



Laboratory of Virology
Department of Virology, Parasitology and Immunology
Faculty of Veterinary Medicine
Ghent University

**Novel insights in the pathogenesis of infectious laryngotracheitis and bronchitis
viruses in chickens**

Vishwanatha Reddy Avalakuppa Papi Reddy

Dissertation submitted in fulfillment of the requirements for the degree of
Doctor of Philosophy (PhD) in Veterinary Sciences, 2016

Promoter
Professor Dr. Hans J. Nauwynck

© Vishwanatha Reddy Avalakuppa Papi Reddy, Laboratory of Virology, Faculty of Veterinary Medicine, Ghent University, Salisburylaan 133, 9820 Merelbeke, Belgium

The author and the promoter give the authorization to consult and copy parts of this work for personal use only. Every other use is subjects to the copyright laws. Permission to reproduce any material contained in this work should be obtained from the author.

Vishwanatha Reddy Avalakuppa Papi Reddy was supported by Indian Council of Agricultural Research - International Fellowship (ICAR IF - 2011/12) and Ghent University special research fund (BOF - 2015).

Men who reject the responsibility of thought and reason can only exist as parasites on the thinking of others. **Ayn Rand**

TABLE OF CONTENTS

List of abbreviations	iii
1. Introduction	1
1.1. Viruses	2
1.1.1. Infectious laryngotracheitis virus (ILTV)	2
1.1.1.1. Background	2
1.1.1.2. Classification	2
1.1.1.3. Structure	5
1.1.1.4. Replication cycle	7
1.1.1.5. Pathogenesis	8
1.1.1.6. Clinical signs and pathology	9
1.1.2. Infectious bronchitis virus (IBV)	10
1.1.2.1. Background	11
1.1.2.2. Classification	12
1.1.2.3. Structure	14
1.1.2.4. Replication cycle	16
1.1.2.5. Pathogenesis	17
1.1.2.6. Clinical signs and pathology	18
1.2. References	19
2. Aims	31
3. Study of ILTV replication characteristics	35
3.1. Replication characteristics of ILTV in the respiratory and conjunctival mucosa	37
3.1.1. Abstract	38
3.1.2. Introduction	38
3.1.3. Materials and methods	40
3.1.4. Results	43
3.1.5. Discussion	50
3.1.6. References	54
3.2. Presence of DNA extracellular traps but not MUC5AC and MUC5B mucin in mucoid plugs/casts of infectious laryngotracheitis virus (ILTV) infected tracheas of chickens	59
3.2.1. Abstract	60
3.2.2. Introduction	60
3.2.3. Materials and methods	62
3.2.4. Results	66
3.2.5. Discussion	72
3.2.6. References	77

4. Study of IBV replication characteristics	83
4.1. Genetic characterization of the Belgian nephropathogenic infectious bronchitis virus (NIBV) reference strain B1648	85
4.1.1. Abstract	86
4.1.2. Introduction	86
4.1.3. Materials and methods	88
4.1.4. Results	91
4.1.5. Discussion	100
4.1.6. References	104
4.2. Productive replication of nephropathogenic infectious bronchitis virus strain B1648 in the peripheral blood monocyctic cells, a strategy for viral dissemination and kidney infection in chickens	111
4.2.1. Abstract	112
4.2.2. Introduction	112
4.2.3. Materials and methods	114
4.2.4. Results	124
4.2.5. Discussion	135
4.2.6. References	143
5. General discussion	151
6. Summary/Samenvatting	173
Curriculum Vitae	183
Acknowledgements	187

LIST OF ABBREVIATIONS

AIHV1	alcelaphine herpesvirus 1
ANOVA	analysis of variance
APN	amino peptidase N
BM	basement membrane
BHV1, 2, 4, 5	bovine herpesvirus 1, 2, 4, 5
CHV1	canine herpesvirus 1
CD	cluster of differentiation
cDNA	complement DNA
CNS	central nervous system
COC	conjunctival organ culture
CCoV	canine coronaviruses
CO ₂	carbon dioxide
CPE	cytopathic effect
CT	cytoplasmic tail
C-terminal	carboxy terminal
2D, 3D	two-dimensional, three-dimensional
DABCO	1,4-diazobicyclo-2.2.2-octane
DMEM	Dulbecco's modified eagle's medium
DNA	deoxyribonucleic acid
DNase I	deoxyribonuclease I
dpi	days post inoculation
dUTP	2'-Deoxyuridine, 5'-Triphosphate
E	early
EAV	equine arteritis virus
EC(M)	extracellular (matrix)
EDTA	ethylene diamine tetra acetic acid
EGF	epidermal growth factor
EHV1, 4,	equine herpesvirus 1, 2,
EID ₅₀	egg infectious dose with a 50% endpoint
E protein	envelope protein
ER	endoplasmic reticulum
ERGIC	endoplasmic reticulum-Golgi intermediate compartment

ET	extracellular tail
FCS	fetal calf serum
FHV1	feline herpesvirus 1
FITC	fluorescein isothiocyanate
FGF-2	fibroblast growth factor 2
G1,-2	globular domain 1,-2,...
GAG	glycosaminoglycan
GaHV1, 2, 3	gallid herpesvirus 1, 2, 3
GAPDH	glyceraldehyde-3-phosphate dehydrogenase
gB, gC	glycoprotein B, glycoprotein C
h	hour
HbX	hepatitis B virus x protein
(H)CMV	(human) cytomegalovirus
HE-staining	haematoxyline-eosine staining
HEPES	4-(2-hydroxyethyl)-1-piperazineethanesulfonic acid
HHV1, 2, 6, 7,8	human herpesvirus 1, 2, 6, 7, 8
HVEM	herpesvirus entry mediator
HIV	human immunodeficiency virus
HSV1 and 2	herpes simplex virus 1 and 2
IB	infectious bronchitis
IBV	infectious bronchitis virus
IE	immediate early
IR	internal repeat
IF	immunofluorescence
Ig	immunoglobulin
IPMA	immunoperoxidase monolayer assay
ILT	infectious laryngotracheitis
ILTV	infectious laryngotracheitis virus
ICTV	international committee on taxonomy of viruses
kbp	kilo base pairs
KUL01	KU Leuven 01
L	late
LDR	linear dynamic range
M41	Massachusetts 41

MCF	malignant catarrhal fever
McHV1	macacine herpesvirus 1
MDBK	Madin-Darby bovine kidney cells
MERS-CoV	Middle East respiratory syndrome coronavirus
MHC	major histocompatibility complex
MIP	maximum intensity projection
M protein	membrane protein
mRNA	messenger RNA
MUC5AC	mucin 5AC
MUC5B	mucin 5B
MuHV1, 4	murine herpesvirus 1, 4
MHV	murine hepatitis virus
NIBV	nephropathogenic infectious bronchitis virus
NK cell	natural killer cell
N protein	nucleocapsid protein
NSP	non-structural protein
N-terminal	amino terminal
OvHV2	ovine herpesvirus 2
ORF	open reading frame
PEDV	porcine epidemic diarrhea virus
PBMC	peripheral blood mononuclear cell
PBS	phosphate-buffered saline
PCR	polymerase chain reaction
PHEV	porcine haemagglutinating encephalomyelitis virus
pi	post inoculation
PMN	polymorphonuclear neutrophil granulocytes
PRCoV	porcine respiratory coronavirus
PRRSV	porcine reproductive and respiratory syndrome virus
PsHV1	psittacid herpesvirus 1
RFLP	restriction fragment length polymorphism
RNA	ribonucleic acid
Roi	region of interest
RT	room temperature
RT-qPCR	real time quantitative polymerase chain reaction

SARS-CoV	severe acute respiratory syndrome
SD	standard deviation
SHV1	swine herpesvirus 1
SPF	specific pathogen free
TG	trigeminal ganglion
TGN	trans Golgi network
Three R's	Refinement, Reduction and Replacement
TOC	tracheal organ culture
TGEV	transmissible gastroenteritis virus
TR	terminal-repeat
TUNEL	terminal deoxynucleotidyl transferase mediated dUTP nick end labeling
UL	unique long
US	unique short
URT	upper respiratory tract
UTR	untranslated region
VZV	Varicella-zoster virus
+ss RNA	positive-sense single-stranded RNA

CHAPTER 1.

INTRODUCTION

1.1. Viruses

1.1.1. Infectious laryngotracheitis virus

Infectious laryngotracheitis virus (ILTV) is a contagious respiratory virus that primarily affects chickens. ILTV can also affect pheasants and peafowls (Crawshaw and Boycott, 1982). ILTV may cause severe production losses due to decreased egg production and/or mortality (Garcia *et al.*, 2013). ILTV transmission commonly occurs by inhalation, direct bird-to-bird contact and indirect by fomites and people (Menendez *et al.*, 2014). Ingestion is also a source of infection, but exposure to nasal epithelium is necessary following ingestion (Garcia *et al.*, 2013; Robertson and Egerton, 1981).

1.1.1.1. Background

In 1925, a new disease was reported in chickens of the United States that was described as trachea-laryngitis (May and Tittsler, 1925). The disease was characterized by nasal exudate, swelling around eyes, dyspnea and expulsion of bloody mucus. However, laryngotracheitis was believed to have existed as early as 1920s (Cover, 1996). Several different names have been used to describe this disease including laryngotracheitis, infectious laryngotracheitis (ILT), infectious bronchitis and avian diphtheria (Beach, 1930). In 1931, the special committee on poultry diseases of the American Veterinary Medical Association adopted the name infectious laryngotracheitis (Garcia *et al.*, 2013). Beaudette was the first to show that ILT was caused by a filterable agent (= virus) (Beaudette, 1937). ILT was the first poultry viral disease for which an effective vaccine was developed (Garcia *et al.*, 2013).

1.1.1.2. Classification

The International Committee on Taxonomy of Viruses (ICTV) has given a classification of herpesviruses (www.ictvonline.org) (Davison, 2010; Davison *et al.*, 2009). Herpesviruses belong to the order *Herpesvirales*, which contain three families, three subfamilies, seventeen genera and ninety species (Davison, 2010). *Herpesviridae*, *Alloherpesviridae* and *Malacoherpesviridae* are the three families within the *Herpesvirales*. The *Herpesviridae* contain viruses of mammals, birds and reptiles. *Alloherpesviridae* contain viruses of fish and frog, and *Malacoherpesviridae*

contain viruses of bivalves (Davison *et al.*, 2009). *Alphaherpesvirinae*, *Betaherpesvirinae* and *gammaherpesvirinae* are three subfamilies of the *Herpesviridae* family.

Alphaherpesvirinae

Alphaherpesvirinae is an extensive subfamily that contains numerous mammalian and avian viruses (Thiry *et al.*, 2005). Alphaherpesviruses have a short life cycle of 8 to 12 hours, grow rapidly, lyse infected cells, and are capable to establish latency primarily in sensory ganglia (Davison *et al.*, 2009; Fuchs *et al.*, 2000; Thiry *et al.*, 2005). Some alphaherpesviruses are found to have a broad host range (Davison *et al.*, 2009). The *alphaherpesvirinae* contains four genera, namely *Simplexvirus*, *Varicellovirus*, *Mardivirus* and *Iltoivirus* (Roizman and Baines, 1991). Herpes simplex virus 1 (HSV1), herpes simplex virus 2 (HSV2) and bovine herpes virus 2 (BHV2) are species under the genus *Simplexvirus*. The best-known species in the genus *Varicellovirus* are swine herpesvirus 1 (SHV1), bovine herpesvirus 1 (BHV1), bovine herpesvirus 2 (BHV2), equine herpesvirus 1 (EHV1), equine herpesvirus 4 (EHV4), canine herpesvirus 1 (CHV1) and feline herpesvirus 1 (FHV1) (Davison, 2010; Davison *et al.*, 2009). Gallid herpesvirus type 2 and 3 (GaHV2 and 3), Anatid herpesvirus 1, Columbidae herpesvirus 1 and Meleagrid herpesvirus 1 are avian alphaherpesviruses under genus *Mardivirus* (Gailbreath and Oaks, 2008; Gennart *et al.*, 2015; Guo *et al.*, 2009; Hunt and Dunn, 2015; Mahony *et al.*, 2015; Petherbridge *et al.*, 2009; Wozniakowski *et al.*, 2013). Gallid herpesvirus type 1 (GaHV1) and Psittacid herpesvirus 1 (PsHV1) are another group of avian alphaherpesviruses that belong to the genus *Iltoivirus* (Fuchs *et al.*, 2007; Horner *et al.*, 1992; Luppi *et al.*, 2016). An overview of the different avian alphaherpesviruses is represented in Table 1. Here, we will focus on Gallid herpesvirus 1 (ILTV) as this avian herpesvirus was used in the present study.

Betaherpesvirinae

Betaherpesvirinae mainly comprise mammalian viruses. The viruses of this family have a restricted host range. The replication cycle of betaherpesviruses takes 36 hours, which is much longer than for alphaherpesviruses. The viruses go to latency in secretory glands, kidneys and lymphoreticular tissues. The *betaherpesvirinae* contain four genera, namely *Cytomegalovirus*, *Muromegalovirus*, *Roseolovirus* and

Proboscivirus (Davison *et al.*, 2009; Roizman and Baines, 1991). Human herpesvirus 5 (HHV5) is the prototype of beta herpesviruses in the genus *Cytomegalovirus*, and is also called human cytomegalovirus (CMV).

Table 1. Overview of avian alphaherpesviruses.

Genus	Virus species	Acronym	Natural host	Clinical signs
Iltovirus	Gallid herpesvirus 1	GaHV1	Chickens	Respiratory disease (ILT)
	Psittacid herpesvirus 1	PsHV1	Psittacine birds	Pacheco's Disease (PD)
Mardivirus	Anatid herpesvirus 1	AnHV1	Ducks	Duck virus enteritis (DVE)/Duck plague
	Columbid herpesvirus 1	CoHV-1	Pigeons, owls and falcons	Respiratory and digestive disease
	Gallid herpesvirus 2	GaHV2	Chickens	Lymphoproliferative disease (MDV)
	Gallid herpesvirus 3	GaHV3	Chickens	Nonpathogenic MDV serotype 2
	Meleagrid herpesvirus 1	MeHV1	Turkey	Nonpathogenic herpesvirus of turkeys (HVT)

Gammaherpesvirinae

Gammaherpesviruses are generally lymphotropic and establishes latency in lymphocytes. The *gammaherpesvirinae* contains four genera, namely *Macavirus*, *Percavirus*, *Lymphocryptovirus* and *Rhadinovirus* (Ackermann, 2006; Davison *et al.*, 2009; Roizman and Baines, 1991). Human herpesvirus 4 (HHV4) or Epstein-Barr virus (EBV) is the prototype of gammaherpesvirus under the genus *Lymphocryptovirus*. Bovine herpesvirus 4 (BHV4), murine herpesvirus 4 (MuHV4) and human herpesvirus 8 (HHV8 or Kaposi's sarcoma-associated herpesvirus) are species under the genus *Rhadinovirus* (Andrei and Snoeck, 2015; O'Connor and Kedes, 2007). The species under genus *Percavirus* are equine herpesvirus 2 and 5 (EHV2 and EHV5). Alcelaphine herpesvirus 1 (AIHV1) and ovine herpesvirus 2 (OvHV2) are under *Macavirus* genus (Davison *et al.*, 2009; Ziak *et al.*, 2014). Macaviruses cause malignant catarrhal fever (MCF), a fatal disease of artiodactyla species (Farquharson, 1946; Ricer, 2015).

1.1.1.3. Structure

Based on electronmicrographs, ILTV demonstrated to have hexagonal nucleocapsid with icosahedral symmetry, a typical morphology of herpesvirions (Garcia *et al.*, 2013; Granzow *et al.*, 2001; Portz *et al.*, 2008). The four distinct structures of ILTV are genome, capsid, tegument and envelope (Figure 1).

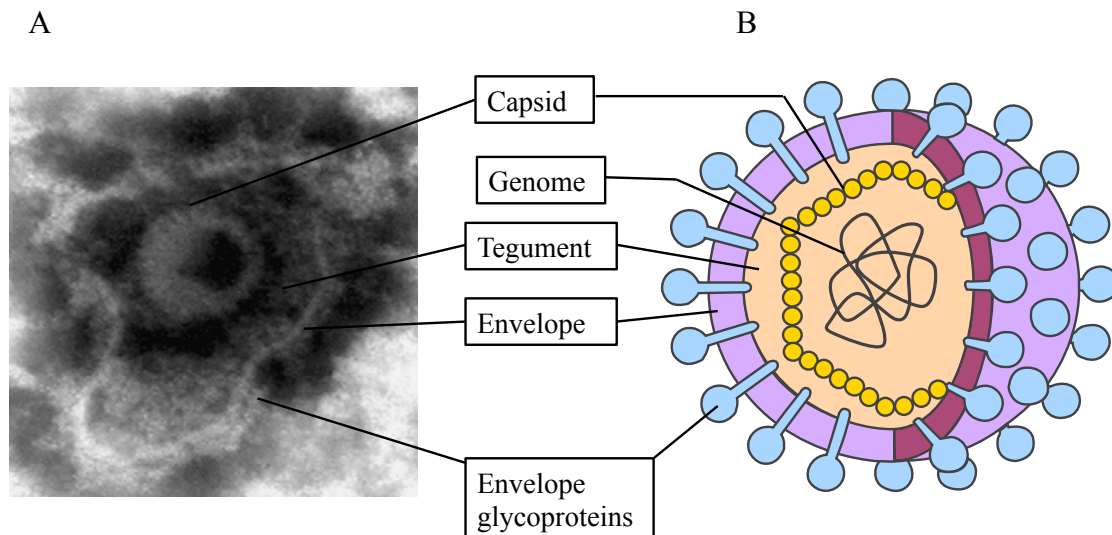


Figure 1. Structure of an ILTV virion. (A) Transmission electron microscopy image of an ILTV particle [adapted from Portz *et al.* (2008)]. (B) Schematic structure of a virion. Distinct structures of ILTV are genome, capsid, tegument and envelope.

ILTV has a double stranded DNA genome of approximately 150 kilo base pairs (kbp). It consists of long and short unique regions (U_L and U_S) interspersed with inverted repeat sequences, such as internal repeat (IR) and terminal repeat (TR) sequences (Figure 2) (Fuchs *et al.*, 2007).

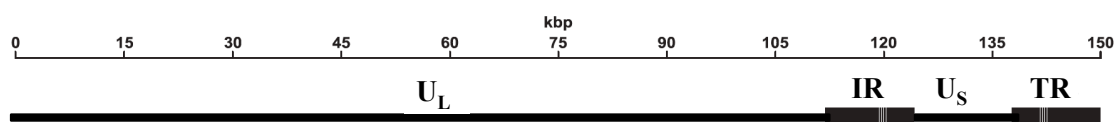


Figure 2. Double-stranded DNA genome of ILTV. Genome of 150 kbp in size consists of long and short unique regions (U_L , U_S), and of inverted repeats (IR, TR) flanking the U_S region [adapted from Fuchs *et al.* (2007)].

Table 2. Identified gene products of ILTV [adapted from *Fuchs et al. (2007)*].

Gene	Protein	Amino acids	Expected masses (kDa)
UL0	ILTV-specific-nuclear protein	506	57.0
UL(-1)	Iltovirus-specific-nuclear protein	501	57.6
ORF A	Iltovirus-specific protein	376	41.3
ORF B	Iltovirus-specific protein	340	38.1
ORF C	Iltovirus-specific protein	354	37.4
ORF D	Iltovirus-specific protein	374	41.5
ORF E	Iltovirus-specific protein	411	45.1
UL10	gM homologue, envelope protein	393	43.1
UL22	gH, envelope glycoprotein	804	89.4
UL27	gB, envelope glycoprotein	883	100.2
UL31	Nuclear protein	314	35.4
UL37	Tegument protein	1022	113.0
UL44	gC, envelope glycoprotein	414	46.4
UL46	Tegument protein	557	62.7
UL47	Tegument protein	623	70.0
UL48	Tegument protein	396	44.6
UL49	Tegument protein	266	30.4
UL49.5	gN, envelope glycoprotein	117	12.7
US4	gG, secreted glycoprotein	292	31.7
US5	gJ, secreted glycoprotein	985, 611	106.5, 66.8

The ILTV genome contains 79 open reading frames (ORFs), which have been predicted to encode proteins. The majority of ILTV ORFs are homologues to ORFs of other alphaherpesviruses, such as HSV1. ORFs A, B, C, D, E, F, U_L-0 and U_L-1 are specific to *Iltovirus* (Fuchs *et al.*, 2007; Veits *et al.*, 2003). Identified ORFs with gene products of ILTV are given in Table 2. The DNA is present in an icosahedral nucleocapsid of about 100 nm in diameter, which is made of elongated hollow 162 capsomers-150 hexamers and 12 pentamers. Tegument is a layer of globular material that surrounds the capsid protein. ILTV is reported to have large amounts of tegument proteins (Granzow *et al.*, 2001). A lipoprotein membrane envelope encloses the nucleocapsid with many glycoprotein spikes on its surface. Viral glycoproteins gB,

gC, gD, gE, gG, gH, gI, gJ, gK, gL, gM and gN are homologues of HSV1 (Thureen and Keeler, 2006). In addition to protein encoding genes, ILTV also encodes short RNAs (approximately 22 nt) known as micro RNAs. The micro RNAs role in silencing of viral/host transcription/translation is not known (Garcia *et al.*, 2013; Rachamadugu *et al.*, 2009).

1.1.1.4. Replication cycle

The replication cycle of ILTV is similar to other alphaherpesviruses, such as HSV1 (Guo *et al.*, 1993; Mettenleiter *et al.*, 2009; Roizman and Taddeo, 2007). The replication of alphaherpesviruses usually starts with the initial attachment of envelope glycoproteins (gC) to cell surface heparan sulphate (Kingsley and Keeler, 1999). Viral glycoproteins gB, gD and gH-L complex are involved in enhancement of virus attachment to the host cell surface (Akhtar and Shukla, 2009; Eisenberg *et al.*, 2012). In case of ILTV, the envelope gC lacks a positively charged heparan sulphate binding region that is conserved in other alphaherpesvirus homologues (Kingsley *et al.*, 1994; Kingsley and Keeler, 1999; Pavlova *et al.*, 2010). Thus, it seems that ILTV does not use heparan sulphate as its primary host cell receptor. After initial attachment, the nucleocapsid is released into the cytoplasm and transported to the nucleus. Upon injection of the viral genome in the nucleus via the nucleopore, viral DNA replication and transcription occur. All viral proteins are synthesized in the cytoplasm of the cell (Guo *et al.*, 1993; Zaichick *et al.*, 2011). In general, the alphaherpesvirus genome transcription strictly follows a regulated cascade. The viral genes are transcribed at different time points and are clustered into immediate early (IE), early (E) and late (L) genes (Hones and Roizman, 1974; Nicoll *et al.*, 2012). Commonly, IE and E genes, and their products regulate transcription of L genes. The ILTV genes are not strictly regulated and found to be quite leaky (Mahmoudian *et al.*, 2012). The ILTV genes are differentiated into IE, E, E/L and L genes. The cascade patterns of ILTV gene expression are as follows. First several enzymes and DNA binding proteins are expressed, which are required for DNA replication, e.g. DNA polymerase and thymidine kinase. After DNA replication, viral structural proteins like capsid, tegument and envelope glycoproteins are expressed (Mahmoudian *et al.*, 2012; Prideaux *et al.*, 1992). The newly synthesized DNA concatemers cleaves into monomeric units and assemble with capsids to form nucleocapsids (Ben-Porat and Tokazewski, 1977). The DNA encapsidation takes place in the nucleus. The

assembled nucleocapsids exploit an envelopment/de-envelopment mechanism for transport to the cytosol (Mettenleiter *et al.*, 2006; Skepper *et al.*, 2001). The nucleocapsids acquire an envelope by budding through the inner lamellae of the nuclear membrane. The primary enveloped nucleocapsids, undergo a fusion with the outer nuclear membrane, which leads to release of de-enveloped/naked nucleocapsids into the cytoplasm (Skepper *et al.*, 2001). In cytoplasm, main tegument proteins added to the nucleocapsids, which obtain their final envelope by budding into glycoprotein-containing Golgi derived vesicles (Mettenleiter *et al.*, 2006). Enveloped mature virions released by cell lysis/exocytosis and vacuolar membrane fusion (Granzow *et al.*, 2001; Guo *et al.*, 1993; Mettenleiter, 2002; Mettenleiter *et al.*, 2006; Mettenleiter and Minson, 2006).

1.1.1.5. Pathogenesis

ILTV enters its host through upper respiratory and ocular routes. After natural entry of virus through nostrils or eyes, it primarily replicates in the epithelium of larynx and tracheal mucosae (Garcia *et al.*, 2013; Guy and Bagust, 2003). However, the exact replication characteristics and invasion mechanisms of ILTV at the respiratory mucosa are not clearly understood. ILTV also replicates in the conjunctiva, respiratory sinuses, air sacs and lungs (Figure 3). During the first week of infection, ILTV replication in the larynx and trachea, leads to epithelial damage and hemorrhages (Bagust and Johnson, 1995; Bagust *et al.*, 2000; Garcia *et al.*, 2013). Several studies have shown that active replication of ILTV slows down after 6 days post inoculation (dpi), and virus may remain at very low levels up to 10 dpi (Bagust and Johnson, 1995; Garcia *et al.*, 2013). ILTV is reported to spread to trigeminal ganglion (TG) of chickens, after 4-7 days of tracheal infection (Bagust, 1986; Bagust *et al.*, 1986). TG is the principal site of latency for ILTV. The establishment of latency is similar with that of other herpesviruses, and is the biological survival mechanism, which enables ILTV to evade host defense mechanisms (Bagust, 1986). The latent virus persists in the flock over generations, and act as source of ILTV infection during stress (Bagust *et al.*, 2000). The onset of egg laying and mixing of chickens with unfamiliar birds are important stressors, which lead to reactivation of virus and spontaneous outbreaks of infection (Fuchs *et al.*, 2007).

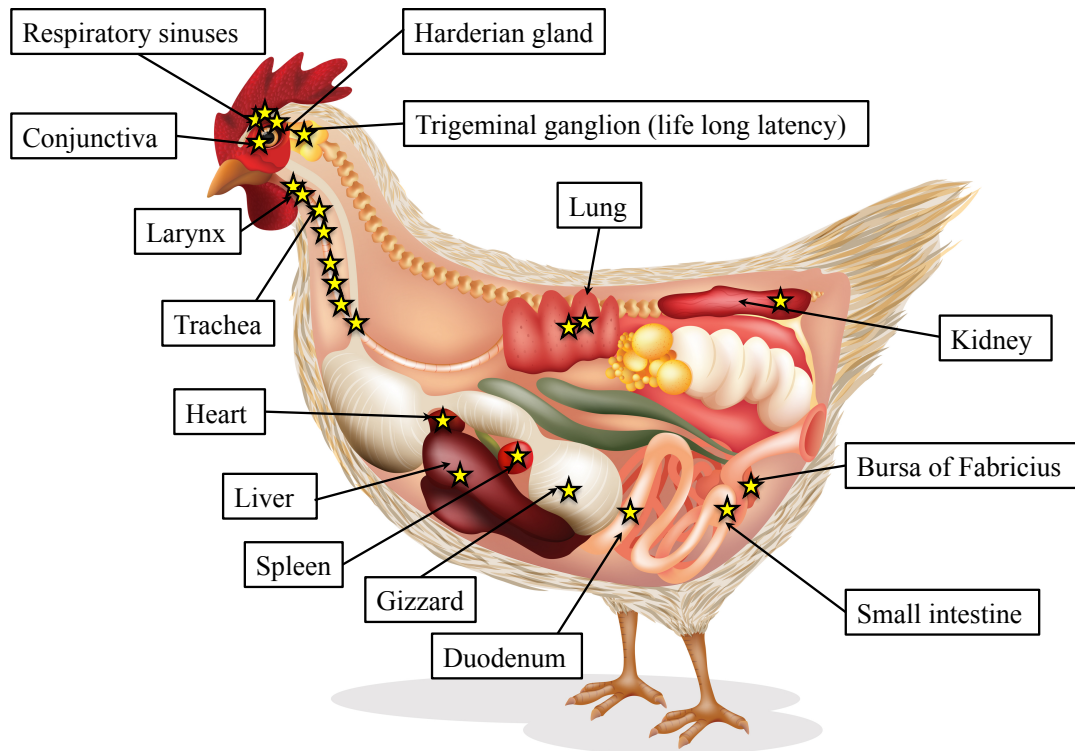


Figure 3. ILTV pathogenesis. Stars represent infectious virus. Star number and infectivity are directly proportional to each other. ILTV replicates in the epithelium of larynx, trachea, conjunctiva, respiratory sinuses, air sacs and lungs. Recently, ILTV was observed in kidneys, spleen, liver, heart, gizzard, small and large intestines, bursa Fabricicus and Harderian gland. ILTV establishes a lifelong latency in trigeminal ganglion.

Very recently, ILTV was reported in extra respiratory tissues like kidneys, spleen, liver, heart, stomach, intestines, bursa Fabricicus and Harderian glands (Roy *et al.*, 2015; Zhao *et al.*, 2013). Otherwise, still there is no clear information on viremic phase of ILTV infection (Garcia *et al.*, 2013).

1.1.1.6. Clinical signs and Pathology

The clinical signs of ILT have been described into a mild and severe form. The mild form of the disease is characterized by nasal discharge, mild respiratory rales, mild conjunctivitis, reduced egg production and no mortality (Bagust *et al.*, 2000). Clinical signs during a severe form are marked by dyspnea, open mouth breathing with expectoration of bloody mucoid material, severe conjunctivitis, high morbidity, and moderate to severe mortality (Fuchs *et al.*, 2007; Garcia *et al.*, 2013). The clinical signs were reported in chickens of all ages but the most characteristic signs observed

in adult birds (Garcia *et al.*, 2013). The important pathological changes of ILT are hemorrhages and diphtheritic changes in larynx and trachea, and presence of mucoid plugs/casts in the trachea (Garcia *et al.*, 2013). An overview of clinical signs and pathology following ILTV infection is shown in Figure 4.

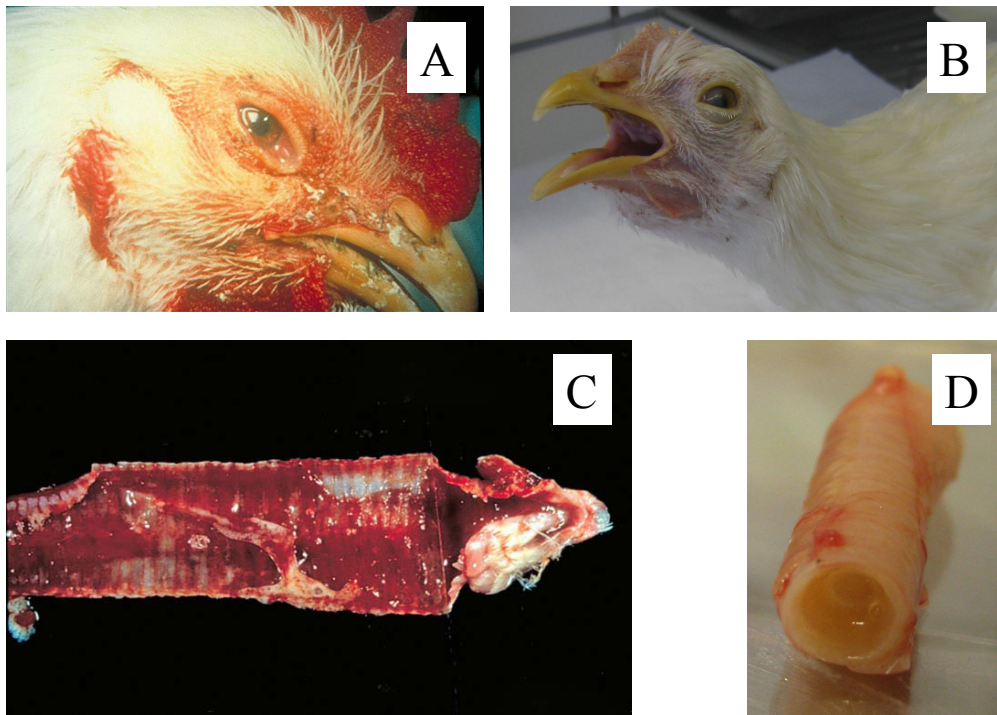


Figure 4. ILTV clinical signs and pathology. (A) Conjunctivitis, (B) open mouth breathing, (C) blood and mucus in larynx and trachea, and (D) mucoid plugs/casts in trachea (figures 4A and 4D adapted from a North Carolina State University fact Sheet entitled “Infectious Laryngotracheitis Virus (ILT)” by Donna K. Carver).

1.1.2. Infectious bronchitis virus

Infectious bronchitis virus (IBV) is the etiological agent of the disease infectious bronchitis (IB). IB is probably the most economically important viral respiratory disease of poultry industry, after avian influenza and Newcastle disease (Cook *et al.*, 2012). IBV is a highly contagious respiratory pathogen of chickens. Partridge, guinea fowl, geese, pigeon, duck and peafowl are also susceptible to IBV infection (Cavanagh, 2005, 2007). IBV affects both meat-type and egg-laying birds. Currently, several serotypes of IBV exist, and new variant types emerge due to increased point mutations and recombination events (Jackwood, 2012).

1.1.2.1. Background

IB was reported in young chickens as a new respiratory disease in North Dakota, United States in 1931 (Fabricant, 1998; Schalk and Hawn, 1931). In 1936, the causative agent of IB was demonstrated to be a filterable agent (= virus) (Beach and Schalm, 1936). IBV was first cultivated in embryonated chicken eggs in 1937 (Beaudette and Hudson, 1937). In the early 1950s, a first IBV variant was reported in the US, and found that vaccines did not cross protect or cross neutralize these variants (Fabricant, 1998; Jungherr *et al.*, 1956). Later new variant strains and serotypes were reported all over the world. In the beginning of the 1950s, the well-known respiratory Massachusetts (Mass) type of IBV was reported in the US. Subsequently, Mass-type (prototype: M41) strains have been reported worldwide and new variants emerged (Hopkins, 1974). In the 1950s, an IBV type was reported to infects the reproductive tract, and which affects egg production and quality in laying chickens (Van Roeckel *et al.*, 1942). In the 1960s, new emerging and fatal nephropathogenic IBV strains were described in the US, Australia, and later all over the world. In the last 15 years, nephropathogenic IBV strains have been emerging as most predominant IBV strains and remained as most feared disease in commercial poultry (Abdel-Moneim *et al.*, 2006; Bayry *et al.*, 2005; De Wit *et al.*, 2015; Lim *et al.*, 2011; Liu and Kong, 2004; Mahmood *et al.*, 2011; Meir *et al.*, 2004; Seger *et al.*, 2016; Toffan *et al.*, 2013a; Zanaty *et al.*, 2016; Ziegler *et al.*, 2002). The B1648 strain was responsible for outbreaks of kidney disease in chicken farms in Belgium, The Netherlands and Northern France, and was first isolated in 1984 (Meulemans *et al.*, 1987; Pensaert and Lambrechts, 1994). Currently, the B1648 strain or its variants are still circulating in Europe and North Africa (Bochkov *et al.*, 2006; Ducatez *et al.*, 2009; Krapež *et al.*, 2010; Toffan *et al.*, 2013b). In the 1970s and 1990s, IBV was shown to infect the intestinal tract with no apparent effect on the gut function (Alexander and Gough, 1977, 1978; Ambali and Jones, 1990). In Europe, currently, 4/91, D274, Mass 41, Italy 02 and QX are recognized as important circulating serotypes (Cavanagh, 2007; Cook *et al.*, 2012). Here, we will focus on nephropathogenic B1648 and respiratory M41 strains as these IBV strains were used in the present PhD thesis work (Lambrechts *et al.*, 1993; Pensaert and Lambrechts, 1994; Pensaert *et al.*, 1981).

1.1.2.2. Classification

Coronaviruses belong to the order *Nidovirales*, which contain four families, namely *Coronaviridae*, *Arteriviridae*, *Roniviridae*, and *Mesoniviridae*. *Coronaviridae* and *Arteriviridae* families represent economically important viruses of mammals and birds. *Coronavirinae* and *Torovirinae* are two subfamilies of the *Coronaviridae* family (Table 3). The *coronavirinae* contain four genera, namely *Alphacoronavirus*, *Betacoronavirus*, *Gammacoronavirus* and *Deltacoronavirus* (www.ictvonline.org) (Gorbalenya *et al.*, 2006). An overview of the different viruses of the family *Coronaviridae* is represented in Table 3.

Transmissible gastroenteritis virus (TGEV), canine coronaviruses (CCoV), feline coronaviruses and porcine respiratory coronavirus (PRCoV) are classified in the genus *Alphacoronavirus* and species *Alphacoronavirus 1*. Porcine epidemic diarrhea virus (PEDV), human coronaviruses 229E and NL63, and bat coronaviruses are other important coronaviruses in the genus *Alphacoronavirus* (Cavanagh, 2005). The well-known species in the genus *Betacoronavirus* are murine hepatitis virus (MHV), porcine haemagglutinating encephalomyelitis virus (PHEV) and human coronavirus OC43. Recently reported, severe acute respiratory syndrome (SARS-CoV) coronavirus and Middle East respiratory syndrome coronavirus (MERS-CoV) are other important coronaviruses in the genus *Betacoronavirus* (Cavanagh, 2005; Drexler *et al.*, 2014).

The coronaviruses under the genera *Gammacoronavirus* and *Deltacoronavirus* infect birds (Woo *et al.*, 2012). The better-known gammacoronaviruses are coronaviruses of domestic chickens (*Gallus gallus*), turkey (*Meleagris gallopavo*), pheasant (*Phasianus colchicus*), mallard duck (*Anas platyrhynchos*), greylag goose (*Anser anser*) and pigeon (*Columbia livia*) (Cavanagh, 2005, 2007). *Deltacoronavirus* genus contains viruses of pigs and wild birds. Recently, many important deltacoronaviruses were reported from free range and wild bird species (Woo *et al.*, 2012).

Table 3. Overview of the family *Coronaviridae* (adapted from Desmarests Ph.D. dissertation, 2016).

Subfamily	Genus	Species	Subspecies		
<i>Coronavirinae</i>	<i>Alphacoronavirus</i>	<i>Alphacoronavirus 1</i>	<i>Canine coronavirus type I and II</i>		
			<i>Feline coronavirus type I and II</i>		
			Porcine respiratory coronavirus		
			Transmissible gastroenteritis virus		
			Ferret coronaviruses		
			<i>Alphacoronavirus 2</i>		
			<i>Human coronavirus 229E</i>		
			<i>Human coronavirus NL63</i>		
			<i>Porcine epidemic diarrhea virus</i>		
			<i>Miniopterus bat coronavirus HKU8</i>		
<i>Betacoroanvirus</i>	<i>Betacoronavirus 1</i>	Bovine coronavirus			
		Human coronavirus OC43			
		Equine coronavirus			
		Human enteric coronavirus			
		Porcine haemagglutinating encephalomyelitis virus			
		Canine respiratory coronavirus			
		<i>Human coronavirus HKU1</i>			
		<i>Murine coronavirus</i>			
		<i>Severe acute respiratory syndrome virus</i>			
		<i>Middle East respiratory syndrome virus</i>			
<i>Gammacoronavirus</i>	<i>Avian coronavirus</i>	Infectious bronchitis virus			
		Turkey coronavirus			
		Duck coronavirus			
		Pigeon coronavirus			
		Goose coronavirus			
		Pheasant coronavirus			
		<i>Cetacean coronavirus</i>			
		Beluga whale coronavirus SW1			
		<i>Deltacoronavirus</i>	<i>Bulbul coronavirus HKU11</i>	<i>Thrush coronavirus HKU12</i>	
				<i>Munia coronavirus HKU13</i>	
<i>Sparrow coronavirus HKU17</i>					
<i>Magpie robin coronavirus HKU18</i>					
<i>Night heron coronavirus HKU19</i>					
<i>Wigeon coronavirus HKU20</i>					
<i>Torovirinae</i>	<i>Bafinivirus</i>			<i>White bream virus</i>	
				<i>Torovirus</i>	<i>Bovine torovirus</i>
					<i>Equine torovirus</i>
					<i>Porcine torovirus</i>
		<i>Human torovirus</i>			

1.1.2.3. Structure

IB viral particles are round to pleomorphic in shape with a mean diameter of approximately 120 nm (Figure 5B) (Cavanagh, 2007). IBV is an enveloped virus with club shaped surface projections (spike proteins) (Cavanagh, 2007; Cavanagh and Naqi, 2003).

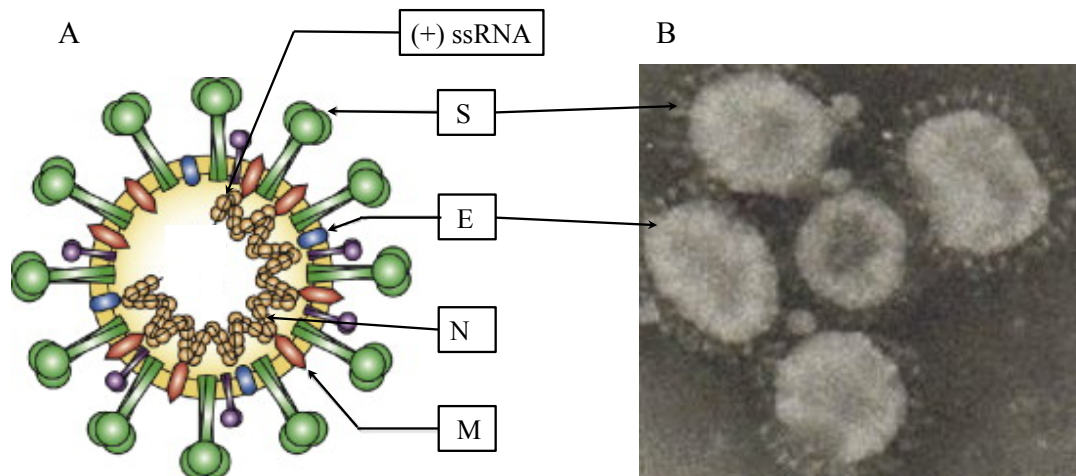


Figure 5. Structure of an IBV virion. (A) Schematic structure of an IBV virion. The nucleocapsid (N) protein surrounds the RNA (+ss RNA). The N protein is surrounded by a lipid envelope in which three structural proteins are inserted, the spike (S), the envelope (E) and the membrane protein (M). (B) Electron micrograph of IBV virion negatively stained with phosphotungstic acid. [Adapted from Cook (1983)].

IBV has a positive-sense single-stranded RNA (+ss RNA) genome with the size of around 27.6 kilobases (kb) (Figure 5). The genome has a methylated cap and poly (A) tail at its 5' and 3' end, respectively. The positive-sense single stranded RNA directly acts as mRNA for the synthesis of viral replicative proteins through translation of open reading frames (ORFs). IBV genome contains at least ten ORFs in the order 5' UTR-1a-1b-S-3a-3b-EM-5a-5b-N-3'UTR (Figure 6). 5'UTR and UTR3' are untranslated regions of around 500 nucleotides, which mediate physical interactions with viral replicase proteins (Liu *et al.*, 2007).

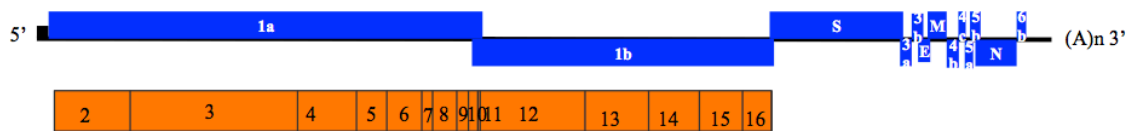


Figure 6. Genome of IBV (+ss RNA). Genome of 27.6 kilobases in size, and consists of a methylated cap and poly (A) tail at its 5' and 3' end. Open reading frame (ORF) 1a and 1b accounts two-thirds of genome, and encode non-structural proteins (NSPs). S, E, M and N are structural protein genes. 3a, 3b, 4a, 4b, 5a, 5b and 6a, 6b are accessory genes (NSPs) (Cavanagh, 2005).

Gene 1 (replicase transcriptase complex) contains two overlapping ORFs, namely ORF 1a and 1b, which make up two-thirds (20 kb) of the viral genome. A ribosomal frame shift mechanism mediates translation of ORF1b. ORF1a and 1b encodes 15 non-structural proteins (NSPs), which are associated with RNA replication, transcription, aspects of pathogenesis and other still unknown functions. The known NSPs of ORF1a and 1b, are RNA-dependent RNA-polymerase, chymotrypsin like main protease, papain like protease 1 and 2, 3C-like protease, ADP-ribose binding protein, Helicase, exoribonuclease, and 2'-O-ribose methyltransferase and other NSPs (Gorbalenya *et al.*, 2006; Hurst *et al.*, 2010; Mielech *et al.*, 2014; van Hemert *et al.*, 2008). The remaining 3' one third of the genome contains ORFs 2, 3, 4 and 6, which encodes spike (S), envelope (E), membrane (M) and nucleocapsid (N) structural proteins, respectively. ORF 3 and ORF 5 encode accessory proteins 3a, 3b, 5a and 5b, which are interspersed between structural proteins. The exact roles of these accessory proteins are largely not known.

The spike glycoprotein is assembles into trimers on the surface of virions to give the crown-like appearance or corona-like appearance (Belouzard *et al.*, 2012). The spike protein is a leading mediator of viral entry. The spike protein (\approx 1160 amino acids) is cleaved into two subunits, namely N-terminal S1 subunit (\approx 520 amino acids) and C-terminal S2 subunit (\approx 620 amino acids) (Belouzard *et al.*, 2012; Cavanagh *et al.*, 1992). S1 is the most variable domain, and consists of virus neutralization and serotype specific determinants. S1 part is responsible for attachment of the virus to receptors on host cells (Casais *et al.*, 2003). S2 activates virus-cell fusion processes (Weiss and Navas-Martin, 2005). The envelope (E/3c) protein is a small membrane non-glycosylated protein. E protein has an important role in virus assembly. In addition, E protein was reported to play a role in ion channel activity, multiple

membrane topologies and virulence (Nieto-Torres *et al.*, 2014; Ruch and Machamer, 2012). The membrane (M) protein is a glycosylated, and most abundant envelope protein. Together with the E protein, the M protein plays crucial roles in virus morphogenesis, assembly and budding (Baudoux *et al.*, 1998; Vennema *et al.*, 1996). The nucleocapsid (N) protein is a highly phosphorylated structural protein. N protein has multiple functions, namely viral packaging, replication, transcription, translation, assembly, viral core formation and signal transduction (McBride *et al.*, 2014).

1.1.2.4. Replication cycle

IBV replication takes place in the cytoplasm of the cell, and it is similar to other coronaviruses (Cavanagh and Naqi, 2003). The coronavirus replication cycle involves five steps: entry, genome replication, transcription, assembly and release. The viral spike protein and cell surface receptor interaction mediates the initial attachment and membrane fusion event of coronavirus entry. Coronaviruses have evolved with different cell surface receptors for virus entry. For example, many alphacoronaviruses use aminopeptidase N (APN), MHV utilize CEACAM1, SARS-CoV use angiotensin-converting enzyme 2 (ACE2) and MERS-CoV use dipeptidyl-peptidase 4 (DPP4), to gain entry into cells (Cui *et al.*, 2013; Fehr and Perlman, 2015; Li *et al.*, 2003; Williams *et al.*, 1991). Sialic acid is a cell surface receptor for IBV entry (Mork *et al.*, 2014; Winter *et al.*, 2006).

Following attachment and fusion, the viral nucleocapsid is released into the cytoplasm. The viral RNA genome directly synthesizes polyproteins pp 1a and pp 1ab by frame shift mechanism. Subsequently, pp 1a and pp 1ab cleave into individual NSPs (Ziebuhr *et al.*, 2000). NSPs assemble into a replication transcription complex (RTC) where genome replication and transcription of subgenomic RNAs occur. Then, translation of S, E and M structural proteins occur, and these proteins embed into endoplasmic reticulum (ER) membrane. The structural proteins move through the endoplasmic reticulum-Golgi intermediate compartment (ERGIC) (de Haan and Rottier, 2005; Krijnse-Locker *et al.*, 1994; Tooze *et al.*, 1984). During this secretory pathway transport posttranslational modifications take place, and all proteins mature and assemble. The assembled virions are then transported to the plasma membrane surface in vesicles and are released by exocytosis (Fehr and Perlman, 2015).

1.1.2.5. Pathogenesis

IBV primarily replicates in the epithelium of the upper respiratory tract (URT) (Cavanagh, 2007; Raj and Jones, 1997b). Virus was shown to replicate mainly in ciliated and mucus producing cells of the epithelium (Nakamura *et al.*, 1996). However, the precise replication kinetics of IBV at the URT are unknown.

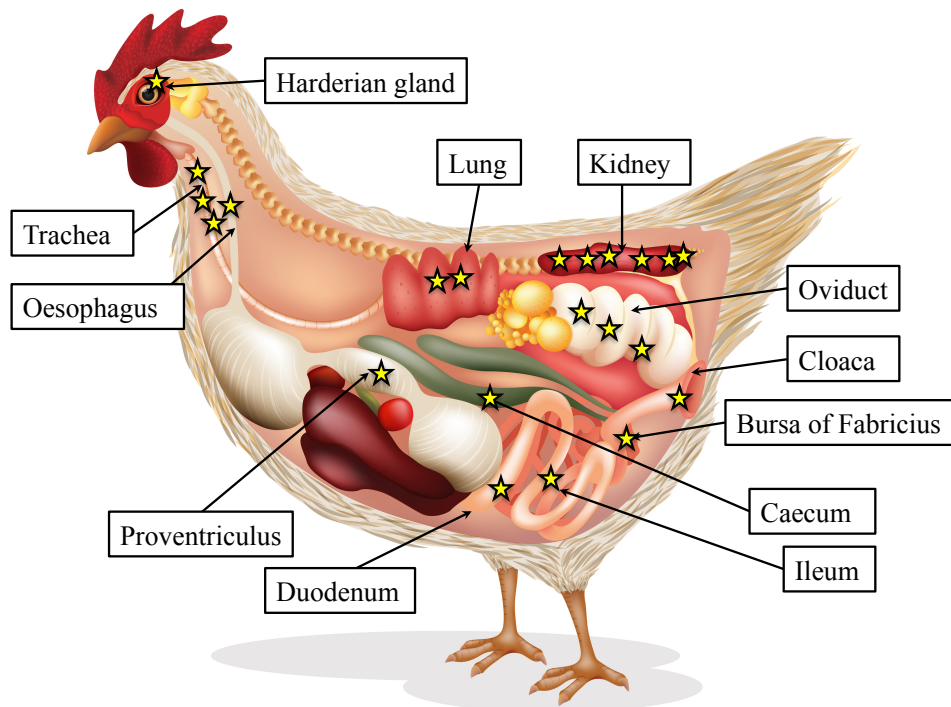


Figure 7. IBV replicates at many epithelial surfaces. Stars represent infectious virus. Star number and infectivity are directly proportional to each other. IBV shows tropism to the trachea, lungs, kidneys, oviduct, oesophagus, duodenum, ileum, bursa of Fabricius, caecum and Harderian gland (Cavanagh, 2005).

High viral titers are observed in the URT between 2 and 5 dpi (Nakamura *et al.*, 1991; Otsuki *et al.*, 1990; Raj and Jones, 1996). IBV also replicates in the lungs and airsacs (Janse *et al.*, 1994; Nauwynck and Pensaert, 1988). In addition to the respiratory tract, IBV has a tropism for the epithelium of many other tissues, including kidneys, reproductive tract, gastrointestinal tract (oesophagus, proventriculus, duodenum, jejunum, bursa of Fabricius, caecal tonsils, rectum and cloaca) and testes (Figure 7) (Alexander and Gough, 1978; Ambali and Jones, 1990; Brown *et al.*, 1987; Cook, 1971, 1984; El-Houadfi *et al.*, 1986; Gallardo *et al.*, 2011; Jones and Jordan, 1971; Lucio and Fabricant, 1990; Raj and Jones, 1996; Villarreal *et al.*, 2007).

Nephropathogenic IBV replicates in collecting ducts and tubules, Henle's loops and distal convoluted tubules of kidneys (Chen *et al.*, 1996; Chong and Apostolov, 1982; Owen *et al.*, 1991). In some cases, IBV may persist in kidneys of chickens (Bhattacharjee *et al.*, 1995; Jones and Ambali, 1987; Raj and Jones, 1997a). Up till now, there are poor reports on the viremic phase of IBV infection.

1.1.2.6. Clinical signs and pathology

The characteristic respiratory signs of IB are tracheal rales, coughing, gasping, nasal discharge, and huddling together (Jackwood and de Wit, 2013). The classical clinical signs of nephropathogenic IBV disease are increased water consumption, watery droppings, low body weight gain and increased mortality (Cook *et al.*, 2012; Meulemans *et al.*, 1987; Pensaert and Lambrechts, 1994). Decreased egg production and quality (thin shelled and misshapen), and cystic dilatation of the oviducts (IBV QX type) are shown in oviduct infected chickens (Awad *et al.*, 2016; Benyeda *et al.*, 2009; Broadfoot *et al.*, 1954; de Wit *et al.*, 2011; Hewson *et al.*, 2014; Maiti *et al.*, 1985). In general, QX type has been reported to be associated with cystic oviducts (false layers syndrome), nephritis and respiratory distress (Benyeda *et al.*, 2009; de Wit *et al.*, 2011). Presence of caseous or cloudy exudate in the tracheal and bronchi mucosa is pathological changes of respiratory IB. The important pathological changes of nephropathogenic IB are dehydrated carcasses, enlarged and pale kidneys with urates in the collecting tubules (Cook *et al.*, 2012; Ignjatovic and Sapats, 2000; Meulemans *et al.*, 1987). An overview of clinical signs and pathology following IBV infection is shown in Figure 8.

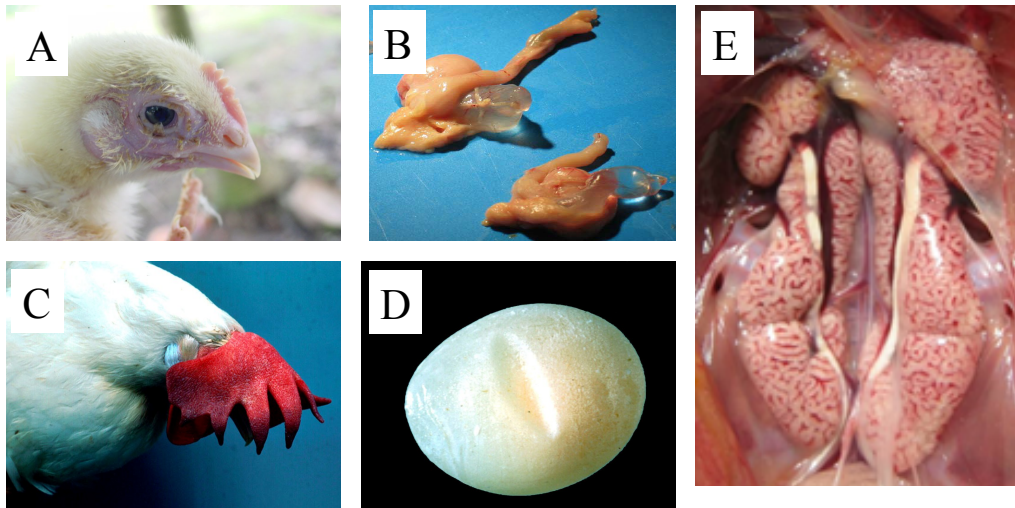


Figure 8. IB clinical signs and pathology. (A) Ephiphora, (B) cystic dilatation of the oviduct (IBV QX strain), (C) depression, (D) thin shelled eggs and (E) enlarged kidneys (figures 8A, 8C and 8D are adapted from atlas of avian diseases, Cornell University, figure 8B is adapted from de Wit *et al.* (2011) and figure 8E is from Dr. Kannan Ganapathy, University of Liverpool).

1.2. References

- Abdel-Moneim, A.S., El-Kady, M.F., Ladman, B.S., Gelb, J., Jr., 2006. S1 gene sequence analysis of a nephropathogenic strain of avian infectious bronchitis virus in Egypt. *Virology* 3, 78.
- Ackermann, M., 2006. Pathogenesis of gammaherpesvirus infections. *Veterinary Microbiology* 113, 211-222.
- Akhtar, J., Shukla, D., 2009. Viral entry mechanisms: cellular and viral mediators of herpes simplex virus entry. *FEBS Journal* 276, 7228-7236.
- Alexander, D.J., Gough, R.E., 1977. Isolation of avian infectious bronchitis virus from experimentally infected chickens. *Research in Veterinary Science* 23, 344-347.
- Alexander, D.J., Gough, R.E., 1978. A long-term study of the pathogenesis of infection of fowls with three strains of avian infectious bronchitis virus. *Research in Veterinary Science* 24, 228-233.
- Ambali, A.G., Jones, R.C., 1990. Early pathogenesis in chicks of infection with an enterotropic strain of infectious bronchitis virus. *Avian Diseases* 34, 809-817.
- Andrei, G., Snoeck, R., 2015. Kaposi's sarcoma-associated herpesvirus: the role of lytic replication in targeted therapy. *Current Opinion in Infectious Diseases* 28, 611-624.
- Awad, F., Chhabra, R., Forrester, A., Chantrey, J., Baylis, M., Lemiere, S., Hussein, H.A., Ganapathy, K., 2016. Experimental infection of IS/885/00-like

- infectious bronchitis virus in specific pathogen free and commercial broiler chicks. *Res Vet Sci* 105, 15-22.
- Bagust, T.J., 1986. Laryngotracheitis (Gallid-1) herpesvirus infection in the chicken. 4. Latency establishment by wild and vaccine strains of ILT virus. *Avian Pathol* 15, 581-595.
- Bagust, T.J., Calnek, B.W., Fahey, K.J., 1986. Gallid-1 herpesvirus infection in the chicken. 3. Reinvestigation of the pathogenesis of infectious laryngotracheitis in acute and early post-acute respiratory disease. *Avian Dis* 30, 179-190.
- Bagust, T.J., Johnson, M.A., 1995. Avian infectious laryngotracheitis: virus-host interactions in relation to prospects for eradication. *Avian Pathol* 24, 373-391.
- Bagust, T.J., Jones, R.C., Guy, J.S., 2000. Avian infectious laryngotracheitis. *Rev Sci Tech* 19, 483-492.
- Baudoux, P., Carrat, C., Besnardeau, L., Charley, B., Laude, H., 1998. Coronavirus pseudoparticles formed with recombinant M and E proteins induce alpha interferon synthesis by leukocytes. *J Virol* 72, 8636-8643.
- Bayry, J., Goudar, M.S., Nighot, P.K., Kshirsagar, S.G., Ladman, B.S., Gelb, J., Ghalsasi, G.R., Kolte, G.N., 2005. Emergence of a nephropathogenic avian infectious bronchitis virus with a novel genotype in India. *J Clin Microbiol* 43, 916-918.
- Beach, J.R., 1930. The Virus of Laryngotracheitis of Fowls. *Science* 72, 633-634.
- Beach, J.R., Schalm, O.W., 1936. A filterable virus, distinct from that of laryngotracheitis, the cause of respiratory disease of chicks. *Poultry Science* 15, 199-206.
- Beaudette, F., Hudson, C.B., 1937. Cultivation of the virus of infectious bronchitis. *J Am Vet Med Assoc* 90, 51-58.
- Beaudette, F.R., 1937. Infectious laryngotracheitis virus. *Poultry Science* 16, 103-105.
- Belouzard, S., Millet, J.K., Licitra, B.N., Whittaker, G.R., 2012. Mechanisms of coronavirus cell entry mediated by the viral spike protein. *Viruses* 4, 1011-1033.
- Ben-Porat, T., Tokazewski, S.A., 1977. Replication of herpesvirus DNA. II. Sedimentation characteristics of newly synthesized DNA. *Virology* 79, 292-301.
- Benyeda, Z., Mató, T., Süveges, T., Szabó, E., Kardi, V., Abonyi-Tóth, Z., Rusvai, M., Palya, V., 2009. Comparison of the pathogenicity of QX-like, M41 and 793/B infectious bronchitis strains from different pathological conditions. *Avian Pathol* 38, 449-456.

- Bhattacharjee, P.S., Carter, S.D., Savage, C.E., Jones, R.C., 1995. Re-excretion of infectious bronchitis virus in chickens induced by cyclosporin. *Avian Pathol* 24, 435-441.
- Bochkov, Y.A., Batchenko, G.V., Shcherbakova, L.O., Borisov, A.V., Drygin, V.V., 2006. Molecular epizootiology of avian infectious bronchitis in Russia. *Avian Pathol* 35, 379-393.
- Broadfoot, D.I., Pomeroy, B.S., Smith, W.M., Jr., 1954. Effect of infectious bronchitis on egg production. *J Am Vet Med Assoc* 124, 128-130.
- Brown, T.P., Glisson, J.R., Rosales, G., Villegas, P., Davis, R.B., 1987. Studies of avian urolithiasis associated with an infectious bronchitis virus. *Avian Dis* 31, 629-636.
- Casais, R., Dove, B., Cavanagh, D., Britton, P., 2003. Recombinant avian infectious bronchitis virus expressing a heterologous spike gene demonstrates that the spike protein is a determinant of cell tropism. *J Virol* 77, 9084-9089.
- Cavanagh, D., 2005. Coronaviruses in poultry and other birds. *Avian Pathol* 34, 439-448.
- Cavanagh, D., 2007. Coronavirus avian infectious bronchitis virus. *Vet Res* 38, 281-297.
- Cavanagh, D., Davis, P.J., Cook, J.K., 1992. Infectious bronchitis virus: evidence for recombination within the Massachusetts serotype. *Avian Pathol* 21, 401-408.
- Cavanagh, D., Naqi, S.A., 2003. *Infectious Bronchitis*, Vol 11, 11 Edition. Iowa state press, Ames, Iowa.
- Chen, B.Y., Hosi, S., Nunoya, T., Itakura, C., 1996. Histopathology and immunohistochemistry of renal lesions due to infectious bronchitis virus in chicks. *Avian Pathol* 25, 269-283.
- Chong, K.T., Apostolov, K., 1982. The pathogenesis of nephritis in chickens induced by infectious bronchitis virus. *J Comp Pathol* 92, 199-211.
- Cook, J.K., 1971. Recovery of infectious bronchitis virus from eggs and chicks produced by experimentally inoculated hens. *J Comp Pathol* 81, 203-211.
- Cook, J.K., 1983. Isolation of a new serotype of infectious bronchitis-like virus from chickens in England. *Vet Rec* 112, 104-105.
- Cook, J.K., 1984. The classification of new serotypes of infectious bronchitis virus isolated from poultry flocks in Britain between 1981 and 1983. *Avian Pathol* 13, 733-741.
- Cook, J.K., Jackwood, M., Jones, R.C., 2012. The long view: 40 years of infectious bronchitis research. *Avian Pathol* 41, 239-250.

- Cover, S.M., 1996. The early history of infectious laryngotracheitis virus. *Avian Dis* 40, 494-500.
- Crawshaw, G.J., Boycott, B.R., 1982. Infectious laryngotracheitis in peafowl and pheasants. *Avian Dis* 26, 397-401.
- Cui, J., Eden, J.S., Holmes, E.C., Wang, L.F., 2013. Adaptive evolution of bat dipeptidyl peptidase 4 (dpp4): implications for the origin and emergence of Middle East respiratory syndrome coronavirus. *Virology* 10, 304.
- Davison, A.J., 2010. Herpesvirus systematics. *Vet Microbiol* 143, 52-69.
- Davison, A.J., Eberle, R., Ehlers, B., Hayward, G.S., McGeoch, D.J., Minson, A.C., Pellett, P.E., Roizman, B., Studdert, M.J., Thiry, E., 2009. The order Herpesvirales. *Arch Virol* 154, 171-177.
- de Haan, C.A., Rottier, P.J., 2005. Molecular interactions in the assembly of coronaviruses. *Adv Virus Res* 64, 165-230.
- De Wit, J.J., Brandao, P., Torres, C.A., Koopman, R., Villarreal, L.Y., 2015. Increased level of protection of respiratory tract and kidney by combining different infectious bronchitis virus vaccines against challenge with nephropathogenic Brazilian genotype subcluster 4 strains. *Avian Pathol* 44, 352-357.
- de Wit, J.J., Nieuwenhuisen-van Wilgen, J., Hoogkamer, A., van de Sande, H., Zuidam, G.J., Fabri, T.H., 2011. Induction of cystic oviducts and protection against early challenge with infectious bronchitis virus serotype D388 (genotype QX) by maternally derived antibodies and by early vaccination. *Avian Pathol* 40, 463-471.
- Drexler, J.F., Corman, V.M., Drosten, C., 2014. Ecology, evolution and classification of bat coronaviruses in the aftermath of SARS. *Antiviral Res* 101, 45-56.
- Ducatez, M.F., Martin, A.M., Owoade, A.A., Olatoye, I.O., Alkali, B.R., Maikano, I., Snoeck, C.J., Sausy, A., Cordioli, P., Muller, C.P., 2009. Characterization of a new genotype and serotype of infectious bronchitis virus in Western Africa. *J Gen Virol* 90, 2679-2685.
- Eisenberg, R.J., Atanasiu, D., Cairns, T.M., Gallagher, J.R., Krummenacher, C., Cohen, G.H., 2012. Herpes virus fusion and entry: a story with many characters. *Viruses* 4, 800-832.
- El-Houadfi, M., Jones, R.C., Cook, J.K., Ambali, A.G., 1986. The isolation and characterisation of six avian infectious bronchitis viruses isolated in Morocco. *Avian Pathol* 15, 93-105.
- Fabricant, J., 1998. The early history of infectious bronchitis. *Avian Dis* 42, 648-650.
- Farquharson, J., 1946. Malignant catarrhal fever. *Br Vet J* 102, 127-130.

- Fehr, A.R., Perlman, S., 2015. Coronaviruses: an overview of their replication and pathogenesis. *Methods Mol Biol* 1282, 1-23.
- Fuchs, W., Veits, J., Helferich, D., Granzow, H., Teifke, J.P., Mettenleiter, T.C., 2007. Molecular biology of avian infectious laryngotracheitis virus. *Vet Res* 38, 261-279.
- Fuchs, W., Ziemann, K., Teifke, J.P., Werner, O., Mettenleiter, T.C., 2000. The non-essential UL50 gene of avian infectious laryngotracheitis virus encodes a functional dUTPase which is not a virulence factor. *J Gen Virol* 81, 627-638.
- Gailbreath, K.L., Oaks, J.L., 2008. Herpesviral inclusion body disease in owls and falcons is caused by the pigeon herpesvirus (columbid herpesvirus 1). *J Wildl Dis* 44, 427-433.
- Gallardo, R.A., Hoerr, F.J., Berry, W.D., van Santen, V.L., Toro, H., 2011. Infectious bronchitis virus in testicles and venereal transmission. *Avian Dis* 55, 255-258.
- Garcia, M., Spatz, S., Guy, J.S., 2013. *Laryngotracheitis*, Vol 13. Ames: Blackwell, 161-179 pp.
- Gennart, I., Coupeau, D., Pejakovic, S., Laurent, S., Rasschaert, D., Muylkens, B., 2015. Marek's disease: Genetic regulation of gallid herpesvirus 2 infection and latency. *Vet J* 205, 339-348.
- Gorbalenya, A.E., Enjuanes, L., Ziebuhr, J., Snijder, E.J., 2006. Nidovirales: evolving the largest RNA virus genome. *Virus Res* 117, 17-37.
- Granzow, H., Klupp, B.G., Fuchs, W., Veits, J., Osterrieder, N., Mettenleiter, T.C., 2001. Egress of alphaherpesviruses: comparative ultrastructural study. *J Virol* 75, 3675-3684.
- Guo, P., Scholz, E., Turek, J., Nodgreen, R., Maloney, B., 1993. Assembly pathway of avian infectious laryngotracheitis virus. *Am J Vet Res* 54, 2031-2039.
- Guo, Y., Shen, C., Cheng, A., Wang, M., Zhang, N., Chen, S., Zhou, Y., 2009. Anatid herpesvirus 1 CH virulent strain induces syncytium and apoptosis in duck embryo fibroblast cultures. *Vet Microbiol* 138, 258-265.
- Guy, J.S., Bagust, T.J., 2003. *Diseases of Poultry*, Vol 11 Ames: Blackwell.
- Hewson, K.A., Robertson, T., Steer, P.A., Devlin, J.M., Noormohammadi, A.H., Ignjatovic, J., 2014. Assessment of the potential relationship between egg quality and infectious bronchitis virus infection in Australian layer flocks. *Aust Vet J* 92, 132-138.
- Honess, R.W., Roizman, B., 1974. Regulation of herpesvirus macromolecular synthesis. I. Cascade regulation of the synthesis of three groups of viral proteins. *J Virol* 14, 8-19.
- Hopkins, S.R., 1974. Serological comparisons of strains of infectious bronchitis virus using plaque-purified isolants. *Avian Dis* 18, 231-239.

- Horner, R.F., Parker, M.E., Abrey, A.N., Kaleta, E.F., Prozesky, L., 1992. Isolation and identification of psittacid herpesvirus 1 from imported psittacines in South Africa. *J S Afr Vet Assoc* 63, 59-62.
- Hunt, H.D., Dunn, J.R., 2015. The Influence of Major Histocompatibility Complex and Vaccination with Turkey Herpesvirus on Marek's Disease Virus Evolution. *Avian Dis* 59, 122-129.
- Hurst, K.R., Ye, R., Goebel, S.J., Jayaraman, P., Masters, P.S., 2010. An interaction between the nucleocapsid protein and a component of the replicase-transcriptase complex is crucial for the infectivity of coronavirus genomic RNA. *J Virol* 84, 10276-10288.
- Ignjatovic, J., Sapats, S., 2000. Avian infectious bronchitis virus. *Rev Sci Tech* 19, 493-508.
- Jackwood, M.W., 2012. Review of infectious bronchitis virus around the world. *Avian Dis* 56, 634-641.
- Jackwood, M.W., de Wit, J.J., 2013. *Diseases of Poultry*. Blackwell Publishing Professional, Ames, IA.
- Janse, E.M., van Roozelaar, D., Koch, G., 1994. Leukocyte subpopulations in kidney and trachea of chickens infected with infectious bronchitis virus. *Avian Pathol* 23, 513-523.
- Jones, R.C., Ambali, A.G., 1987. Re-excretion of an enterotropic infectious bronchitis virus by hens at point of lay after experimental infection at day old. *Vet Rec* 120, 617-618.
- Jones, R.C., Jordan, F.T., 1971. The site of replication of infectious bronchitis virus in the oviduct of experimentally infected hens. *Vet Rec* 89, 317-318.
- Jungherr, E.L., Chomiak, T.W., Luginbuhl, R.E. 1956. Immunologic differences in strains of infectious bronchitis virus. In *In Proceedings of 60th Annual Meeting of the United States Livestock Sanitary Association (Chicago, IL, USA)*, 203-209.
- Kingsley, D.H., Hazel, J.W., Keeler, C.L., Jr., 1994. Identification and characterization of the infectious laryngotracheitis virus glycoprotein C gene. *Virology* 203, 336-343.
- Kingsley, D.H., Keeler, C.L., Jr., 1999. Infectious laryngotracheitis virus, an alpha herpesvirus that does not interact with cell surface heparan sulfate. *Virology* 256, 213-219.
- Krapež, U., Slavec, B., Barlič-Maganja, D., Rojs, O.Z., 2010. Molecular analysis of infectious bronchitis viruses isolated in Slovenia between 1990 and 2005: a retrospective study. *Virus Genes* 41, 414-416.
- Krijnse-Locker, J., Ericsson, M., Rottier, P.J., Griffiths, G., 1994. Characterization of the budding compartment of mouse hepatitis virus: evidence that transport

- from the RER to the Golgi complex requires only one vesicular transport step. *J Cell Biol* 124, 55-70.
- Lambrechts, C., Pensaert, M., Ducatelle, R., 1993. Challenge experiments to evaluate cross-protection induced at the trachea and kidney level by vaccine strains and Belgian nephropathogenic isolates of avian infectious bronchitis virus. *Avian Pathol* 22, 577-590.
- Li, W., Moore, M.J., Vasilieva, N., Sui, J., Wong, S.K., Berne, M.A., Somasundaran, M., Sullivan, J.L., Luzuriaga, K., Greenough, T.C., Choe, H., Farzan, M., 2003. Angiotensin-converting enzyme 2 is a functional receptor for the SARS coronavirus. *Nature* 426, 450-454.
- Lim, T.H., Lee, H.J., Lee, D.H., Lee, Y.N., Park, J.K., Youn, H.N., Kim, M.S., Lee, J.B., Park, S.Y., Choi, I.S., Song, C.S., 2011. An emerging recombinant cluster of nephropathogenic strains of avian infectious bronchitis virus in Korea. *Infect Genet Evol* 11, 678-685.
- Liu, P., Li, L., Millership, J.J., Kang, H., Leibowitz, J.L., Giedroc, D.P., 2007. A U-turn motif-containing stem-loop in the coronavirus 5' untranslated region plays a functional role in replication. *RNA* 13, 763-780.
- Liu, S., Kong, X., 2004. A new genotype of nephropathogenic infectious bronchitis virus circulating in vaccinated and non-vaccinated flocks in China. *Avian Pathol* 33, 321-327.
- Lucio, B., Fabricant, J., 1990. Tissue tropism of three cloacal isolates and Massachusetts strain of infectious bronchitis virus. *Avian Dis* 34, 865-870.
- Luppi, M.M., Luiz, A.P., Coelho, F.M., Ecco, R., da Fonseca, F.G., Resende, M., 2016. Genotypic characterization of psittacid herpesvirus isolates from Brazil. *Braz J Microbiol* 47, 217-224.
- Mahmood, Z.H., Sleman, R.R., Uthman, A.U., 2011. Isolation and molecular characterization of Sul/01/09 avian infectious bronchitis virus, indicates the emergence of a new genotype in the Middle East. *Vet Microbiol* 150, 21-27.
- Mahmoudian, A., Markham, P.F., Noormohammadi, A.H., Browning, G.F., 2012. Kinetics of transcription of infectious laryngotracheitis virus genes. *Comp Immunol Microbiol Infect Dis* 35, 103-115.
- Mahony, T.J., Hall, R.N., Walkden-Brown, S., Meers, J., Gravel, J.L., West, L., Hardy, V., Islam, A.F., Fowler, E.V., Mitter, N., 2015. Genomic deletions and mutations resulting in the loss of eight genes reduce the in vivo replication capacity of Meleagrid herpesvirus 1. *Virus Genes* 51, 85-95.
- Maiti, N.K., Sharma, S.N., Sambyal, D.S., 1985. Isolation of infectious bronchitis virus from intestine and reproductive organs of laying hens with dropped egg production. *Avian Dis* 29, 509-513.
- May, H.G., Tittsler, R.P., 1925. Tracheolaryngitis in poultry. *J Am Vet Med Assoc* 67, 229-231.

- McBride, R., van Zyl, M., Fielding, B.C., 2014. The coronavirus nucleocapsid is a multifunctional protein. *Viruses* 6, 2991-3018.
- Meir, R., Rosenblut, E., Perl, S., Kass, N., Ayali, G., Perk, S., Hemsani, E., 2004. Identification of a novel nephropathogenic infectious bronchitis virus in Israel. *Avian Dis* 48, 635-641.
- Menendez, K.R., Garcia, M., Spatz, S., Tablante, N.L., 2014. Molecular epidemiology of infectious laryngotracheitis: a review. *Avian Pathol* 43, 108-117.
- Mettenleiter, T.C., 2002. Herpesvirus assembly and egress. *J Virol* 76, 1537-1547.
- Mettenleiter, T.C., Klupp, B.G., Granzow, H., 2006. Herpesvirus assembly: a tale of two membranes. *Curr Opin Microbiol* 9, 423-429.
- Mettenleiter, T.C., Klupp, B.G., Granzow, H., 2009. Herpesvirus assembly: an update. *Virus Res* 143, 222-234.
- Mettenleiter, T.C., Minson, T., 2006. Egress of alphaherpesviruses. *J Virol* 80, 1610-1611; author reply 1611-1612.
- Meulemans, G., Carlier, M.C., Gonze, M., Petit, P., Vandebroek, M., 1987. Incidence, characterisation and prophylaxis of nephropathogenic avian infectious bronchitis viruses. *Vet Rec* 120, 205-206.
- Mielech, A.M., Chen, Y., Mesecar, A.D., Baker, S.C., 2014. Nidovirus papain-like proteases: multifunctional enzymes with protease, deubiquitinating and deISGylating activities. *Virus Res* 194, 184-190.
- Mork, A.K., Hesse, M., Abd El Rahman, S., Rautenschlein, S., Herrler, G., Winter, C., 2014. Differences in the tissue tropism to chicken oviduct epithelial cells between avian coronavirus IBV strains QX and B1648 are not related to the sialic acid binding properties of their spike proteins. *Vet Res* 45, 67.
- Nakamura, K., Cook, J.K., Otsuki, K., Huggins, M.B., Frazier, J.A., 1991. Comparative study of respiratory lesions in two chicken lines of different susceptibility infected with infectious bronchitis virus: histology, ultrastructure and immunohistochemistry. *Avian Pathol* 20, 241-257.
- Nakamura, K., Imai, K., Tanimura, N., 1996. Comparison of the effects of infectious bronchitis and infectious laryngotracheitis on the chicken respiratory tract. *J Comp Pathol* 114, 11-21.
- Nauwynck, H., Pensaert, M. 1988. Studies on the pathogenesis of infections with a nephropathogenic variant of infectious bronchitis virus in chickens. In: 1st International Symposium on Infectious Bronchitis, Raischholzhausen, Germany, 113-119.
- Nicoll, M.P., Proenca, J.T., Efstathiou, S., 2012. The molecular basis of herpes simplex virus latency. *FEMS Microbiol Rev* 36, 684-705.

- Nieto-Torres, J.L., DeDiego, M.L., Verdia-Baguena, C., Jimenez-Guardeno, J.M., Regla-Nava, J.A., Fernandez-Delgado, R., Castano-Rodriguez, C., Alcaraz, A., Torres, J., Aguilera, V.M., Enjuanes, L., 2014. Severe acute respiratory syndrome coronavirus envelope protein ion channel activity promotes virus fitness and pathogenesis. *PLoS Pathog* 10, e1004077.
- O'Connor, C.M., Kedes, D.H., 2007. Rhesus monkey rhadinovirus: a model for the study of KSHV. *Curr Top Microbiol Immunol* 312, 43-69.
- Otsuki, K., Huggins, M.B., Cook, J.K., 1990. Comparison of the susceptibility to avian infectious bronchitis virus infection of two inbred lines of white leghorn chickens. *Avian Pathol* 19, 467-475.
- Owen, R.L., Cowen, B.S., Hattel, A.L., Naqi, S.A., Wilson, R.A., 1991. Detection of viral antigen following exposure of one-day-old chickens to the Holland 52 strain of infectious bronchitis virus. *Avian Pathol* 20, 663-673.
- Pavlova, S.P., Veits, J., Blohm, U., Maresch, C., Mettenleiter, T.C., Fuchs, W., 2010. In vitro and in vivo characterization of glycoprotein C-deleted infectious laryngotracheitis virus. *J Gen Virol* 91, 847-857.
- Pensaert, M., Lambrechts, C., 1994. Vaccination of chickens against a Belgian nephropathogenic strain of infectious bronchitis virus B1648 using attenuated homologous and heterologous strains. *Avian Pathol* 23, 631-641.
- Pensaert, M.B., Debouck, P., Reynolds, D.J., 1981. An immunoelectron microscopic and immunofluorescent study on the antigenic relationship between the coronavirus-like agent, CV 777, and several coronaviruses. *Arch Virol* 68, 45-52.
- Petherbridge, L., Xu, H., Zhao, Y., Smith, L.P., Simpson, J., Baigent, S., Nair, V., 2009. Cloning of Gallid herpesvirus 3 (Marek's disease virus serotype-2) genome as infectious bacterial artificial chromosomes for analysis of viral gene functions. *J Virol Methods* 158, 11-17.
- Portz, C., Beltrao, N., Furian, T.Q., Junior, A.B., Macagnan, M., Griebeler, J., Lima Rosa, C.A., Colodel, E.M., Driemeier, D., Back, A., Barth Schatzmayr, O.M., Canal, C.W., 2008. Natural infection of turkeys by infectious laryngotracheitis virus. *Vet Microbiol* 131, 57-64.
- Prideaux, C.T., Kongsuwan, K., Johnson, M.A., Sheppard, M., Fahey, K.J., 1992. Infectious laryngotracheitis virus growth, DNA replication, and protein synthesis. *Arch Virol* 123, 181-192.
- Rachamadugu, R., Lee, J.Y., Wooming, A., Kong, B.W., 2009. Identification and expression analysis of infectious laryngotracheitis virus encoding microRNAs. *Virus Genes* 39, 301-308.
- Raj, G.D., Jones, R.C., 1996. Immunopathogenesis of infection in SPF chicks and commercial broiler chickens of a variant infectious bronchitis virus of economic importance. *Avian Pathol* 25, 481-501.

- Raj, G.D., Jones, R.C., 1997a. Effect of T-cell suppression by cyclosporin on primary and persistent infections of infectious bronchitis virus in chickens. *Avian Pathol* 26, 257-276.
- Raj, G.D., Jones, R.C., 1997b. Infectious bronchitis virus: Immunopathogenesis of infection in the chicken. *Avian Pathol* 26, 677-706.
- Ricer, L., 2015. Malignant catarrhal fever in a Red Angus cow. *Can Vet J* 56, 83-85.
- Robertson, G.M., Egerton, J.R., 1981. Replication of infectious laryngotracheitis virus in chickens following vaccination. *Aust Vet J* 57, 119-123.
- Roizman, B., Baines, J., 1991. The diversity and unity of Herpesviridae. *Comp Immunol Microbiol Infect Dis* 14, 63-79.
- Roizman, B., Taddeo, B. 2007. The strategy of herpes simplex virus replication and takeover of the host cell, In: Arvin, A., Campadelli-Fiume, G., Mocarski, E., Moore, P.S., Roizman, B., Whitley, R., Yamanishi, K. (Eds.) *Human Herpesviruses: Biology, Therapy, and Immunoprophylaxis*. Cambridge.
- Roy, P., Fakhrul Islam, A.F., Burgess, S.K., Hunt, P.W., McNally, J., Walkden-Brown, S.W., 2015. Real-time PCR quantification of infectious laryngotracheitis virus in chicken tissues, faeces, isolator-dust and bedding material over 28 days following infection reveals high levels in faeces and dust. *J Gen Virol* 96, 3338-3347.
- Ruch, T.R., Machamer, C.E., 2012. The coronavirus E protein: assembly and beyond. *Viruses* 4, 363-382.
- Schalk, A.F., Hawn, M.C., 1931. An apparent new respiratory disease of chicks. *J Am Vet Med Assoc* 78, 413-422.
- Seger, W., GhalyanchiLangeroudi, A., Karimi, V., Madadgar, O., Marandi, M.V., Hashemzadeh, M., 2016. Genotyping of infectious bronchitis viruses from broiler farms in Iraq during 2014-2015. *Arch Virol* 161, 1229-1237.
- Skepper, J.N., Whiteley, A., Browne, H., Minson, A., 2001. Herpes simplex virus nucleocapsids mature to progeny virions by an envelopment --> deenvelopment --> reenvelopment pathway. *J Virol* 75, 5697-5702.
- Thiry, E., Meurens, F., Muylkens, B., McVoy, M., Gogev, S., Thiry, J., Vanderplasschen, A., Epstein, A., Keil, G., Schynts, F., 2005. Recombination in alphaherpesviruses. *Rev Med Virol* 15, 89-103.
- Thureen, D.R., Keeler, C.L., Jr., 2006. Psittacid herpesvirus 1 and infectious laryngotracheitis virus: Comparative genome sequence analysis of two avian alphaherpesviruses. *J Virol* 80, 7863-7872.
- Toffan, A., Bonci, M., Bano, L., Bano, L., Valastro, V., Vascellari, M., Capua, I., Terregino, C., 2013a. Diagnostic and clinical observation on the infectious bronchitis virus strain Q1 in Italy. *Vet Ital* 49, 347-355.

- Toffan, A., Bonci, M., Bano, L., Valastro, V., Vascellari, M., Capua, I., Terregino, C., 2013b. Diagnostic and clinical observation on the infectious bronchitis virus strain Q1 in Italy. *Vet Ital* 49, 347-355.
- Tooze, J., Tooze, S., Warren, G., 1984. Replication of coronavirus MHV-A59 in sac-cells: determination of the first site of budding of progeny virions. *Eur J Cell Biol* 33, 281-293.
- van Hemert, M.J., van den Worm, S.H., Knoops, K., Mommaas, A.M., Gorbalenya, A.E., Snijder, E.J., 2008. SARS-coronavirus replication/transcription complexes are membrane-protected and need a host factor for activity in vitro. *PLoS Pathog* 4, e1000054.
- Van Roeckel, H., Bullis, K.L., Flint, O.S., Clarke, M.K. 1942. Poultry disease control service (Masachusetts Agricultural Experiment Station Poultry disease control service), 99-103.
- Veits, J., Mettenleiter, T.C., Fuchs, W., 2003. Five unique open reading frames of infectious laryngotracheitis virus are expressed during infection but are dispensable for virus replication in cell culture. *J Gen Virol* 84, 1415-1425.
- Vennema, H., Godeke, G.J., Rossen, J.W., Voorhout, W.F., Horzinek, M.C., Opstelten, D.J., Rottier, P.J., 1996. Nucleocapsid-independent assembly of coronavirus-like particles by co-expression of viral envelope protein genes. *EMBO J* 15, 2020-2028.
- Villarreal, L.Y., Brandao, P.E., Chacon, J.L., Assayag, M.S., Maiorka, P.C., Raffi, P., Saidenberg, A.B., Jones, R.C., Ferreira, A.J., 2007. Orchitis in roosters with reduced fertility associated with avian infectious bronchitis virus and avian metapneumovirus infections. *Avian Dis* 51, 900-904.
- Weiss, S.R., Navas-Martin, S., 2005. Coronavirus pathogenesis and the emerging pathogen severe acute respiratory syndrome coronavirus. *Microbiol Mol Biol Rev* 69, 635-664.
- Williams, R.K., Jiang, G.S., Holmes, K.V., 1991. Receptor for mouse hepatitis virus is a member of the carcinoembryonic antigen family of glycoproteins. *Proc Natl Acad Sci U S A* 88, 5533-5536.
- Winter, C., Schwegmann-Wessels, C., Cavanagh, D., Neumann, U., Herrler, G., 2006. Sialic acid is a receptor determinant for infection of cells by avian Infectious bronchitis virus. *J Gen Virol* 87, 1209-1216.
- Woo, P.C., Lau, S.K., Lam, C.S., Lau, C.C., Tsang, A.K., Lau, J.H., Bai, R., Teng, J.L., Tsang, C.C., Wang, M., Zheng, B.J., Chan, K.H., Yuen, K.Y., 2012. Discovery of seven novel Mammalian and avian coronaviruses in the genus deltacoronavirus supports bat coronaviruses as the gene source of alphacoronavirus and betacoronavirus and avian coronaviruses as the gene source of gammacoronavirus and deltacoronavirus. *J Virol* 86, 3995-4008.

- Wozniakowski, G.J., Samorek-Salamonowicz, E., Szymanski, P., Wencel, P., Houszka, M., 2013. Phylogenetic analysis of Columbid herpesvirus-1 in rock pigeons, birds of prey and non-raptorial birds in Poland. *BMC Vet Res* 9, 52.
- Zaichick, S.V., Bohannon, K.P., Smith, G.A., 2011. Alphaherpesviruses and the cytoskeleton in neuronal infections. *Viruses* 3, 941-981.
- Zanaty, A., Arafa, A.S., Hagag, N., El-Kady, M., 2016. Genotyping and pathotyping of diversified strains of infectious bronchitis viruses circulating in Egypt. *World J Virol* 5, 125-134.
- Zhao, Y., Kong, C., Cui, X., Cui, H., Shi, X., Zhang, X., Hu, S., Hao, L., Wang, Y., 2013. Detection of infectious laryngotracheitis virus by real-time PCR in naturally and experimentally infected chickens. *PLoS One* 8, e67598.
- Ziak, J., Koptidesova, D., Oveckova, I., Rejholcova, O., Kopacek, J., Kudelova, M., Zelnik, V., 2014. Ovine herpesvirus 1 (OVHV-1) thymidine kinase locus sequence analysis: evidence that OVHV-1 belongs to the Macavirus genus of the Gammaherpesvirinae subfamily. *Acta Virol* 58, 190-193.
- Ziebuhr, J., Snijder, E.J., Gorbalenya, A.E., 2000. Virus-encoded proteinases and proteolytic processing in the Nidovirales. *J Gen Virol* 81, 853-879.
- Ziegler, A.F., Ladman, B.S., Dunn, P.A., Schneider, A., Davison, S., Miller, P.G., Lu, H., Weinstock, D., Salem, M., Eckroade, R.J., Gelb, J., Jr., 2002. Nephropathogenic infectious bronchitis in Pennsylvania chickens 1997-2000. *Avian Dis* 46, 847-858.

CHAPTER 2.

AIMS

Avian respiratory viruses are an important cause of economic losses to the worldwide poultry industry. The main losses are due to decreased egg production and quality, reduced growth and mortality. The use of diagnostics, vaccines and antimicrobials to diagnose, prevent and treat secondary infections are other ancillary factors that cause additional losses. Infectious laryngotracheitis virus (ILT) and infectious bronchitis virus (IBV) are economically the most important avian respiratory viruses. In general, ILT and IBV show tropism primarily to the epithelium of the respiratory mucosa. However, the ILT and IBV clinical features are different and evolved completely into different directions. Hence, in this thesis, the pathogenesis of ILT and IBV were examined under *in vitro* and *in vivo* conditions, to elucidate the reasons for the differences in their clinical features.

Infectious laryngotracheitis virus

ILT enters chickens through respiratory and ocular routes. After entry, initial virus replication takes place in the respiratory and conjunctival epithelial cells. Then, ILT invades through the basement membrane (BM) to disseminate in the underlying lamina propria. However, the exact replication kinetics and invasion strategies of ILT at the primary replication site are not well understood. In order to get an answer to this question *in vitro* tracheal and conjunctival mucosa explant models of chickens were established (**Chapter 3.1**).

During acute ILT infection, the formation of mucoid plugs/casts in the trachea is the main cause for suffocation and mortality of chickens. Although it has been supposed that the trachea obstruction is due to mucus hypersecretion, there are no published reports to support this assumption. This lacuna will be addressed in **Chapter 3.2**.

Infectious bronchitis virus

Massachusetts (Mass) type IBV (prototype: M41) is a well-known respiratory IBV strain. Some IBV strains are nephropathogenic (NIBV), i.e. they cause additionally severe kidney infection. The virulent NIBV infection is characterized by wet droppings, increased water consumption, loss of body weight gain and increased mortality. In the last 15 years, diverse new variants of NIBV emerged as predominant IBV strains.

The NIBV strain B1648 was first isolated in 1984, in Flanders, Belgium. Despite intensive vaccination, B1648 and its variants are still circulating in Europe and North Africa.

In the present thesis the complete genome of Belgian nephropathogenic IBV reference strain was identified to understand its evolutionary relationship with other IBV strains, and to determine possible genetic factors that may be associated with the nephropathogenic nature of this strain (**Chapter 4.1.**). Further, it is unknown why NIBV has a strong tropism for the kidneys. This was addressed in **Chapter 4.2.**

CHAPTER 3.

Study of infectious laryngotracheitis virus (ILTV) replication characteristics

CHAPTER 3.1.

The replication characteristics of infectious laryngotracheitis virus (ILTV) in the respiratory and conjunctival mucosa

Vishwanatha R.A.P. Reddy, Lennert Steukers, Yewei Li, Walter Fuchs, Alain
Vanderplasschen and Hans J. Nauwynck

Avian Pathology (2014), 43 (5): 450-7

3.1.1. Abstract

Avian infectious laryngotracheitis virus (ILTV) is an alphaherpesvirus of poultry that is spread worldwide. ILTV enters its host via respiratory tract and eyes. Although it is known for a long time, the replication characteristics of ILTV in the respiratory and conjunctival mucosa are still poorly studied. To study the replication characteristics of ILTV in chicken tracheal and conjunctival mucosa, two *in vitro* explant models were developed. Light microscopy and a fluorescent terminal deoxynucleotidyl transferase mediated dUTP nick end labeling (TUNEL) staining were used to evaluate the viability of mucosal explants. The mucosal explants were viable up to the end of the experiment at 96h of cultivation. The tracheal and conjunctival mucosal explants were inoculated with ILTV and collected at 0, 24, 48 and 72h post inoculation (pi). ILTV spread in a plaquewise manner in both mucosae. A reproducible quantitative analysis of this mucosal spread was evaluated by measuring plaque numbers, plaque latitude and invasion depth underneath the basement membrane (BM). No major differences in the plaque numbers were observed over time. Plaque latitude progressively increased over time up to $70.4 \pm 12.9 \mu\text{m}$ in trachea and $97.8 \pm 9.5 \mu\text{m}$ in conjunctiva at 72h pi. The virus had difficulties to cross the BM. Only from 48h pi BM crossing was found and at 72h pi it was observed in 56% (trachea) and 74% (conjunctiva) of the plaques. Viability analysis of infected explants indicated that ILTV blocks apoptosis in infected cells of both mucosae but activates apoptosis in bystander cells.

3.1.2. Introduction

Infectious laryngotracheitis virus (ILTV) is an avian herpesvirus, classified within the order *Herpesvirales*, family *Herpesviridae*, subfamily *Alphaherpesvirinae* and genus *Iltovirus*. ILTV is taxonomically designated as *Gallid herpesvirus 1* (GaHV1) (Davison, 2010). ILTV is a contagious respiratory virus of chickens with an active cytolytic replication that takes place in the epithelium of trachea, larynx and conjunctiva, which may lead to severe mucosal epithelial damage and hemorrhages. These pathological changes lead to “infectious laryngotracheitis” (ILT) (Bang and Bang, 1967; Guy and Bagust, 2003). During ILTV infection, it is not clear if a viremia occurs (Bagust, 1986; Guy and Bagust, 2003; Zhao *et al.*, 2013). After an acute phase of infection, ILTV, like other alphaherpesviruses, establishes a lifelong latency within the trigeminal ganglion of the central nervous system (CNS). During

stress, reactivation of the virus may occur, leading to the spread of ILTV to susceptible contact animals (Fuchs *et al.*, 2007). The characteristic clinical signs of ILT during a mild form are nasal discharge, conjunctivitis and drop in egg production. During a severe form, additional signs are gasping, bloody mucus expectoration, dyspnea and death due to asphyxia (Fuchs *et al.*, 2007). ILT has an economic impact by causing severe production losses due to a high morbidity and mortality and by mass vaccination (Jones, 2010).

ILTV enters its host via respiratory and ocular routes. After its entry, initial virus replication takes place in the epithelium of the respiratory and conjunctival mucosa (Guy and Bagust, 2003). Afterwards, ILTV may invade through the basement membrane (BM). During evolution of all animal species, most alphaherpesviruses have acquired intriguing tools to invade through the BM of the mucosa and to disseminate in the underlying lamina propria (Glorieux *et al.*, 2009; Steukers *et al.*, 2012). The precise replication characteristics and invasion mechanism of ILTV at the primary replication site, i.e. in the respiratory and conjunctival mucosa are unknown.

Replication characteristics of ILTV in the respiratory and conjunctival mucosa may be investigated by performing animal experiments (Bang and Bang, 1967; Kirkpatrick *et al.*, 2006). However, *in vivo* studies are more and more contested due to ethical reasons. Furthermore, animal experiments are prone to large inter-animal variation. Hence, a fully standardized *in vitro* model, which mimics the *in vivo* situation, is useful to study host-virus interactions during the early stages of infection.

The tracheal organ culture (TOC) system is commonly used to study host-pathogen interactions (Reemers *et al.*, 2009). Generally, tracheal rings from chicks or 19-day-old chicken embryos are used for tracheal organ cultures (Jones and Hennion, 2008; Zhang *et al.*, 2012). TOC has already been used for a long time for diagnosis and pathogenesis studies of ILTV (Bagust, 1986; Ide, 1978). The viability of TOCs has generally been analysed by two methods: one based on the ciliary beating and another based on the ciliary removal of latex beads (Anderton *et al.*, 2004). However, these two methods evaluate only the epithelium viability and do not control the viability of the lamina propria of the tracheal mucosa and the underlying submucosa. The chicken conjunctival organ culture (COC) has also been used to study host-virus interactions (Darbyshire *et al.*, 1976) but viability analysis was not performed. To study

replication characteristics and invasion mechanism of ILTV through the BM towards the lamina propria and the underlying submucosa, it is crucial to keep these layers viable.

The aims of the present study were (i) to evaluate quantitatively the replication characteristics of ILTV in *in vitro* models of chicken tracheal and conjunctival mucosa explants and (ii) to analyse cell viability of infected mucosal explants. Hence, an *in vitro* tracheal and conjunctival organ cultures were established. The tracheal and conjunctival mucosa explants (organs) were placed on fine-meshed gauze and maintained for 96h at an air-liquid interface. A viability analysis was performed using light microscopy (ciliary beating) and fluorescence microscopy (TUNEL-positive cells). The mucosal explants were inoculated with ILTV. ILTV replication kinetics was quantitatively evaluated by measuring plaque number, plaque latitude and invasion depth underneath the BM in tracheal and conjunctival mucosa explants (organs). A viability analysis of infected mucosal explants was performed to examine the outcome of an ILTV infection in these mucosae.

3.1.3. Materials and Methods

3.1.3.1. Virus

A pathogenic Belgian isolate of ILTV (U76/1035) was used in this study (Meulemans and Halen, 1978). Stock virus was propagated in primary chicken embryo kidney cells that were collected from 19-day-old embryonated specific pathogen free (SPF) eggs by trypsin digestion. Cells were grown in minimum essential medium (Gibco) supplemented with 2% fetal calf serum (Gibco). Virus titration was performed on the chorioallantoic membrane of 10-day-old chicken embryos to determine EID₅₀/ml. The ILTV strain obtained was from unknown passages. From which a second passage was produced and utilized for inoculation of explants.

3.1.3.2. Isolation and cultivation of chicken tracheal and conjunctival explants

This study was in agreement with the guidelines of the Local Ethical and Animal Welfare Committee of the Faculty of Veterinary Medicine of Ghent University. SPF chickens were euthanized by intravenous injection of sodium pentobarbital (100 mg/kg body weight) in the brachial wing vein. Tracheas and conjunctivas were

collected from three four to eight week old chickens. Tracheas were carefully split into two equal halves with sharp surgical blades (Swann-Morton). Conjunctival mucosa folds were carefully dissected from the underlying layers. Tracheal and conjunctival mucosal explants covering a total area of 10 mm² were made and placed on fine-meshed gauze in six-well culture plates (Nunc), epithelium upwards. The explants were maintained in serum-free medium (50% Ham's F12 (Gibco)/50% DMEM (Gibco)) supplemented with 100 U/mL penicillin (Continental Pharma), 0.1 mg/mL streptomycin (Certa), 1 µg/mL gentamycin (Gibco) and 25 mM HEPES (Gibco). The epithelium of the explants was slightly immersed in the fluid to achieve an air liquid interface, i.e. with just a thin film of fluid covering the epithelium. During the entire cultivation period, medium was not replaced. Explants were maintained up to 96 hours at 37°C and 5% CO₂.

3.1.3.3. Ciliary beating

Ciliary beating of the tracheal explants was checked on a daily basis with a light microscope (Olympus CKX 31) at objective magnification x20.

3.1.3.4. Viability analysis by TUNEL assay

A viability analysis was performed in three independent experiments. Tracheal and conjunctival mucosa explants were collected at 0, 24, 48, 72 and 96h of *in vitro* cultivation. The In Situ Cell Death Detection Kit (Fluorescein) based on terminal deoxynucleotidyl transferase mediated dUTP nick end labeling (TUNEL) (Roche diagnostics GmbH, Mannheim, Germany) was used to detect apoptotic cells. The test was performed according to the manufacturer's guidelines. Hoechst 33342 (Molecular Probes) was used to visualize cell nuclei. The percentage of TUNEL-positive cells was determined in five randomly selected fields of 100 cells in both epithelium and lamina propria with a fluorescence microscope (Leica DM RBE microscope, Leica Microsystems).

3.1.3.5. Inoculation of GaHV1 (ILTV) and evaluation of mucosal spread

Tracheas and conjunctivas of three chickens were used. Explants were inoculated at 24h of cultivation with ILTV (U76/1035). For the inoculation, explants were taken from their gauze and placed at the bottom of a 24-well plate with the epithelial surface upwards. Explants were washed twice with warm serum-free medium and inoculated

with 1 ml of a virus stock containing $10^{6.0}$ EID₅₀ (1h, 37°C, 5% CO₂). After one hour, inoculated explants were washed three times with warm medium and placed back on the gauze. Explants were collected at 0, 24, 48 and 72h pi, embedded in Methocel[®] (Fluka) and frozen at -70°C. Inoculation was performed for three different chickens. For each chicken, one explant was collected at each time point post inoculation. As a parameter of productive replication, we have checked viral titers in the supernatant of inoculated explants in one replicate.

3.1.3.6. Immunofluorescence staining

At 0, 24, 48 and 72h pi, 150 consecutive cryosections of 15 µm were made from the frozen explants and the cryosections were fixed in methanol (25 min, -20°C). The cryosections were first stained for collagen IV, which is abundantly present in the BM and connective tissue, and next for ILTV antigens. The cryosections were incubated (1h, 37°C) with goat anti-collagen IV antibodies (Southern Biotech) (1:50 in PBS), after which cryosections were washed three times (PBS) and incubated (1h, 37°C) with biotinylated rabbit anti-goat IgG antibodies (1:100 in PBS) and washed three times after incubation. Then, cryosections were incubated (1h, 37°C) simultaneously with streptavidin-Texas Red (Molecular Probes) (1:50 in PBS) and mouse monoclonal anti-ILTV gC antibodies (1:50 in PBS) (The monoclonal antibody against ILTV gC was provided by the Institute of Molecular Biology, Friedrich-Loeffler-Institute, Federal Research Institute for Animal Health, Boddenblick 5A, 17493 Greifswald-InseldRiems, Germany). Subsequently, after washing, the sections were incubated (1h, 37°C) with FITC-labelled goat anti-mouse IgG antibodies (Molecular Probes) (1:100 in PBS). Finally, after washing, the sections were incubated (10min, RT) with Hoechst 33342 (1:100 in PBS), washed and mounted with glycerin-DABCO (Janssen Chimica).

3.1.3.7. Evaluation of ILTV mucosal spread

A confocal microscope (Leica TCS SPE confocal microscope) was used for the analysis of ILTV replication in mucosal explants. Solid-state lasers were used to excite Texas Red (561 nm) and FITC (488 nm) fluorophores. We have analysed replication characteristics of ILTV by a reproducible quantitative analysis system described by Glorieux et al. (2009). Briefly, at 24, 48 and 72h pi, the average number of plaques were counted in a surface area of 8 mm² of the explants (150 consecutive

cryosections) derived from both trachea and conjunctiva. Using the Leica confocal software, plaque dimensions, latitude and invasion depth (distance covered by ILTV underneath the BM) were measured at the maximal size for at least 10 different plaques per chicken at 0, 24, 48 and 72h pi. Maximum intensity projection (MIP) or Extended focus image of the confocal microscope was used to display three-dimensional information of the plaque. We have excluded borders and edges of the explant from analysis, i.e. only middle regions of the explant were considered for analysis.

3.1.3.8. Cell viability in ILTV infected tracheal and conjunctival mucosa

The TUNEL assay was performed to detect apoptotic cells in infected tracheal and conjunctival mucosa explants. Immunofluorescence stainings were performed to detect ILTV antigens. The protocol of both techniques is described above. TUNEL-positive cells were counted at 0, 24, 48 and 72h pi. Two regions of interest were taken into account for calculation: (i) regions containing ILTV-negative cells and (ii) regions containing ILTV-positive cells (plaque). In an ILTV-negative region, 10 randomly selected fields of 100 cells were evaluated in both epithelium and lamina propria. In ILTV-positive cells region, 10 randomly selected ILTV plaques were evaluated in both epithelium and lamina propria. The experiment was performed in triplicate.

3.1.3.9. Statistical analysis

Sigma Plot (Systat Software, Inc., San Jose, CA) software was used to analyse the data statistically for one-way analysis of variance (ANOVA). The results of three independent experiments are shown as means \pm standard deviation (SD) and *P* values of < 0.05 were considered significant.

3.1.4. Results

3.1.4.1. Ciliary beating

The ciliary beating of the tracheal explants was normal up till the end of the study (96h of cultivation).

3.1.4.2. Viability of tracheal and conjunctival mucosa explants

The viability of the tracheal and conjunctival mucosa explants was assessed based on the percentage of TUNEL-positive cells. We did not observe a significant increase in the number of positive cells at 0, 24, 48, 72 and 96h of *in vitro* cultivation for both the epithelium and the lamina propria (Table 1). The percentage of TUNEL-positive cells in the epithelium of trachea and conjunctiva ranged from $0.0 \pm 0.0\%$ to $0.9 \pm 0.1\%$ at 0 and 96h, respectively. In the lamina propria of trachea and conjunctiva, the percentage of TUNEL-positive cells ranged from $0.0 \pm 0.0\%$ to $1.4 \pm 1.8\%$ at 0 and 96h respectively. Negligible TUNEL-positive cells were observed in the tracheal cartilage.

Table 1. Apoptosis in the epithelium and lamina propria of chicken tracheal mucosa explants during *in vitro* cultivation. Values are given for three independent experiments as means \pm SD.

Tissue	Layer	% of TUNEL positive cells at ... hours of <i>in vitro</i> cultivation				
		0	24	48	72	96
Trachea	Epithelium	0.0 ± 0.0	0.3 ± 0.2	0.3 ± 0.3	0.6 ± 0.2	0.7 ± 1.1
	Lamina propria	0.0 ± 0.0	0.4 ± 0.2	0.8 ± 0.5	0.9 ± 0.3	1.4 ± 1.8
Conjunctiva	Epithelium	0.0 ± 0.0	0.4 ± 0.3	0.5 ± 0.2	0.7 ± 0.2	0.9 ± 0.1
	Lamina propria	0.2 ± 0.1	0.7 ± 0.1	0.7 ± 0.2	1.0 ± 0.2	1.2 ± 0.1

3.1.4.3. GaHV1 (ILTV) interactions with tracheal and conjunctival mucosa

3.1.4.3.1. Evaluation of ILTV mucosal spread - Inoculation of chicken tracheal and conjunctival mucosa explants with ILTV led to the formation of viral antigen positive plaques (group of closely connected cells) in the mucosa. At 0h, no infection was observed. At 24, 48 and 72h pi clear ILTV infected plaques were found in the tracheal and conjunctival mucosa. Representative images of plaques at 24h pi are illustrated in Figure 1. We have observed ILTV infection only in the epithelial cells. We did not observe infection at the edges and ventral region of the cryosections. Dissemination kinetics of plaques in the mucosa was evaluated by measuring the plaque number, maximal plaque latitude and invasion depth underneath the BM at 0, 24, 48 and 72h pi. The viral titers in the supernatant of inoculated explants were increased from $10^{2.7}$ EID₅₀/ml at 24h pi to $10^{4.3}$ EID₅₀/ml 72h pi.

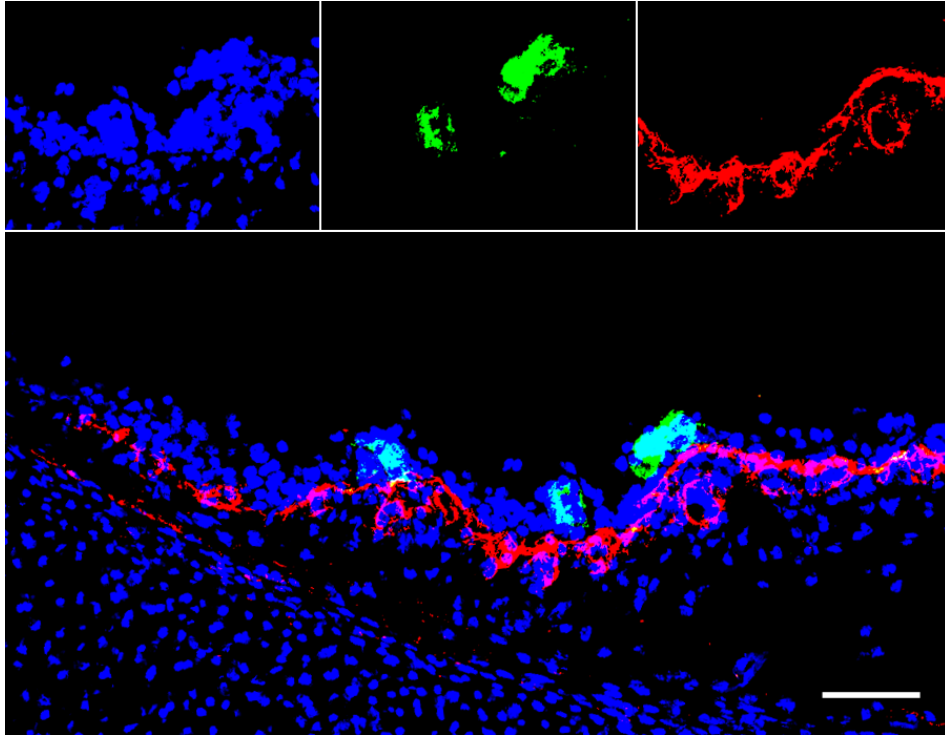


Figure 1. Representative confocal photomicrographs illustrating three ILTV-positive plaques in the epithelium of tracheal mucosa at 24h pi. Images for individual channels are shown on top row from left to right (Cell nuclei is blue, ILTV antigen is green and Collagen IV is red fluorescence) and a larger merged image on a down row. Colocalization of viral antigen with collagen IV is visualised by yellow color. Scale bar represents 50 μm .

3.1.4.3.2. Plaque Number - Mucosal explants covering a total area of 10 mm^2 were evaluated using Leica confocal microscope. We have excluded borders and edges of the explant for analysis. Results of the average number of plaques are given per 8 mm^2 or per one explant (150 consecutive cryosections). Mean values \pm SD are represented in Figure 2 for three independent experiments. The number of plaques slightly increased in time.

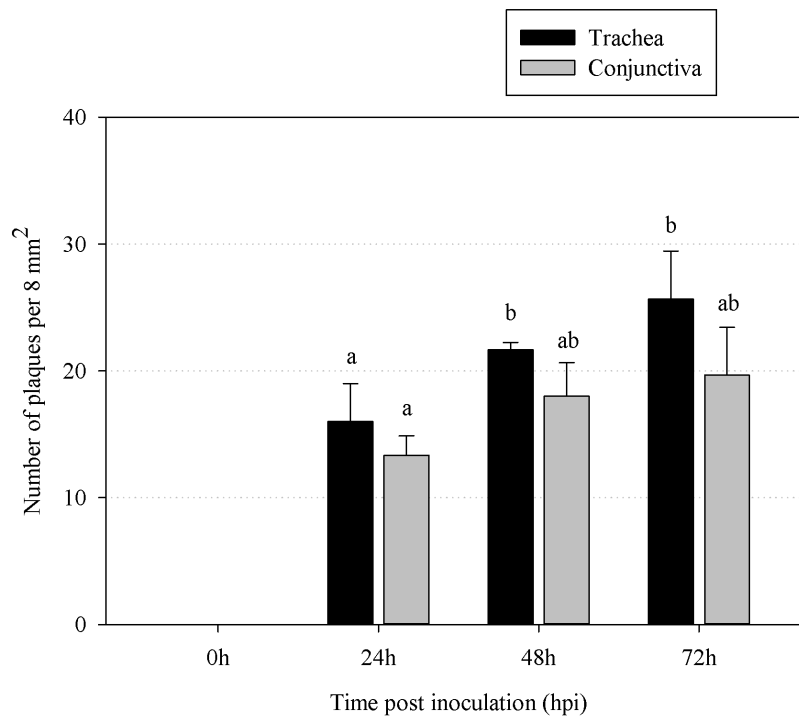
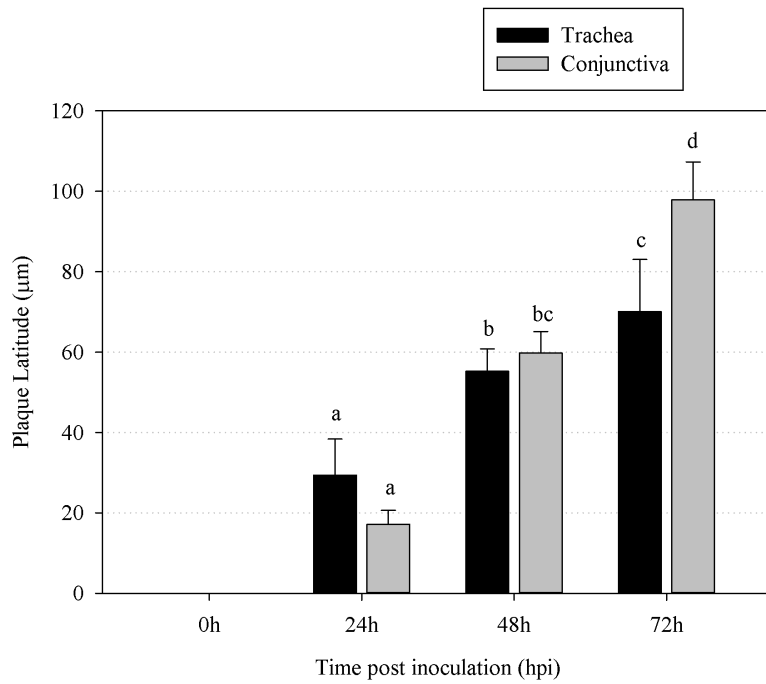


Figure 2. The number of plaques was determined at 0, 24, 48 and 72h pi. For each chicken, 150 consecutive cryosections were analysed at every time point to count plaques. Bars with different letters are significantly different from each other ($P < 0.05$).

3.1.4.3.3. Plaque latitude - Plaque latitudes were measured using Leica confocal software. Mean values \pm SD are represented in Figure 3a for three independent experiments. The plaque latitude increased steadily over time from 0 to 72h pi. In the tracheal mucosa the latitude increased from $29.4 \pm 9.0 \mu\text{m}$ (24h pi), to $55.4 \pm 5.6 \mu\text{m}$ (48h pi) and $70.4 \pm 12.9 \mu\text{m}$ (72h pi). In the conjunctiva increased from $17.2 \pm 3.4 \mu\text{m}$ (24h pi), to $59.8 \pm 5.3 \mu\text{m}$ (48h pi) and $97.8 \pm 9.5 \mu\text{m}$ (72h pi).

a)



b)

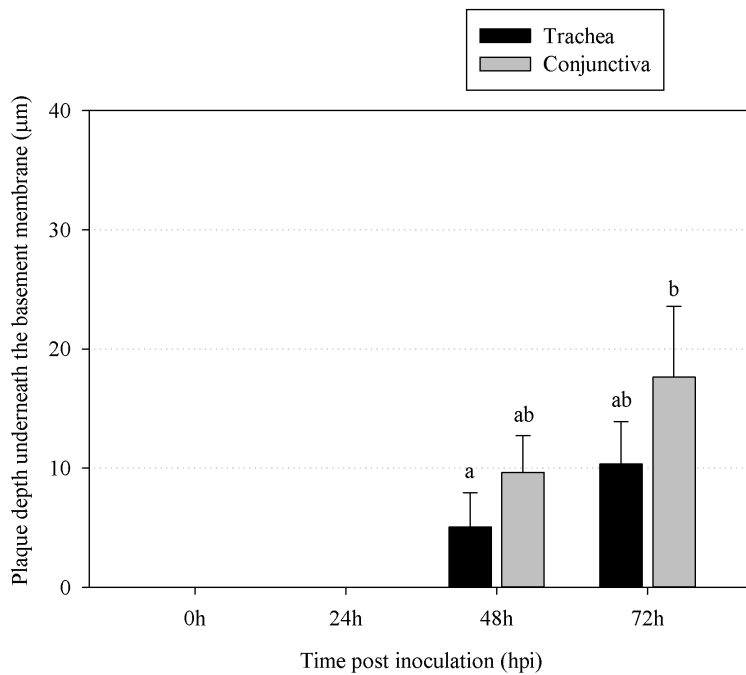


Figure 3. Evolution of plaque latitude (a) and invasion depth (b) underneath the basement membrane at 0, 24, 48 and 72h pi. Data are represented as means of 10 plaques at maximal size for three different independent experiments \pm SD (error bars). Bars with different letters are significantly different from each other ($P < 0.05$).

3.1.4.3.4. Plaque invasion depth - Plaque invasion is the vertical spread of ILTV in mucosa. Plaque invasion depth is the distance covered by ILTV-infected tissue underneath the BM (Glorieux et al., 2009). Plaque invasion depths were measured using Leica confocal software. The evolution of ILTV plaque formation at 0, 24, 48 and 72h pi in trachea and conjunctiva are illustrated in Figure 4. At 0 and 24h pi, infected plaques did not cross the BM. ILTV starts BM invasion slowly, as infected plaques only crossed the BM between 24h and 48h pi. At 48h pi, about 31% of the plaques showed invasion through the BM of trachea and about 43% of the plaques showed invasion through the BM of conjunctiva. At 72h pi, this percentage increased to 56% in trachea and 74% in conjunctiva. Mean values \pm SD are represented in Figure 3b for three independent experiments. The average depths underneath the BM increased from $5.1 \pm 2.9 \mu\text{m}$ at 48h pi to $10.3 \pm 3.6 \mu\text{m}$ at 72h pi among all plaques of tracheal mucosa. In conjunctival mucosa, the average depths underneath the BM increased from $9.6 \pm 3.1 \mu\text{m}$ at 48h pi to $17.6 \pm 6 \mu\text{m}$ at 72h pi among all plaques.

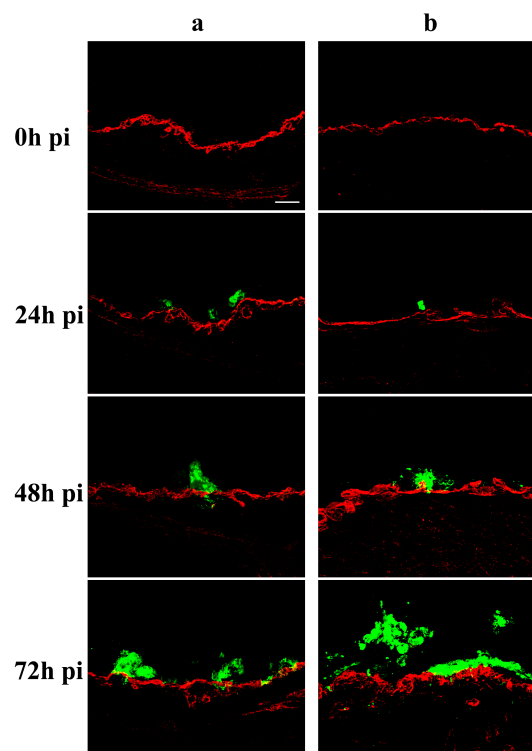


Figure 4. Representative confocal photomicrographs illustrating the evolution over time of ILTV induced plaques in tracheal (a) and conjunctival mucosa (b). Green fluorescence visualises ILTV antigens. Collagen IV is visualised by red fluorescence. Scale bar represents $50 \mu\text{m}$.

3.1.4.4. Cell viability in ILTV infected tracheal and conjunctival mucosa

After inoculation with ILTV, a large number of cells were ILTV infected. A small number of TUNEL-positive cells were observed in both regions of ILTV-infected and non-infected cells (Table 2). In ILTV-infected regions, TUNEL-positive cells were usually observed in the vicinity of ILTV-infected cells. ILTV-infected cells were mostly not TUNEL-positive. In tracheal and conjunctival epithelium, the percentage of ILTV-positive cells that were TUNEL-positive ranged from 0.4 % at 24h to 1.4% at 72h pi. A representative confocal image illustrating TUNEL-positive cells in the vicinity of ILTV-infected cells but not in the ILTV-infected plaque is given in Figure 5.

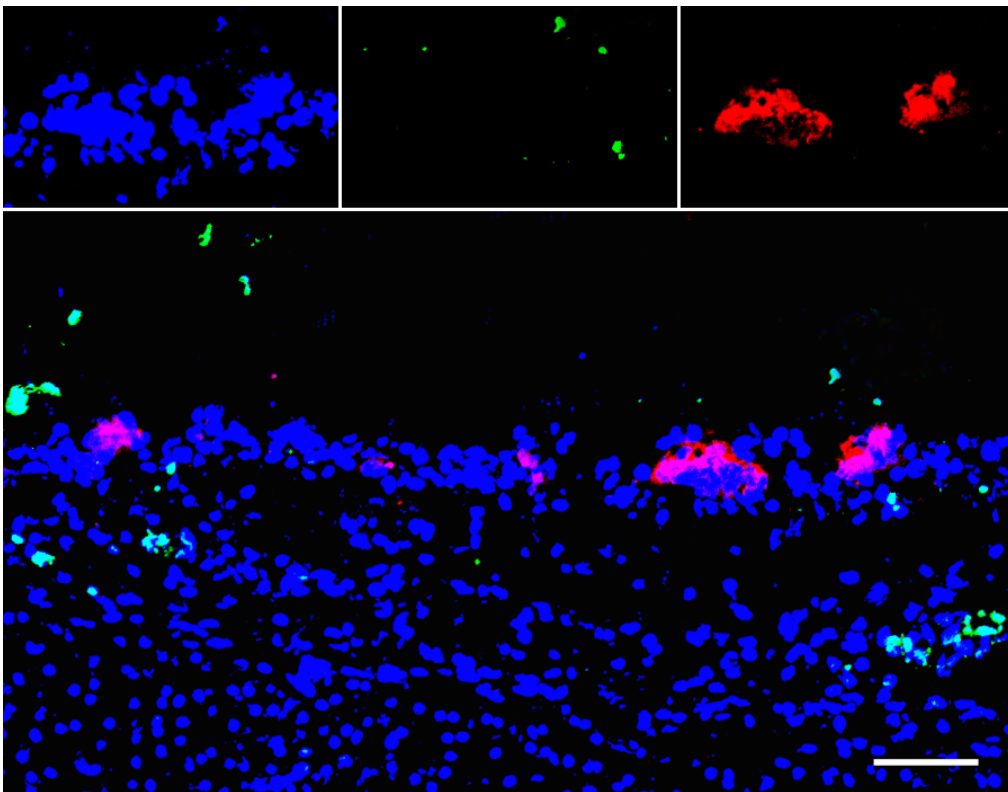


Figure 5. Representative confocal photomicrographs illustrating a small number of TUNEL-positive (apoptotic) cells in a region of ILTV-positive cells. Images for individual channels are shown on top row from left to right (Cell nuclei is blue, Apoptotic cell is green and Viral antigen is red fluorescence) and a larger merged image on a down row. TUNEL-positive cells were usually present in the vicinity of ILTV-infected cells. ILTV-infected cells were in general not apoptotic. Scale bar represents 50 μm .

Table 2. Percentage of TUNEL-positive cells in both epithelium and lamina propria of a region of ILTV-negative and of a region of ILTV-positive cells (plaque) at 0, 24, 48 and 72 h post inoculation (pi). Values are given for three independent experiments as means \pm SD.

Tissue	Layer	% of TUNEL positive cells at ... hours of in vitro cultivation			
		0	24	48	72
Trachea	ILTV ⁻ Epithelium	0.4 \pm 0.1	0.8 \pm 0.2	0.7 \pm 0.1	1.3 \pm 0.5
	ILTV ⁻ Lamina propria	0.7 \pm 0.2	1.1 \pm 0.3	1.3 \pm 0.2	2.5 \pm 1.0
	ILTV ⁺ Epithelium	ND	1.1 \pm 0.1	3.9 \pm 1.2*	4.2 \pm 1.1*
	ILTV ⁺ Lamina propria	ND	5.3 \pm 1.2*	7.1 \pm 1.1*	6.4 \pm 0.9*
Conjunctiva	ILTV ⁻ Epithelium	0.6 \pm 0.1	1.0 \pm 0.2	0.9 \pm 0.3	1.4 \pm 0.1
	ILTV ⁻ Lamina propria	1.0 \pm 0.2	0.9 \pm 0.1	1.6 \pm 0.3	2.1 \pm 0.4
	ILTV ⁺ Epithelium	ND	1.6 \pm 0.2*	4.9 \pm 1.5*	3.2 \pm 1.3
	ILTV ⁺ Lamina propria	ND	4.9 \pm 1.3*	9.0 \pm 2.3	8.3 \pm 1.4*

ND = not determined; no ILTV-positive cells were found.

* Significant differences compared with the control (ILTV negative tissue) at $P < 0.05$ level.

3.1.5. Discussion

In the present study, (i) chicken tracheal and conjunctival mucosa explants were established, (ii) replication kinetics of ILTV were investigated in tracheal and conjunctival mucosa and (iii) cell viability was analysed in ILTV infected tracheal and conjunctival mucosa explants.

Even though *in vivo* laboratory animals are the best system for studying host-pathogen interactions, physiological inter-individual differences and different environmental conditions are important drawbacks. The use of an *in vitro* culture offers the opportunity to study host-pathogen interactions under more controlled conditions. In cell cultures, cell-cell and cell-extracellular matrix interactions are reduced due to the lack of a three-dimensional architecture of the culture (Freshney, 2005). *In vitro* explant (organ) cultures are excellent alternative models that mimic natural conditions. The *in vitro* explant (organ) cultures are in line with the three Rs principle, i.e. Reduction (reduction of number of animals), Replacement (no use of living animals) and Refinement (minimizing the pain) (Russell and Burch, 1959). A major advantage of the *in vitro* explant (organ) model is that explants of the same animals can be used to compare different viral strains.

The culture technique that was used in this study for chicken tracheal and conjunctival explants (organs) is similar to that of porcine (Glorieux *et al.*, 2007), bovine (Steukers *et al.*, 2012), equine (Vandekerckhove *et al.*, 2009) and human (Glorieux *et al.*, 2011) respiratory explants. To our knowledge, there are no reports on the viability of cells in the epithelial layers, lamina propria and underlying connective tissue of chicken TOC and COC. Hence, in this study the viability of epithelial cells and cells in the lamina propria of TOC and COC were evaluated by quantifying TUNEL-positive cells at 0, 24, 48, 72 and 96h of *in vitro* cultivation. The TUNEL-positive cells remained below 1.5% up to 96h of cultivation in both epithelium and lamina propria of TOC and COC. Thus, we can state that TOC and COC were successfully maintained for at least 96h in culture at an air-liquid interface without significant changes in tissue viability.

The chicken tracheal and conjunctival explants were susceptible to an ILTV infection. The infection pattern of ILTV in the mucosal explants is mimicking extremely well the *in vivo* observations made by the Bang and Bang (1967). The purpose of the present study was to analyse the behavior of ILTV in the mucosa by immunofluorescence and mathematical quantitative analysis using confocal microscopy and software Image J, as described for the first time by Glorieux *et al.* (2009). By doing this, a complete three-dimensional picture of the horizontal and vertical spread of ILTV in the mucosa was obtained. This novel approach is an ideal tool for studying cellular and molecular aspects of the invasion mechanisms of pathogens (Glorieux *et al.*, 2011; Glorieux *et al.*, 2009; Steukers *et al.*, 2012; Vandekerckhove *et al.*, 2010). It allows a thorough comparison of different alphaherpesvirus replication kinetics in their respective species. The ILTV induced plaques were present in the epithelial layer starting from 24h pi. The plaque latitude increased in time. The ILTV infected plaques started to cross the basement membrane from 48h pi.

Mucosa explant models of porcine, equine, human and bovine origin were developed in our laboratory to study virus-host interactions and mucosal invasion. By using these explants, invasion processes of different alphaherpesviruses (EHV1, EHV4, BHV1, SHV1 and HSV1) have already been described. Based on their invasion mechanism, alphaherpesviruses can be classified into three types: (i) EHV4 shows replication in the respiratory epithelial cells without invasion through the BM, (ii) BHV1, SHV1 and HSV1 exhibit a plaquewise spread through the BM in the *in vitro* explant model and (iii) EHV1 spreads only laterally and does not breach through the BM (similar to

EHV4) but invades deeper tissues of the respiratory tract via infected leukocytes which function as Trojan horses (Glorieux *et al.*, 2011; Glorieux *et al.*, 2009; Steukers *et al.*, 2012; Vandekerckhove *et al.*, 2010).

When comparing replication kinetics of ILTV in trachea and conjunctiva, we observed some interesting findings. At 72h pi, the plaque latitude in the conjunctival mucosa was significantly larger compared to that in the tracheal mucosa. The percentage of the plaques that penetrated through the BM was larger in conjunctiva (48h pi: 43% and 72h pi: 74%) compared to the trachea (48h pi: 31% and 72h pi: 56%). Plaque latitude and invasion depth kinetics indicated that at later time points (48 and 72h pi) ILTV showed a more extensive replication in conjunctival mucosa compared to the tracheal mucosa. The differences in the replication kinetics of ILTV are likely due to variation in its tropism for trachea and conjunctiva. Kirkpatrick *et al.* (2006) observed that there is a variation in ILTV in its tropism for trachea or conjunctiva. In the future, the replication characteristics of different ILTV strains on mucosal explants may help to understand their tropism for trachea and conjunctiva.

In BHV1, SHV1 and HSV1 infection, the lateral mucosal spread and vertical invasion depth evolved similarly with increasing time pi. In the case of ILTV, the invasion through the BM was very restricted. At 48h pi 30.9% of the plaques in trachea and 43.3% of the plaques in conjunctiva were crossing the BM. This finding is in contrast with plaques induced by SHV1, HSV1 and BHV1. With SHV1 and HSV1, 100% of the plaques crossed the BM at 24h pi (Glorieux *et al.*, 2011; Glorieux *et al.*, 2009). With BHV1, 90% of the plaques went through the BM at 48h pi (Steukers *et al.*, 2011). ILTV may not have developed enough tools to breach quickly through the BM like BHV1, SHV1 and HSV1. The restricted ILTV invasion through the BM agrees with the *in vivo* pathogenesis of ILTV, where no clear evidence exists for viremia (Bagust, 1986; Guy and Bagust, 2003). Otherwise, invasion of ILTV through the BM of trachea and conjunctiva is evidently corroborated. Indeed, (Zhao *et al.*, 2013) detected ILTV in most of the internal organs of infected chickens.

Although speculative, a hypothesis can be formed to explain the restricted ILTV invasion through the BM in chickens compared to the invasion of other alphaherpesviruses in their respective species. Viral structural components and BM composition should be considered. The structural glycoproteins present on the surface

of alphaherpesviruses and alphaherpesvirus-infected cells together with up-regulated cellular proteases are putative candidates for helping the virus to cross the BM. Several proteolytic enzymes, including trypsin-like proteases, have been shown to break down the BM and extracellular matrix and trypsin-like serine protease was found to be involved in the SHV1 invasion through the BM (Barrett *et al.*, 2003; Glorieux *et al.*, 2011). A rapid breakdown of BM components is most probably facilitating the SHV1 invasion. Alphaherpesviruses use the glycoprotein E/glycoprotein I (gE/gI) complex to spread directly from cell to cell through cell junctions (Devlin *et al.*, 2006). In case of BHV1, the gE/gI complex also efficiently mediates invasion through the BM (Steukers, 2013). The involvement of trypsin-like serine proteases and/or gE/gI complex in the ILTV invasion needs to be addressed. Characteristics of the BM may also play a role in the restricted ILTV invasion. The heterogeneous components in the BM interact and form a sheet of fibers. These intermolecular interactions in the BM might be stronger in chickens compared to mammals and prevent better the entry of pathogens (Fitch *et al.*, 1982; LeBleu *et al.*, 2007; Mayne *et al.*, 1982; Mayne and Zettergren, 1980). Several questions on why ILTV has problems to cross the BM are still not answered. Do certain components or total thickness of the BM play a role in its barrier function against ILTV invasion (Steukers *et al.*, 2012)? Or did ILTV not develop a mechanism during evolution to invade quickly through the BM? Tracheal and conjunctival mucosal explants are ideal tools to address these questions.

The effect of ILTV on the cell viability of tracheal and conjunctival mucosa was analysed by a TUNEL assay. A large number of epithelial cells were ILTV-positive. But, only a few ILTV-infected cells were TUNEL-positive, even at 72h pi. Our studies are consistent with previous reports demonstrating that low levels of apoptosis were observed in cells infected with other alphaherpesviruses HSV2-, SHV1- and HSV1 (Aleman *et al.*, 2001; Asano *et al.*, 1999; Glorieux *et al.*, 2011). Further, TUNEL-positive cells were predominantly restricted to the vicinity of ILTV-infected cells. These TUNEL-positive cells might be local leukocytes that respond to the productive ILTV infection, as seen in SHV1 and HSV2 (Aleman *et al.*, 2001; Asano *et al.*, 1999). Or these apoptotic cells may be uninfected bystander cells present in the vicinity of infected cells (Aleman *et al.*, 2001). ILTV-infected cells may release some pro-apoptotic components or cytokines to induce apoptosis. This could be an ILTV strategy to sustain the infection in the mucosa. Several publications have shown that

alphaherpesviruses (HSV1, HSV2, SHV1 and BHV1) evade the immune system by inhibiting apoptosis of infected cells (Aleman *et al.*, 2001; Asano *et al.*, 1999; Galvan and Roizman, 1998; Jerome *et al.*, 1999; Winkler *et al.*, 1999). More specifically, alphaherpesviruses usually evades natural killer (NK) cell- and T-lymphocyte-dependent antiviral pathways and maintain the viability of infected cells (Aleman *et al.*, 2001; Favoreel *et al.*, 2000; Han *et al.*, 2007; Murugin *et al.*, 2011; Orange *et al.*, 2002; Winkler *et al.*, 1999). There are reports that ILTV suppresses apoptosis of infected primary cells (Burnside and Morgan, 2011; Lee *et al.*, 2012). However, to our knowledge there are no reports on the effect of ILTV on apoptosis in infected cells of tracheal and conjunctival mucosae. Therefore, our current *in vitro* study indicates that ILTV blocks apoptosis in infected epithelial cells of tracheal and conjunctival mucosa. Furthermore, it may induce apoptosis of neighboring uninfected cells. Usually viruses alter host immune responses to their benefit. It may protect infected cells against an attack by the immune system. This allows infected epithelial cells to survive long enough to support replication. Further, surviving epithelial cells may ensure that virus could breach the BM, reach the lamina propria and finally enhance mucosal invasion in the infection process. By doing this ILTV may easily reach sensory nerves and the trigeminal ganglion, the site of latency. All these mechanisms help ILTV to sustain life-long infection. The exact viral factors involved in the inhibition of apoptosis of infected cells and the activation of apoptosis in the surrounding cells will be identified in the near future.

3.1.6. Acknowledgements

The authors acknowledge Magda De Keyzer and Lieve Sys for their excellent technical assistance, Thierry van den Berg for providing the virus and Zeger Van den Abeele, Loes Geypen and Bart Ellebaut for their help with handling and euthanizing the chickens.

3.1.7. References

Aleman, N., Quiroga, M.I., Lopez-Pena, M., Vazquez, S., Guerrero, F.H., Nieto, J.M., 2001. Induction and inhibition of apoptosis by pseudorabies virus in the trigeminal ganglion during acute infection of swine. *J Virol* 75, 469-479.

- Anderton, T.L., Maskell, D.J., Preston, A., 2004. Ciliostasis is a key early event during colonization of canine tracheal tissue by *Bordetella bronchiseptica*. *Microbiology* 150, 2843-2855.
- Asano, S., Honda, T., Goshima, F., Watanabe, D., Miyake, Y., Sugiura, Y., Nishiyama, Y., 1999. US3 protein kinase of herpes simplex virus type 2 plays a role in protecting corneal epithelial cells from apoptosis in infected mice. *J Gen Virol* 80 (Pt 1), 51-56.
- Bagust, T.J., 1986. Laryngotracheitis (Gallid-1) herpesvirus infection in the chicken. 4. Latency establishment by wild and vaccine strains of ILT virus. *Avian Pathol* 15, 581-595.
- Bang, B.G., Bang, F.B., 1967. Laryngotracheitis virus in chickens. A model for study of acute nonfatal desquamating rhinitis. *J Exp Med* 125, 409-428.
- Barrett, A.J., Tolle, D.P., Rawlings, N.D., 2003. Managing peptidases in the genomic era. *Biol Chem* 384, 873-882.
- Burnside, J., Morgan, R., 2011. Emerging roles of chicken and viral microRNAs in avian disease. *BMC Proc* 5 Suppl 4, S2.
- Darbyshire, J.H., Cook, J.K., Peters, R.W., 1976. Organ culture studies on the efficiency of infection of chicken tissues with avian infectious bronchitis virus. *Br J Exp Pathol* 57, 443-454.
- Davison, A.J., 2010. Herpesvirus systematics. *Vet Microbiol* 143, 52-69.
- Devlin, J.M., Browning, G.F., Gilkerson, J.R., 2006. A glycoprotein I- and glycoprotein E-deficient mutant of infectious laryngotracheitis virus exhibits impaired cell-to-cell spread in cultured cells. *Arch Virol* 151, 1281-1289.
- Favoreel, H.W., Nauwynck, H.J., Pensaert, M.B., 2000. Immunological hiding of herpesvirus-infected cells. *Arch Virol* 145, 1269-1290.
- Fitch, J.M., Gibney, E., Sanderson, R.D., Mayne, R., Linsenmayer, T.F., 1982. Domain and basement membrane specificity of a monoclonal antibody against chicken type IV collagen. *J Cell Biol* 95, 641-647.
- Freshney, R.I., 2005. *Culture of Animal Cells: A manual of Basic Technique*, Vol 5th edition. Hoboken: Wiley-Blackwell.
- Fuchs, W., Veits, J., Helferich, D., Granzow, H., Teifke, J.P., Mettenleiter, T.C., 2007. Molecular biology of avian infectious laryngotracheitis virus. *Vet Res* 38, 261-279.
- Galvan, V., Roizman, B., 1998. Herpes simplex virus 1 induces and blocks apoptosis at multiple steps during infection and protects cells from exogenous inducers in a cell-type-dependent manner. *Proc Natl Acad Sci U S A* 95, 3931-3936.
- Glorieux, S., Bachert, C., Favoreel, H.W., Vandekerckhove, A.P., Steukers, L., Rekecki, A., Van den Broeck, W., Goossens, J., Croubels, S., Clayton, R.F.,

- Nauwynck, H.J., 2011. Herpes simplex virus type 1 penetrates the basement membrane in human nasal respiratory mucosa. *PLoS One* 6, e22160.
- Glorieux, S., Favoreel, H.W., Meesen, G., de Vos, W., Van den Broeck, W., Nauwynck, H.J., 2009. Different replication characteristics of historical pseudorabies virus strains in porcine respiratory nasal mucosa explants. *Vet Microbiol* 136, 341-346.
- Glorieux, S., Van den Broeck, W., van der Meulen, K.M., Van Reeth, K., Favoreel, H.W., Nauwynck, H.J., 2007. In vitro culture of porcine respiratory nasal mucosa explants for studying the interaction of porcine viruses with the respiratory tract. *J Virol Methods* 142, 105-112.
- Guy, J.S., Bagust, T.J., 2003. *Diseases of Poultry*, Vol 11 Ames: Blackwell.
- Han, J.Y., Sloan, D.D., Aubert, M., Miller, S.A., Dang, C.H., Jerome, K.R., 2007. Apoptosis and antigen receptor function in T and B cells following exposure to herpes simplex virus. *Virology* 359, 253-263.
- Ide, P.R., 1978. Sensitivity and specificity of the fluorescent antibody technique for detection of infectious laryngotracheitis virus. *Can J Comp Med* 42, 54-62.
- Jerome, K.R., Fox, R., Chen, Z., Sears, A.E., Lee, H., Corey, L., 1999. Herpes simplex virus inhibits apoptosis through the action of two genes, Us5 and Us3. *J Virol* 73, 8950-8957.
- Jones, B.V., Hennion, R.M., 2008. The preparation of chicken tracheal organ cultures for virus isolation, propagation, and titration. *Methods Mol Biol* 454, 103-107.
- Jones, R.C., 2010. Viral respiratory diseases (ILT, aMPV infections, IB): are they ever under control? *Br Poult Sci* 51, 1-11.
- Kirkpatrick, N.C., Mahmoudian, A., Colson, C.A., Devlin, J.M., Noormohammadi, A.H., 2006. Relationship between mortality, clinical signs and tracheal pathology in infectious laryngotracheitis. *Avian Pathol* 35, 449-453.
- LeBleu, V.S., Macdonald, B., Kalluri, R., 2007. Structure and function of basement membranes. *Exp Biol Med (Maywood)* 232, 1121-1129.
- Lee, J., Bottje, W.G., Kong, B.W., 2012. Genome-wide host responses against infectious laryngotracheitis virus vaccine infection in chicken embryo lung cells. *BMC Genomics* 13, 143.
- Mayne, R., Wiedemann, H., Dessau, W., Von der Mark, K., Bruckner, P., 1982. Structural and immunological characterization of type IV collagen isolated from chicken tissues. *Eur J Biochem* 126, 417-423.
- Mayne, R., Zettergren, J.G., 1980. Type IV collagen from chicken muscular tissues. Isolation and characterization of the pepsin-resistant fragments. *Biochemistry* 19, 4065-4072.

- Meulemans, G., Halen, P., 1978. Some physico-chemical and biological properties of a Belgian strain (U 76/1035) of infectious laryngotracheitis virus. *Avian Pathol* 7, 311-315.
- Murugin, V.V., Zuikova, I.N., Murugina, N.E., Shulzhenko, A.E., Pinegin, B.V., Pashenkov, M.V., 2011. Reduced degranulation of NK cells in patients with frequently recurring herpes. *Clin Vaccine Immunol* 18, 1410-1415.
- Orange, J.S., Fasset, M.S., Koopman, L.A., Boyson, J.E., Strominger, J.L., 2002. Viral evasion of natural killer cells. *Nat Immunol* 3, 1006-1012.
- Reemers, S.S., Groot Koerkamp, M.J., Holstege, F.C., van Eden, W., Vervelde, L., 2009. Cellular host transcriptional responses to influenza A virus in chicken tracheal organ cultures differ from responses in in vivo infected trachea. *Vet Immunol Immunopathol* 132, 91-100.
- Russell, W.M.S., Burch, R.L., 1959. *The principles of humane experimental technique*. Methuen, London, UK.
- Steukers, L., Vandekerckhove, A.P., Van den Broeck, W., Glorieux, S., Nauwynck, H.J., 2011. Comparative analysis of replication characteristics of BoHV-1 subtypes in bovine respiratory and genital mucosa explants: a phylogenetic enlightenment. *Vet Res* 42, 33.
- Steukers, L., Vandekerckhove, A.P., Van den Broeck, W., Glorieux, S., Nauwynck, H.J., 2012. Kinetics of BoHV-1 dissemination in an in vitro culture of bovine upper respiratory tract mucosa explants. *ILAR J* 53, E43-54.
- Vandekerckhove, A., Glorieux, S., Broeck, W.V., Gryspeerdt, A., van der Meulen, K.M., Nauwynck, H.J., 2009. In vitro culture of equine respiratory mucosa explants. *Vet J* 181, 280-287.
- Vandekerckhove, A.P., Glorieux, S., Gryspeerdt, A.C., Steukers, L., Duchateau, L., Osterrieder, N., Van de Walle, G.R., Nauwynck, H.J., 2010. Replication kinetics of neurovirulent versus non-neurovirulent equine herpesvirus type 1 strains in equine nasal mucosal explants. *J Gen Virol* 91, 2019-2028.
- Winkler, M.T., Doster, A., Jones, C., 1999. Bovine herpesvirus 1 can infect CD4(+) T lymphocytes and induce programmed cell death during acute infection of cattle. *J Virol* 73, 8657-8668.
- Zhang, S., Jian, F., Zhao, G., Huang, L., Zhang, L., Ning, C., Wang, R., Qi, M., Xiao, L., 2012. Chick embryo tracheal organ: a new and effective in vitro culture model for *Cryptosporidium baileyi*. *Vet Parasitol* 188, 376-381.
- Zhao, Y., Kong, C., Cui, X., Cui, H., Shi, X., Zhang, X., Hu, S., Hao, L., Wang, Y., 2013. Detection of infectious laryngotracheitis virus by real-time PCR in naturally and experimentally infected chickens. *PLoS One* 8, e67598.

CHAPTER 3.2.

Presence of DNA extracellular traps but not MUC5AC and MUC5B mucin in mucoid plugs/casts of infectious laryngotracheitis virus (ILTV) infected tracheas of chickens

Vishwanatha R.A.P. Reddy, Ivan Trus and Hans J. Nauwynck

Virus Research (2017), 227: 135-142

3.2.1. Abstract

Although it has been speculated that the tracheal obstructions and asphyxiation during acute infectious laryngotracheitis (ILT) are due to mucoid plugs/casts formed by mucus hypersecretion, there are no reports demonstrating this. Hence, in the present study, we first examined if the main respiratory mucins, MUC5AC and MUC5B, are expressed in the mucosae of larynx, trachea and bronchi of mock-inoculated and ILTV infected chickens. Second, the tracheas with plugs/casts were stained for mucins (MUC5AC and MUC5B) and nuclear material (traps). MUC5AC and MUC5B were produced by the mucosae of larynx, trachea and bronchi of mock-inoculated chickens. Interestingly, MUC5AC and MUC5B were exclusively present in the dorsal tracheal region of the cranial and middle part of trachea of mock-inoculated chickens. In ILTV infected chickens, the tracheal lumen diameter was almost 40% reduced and was associated with a strongly increased tracheal mucosal thickness. MUC5AC and MUC5B were scarcely observed in larynx, trachea and bronchi, and in tracheal plugs/casts of ILTV infected birds. Surprisingly, DNA fibrous structures were observed in connection with nuclei of $10.0 \pm 7.3\%$ cells, present in tracheal plugs/casts. Upon inoculation of isolated blood heterophils with ILTV, DNA fibrous structures were observed in $2.0 \pm 0.1\%$ nuclei of ILTV inoculated blood heterophils at 24 hours post inoculation (hpi). In conclusion, the tracheal obstructions and suffocation of ILTV infected chickens are due to a strong thickening of the mucosa (inflammation) resulting in a reduced tracheal lumen diameter and the presence of mucoid plugs/casts containing stretched long DNA-fibrous structures (traps) but not MUC5AC and MUC5B mucins.

3.2.2. Introduction

Avian infectious laryngotracheitis virus remains a threat to the worldwide commercial poultry industry by decreased egg production, delayed growth and mortality (Fuchs *et al.*, 2007). ILTV belongs to the order *Herpesvirales*, family *Herpesviridae*, subfamily *Alphaherpesvirinae* and genus *Iltovirus* (Davison, 2010). ILTV replicates in the epithelial cell of the larynx, trachea, and conjunctiva mucosae, and invades underlying layers in a restricted manner (Garcia *et al.*, 2013; Reddy *et al.*, 2014). ILTV is usually highly cytolytic in the larynx and trachea mucosae, which may lead to severe mucosal epithelial damage and hemorrhages. The above pathological

changes cause the typical ILT clinical signs: coughing, nasal discharge, and conjunctivitis during a mild form and marked dyspnea, gasping, open mouth breathing and expectoration of bloody mucoïd material during a severe form (Bagust *et al.*, 2000; Garcia *et al.*, 2013). Mucoïd casts/plugs in the trachea obstruct airways and predispose chickens to die due to asphyxiation (Bagust *et al.*, 2000; Linares *et al.*, 1994).

After an acute laryngotracheitis infection, ILTV can establish a lifelong latency in the trigeminal ganglion of the central nervous system (Garcia *et al.*, 2013). Stress during rehousing with unfamiliar birds and onset of egg production cause sporadic reactivation followed by active replication of ILTV and horizontal transmission of ILTV to susceptible contact animals (Bagust *et al.*, 2000; Fuchs *et al.*, 2007).

Mucus is a viscoelastic and biopolymeric hydrogel, which coats the moist non-keratinized surface of mucosa. Mucus serves as a major protective layer on the mucosa, by forming a semipermeable barrier that enables the exchange of nutrients, gases and water, while being impermeable to most pathogens/foreign particles (Vareille *et al.*, 2011; Yang *et al.*, 2012). The mucus layer thickness differs among the species, location in the respiratory tract and health status. The major components of respiratory mucus are mucins. Up till now, at least 9 mucin genes have been reported in human airway mucus, with MUC5AC and MUC5B being the major gel forming mucins (Corfield, 2015). Mucin types may change during disease (Rose and Voynow, 2006) and many respiratory viruses stimulate mucus production in respiratory mucosa (Vareille *et al.*, 2011). During an acute ILTV infection, mucoïd plugs/casts are formed in the trachea and obstruction may lead to chicken mortality (Linares *et al.*, 1994). It has been postulated that the mucoïd plugs/casts are formed due to mucus hypersecretion, however there are no hard data proving this (Garcia *et al.*, 2013; Linares *et al.*, 1994).

In the present study, first we examined the expression of MUC5AC and MUC5B in the mucosae of larynx, trachea and bronchi of the mock-inoculated and ILTV infected chickens by immunofluorescence staining. Second, the tracheal lumen diameter and mucosal thickness were compared between the mock-inoculated and ILTV infected chickens to understand their role in obstruction of the trachea. Third, tracheas with mucoïd plugs/casts from euthanized ILTV infected chickens showing respiratory

distress were stained for MUC5AC and MUC5B and for DNA fibrous structures (extracellular network). Finally, the effect of ILTV on the formation of DNA fibrous-like structures from nuclei of blood heterophils was analyzed (Chuammitri *et al.*, 2009; Cortjens *et al.*, 2016; Funchal *et al.*, 2015; Goldmann and Medina, 2012; Raftery *et al.*, 2014; Zawrotniak and Rapala-Kozik, 2013).

3.2.3. Materials and Methods

3.2.3.1. ILTV (U76/1035) inoculation

Six 12 weeks specific pathogen free (SPF) White Leghorn chickens were individually tagged and housed in two experimental rooms. Drinking water and feed were provided *ad libitum*. A pathogenic Belgian isolate of ILTV (U76/1035) was used in this study (Meulemans and Halen, 1978; Reddy *et al.*, 2014). Before the start of the experiment, an acclimatization period of one-week was respected. At the age of 13 weeks, three chickens (group 1) were inoculated with the virulent ILTV (U76/1035) via intratracheal (300 μ l), nasal (50 μ l each nostril) and ocular routes (50 μ l each eye) with 10^4 EID₅₀/500 μ l. The second group of three animals was mock-inoculated with PBS and served as non-infected control. This study was in agreement with the guidelines of the Local Ethical and Animal Welfare Committee of the Faculty of Veterinary Medicine of Ghent University (EC 2015/81).

3.2.3.2. Clinical signs

Clinical signs were recorded daily until 5 days post inoculation (dpi), with special emphasis on bird breathing.

3.2.3.3. Euthanasia and collection of mock-inoculated and ILTV infected larynx, trachea and bronchi, and ILTV infected trachea with mucoïd plugs/casts

Larynx, trachea and bronchi were collected from three mock-inoculated (5 dpi) and three ILTV infected chickens (5 dpi). Equal sized tissues were prepared, embedded in Methocel[®] (Fluka) and frozen at -70°C.

In order to have a good yield of mucoïd plugs/casts in ILTV infected tracheal mucosa, chickens were humanely euthanized when they showed marked gasping and open mouth breathing with an extended neck (5 dpi). During necropsy, tracheas with mucoïd plugs/casts were collected in a gelatin capsule (size 000, Nova, Belgica

T.O.P. nv). The schematic procedure for collecting tracheas with mucoid plugs/casts from ILTV infected chickens is illustrated in Figure 1. Briefly, a trachea containing a mucoid plug/cast was placed vertically in a gelatin capsule. The gelatin capsule with trachea containing a mucoid plug/cast was immediately embedded in Methocel[®] in plastic tubes (Fluka) and were snap frozen for immunofluorescence staining.

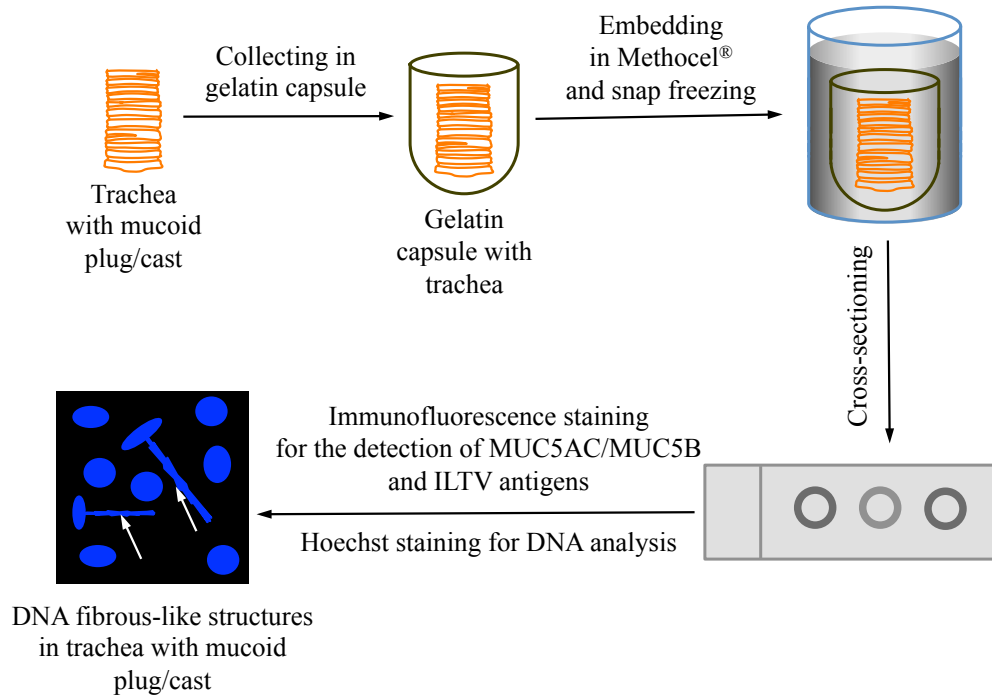


Figure 1. Schematic procedure of the collection of ILTV infected trachea with mucoid plug/cast in a gelatin capsule and of the evaluation of the results. A trachea containing a mucoid plug/cast was placed vertically in a gelatin capsule. The gelatin capsule with a trachea containing a mucoid plug/cast was immediately embedded in Methocel[®] and snap frozen. Cross-cryosections were made and processed for the detection of MUC5AC/MUC5B and ILTV antigens by immunofluorescence and for the detection of DNA fibrous structures by Hoechst staining.

3.2.3.4. Immunofluorescence staining for MUC5AC and MUC5B in laryngeal, tracheal and bronchial mucosae of mock-inoculated chickens

Immunofluorescence staining was performed to determine MUC5AC and MUC5B secretion in the mucosae of larynx, trachea and bronchi of mock-inoculated chickens. Cryosections of 10 μm were made from larynx, trachea and bronchi, fixed in 4% paraformaldehyde for 20 min at 4°C and permeabilized in 0.1% Triton[®] X-100 for 10 min at room temperature. For MUC5AC staining, the sections were incubated with mouse anti-MUC5AC monoclonal IgG₁ antibodies as primary antibody (45M1,

LifeSpan Biosciences, 1:100) and FITC labeled goat anti-mouse IgG polyclonal antibodies as secondary antibody (Molecular Probes, 1:200). For MUC5B staining, the sections were incubated with rabbit anti-MUC5B polyclonal antibodies as primary antibody (H-300, Santa Cruz Biotechnology, 1:100) and FITC labeled goat anti-rabbit IgG polyclonal antibodies as secondary antibody (Molecular Probes, 1:200). All antibodies were diluted in 10 mM phosphate buffer saline (PBS) and incubated for 1 h at 37°C. Two washings with PBS (10 min/each) were performed after each incubation step. The nuclei were counterstained with Hoechst 33342 (Molecular Probes, 1:100) for 10 min at room temperature. The sections were then washed twice and mounted with glycerin-DABCO (Sigma).

3.2.3.5. Immunofluorescence staining for MUC5AC/MUC5B and ILTV in laryngeal, tracheal and bronchial mucosae, and trachea with mucoid plugs/casts of ILTV infected chickens

Cryosections of 10 µm were made from ILTV infected larynx, trachea and bronchi, and trachea filled with mucoid plugs/casts. ILTV infected laryngeal, tracheal and bronchial mucosae and trachea with mucoid plugs/casts were visualized for MUC5AC, MUC5B and ILTV using the same technique as for the cryosections of laryngeal, tracheal and bronchial mucosae of mock-inoculated chickens. To visualize ILTV infection in laryngeal, tracheal and bronchial mucosae and trachea with mucoid plugs/casts, cryosections were incubated with mouse monoclonal anti-ILTV gC antibodies as primary antibody (1:50) (kindly provided by Walter Fuchs, Institute of Molecular Biology, Friedrich-Loeffler-Institute, Federal Research Institute for Animal Health, Greifswald-Insel Riems, Germany) and FITC labeled goat anti-mouse IgG polyclonal antibodies as secondary antibody (Molecular Probes, 1:100). To determine if mucin-producing cells were infected with ILTV, double immunofluorescence stainings were performed for MUC5B and ILTV. Hoechst was used to visualize cell nuclei. A confocal microscope (Leica TCS SPE confocal microscope) was used for the analysis of the presence of mucin and ILTV infected cells in laryngeal, tracheal and bronchial mucosae and trachea with mucoid plugs/casts.

3.2.3.5.1. Measurement of the diameter of tracheal lumen and the thickness of tracheal mucosa

The tracheal lumen diameter and mucosal thickness were evaluated in the mock-inoculated and ILTV infected chickens by using a confocal microscope. The epithelial layer and lamina propria layer were measured as mucosal thickness (Nunoya *et al.*, 1987). Ten randomly selected regions were considered for measurement in each chicken. The measurement was performed in tracheal rings of three mock-inoculated and three ILTV infected chickens. Student's t-test was used to compare the diameter of the tracheal lumen and the tracheal mucosal thickness between ILTV infected and control groups ($M \pm SD$, $n=3$).

3.2.3.6. Isolation of blood heterophils, inoculation of ILTV and immunostaining

Five ml blood was collected on heparin (15 IU/ml) (Leo) from the brachial wing vein of chickens. Heterophils were isolated from chicken whole blood by PolymorphprepTM gradient centrifugation as described by the manufacturer (Nycomed pharma). Polymorphonuclear cells were resuspended in RPMI-1640 (Gibco) medium containing 10% fetal calf serum (FCS, Gibco), 100 U/ml penicillin (Continental Pharma), 0.1 mg/ml streptomycin (Certa), 1 μ g/ml gentamycin (Gibco), and 1% non-essential amino acids (Gibco). Heterophil's viability was determined with 0.1% trypan blue and heterophil's morphology was analysed using Diff-Quick stained cytopsin preparations of cell suspensions. Mean viability of the isolated heterophils was $98.0 \pm 1.7\%$ (range between 96 and 99%, $n=3$). Mean purity of the heterophils was $95.7 \pm 1.5\%$ (range between 94 and 97%, $n=3$). Afterwards, 2×10^6 cells/ml were seeded in a 24-well plate (Nunc) and cultivated at 37°C with 5% CO₂. After one hour of cultivation, polymorphonuclear cells were inoculated with ILTV at a multiplicity of infection (m.o.i.) of 0.5. After 1 h of incubation (37°C, 5% CO₂), cells were washed two times with warm RPMI-1640 medium. Cells were collected at 0, 12 and 24 hpi to make cytopsin, and were visualized for ILTV using the same technique as for the cryosections of tracheas with mucoid plugs/casts. The nuclei were counterstained with Hoechst. All experiments were performed in triplicate. Immunostainings were analysed by confocal microscopy.

3.2.4. Results

3.2.4.1. Clinical signs and euthanasia

After ILTV inoculation, one chicken showed coughing at 2 dpi, and two chickens showed mild gasping at 3 dpi. At 4 dpi, all three chickens showed mild gasping and open mouth breathing. At 3 and 4 dpi, chickens were still active. Appetite of the ILTV infected chickens was normal until 4 dpi. Only at 5 dpi, severe gasping, marked dyspnea, expectoration of mucus and open mouth breathing with an extended neck were observed in all three ILTV inoculated chickens. Chickens were euthanized at 5 dpi. At necropsy, intraluminal mucoid plugs/casts were observed that completely filled the trachea of ILTV infected chickens (Figure 2C). None of the mock-inoculated chickens showed clinical signs during the whole experiment. Mucoid plugs/casts were not observed in tracheal lumen of mock-inoculated chickens (Figure 2A).

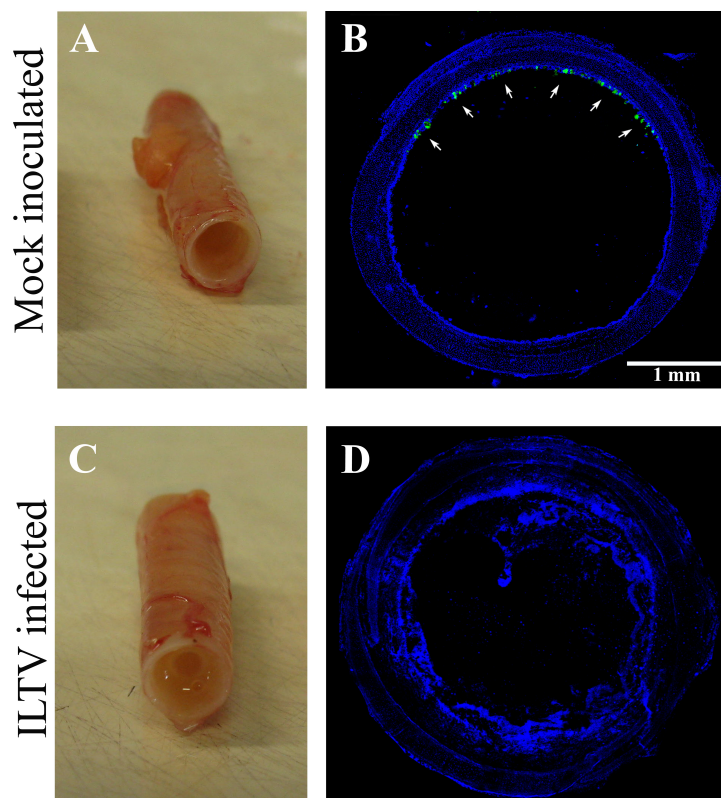


Figure 2. Representative macroscopic picture and confocal photomicrographs of a mock-inoculated trachea (A and B) and an ILTV infected trachea with an intraluminal mucoid plug/cast (C and D) after euthanasia (5 dpi). (A) Tracheal ring from a mock-inoculated chicken, free of plugs. (B) MUC5AC was exclusively distributed (arrows)

in the dorsal region of the trachea. (C) Tracheal ring from a chicken at 5 days post ILTV inoculation; note the obstruction with a jelly plug. (D) Epithelial cell layer was almost completely destroyed, submucosa was swollen and mucins were hardly observed in ILTV infected tracheal mucosa and mucoid plugs/casts. Green fluorescence visualises MUC5AC (arrows). Cell nuclei were stained with Hoechst (blue).

3.2.4.2. MUC5AC and MUC5B production in laryngeal, tracheal and bronchial mucosae of mock-inoculated chickens

MUC5AC and MUC5B were produced by the epithelial cells of laryngeal, tracheal and bronchial mucosae of mock-inoculated chickens. More MUC5B was produced compared to MUC5AC in laryngeal, tracheal and bronchial mucosae of mock-inoculated chickens (Table 1). The MUC5AC and MUC5B protein domain organization is similar between humans and chickens and therefore the affinity is predicted to be similar (Lang *et al.*, 2006). In our laboratory, MUC5AC and MUC5B immunofluorescence staining was compared simultaneously with respiratory mucosae of chickens, humans and pigs (Yang, 2015). MUC5AC production was higher than that of MUC5B in the respiratory tract of humans and pigs whereas the situation was reversed in chickens (Kirkham *et al.*, 2002; Rose and Voynow, 2006; Yang, 2015).

Table 1. MUC5AC and MUC5B expression in the normal and ILTV infected respiratory mucosa, and ILTV infected mucoid plugs/casts.

Infection status	Tissue/casts	Immunofluorescence score*	
		MUC5AC	MUC5B
Mock-infected	Larynx (dorsal mucosa)	++	+++
	Trachea (dorsal mucosa)	++	+++
	Bronchi	+/-	++
ILTV	Larynx	+/-	+/-
	Trachea	+/-	+/-
	Bronchi	+/-	+/-
	Mucoid plugs/casts	+/-	+/-

Score for Positive cells *: +/- <1% of the cells; + 1-5%; ++ 6-15%; +++ 16-30%; +++++ >30%

In general, MUC5AC and MUC5B production was higher in larynx and trachea than in bronchi (Table 1). Representative confocal images of the production of MUC5AC and MUC5B in tracheal mucosa of mock-inoculated chickens are illustrated in Figure

3. Interestingly, MUC5AC and MUC5B were exclusively distributed in the dorsal tracheal region of the tracheal mucosa. The dorsal distribution of MUC5AC and MUC5B was predominantly observed in the cranial and middle part of the trachea. In the caudal part of the trachea, MUC5AC and MUC5B were distributed in lateral and ventral sides along with dorsal distribution. A representative confocal image of MUC5AC distribution in the dorsal region of the cranial tracheal ring is presented in Figure 2B.

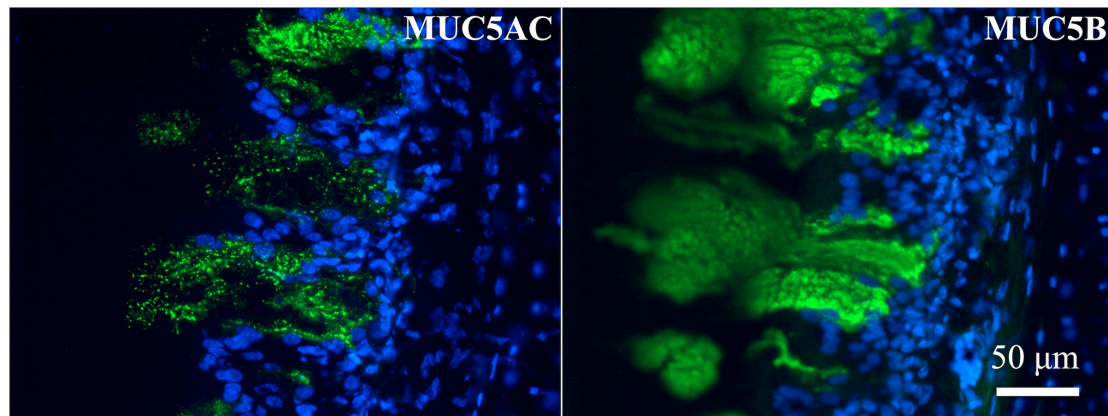


Figure 3. Confocal photomicrographs illustrating the production of MUC5AC and MUC5B in tracheal mucosa of mock-inoculated chicken. MUC5B production was higher compared to MUC5AC. Green fluorescence visualises MUC5AC and MUC5B. Cell nuclei were stained with Hoechst (blue).

3.2.4.3. Immunofluorescence staining for MUC5AC/MUC5B and ILTV in laryngeal, tracheal and bronchial mucosae, and trachea with muroid plugs/casts of ILTV infected chickens

ILTV infected laryngeal, tracheal and bronchial mucosae, and trachea with muroid plugs/casts were stained for MUC5AC, MUC5B and ILTV. Immunofluorescence staining showed that the epithelial cell layer was desquamated (Figure 2D). The epithelial and lamina propria layers were observed to be swollen in ILTV infected tracheal mucosa, and that was suggestive of marked tracheal edema, congestion and thickened tracheal mucosa (Figure 2B and 2D). Thus, the tracheal lumen diameter and mucosal thickness were measured to address differences between control and ILTV infected groups.

3.2.4.3.1. Measurement of the diameter of the tracheal lumen and the thickness of tracheal mucosa

The tracheal lumen diameter and mucosal thickness were measured using Leica confocal software (Figure 4). The mean diameter for the ILTV infected group was $1318.8 \pm 24.3 \mu\text{m}$, while for the control group the diameter was $2010.2 \pm 62.9 \mu\text{m}$. The mean tracheal mucosal thickness on top of the cartilaginous layer for the ILTV infected group was $685.5 \pm 55.5 \mu\text{m}$, whereas that for the control group thickness was $105.1 \pm 4.0 \mu\text{m}$. The tracheal lumen diameter and the mucosal thickness were significantly different between the infected and control groups ($P < 0.05$).

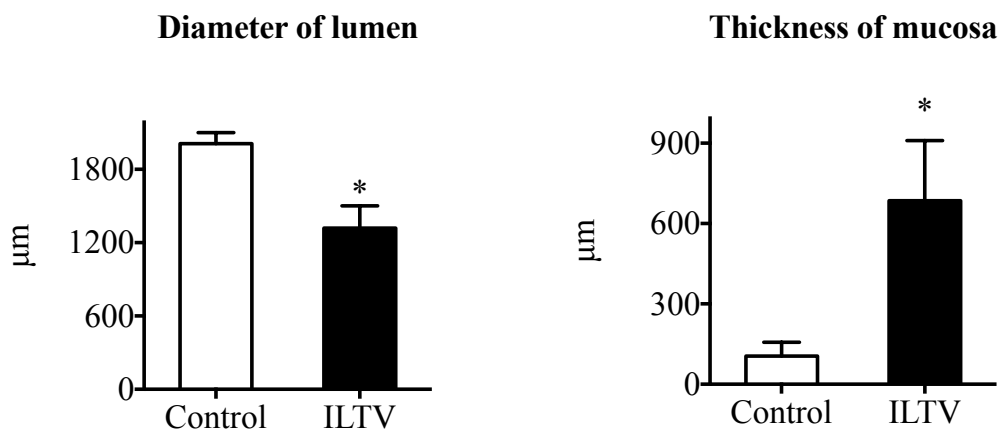


Figure 4. The diameter of the tracheal lumen and the mucosal thickness. The diameter of tracheal lumen and the tracheal mucosal thickness were evaluated from ILTV infected and control chickens. Mean and standard deviation (SD) are shown for each group. An asterisk (*) indicates statistically significant difference ($P < 0.05$) between ILTV infected and control groups.

3.2.4.3.2. MUC5AC and MUC5B were scarce in ILTV infected laryngeal, tracheal and bronchial mucosae, and trachea with mucoid plugs/casts

MUC5AC and MUC5B were sparsely observed in the ILTV infected laryngeal, tracheal and bronchial mucosae, and trachea containing mucoid plugs/casts (Table 1, and Figure 2D and 5). Further, ILTV infected cells were hardly observed in laryngeal, tracheal and bronchial mucosae, and were not observed in the trachea containing mucoid plugs/casts. Surprisingly, the nuclei of $10.0 \pm 7.3\%$ of the cells contained DNA fibrous-like structures linked with the nucleus in the mucoid plugs/casts. The DNA fibrous-like structures in the mucoid plugs/casts were identified as stretched long DNA fibrous threads of $17.8 \pm 6.5 \mu\text{m}$ in length (Figure 6). These DNA fibrous

structures originated from nuclei and protruded beyond the cell margins in the environment. The DNA fibrous-like structures connected to nuclei of ILTV infected trachea with mucoid plugs/casts were very similar to extracellular networks of DNA as reported by Chuammitri et al. (2009), Goldmann and Medina, (2012), Zawrotniak and Rapala-Kozik (2013), Raftery (2014), Funchal (2015) and Cortjens (2016) in neutrophils and heterophils. The percentage of DNA fibrous-like structures was determined in 10 randomly selected fields of 300 cells that were present in mucoid plugs/casts. The DNA fibrous-like structures were mainly present at the periphery of the mucoid plugs/casts (in the area of desquamated epithelial layer). The DNA fibrous-like structures were not observed in mock-inoculated chickens.

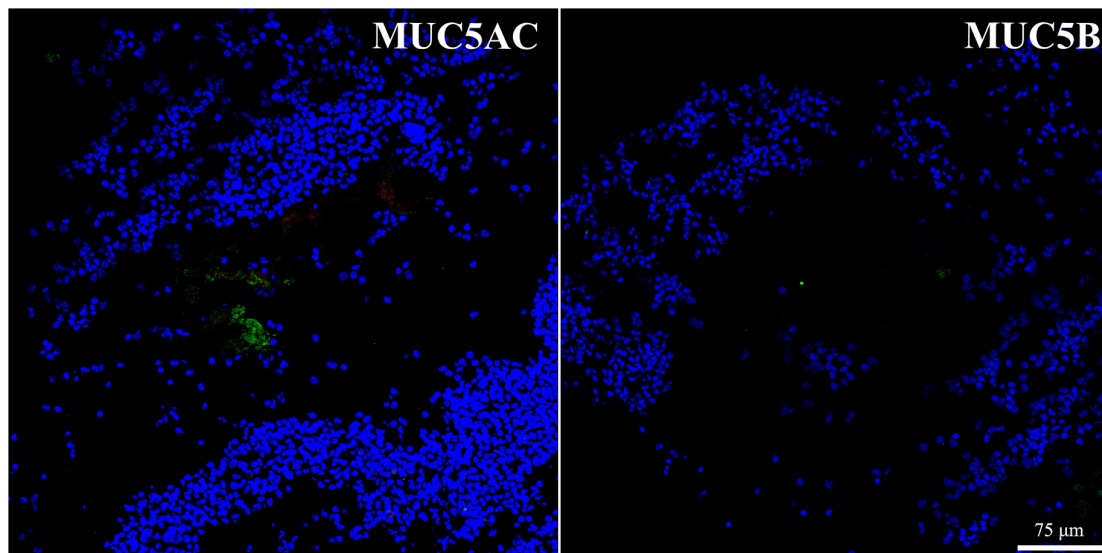


Figure 5. Immunofluorescence of MUC5AC and MUC5B in the trachea with mucoid plugs/casts of ILTV infected chickens. MUC5AC and MUC5B were scarcely present in the trachea with mucoid plugs/casts of ILTV infected chickens. Green fluorescence visualises MUC5AC and MUC5B. Cell nuclei were stained with Hoechst (blue).

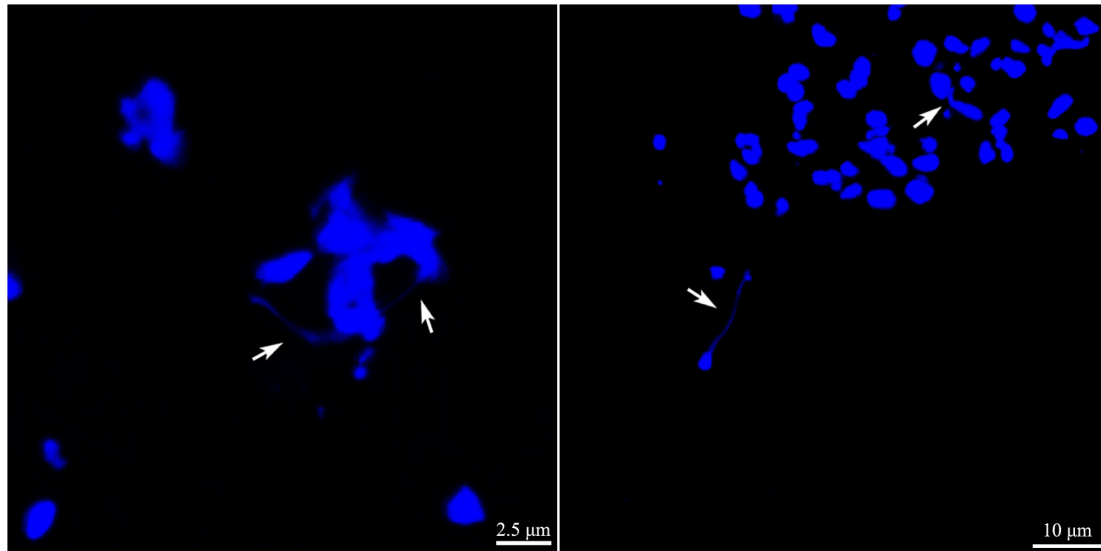


Figure 6. . Fluorescent images taken by means of confocal microscopy from nuclei of trachea with mucoïd plugs/casts of ILTV infected chickens at 5 dpi. DNA fibrous-like structures from nuclei of trachea with mucoïd plugs/casts were present (arrows). Cell nuclei were stained with Hoechst (blue).

We have hypothesized that cells showing these DNA fibrous-like structures in the mucoïd plugs/casts could be immune cells, especially macrophages and heterophils. Hence, the KUL01 marker (marker for monocytes and macrophages) was used to check the cell type that shows DNA fibrous-like structures in the mucoïd plugs/casts. These cells were not monocytes/macrophages. Further, ILTV interactions were evaluated in peripheral blood mononuclear cells (PBMCs). The DNA fibrous-like structures were not observed in ILTV inoculated PBMCs. Currently, there are no markers available specific for heterophils of chickens. Therefore, it was not possible to check whether the DNA fibrous-like structures were formed by heterophils in the trachea containing mucoïd plugs/casts. As an alternative, an ILTV inoculation experiment with isolated blood heterophils was performed.

3.2.4.4. DNA fibrous-like structures from nuclei of ILTV inoculated blood heterophils

The percentage of heterophils with DNA fibrous-like structures was determined in 10 randomly selected fields of ILTV inoculated blood heterophils. At 24 hpi, only 2.0 ± 0.1 % nuclei of ILTV inoculated blood heterophils showed DNA fibrous-like structures, suggesting that heterophils are most probably not the only cells that have DNA fibrous structures in tracheas containing mucoïd plugs/casts. These structures

were not observed at 0 and 12 hpi, and in the control heterophils (Figure 7). We have started to work on the role of other cell types in the formation of DNA fibrous-like structures in tracheas with mucoid plugs/casts. The results of that work will be published in a future paper.

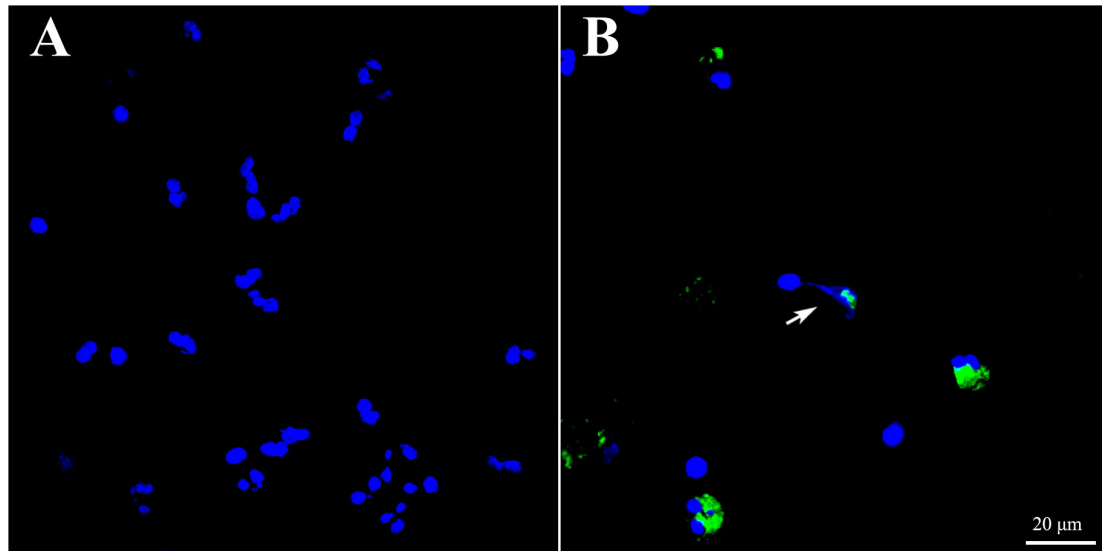


Figure 7. Confocal photomicrographs of mock-inoculated (A) and ILTV inoculated heterophils (B). Mock-inoculated blood heterophils with segmented nuclei. DNA fibrous-like structures from nuclei of ILTV inoculated blood heterophils were similar to neutrophil/heterophil extracellular networks (arrows). Green fluorescence visualises ILTV antigens taken up by the heterophils. Cell nuclei were stained with Hoechst (blue).

3.2.5. Discussion

During acute ILTV infection, the formation of mucoid plugs/casts in the trachea is the main cause for asphyxiation and mortality in chickens (Linares *et al.*, 1994). Although it has been postulated that the trachea obstruction is due to mucus hypersecretion (Garcia *et al.*, 2013; Linares *et al.*, 1994), there are no published reports supporting this hypothesis. Thus, we wished to determine if there is any change of mucin secretion in ILTV infected animals leading to plugs/casts in the lumen of the trachea.

MUC5AC and MUC5B mucins were extensively produced in the superficial epithelium of laryngeal, tracheal and bronchial mucosae of mock-inoculated chickens. This is in line with the respiratory mucosa of humans and pigs (Kirkham *et al.*, 2002). MUC5B expression was more pronounced than that of MUC5AC in laryngeal, tracheal and bronchial mucosae of mock-inoculated chickens, which is opposite to the

situation in humans and pigs (Kirkham *et al.*, 2002; Rose and Voynow, 2006; Yang, 2015). The mucin MUC5AC and MUC5B production was higher in larynx and trachea compared to bronchi. In evolution, the innate defense mechanism of mucins at larynx and trachea, may be anatomically more relevant and necessary to protect against initial entry and interactions of pathogens/foreign substances than at bronchi. This could be the main reason for the higher expression of mucin secretory glands in larynx and trachea than in bronchi.

An important observation of this study was that the MUC5AC and MUC5B mucins were only present at the dorsal tracheal region of the cranial and middle tracheal mucosa. This property may have been developed in evolution to restrict the entry of pathogens/foreign substances via dorsal surface, the area where the air has the largest impact on the mucosa. When the pathogens naturally enter through the respiratory route, they may directly hit the dorsal surface of the mucosa, where they can attach and invade. In evolution, to block the initial entry of pathogens, the mucosa may have developed mucus secretory goblet cells at the dorsal surface. ILTV may have infected mainly the areas without mucus secretory goblet cells (lateral and ventral areas). Earlier in our laboratory, Yang *et al.* (2012 and 2015) have reported that MUC5AC producing tracheal epithelial cells were resistant to alphaherpesvirus of pigs, and alphaherpesvirus mobility was fully blocked in porcine tracheal respiratory mucus. In addition, in chickens we have observed that MUC5B producing primary tracheal epithelial cells were not susceptible to ILTV infection (data not shown). Therefore, we have indicated that ILTV infection may have occurred mainly in non mucin secreting lateral and ventral areas of cranial and middle tracheal mucosa of chickens (Yang, 2015).

In ILTV infected chickens, the tracheal mucosa thickness was nearly 6.5 times higher compared to the tracheal mucosa thickness of control chickens, and which is the main reason for almost 40% reduced diameter of the lumen in infected trachea. The important factors behind the increased tracheal mucosal thickness are most probably marked congestion, severe edema and massive infiltration of heterophils, macrophages, lymphocytes and plasma cells in the mucosa and submucosa (Devlin *et al.*, 2006; Garcia *et al.*, 2013; Hayashi *et al.*, 1985). Thus, the present study strongly corroborates that the increased mucosal thickness and its associated reduced tracheal lumen is one of the important reason for the obstruction of the trachea at 5 dpi of

ILTV causing severe respiratory problems. In the past, many studies have reported that respiratory infection or inflammation is associated with increased mucosal thickness (Bowden *et al.*, 1996; Kita *et al.*, 2009; Nunoya *et al.*, 1987; Sajjan *et al.*, 2004). The mucosal thickness measuring is an established system for determining the degree of tracheal infection in *Mycoplasma gallisepticum* infections of chickens (Gaunson *et al.*, 2000; Nunoya *et al.*, 1987; Sprygin *et al.*, 2011; Zaki *et al.*, 2004). Devlin *et al.* (2006) used the tracheal mucosal thickness to evaluate the virulence of ILTV.

Mucin production was sparsely observed in the ILTV infected mucosa. The results presented here are somewhat in contrast with another study, where hypertrophic goblet cells were observed in the mucosa at 5 dpi with a low virulent ILTV strain (A4557-5) (Russell, 1983). The strain used, virulence of virus, experimental design and conditions, intercurrent infections and detection techniques may explain this discrepancy in mucin secretion.

MUC5AC and MUC5B mucins were scarcely present in the trachea-mucoid plugs/casts, which does not fit with the assumption that the mucoid plugs/casts are associated with mucus hypersecretion (Garcia *et al.*, 2013; Linares *et al.*, 1994). The gel that was present in the ILTV infected tracheae may be explained by the release of a DNA network. Indeed, DNA fibrous-like structures were present in 10% of the cells in the trachea-mucoid plugs/casts. These structures were very similar to the extracellular networks of neutrophils/heterophils (Chuammitri *et al.*, 2009; Cortjens *et al.*, 2016; Funchal *et al.*, 2015; Goldmann and Medina, 2012; Raftery *et al.*, 2014; Zawrotniak and Rapala-Kozik, 2013). A network of DNA may form a jelly substance. The scarce presence of mucin in the trachea-mucoid plugs/casts, and presence of extracellular networks like DNA fibrous structures in the nuclei of the trachea-mucoid plugs/casts of ILT is in line with what has been shown with the sputum and mucus of cystic fibrosis patients (Henke *et al.*, 2004; Lethem *et al.*, 1990; Rubin, 2007). In this sputum and mucus, the DNA source has been reported to be from neutrophils. The extracellular DNA network was shown to be associated with bacterial colonization (Henke *et al.*, 2004; Lundgren and Baraniuk, 1992; Rahman and Gadjeva, 2014). Further, the DNA was reported to give high adhesive and viscoelastic properties to sputum and mucus of cystic fibrosis patients (Lethem *et al.*, 1990; Zawrotniak and Rapala-Kozik, 2013). Similarly, during ILT infection, we have observed that the

trachea-mucoid plugs/casts were highly adhesive and viscoelastic (data not shown), and the DNA fibrous-like structures may be at the basis of this property.

Usually, an extracellular DNA network is a defense mechanism of host cells towards pathogenic microorganisms (Goldmann and Medina, 2012). The extracellular network during an acute ILTV infection may also be a strategy to control virus replication and eliminate the virus in the respiratory mucosa. The formation of an extracellular DNA network generally starts with the loss of the tight organization of the nuclei followed by chromatin decondensation. Then, the characteristic shape of nuclei disappears and chromatin leaks into the cytoplasm. Finally, antimicrobial proteins absorb to the decondensed chromatin, and becomes released DNA into the extracellular milieu (Chuammitri *et al.*, 2009; Goldmann and Medina, 2012). Up till now, heterophils/neutrophils, mast cells and macrophages have been reported to release extracellular networks to trap and kill viruses, bacteria, fungi and parasites (Bruns *et al.*, 2010; Chow *et al.*, 2010; Goldmann and Medina, 2012; Linch *et al.*, 2009; Lippolis *et al.*, 2006; Saitoh *et al.*, 2012; von Kockritz-Blickwede *et al.*, 2008; Yousefi *et al.*, 2008). During an acute ILTV infection, the decondensed DNA fibrous structures may be released either from infiltrated heterophils/other immune cells or from desquamated epithelial cells of the respiratory mucosa (Bagust *et al.*, 2000; Linares *et al.*, 1994). The decondensed DNA fibrous structures may trap cellular debris, proteins, lipids, cations and other non-mucin components, which may have been released due to hemorrhages and necrosis of the mucosa during acute ILTV (Garcia *et al.*, 2013; Lethem *et al.*, 1990; Linares *et al.*, 1994). A DNA network with these trapped substances form together a jelly plug in the trachea and obstruct normal airways of chickens, and may cause asphyxiation.

In cystic fibrosis cases, aerosolized deoxyribonuclease I (DNase I, Dornase Alfa) has been effectively used to treat sputum/mucus casts containing DNA fibrous structures (Rogers, 2007; Shak, 1995; Shak *et al.*, 1990). Thus, aerosol administration of DNase I could be helpful to alleviate the dyspnea, gasping, open mouth breathing and suffocation during an ILTV infection. Further, mucoactive agents such as mucolytics, expectorants and mucokinetics will not be useful to reduce clinical signs of acute ILTV disease (Rogers, 2007).

Secretory mucins such as MUC5AC, MUC5B and MUC2 and membrane-tethered mucins such as MUC1 and MUC4 have been reported to contribute to the innate immune defense and mucociliary clearance in airways of healthy humans (Rose and Voynow, 2006). In chronic airway diseases of humans, MUC5AC, MUC5B, MUC8 and MUC2 mucins have been identified in the sputum samples (Rose and Voynow, 2006). There are fewer reports on the presence of other secretory and membrane-tethered mucins in airways of healthy and diseased chickens, except for MUC5AC and MUC5B. In chickens, there are only a few reports available that demonstrate the presence of several mucin genes based on prediction with bioinformatics tools (MUC2, MUC4, MUC6, MUC13 and MUC16) and mRNA gene expression studies (MUC2) (Fan et al., 2015; Lang et al., 2006). However, the functional roles of these mucins were still unknown (Fan *et al.*, 2015; Lang *et al.*, 2006; Rose and Voynow, 2006). Currently, there are antibodies available only against MUC5AC and MUC5B mucins but not against other secretory and membrane-tethered mucins of airways of chickens. Thus, the presence of other than MUC5AC and MUC5B mucin types cannot be excluded in laryngeal, tracheal and bronchial mucosae of healthy and ILTV infected chickens, and in tracheas containing mucoid plugs/casts of ILTV infected chickens.

Mucoid plug/cast formation with asphyxiation is mainly associated with ILT, when compared with other avian respiratory diseases such as Infectious bronchitis, Newcastle disease, Influenza (H9N2 is an exception) and *Mycoplasma gallisepticum* (Bagust *et al.*, 2000; Garcia *et al.*, 2013; Linares *et al.*, 1994; Nili and Asasi, 2002; Wu *et al.*, 2008). The specific activation of DNA fibrous structure formation during ILT may be the main reason for this difference. In the future, the molecular mechanism will be unraveled.

In summary, MUC5AC and MUC5B were the gel-forming mucins produced by the epithelium of laryngeal, tracheal and bronchial mucosae of mock-inoculated chickens. The presence of other mucin types in healthy airways of chickens cannot be excluded. MUC5AC and MUC5B were present only in the dorsal tracheal region of the cranial and middle part of the tracheal mucosa of mock-inoculated chickens. Tracheas with mucoid plugs/casts of ILTV infected chickens contained DNA fibrous structures connected with nuclei but not MUC5AC and MUC5B mucins. The absence of other mucin types cannot be stated in the airways and tracheas with mucoid plugs/casts of

ILTV infected chickens. Taken together, the tracheal obstructions and suffocation of ILTV infected chickens were associated with the presence of DNA fibrous structures connected with nuclei of cells in tracheas containing mucoid plugs/casts, which together with the swelling of the mucosa reduced the diameter of the tracheal lumen.

3.2.6. Acknowledgements

The authors acknowledge Magda De Keyzer and Lieve Sys for their excellent technical assistance, Thierry van den Berg for providing the virus and Zeger Van den Abeele and Loes Geypen for their help with handling and euthanizing the chickens.

3.2.7. References

- Bagust, T.J., Jones, R.C., Guy, J.S., 2000. Avian infectious laryngotracheitis. *Rev Sci Tech* 19, 483-492.
- Bowden, J.J., Baluk, P., Lefevre, P.M., Schoeb, T.R., Lindsey, J.R., McDonald, D.M., 1996. Sensory denervation by neonatal capsaicin treatment exacerbates *Mycoplasma pulmonis* infection in rat airways. *Am J Physiol* 270, L393-403.
- Bruns, S., Kniemeyer, O., Hasenberg, M., Amanianda, V., Nietzsche, S., Thywissen, A., Jeron, A., Latge, J.P., Brakhage, A.A., Gunzer, M., 2010. Production of extracellular traps against *Aspergillus fumigatus* in vitro and in infected lung tissue is dependent on invading neutrophils and influenced by hydrophobin RodA. *PLoS Pathog* 6, e1000873.
- Chow, O.A., von Kockritz-Blickwede, M., Bright, A.T., Hensler, M.E., Zinkernagel, A.S., Cogen, A.L., Gallo, R.L., Monestier, M., Wang, Y., Glass, C.K., Nizet, V., 2010. Statins enhance formation of phagocyte extracellular traps. *Cell Host Microbe* 8, 445-454.
- Chuammitri, P., Ostojic, J., Andreasen, C.B., Redmond, S.B., Lamont, S.J., Palic, D., 2009. Chicken heterophil extracellular traps (HETs): novel defense mechanism of chicken heterophils. *Vet Immunol Immunopathol* 129, 126-131.
- Corfield, A.P., 2015. Mucins: a biologically relevant glycan barrier in mucosal protection. *Biochim Biophys Acta* 1850, 236-252.
- Cortjens, B., de Boer, O.J., de Jong, R., Antonis, A.F., Sabogal Pineros, Y.S., Lutter, R., van Woensel, J.B., Bem, R.A., 2016. Neutrophil extracellular traps cause airway obstruction during respiratory syncytial virus disease. *J Pathol* 238, 401-411.
- Davison, A.J., 2010. Herpesvirus systematics. *Vet Microbiol* 143, 52-69.

- Devlin, J.M., Browning, G.F., Hartley, C.A., Kirkpatrick, N.C., Mahmoudian, A., Noormohammadi, A.H., Gilkerson, J.R., 2006. Glycoprotein G is a virulence factor in infectious laryngotracheitis virus. *J Gen Virol* 87, 2839-2847.
- Fan, X., Liu, S., Liu, G., Zhao, J., Jiao, H., Wang, X., Song, Z., Lin, H., 2015. Vitamin A Deficiency Impairs Mucin Expression and Suppresses the Mucosal Immune Function of the Respiratory Tract in Chicks. *PLoS One* 10, e0139131.
- Fuchs, W., Veits, J., Helferich, D., Granzow, H., Teifke, J.P., Mettenleiter, T.C., 2007. Molecular biology of avian infectious laryngotracheitis virus. *Vet Res* 38, 261-279.
- Funchal, G.A., Jaeger, N., Czepielewski, R.S., Machado, M.S., Muraro, S.P., Stein, R.T., Bonorino, C.B., Porto, B.N., 2015. Respiratory syncytial virus fusion protein promotes TLR-4-dependent neutrophil extracellular trap formation by human neutrophils. *PLoS One* 10, e0124082.
- Garcia, M., Spatz, S., Guy, J.S., 2013. Laryngotracheitis, Vol 13. Ames: Blackwell, 161-179 pp.
- Gaunson, J.E., Philip, C.J., Whithear, K.G., Browning, G.F., 2000. Lymphocytic infiltration in the chicken trachea in response to *Mycoplasma gallisepticum* infection. *Microbiology* 146 (Pt 5), 1223-1229.
- Goldmann, O., Medina, E., 2012. The expanding world of extracellular traps: not only neutrophils but much more. *Front Immunol* 3, 420.
- Hayashi, S., Odagiri, Y., Kotani, T., Horiuchi, T., 1985. Pathological changes of tracheal mucosa in chickens infected with infectious laryngotracheitis virus. *Avian Dis* 29, 943-950.
- Henke, M.O., Renner, A., Huber, R.M., Seeds, M.C., Rubin, B.K., 2004. MUC5AC and MUC5B Mucins Are Decreased in Cystic Fibrosis Airway Secretions. *Am J Respir Cell Mol Biol* 31, 86-91.
- Kirkham, S., Sheehan, J.K., Knight, D., Richardson, P.S., Thornton, D.J., 2002. Heterogeneity of airways mucus: variations in the amounts and glycoforms of the major oligomeric mucins MUC5AC and MUC5B. *Biochem J* 361, 537-546.
- Kita, T., Fujimura, M., Myou, S., Watanabe, K., Waseda, Y., Nakao, S., 2009. Effects of KF19514, a phosphodiesterase 4 and 1 Inhibitor, on bronchial inflammation and remodeling in a murine model of chronic asthma. *Allergol Int* 58, 267-275.
- Lang, T., Hansson, G.C., Samuelsson, T., 2006. An inventory of mucin genes in the chicken genome shows that the mucin domain of Muc13 is encoded by multiple exons and that ovomucin is part of a locus of related gel-forming mucins. *BMC Genomics* 7, 197.

- Lethem, M.I., James, S.L., Marriott, C., Burke, J.F., 1990. The origin of DNA associated with mucus glycoproteins in cystic fibrosis sputum. *Eur Respir J* 3, 19-23.
- Linares, J.A., Bickford, A.A., Cooper, G.L., Charlton, B.R., Woolcock, P.R., 1994. An outbreak of infectious laryngotracheitis in California broilers. *Avian Dis* 38, 188-192.
- Linch, S.N., Kelly, A.M., Danielson, E.T., Pero, R., Lee, J.J., Gold, J.A., 2009. Mouse eosinophils possess potent antibacterial properties in vivo. *Infect Immun* 77, 4976-4982.
- Lippolis, J.D., Reinhardt, T.A., Goff, J.P., Horst, R.L., 2006. Neutrophil extracellular trap formation by bovine neutrophils is not inhibited by milk. *Vet Immunol Immunopathol* 113, 248-255.
- Lundgren, J.D., Baraniuk, J.N., 1992. Mucus secretion and inflammation. *Pulm Pharmacol* 5, 81-96.
- Meulemans, G., Halen, P., 1978. Some physico-chemical and biological properties of a Belgian strain (U 76/1035) of infectious laryngotracheitis virus. *Avian Pathol* 7, 311-315.
- Nili, H., Asasi, K., 2002. Natural cases and an experimental study of H9N2 avian influenza in commercial broiler chickens of Iran. *Avian Pathol* 31, 247-252.
- Nunoya, T., Tajima, M., Yagihashi, T., Sannai, S., 1987. Evaluation of respiratory lesions in chickens induced by *Mycoplasma gallisepticum*. *Nihon Juigaku Zasshi* 49, 621-629.
- Raftery, M.J., Lalwani, P., Krautkrmer, E., Peters, T., Scharffetter-Kochanek, K., Kruger, R., Hofmann, J., Seeger, K., Kruger, D.H., Schonrich, G., 2014. beta2 integrin mediates hantavirus-induced release of neutrophil extracellular traps. *J Exp Med* 211, 1485-1497.
- Rahman, S., Gadjeva, M., 2014. Does NETosis Contribute to the Bacterial Pathoadaptation in Cystic Fibrosis? *Front Immunol* 5, 378.
- Reddy, V.R., Steukers, L., Li, Y., Fuchs, W., Vanderplasschen, A., Nauwynck, H.J., 2014. Replication characteristics of infectious laryngotracheitis virus in the respiratory and conjunctival mucosa. *Avian Pathol* 43, 450-457.
- Rogers, D.F., 2007. Mucoactive agents for airway mucus hypersecretory diseases. *Respir Care* 52, 1176-1193; discussion 1193-1177.
- Rose, M.C., Voynow, J.A., 2006. Respiratory tract mucin genes and mucin glycoproteins in health and disease. *Physiol Rev* 86, 245-278.
- Rubin, B.K., 2007. Mucus structure and properties in cystic fibrosis. *Paediatr Respir Rev* 8, 4-7.

- Russell, R.G., 1983. Respiratory tract lesions from infectious laryngotracheitis virus of low virulence. *Vet Pathol* 20, 360-369.
- Saitoh, T., Komano, J., Saitoh, Y., Misawa, T., Takahama, M., Kozaki, T., Uehata, T., Iwasaki, H., Omori, H., Yamaoka, S., Yamamoto, N., Akira, S., 2012. Neutrophil extracellular traps mediate a host defense response to human immunodeficiency virus-1. *Cell Host Microbe* 12, 109-116.
- Sajjan, U., Moreira, J., Liu, M., Humar, A., Chaparro, C., Forstner, J., Keshavjee, S., 2004. A novel model to study bacterial adherence to the transplanted airway: inhibition of *Burkholderia cepacia* adherence to human airway by dextran and xylitol. *J Heart Lung Transplant* 23, 1382-1391.
- Shak, S., 1995. Aerosolized recombinant human DNase I for the treatment of cystic fibrosis. *Chest* 107, 65S-70S.
- Shak, S., Capon, D.J., Hellmiss, R., Marsters, S.A., Baker, C.L., 1990. Recombinant human DNase I reduces the viscosity of cystic fibrosis sputum. *Proc Natl Acad Sci U S A* 87, 9188-9192.
- Sprygin, A.V., Elatkin, N.P., Kolotilov, A.N., Volkov, M.S., Sorokina, M.I., Borisova, A.V., Andreychuk, D.B., Mudrak, N.S., Irza, V.N., Borisov, A.V., Drygin, V.V., 2011. Biological characterization of Russian *Mycoplasma gallisepticum* field isolates. *Avian Pathol* 40, 213-219.
- Vareille, M., Kieninger, E., Edwards, M.R., Regamey, N., 2011. The airway epithelium: soldier in the fight against respiratory viruses. *Clin Microbiol Rev* 24, 210-229.
- von Kockritz-Blickwede, M., Goldmann, O., Thulin, P., Heinemann, K., Norrby-Teglund, A., Rohde, M., Medina, E., 2008. Phagocytosis-independent antimicrobial activity of mast cells by means of extracellular trap formation. *Blood* 111, 3070-3080.
- Wu, R., Sui, Z.W., Zhang, H.B., Chen, Q.J., Liang, W.W., Yang, K.L., Xiong, Z.L., Liu, Z.W., Chen, Z., Xu, D.P., 2008. Characterization of a pathogenic H9N2 influenza A virus isolated from central China in 2007. *Arch Virol* 153, 1549-1555.
- Yang, X., 2015. Interactions of Pseudorabies virus and swine Influenza virus with Porcine Respiratory mucus. Ghent University, Merlbeke, Belgium
- Yang, X., Forier, K., Steukers, L., Van Vlierberghe, S., Dubruel, P., Braeckmans, K., Glorieux, S., Nauwynck, H.J., 2012. Immobilization of pseudorabies virus in porcine tracheal respiratory mucus revealed by single particle tracking. *PLoS One* 7, e51054.
- Yousefi, S., Gold, J.A., Andina, N., Lee, J.J., Kelly, A.M., Kozlowski, E., Schmid, I., Straumann, A., Reichenbach, J., Gleich, G.J., Simon, H.U., 2008. Catapult-like release of mitochondrial DNA by eosinophils contributes to antibacterial defense. *Nat Med* 14, 949-953.

Zaki, M.M., Ferguson, N., Leiting, V., Kleven, S.H., 2004. Safety of *Mycoplasma gallisepticum* vaccine strain 6/85 after backpassage in turkeys. *Avian Dis* 48, 642-646.

Zawrotniak, M., Rapala-Kozik, M., 2013. Neutrophil extracellular traps (NETs) - formation and implications. *Acta Biochim Pol* 60, 277-284.

CHAPTER 4.

Study of infectious bronchitis virus (IBV) replication characteristics

CHAPTER 4.1.

Genetic characterization of the Belgian nephropathogenic infectious bronchitis virus (NIBV) reference strain B1648

Vishwanatha R.A.P. Reddy, Sebastiaan Theuns, Inge D.M. Roukaerts, Mark Zeller,
Jelle Matthijnsens and Hans J. Nauwynck

Viruses (2015), 7(8): 4488-506

4.1.1. Abstract

The virulent nephropathogenic infectious bronchitis virus (NIBV) strain B1648 was first isolated in 1984, in Flanders, Belgium. Despite intensive vaccination, B1648 and its variants are still circulating in Europe and North Africa. Here, the full-length genome of this Belgian NIBV reference strain was determined by next generation sequencing (NGS) to understand its evolutionary relationship with other IBV strains, and to identify possible genetic factors that may be associated with the nephropathogenicity. Thirteen open reading frames (ORFs) were predicted in the B1648 strain (5'UTR-1a-1b-S-3a-3b-E-M-4b-4c-5a-5b-N-6b-3'UTR). ORFs 4b, 4c and 6b, which have been rarely reported in literature, were present in B1648 and most of the other IBV complete genomes. According to phylogenetic analysis of the full-length genome, replicase transcriptase complex, spike protein, partial S1 gene and M protein, B1648 strain clustered with the non-Massachusetts type strains NGA/A116E7/2006, UKr 27-11, QX-like ITA/90254/2005, QX-like CK/SWE/0658946/10, TN20/00, RF-27/99, RF/06/2007 and SLO/266/05. Based on the partial S1 fragment, B1648 clustered with the strains TN20/00, RF-27/99, RF/06/2007 and SLO/266/05 and, further designated as B1648 genotype. The full-length genome of B1648 shared the highest sequence homology with UKr 27-11, Gray, JMK, and NGA/A116E7/2006 (91.2 to 91.6%) and was least related with the reference Beaudette and Massachusetts strains (89.7%). Nucleotide and amino acid sequence analyses indicated that B1648 strain may have played an important role in the evolution of IBV in Europe and North Africa. Further, the nephropathogenicity determinants might be located on the 1a, spike, M and accessory proteins (3a, 3b, 4b, 4c, 5a, 5b and 6b). Overall, strain B1648 is distinct from all the strains reported so far in Europe and other parts of the world. However, the interpretations of this chapter should be further confirmed by reverse genetics system (RGS) and *in vivo* chicken experiments.

4.1.2. Introduction

Infectious bronchitis virus (IBV) belongs to the *Nidovirales*, family *Coronaviridae*, subfamily *Coronavirinae* and genus *Gammacoronavirus*. Coronaviruses of turkeys, ducks, pheasants, teal and geese, as well as Beluga whale and Bottlenose dolphin coronaviruses are other known members within this genus (Cavanagh, 2005; Woo *et*

al., 2014). IBV is an enveloped virus with a positive sense single stranded RNA genome.

The genome has a size of approximately 27.6 kb and contains a methylated cap and poly (A) tail at its 5' and 3' end, respectively. IBV contains at least ten open reading frames (ORFs) in the order 5' UTR-1a-1b-S-3a-3b-EM-5a-5b-N-3'UTR (Cavanagh, 2007). Gene 1 or the replicase transcriptase complex gene is the largest gene (20 kb) among the ten ORFs. Gene 1 consists of two overlapping ORFs, namely ORF1a and ORF1b, of which the latter is translated in polyprotein 1ab by a ribosomal frameshift. Furthermore, ORF1a and ORF1b encode 15 non-structural proteins (NSPs), which are required for RNA replication, transcription and other aspects of viral replication and pathogenesis. ORFs 2, 3, 4 and 6 encode four major structural proteins: The spike (S) glycoprotein, the small envelope (E) protein, the membrane (M) glycoprotein and the nucleocapsid (N) protein, respectively. The S protein is cleaved into two subunits, namely S1 and S2, of which S1 is the most variable domain and a major serotype determinant. ORFs 3 and 5 are interspersed between ORFs encoding structural proteins, and encode small non-structural proteins (NSPs), known as 3a, 3b, 5a and 5b (Cavanagh, 2007). Overall, the IBV genome is genetically variable due to the frequent occurrence of point mutations, insertions, deletions and recombination events (Cavanagh, 2007; Kottier *et al.*, 1995; Thor *et al.*, 2011).

IBV affects both broiler and layer chickens. Although chicken flocks are routinely vaccinated with live vaccines, outbreaks of infectious bronchitis have been observed in vaccinated flocks, as there is partial cross-protection between different IBV serotypes (Cook *et al.*, 2001; Lambrechts *et al.*, 1993; Pensaert and Lambrechts, 1994). Hence, serological and molecular characterization of field isolates is very important to select appropriate vaccine strains. IBV has a tropism for the epithelial cells of the respiratory tract, kidney, oviduct and alimentary tract of chickens. In the beginning of the 1950s, the respiratory Massachusetts (Mass) type of IBV was identified in the United States (Hopkins, 1974). Later, Mass-type strains have been isolated all over the world and variants emerged (Cavanagh *et al.*, 1992; Hopkins, 1974; Johnson and Marquardt, 1975).

In Europe, at present, Mass 41, 4/91, D274, Italy 02 and QX are recognized as important circulating serotypes (Cavanagh, 2007; Cook *et al.*, 2012; Kottier *et al.*,

1995; Thor *et al.*, 2011). Some IBV strains were described as nephropathogenic since the respiratory infection was followed by a severe renal disease, which leads to clinical signs such as excessive water consumption and wet droppings and increased mortality. Post-mortem examination of birds that died after a nephropathogenic IBV (NIBV) infection reveals dehydrated carcasses and swollen and pale kidneys with urates in the tubules.

The first nephropathogenic IBV strains were reported in the US (Winterfield and Hitchner, 1962) and Australia (Cumming, 1969), and later in other parts of the world (Meulemans *et al.*, 1987; Song *et al.*, 1998; Wang *et al.*, 1996). Over the past 15 years, the nephropathogenic IBV strains have been emerging as most predominant IBV strains in poultry industry, especially in Asian and Middle Eastern countries (Abdel-Moneim *et al.*, 2006; Bayry *et al.*, 2005; Lim *et al.*, 2011; Mahmood *et al.*, 2011; Meir *et al.*, 2004). Strain B1648 was responsible for outbreaks of kidney disease on chicken farms in Belgium, The Netherlands and Northern France, and was first isolated in 1984 (Cook *et al.*, 2012; Meulemans *et al.*, 1987; Pensaert and Lambrechts, 1994). At present, strain B1648 or its variants are still circulating in Europe and North Africa (Bochkov *et al.*, 2006; Ducatez *et al.*, 2009; Krapež *et al.*, 2010; Toffan *et al.*, 2013b). Based on the spike gene analysis of B1648 strain, some of the European, American and West African non-Massachusetts type strains show close genetic relationship with strain B1648 (Ducatez *et al.*, 2009; Shaw *et al.*, 1996). However, conclusions based on the spike gene or partial spike gene segment analysis should be made cautiously, because the true evolutionary relationship of B1648 with other strains can only be evaluated by complete genome analysis (Ammayappan and Vakharia, 2009; Phillips *et al.*, 2012; Zhao *et al.*, 2013; Zhou *et al.*, 2014). Hence, this paper aims to characterize the complete genome of strain B1648 by means of NGS (Illumina) and aimed to speculate the genetic factors, which might be associated with the nephropathogenic nature of this strain.

4.1.3. Materials and Methods

4.1.3.1. Virus propagation

The virulent nephropathogenic IBV strain, B1648 has been isolated in 1984 (Pensaert and Lambrechts, 1994). Virus stocks were prepared in 10-day-old embryonated SPF

chicken eggs by allantoic route inoculation. Then, virus was propagated in embryos for 48 h at 37 °C. Finally, the allantoic fluid was harvested, cleared by low speed centrifugation and frozen at -70 °C until use.

4.1.3.2. Preparation of RNA for illumina sequencing

The virus infected allantoic fluid was filtered twice using 0.8 µm and 0.45 µm membrane filters. Free and bacterial DNA/RNA was destroyed by the addition of 2 µL of Benzonase Nuclease (Novagen, San Diego, CA, USA), 1 µL of Micrococcal Nuclease (New England Biolabs, Ipswich, MA, USA) and 1 µL of NEBNext® RNase III RNA Fragmentation Module (Invitrogen, Carlsbad, CA, USA) in 7 µL of homemade buffer (1 M Tris, 100 mM CaCl₂ and 30 mM MgCl₂) that were added to 140 µL of allantoic fluid, and incubated for 2 h at 37 °C. Next, 7 µL of EDTA were added to the sample for enzyme inactivation. Extraction of viral RNA was performed using the QIAamp Viral RNA Mini Kit (Qiagen, Hilden, Germany) according to the manufacturer's instructions, but without using carrier RNA. Total RNA was amplified using the Whole Transcriptome Amplification Kit (WTA 2, Sigma Aldrich, St. Louis, MO, USA). Therefore, 0.5 µL Library Synthesis Solution was added to 2.82 µL of RNA, followed by denaturation for 2 min at 95 °C. RNA was cooled to 18 °C and 0.5 µL Library Synthesis Buffer, 0.4 µL Library Synthesis Enzyme and 0.78 µL of water was immediately added to the reaction. The mixture was treated with the following temperature conditions: 18 °C, 25 °C, 37 °C, 42 °C and 70 °C for 10, 10, 30, 10 and 20 min, respectively. Samples were cooled down to 4 °C followed by a brief centrifugation step. A mastermix containing 60.2 µL of nuclease free water, 7.5 µL of Amplification Mix, 1.5 µL of WTA dNTP mix and 0.75 µL Amplification Enzyme was added to the sample and incubated as follows: 94 °C for 2 min and 30 cycles at 94 °C for 30 s and 70 °C for 5 min. The resulting cDNA products were purified with the MSB® Spin PCRapace kit (STRATEC Molecular, Birkenfeld, Germany) according to the instructions of the manufacturer and prepared for Illumina sequencing using the KAPA Library Preparation Kit (Kapa Biosystems, Wilmington, NC, USA), according to the manufacturer's instructions.

4.1.3.3. Illumina sequencing and sequence assembly

Fragments ranging from 350–600 bp were selected using the BluePippin (Sage Science, Beverly, MA, USA) according to the manufacturer's instructions.

Sequencing of the samples was performed on a HiSeq 2500 platform (Illumina, San Diego, CA, USA) for 300 cycles (150 bp paired ends). Raw reads were trimmed for quality and adapters, and were de novo assembled into contigs using SPAdes (Bankevich *et al.*, 2012). Scaffolds were classified using a tBLASTx search against all complete viral genomes in GenBank using an e-value cut-off of 10^{-10} . Scaffolds with a significant tBLASTx hit were retained and used for a second tBlastx search against the GenBank nucleotide database using an E-value of 10^{-4} (Altschul *et al.*, 1990).

4.1.3.4. Genome sequence analysis

Multiple sequence alignments were performed using the ClustalW plug-in in the MEGA software version 5.2.2, followed by manual editing. The B1648 genome, coding sequence and ORF prediction was carried out in <http://covdb.microbiology.hku.hk> and <http://www.jcvi.org/vigor/> (Huang *et al.*, 2008; Wang *et al.*, 2010). Phylogenetic trees were constructed using the maximum-likelihood method. Substitution models were determined for each gene separately. The bootstrap values were determined from 500 replicates of the original data. Nucleotide and amino acid identities were determined using the p-distance model. The complete genome of strain B1648 was compared to 55 relevant respiratory and nephropathogenic complete IBV genomes of North America (USA), Asia (China, Korea and Taiwan), Africa (Nigeria) and Europe (Sweden, Ukraine and Italy). Partial S1 gene sequences (727 nt) of 90 relevant respiratory and nephropathogenic IBV strains of North America (USA), South America (Argentina), Europe (Sweden, Italy, UK, Slovenia, Ukraine and Russia), Asia (China, India, Israel, Korea and Taiwan), Africa (Tunisia, Nigeria and Egypt) and Australia were compared to B1648 strain as well. During B1648 strain outbreak (1984), Mass type strains were other important IBV strains present in the field (Meulemans *et al.*, 1987). Thus, Mass and non-Mass strains nomenclature has been used in this chapter to understand the phylogenetic and pairwise comparisons of B1648 genome in a better way.

4.1.3.5. Recombination analysis

Simplot analysis (SimPlot version 3.5.1) was performed to determine whether the B1648 strain has recombined with other strains during its evolution. Based on the phylogenetic analysis of the complete genome sequence, 10 relevant strains were selected and included in the recombination analysis. The 10 complete genome

sequences were aligned using the ClustalW plug-in in the MEGA software version 5.2.2. The Kimura 2-parameter model was used as a distance model, the window size was 500 bp and step size was 60 bp.

4.1.3.6. Genbank accession number

The full-length genomic sequence of the B1648 strain that was described in this report has been deposited in the GenBank database with accession number KR231009.

4.1.4. Results

4.1.4.1. Genome organization of strain B1648

The complete genome sequence of strain B1648 had a size of 27654 nucleotides (nt), excluding the poly(A)-tail. Thirteen ORFs (5'-1a-1b-S-3a-3b-E-M-4b-4c-5a-5b-N-6b-3') were predicted in the B1648 genome (Table 1). ORFs 4b, 4c and 6b were predicted in the B1648 genome and also in most of the GenBank IBV genomes (Table 2). Among the different regions of the genome, the 5' end untranslated regions (UTR) (518 nt) and 3' end UTR (292 nt) were most conserved (94.8 to 99.5%). On the other hand, the 6b protein was the most variable (15.9 to 96%), followed by 4c (46.4 to 100%), 3b (51.2 to 96.4%) and the Spike protein (56.9 to 86.2%) (Table 2). Deletions, insertions and point mutations were distributed throughout the B1648 genome.

Table 1. Genes, coding regions, nucleotide length and amino acids size of B1648 strain.

Open Reading Frame	Frame	Nucleotide Location	Nucleotide Length (bp)	Amino Acids Size
5' UTR	-	1-518	518	-
1a	+3	519-12368	11,850	3949
1b	+2	12443-20401	7959	2652
Spike	+3	20352-23852	3501	1166
3a	+2	23852-24025	174	57
3b	+1	24025-24219	195	64
Envelope	+2	24200-24484	285	94
Membrane	+3	24477-25154	678	225
4b	+3	25155-25439	285	94
4c	+1	25360-25530	171	56
5a	+2	25514-25711	198	65
5b	+1	25708-25956	249	82
Nucleocapsid	+3	25899-27128	1230	409
6b	+2	27137-27361	225	74
3' UTR	-	27362-27654	292	-

Table 2. Nucleotide and amino acid sequence identity (%) of B1648 genome with relevant genomes of Infectious Bronchitis Virus (IBV).

Strain	Genome	5'	1a	1b	Spike	3a	3b	E (3c)	M	4b	4c	5a	5b	N	6b	3'
Beaudette	89.7	96.2	89.7/91.7	91.9/96.6	80.7/80.7	91.1/94.6	80.1/64.6	88.9/81.8	95.1/93	90.2/85.8	87.1/84.2	83.4/84.8	95.3/90.8	92.4/93.6	93.6/93.9	99.1
California99	90.4	98.1	90.1/91.9	93/97.1	79.2/ 84.1	87.8/82.8	96.6/96.4	92.3/90.7	93.9/91.5	89.6/87.5	89.0/89.7	86.5/88.4	93.6/86.6	93.4/96	68.9/65.2	98.1
Cal5572003	90.4	98.4	90.3/91.3	92.9/97.2	79.5/83	93.7/94.6	89.8/80.7	93.5/91.9	94.4/91.5	83.7/76.9	64.4/50.5	87.1/86.6	94.4/86.6	93.3/94.7	94.3/96	98.1
Cal56b	90.6	97.8	90.7/92.1	92.9/97	77.8/82.8	89.2/85.9	94.8/92.7	91.5/88.2	95.1/93	85.5/82.4	66.0/50.5	88.3/88.4	94.5/90.8	94.1/96.2	93/93.9	98.6
SAIBK	86.8	95.8	86.4/89.4	89.5/95.5	78/81.7	90.9/79.6	76.2/67.1	88.5/85.7	92/90.4	<i>83/82.4</i>	<i>64.4/46.4</i>	87.2/91.9	93.6/89.5	85.7/91.8	NA	97.6
TW2575/98	<i>86.0</i>	<i>95.5</i>	<i>84.8/87.9</i>	<i>88.9/95.7</i>	79.2/81.7	94.8/ 97.3	87.3/80.7	90.5/87	92.7/90.4	83.7/80.6	85.1/81.3	86.3/88.4	92.6/85.2	88.4/92	68.3/65.2	97.1
ArkDPI11	90.8	98.7	90.6/92.2	93/96.9	80.7/83.7	97.4/94.6	96.6/94.6	93/91.9	93.6/92	89.6/87.5	89.9/92.4	86.5/88.4	94.9/89.5	94.2/96.5	94.3/96	98.1
H52	89.6	97.8	89.4/91.5	92.1/96.5	80.9/80.6	85.1/88.9	81.5/67.1	88.9/81.8	95.4/93	88.5/85.8	85.2/78.3	87.8/88.4	92.6/85.2	91.9/94.7	<i>34.7/15.9</i>	98.6
H120	90.4	98.7	89.9/91.7	93.6/97.4	79/81.1	85.1/88.9	80.7/67.1	87.6/76.3	96.2/92.5	88.5/85.8	85.2/78.3	88.4/88.4	95.3/90.8	93.4/94.7	<i>34.7/15.9</i>	99.0
Mass412006	90.8	98.7	91.1/92.6	92.5/97	83.1/82.3	87.8/82.8	96.6/96.4	93.5/ 93.1	93.7/92	89.6/87.5	89.9/92.4	86.5/88.4	94.4/88.1	94.4/96.7	93/93.9	98.6
Mass411985	89.7	96.8	89.6/91.4	92.2/96.7	58.3/80.8	91.1/91.8	81.5/67.1	89.5/83.1	94.8/93	90.9/89.1	89.2/81.3	86.6/83	<i>92.6/83.7</i>	91.9/94.7	NA	98.1
Conn461996	91.1	97.8	91.5/92.7	93.1/97	58.6/82.5	87.8/82.8	96.6/96.4	93.3/93.1	93.6/92	89.6/87.5	89.9/92.4	86.5/88.4	94.9/89.5	94.4/96.7	89.5/91.8	98.6
ITA/90254/2005	90.2	97.1	92.2/94.2	90.8/96.3	80.5/81.8	85.7/79.6	<i>64.1/54</i>	89.2/84.4	95.6/94.6	93.4/92.4	92.7/89.7	90.1/91.9	92.6/86.6	91.3/94.9	97.5/96	99.0
NGA/A116E7/2006	91.6	97.8	92.2/94	93/96.8	81.7/ 84.8	90/79.6	78.1/64.6	92/90.7	89.9/85.5	92.4/90.8	91.9/89.7	93.5/91.9	93.5/88.1	92.8/95.2	94.2/89.7	98.6
Delaware072	88.1	98.4	89.1/90.5	<i>91/94.2</i>	81.4/57.5	92.8/82.8	96.6/96.4	92.9/90.7	94.7/93	88.5/85.8	85.1/78.3	85.3/88.4	94.9/89.5	92.9/94.4	92.9/93.9	98.6
Gray	91.2	98.7	91.8/93.3	92.6/97.2	78.6/ 82.8	97.4/94.6	96.6/94.6	92.6/91.9	<i>88.2/81.6</i>	89.6/85.8	89.9/92.4	86.5/88.4	93.1/86.6	<i>86.1/84.5</i>	94.9/96	<i>96.6</i>
Holte	90.7	98.7	91.5/92.8	92.2/97	<i>79/80.2</i>	91.9/88.9	94.2/88.9	91.4/89.5	94.9/92	87.9/82.4	89.1/84.2	<i>83.3/86.6</i>	95.8/92.2	91.2/93.4	NA	NA
Iowa97	90.6	98.4	91.3/92.4	92.2/97	<i>77.7/82.7</i>	91.9/88.9	94.2/88.9	91.4/89.5	94.5/91.5	87.9/82.4	89.1/84.2	<i>83.3/86.6</i>	95.8/92.2	91.5/93.9	91.5/89.7	96.6
JMK	91.2	98.7	92/93.5	92.5/97	79.1/82.3	97.4/94.6	96/92.7	92.6/91.9	94.1/92	89.6/85.8	89.9/92.4	86.5/88.4	93.1/86.6	93.6/94.9	NA	98.1
CK/CH/LDL/101212	90.4	98.4	89.8/91.6	93.6/97.3	78.8/81.2	85.1/88.9	80.7/67.1	<i>87.6/76.3</i>	96.2/92.5	88.5/85.8	85.2/78.3	87.8/86.6	95.3/90.8	93.2/94.4	<i>34.7/15.9</i>	98.1
CK/SWE/0658946/10	89.5	96.8	90/91.1	91.3/95.8	80/80.8	<i>83.6/76.4</i>	<i>64.9/51.2</i>	93.7/88.2	96.1/95.6	91.3/92.4	92.0/81.3	94.7/98.4	91.2/85.2	89.2/90.4	97.5/96	99.0
KM91	90.0	98.7	91.1/92.6	91.7/96.6	<i>62.4/80.4</i>	87.8/69.5	78.8/74.1	89.6/89.5	94.3/93.5	92.5/92.4	93.6/95.0	86/84.8	93.1/86.6	92.5/95.5	71.4/73.2	96.6
CK/CH/LJL/111054	90.7	98.7	90.2/92.1	93.6/97.3	84.6/82.6	87.8/82.8	96.6/96.4	93.3/93.1	93.7/92	89.6/87.5	89.9/92.4	86.5/88.4	94.9/89.5	94.4/96.7	90.2/91.8	98.6
Ukr27-11	91.2	96.5	89.8/91.7	93.6/97.2	80.8/86.2	98.3/97.3	93/92.7	92.3/91.9	96.9/96.6	97.6/97	96.9/100.0	94.7/93.5	94.4/89.5	93.2/ 95.2	97.5/96	99.0
CK/CH/LDL/110931	90.6	98.7	89.9/91.7	93.6/97.3	80.7/82.4	87.8/82.8	96.6/96.4	93.3/93.1	93.7/92	89.6/87.5	89.9/92.4	86.5/88.4	94.9/89.5	94.4/96.7	90.2/91.8	98.6

Boldface indicates the highest, and italic the lowest, nucleotide and amino acid sequence identity

4.1.4.2. Phylogenetic analysis and comparison alignments of full genomes of IBV strains

The general time reversible model with gamma distribution and invariant sites was used for the construction of a maximum likelihood phylogenetic tree of the 55 relevant respiratory and nephropathogenic complete IBV genomes of North America (USA), Asia (China, Korea and Taiwan), Africa (Nigeria) and Europe (Sweden, Ukraine and Italy) (Figure 1). The phylogenetic analysis of 55 full-length nucleotide sequences of different IBV strains has demonstrated that NGA/A116E7/2006 (non-Mass pathogenic variable type of Nigeria), UKr 27-11 (non-Mass recombinant type of Ukraine), QX-like ITA/90254/2005 (non-Mass type of Italy) and QX-like CK/SWE/0658946/10 (non-Mass type of Sweden) strains clustered most closely with B1648. The B1648 strain has the highest nucleotide sequence homology with strains UKr 27-11, Gray (non-Mass nephropathogen), JMK (non-Mass respiratory pathogen) and NGA/A116E7/2006 (91.2 to 91.6%) (Table 2). Strain B1648 was clustered distinctly from all the Mass type strains. The nucleotide sequence homology to Mass 41 (M41, 1985) and reference (Beaudette) strain was 89.7%.

Full genome

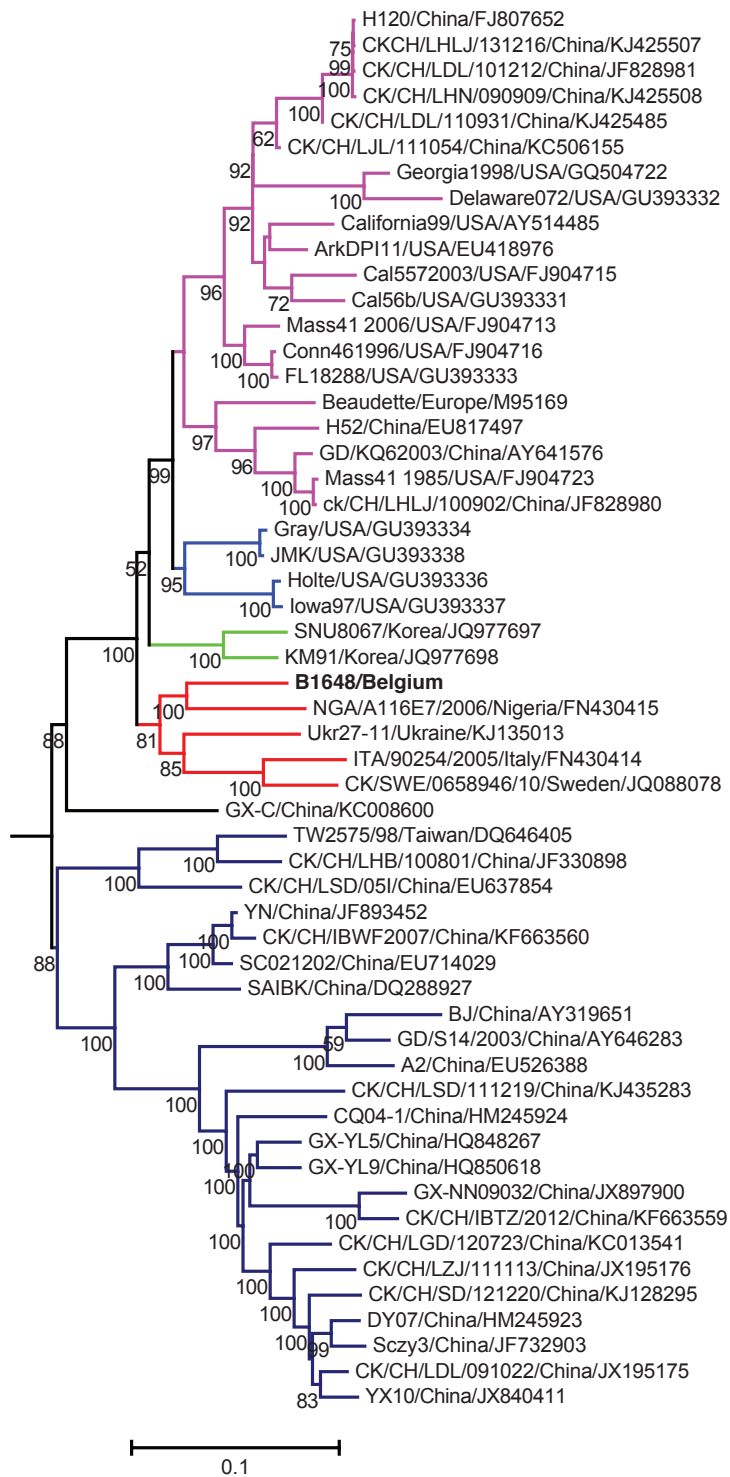
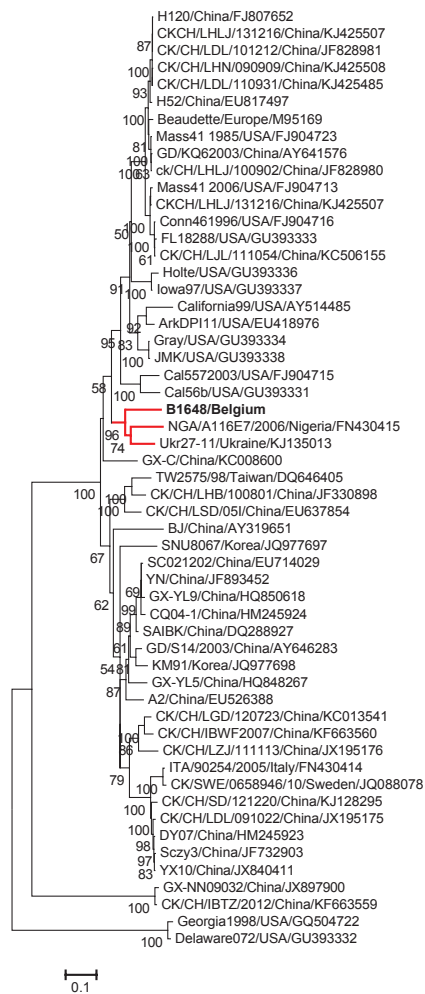


Figure 1. Maximum likelihood phylogenetic tree based on 55 full genome sequences. Bootstrap values ($n = 500$ replicates) of $<50\%$ are not shown. Strain B1648 cluster is shown in red.

4.1.4.3. Phylogenetic analysis and sequence comparison of spike protein (1166 aa) and partial S1 gene (727 nt)

Maximum likelihood trees were constructed for the amino acid sequences of the spike protein and nucleotide sequences of the partial S1 gene using the general time reversible and Tamura 92 models with gamma distribution sites, respectively (Figure 2). The phylogenetic analysis of the spike protein (1166 aa) clustered NGA/A116E7/2006 and Ukr27-11 with B1648 strain. The phylogenetic analysis of 90 partial S1 genes (727 nt) of relevant respiratory and nephropathogenic IBV strains of North America (USA), South America (Argentina), Europe (Sweden, Italy, UK, Slovenia, Ukraine and Russia), Asia (China, India, Israel, Korea and Taiwan), Africa (Tunisia, Nigeria and Egypt) and Australia has clustered B1648 strain with TN20/00 (Tunisian), RF-27/99 and RF/06/2007 (Russian) and SLO/266/05 (Slovenian) strains. The Spike protein of B1648 showed the highest amino acid identities to California99, NGA/A116E7/2006 and Ukr27-11 (84.1 to 86.2%). The partial S1 gene of B1648 strain showed the highest nucleotide homology with strains SLO/266/05, RF/06/2007, RF-27/99 and TN20/00 (89.4 to 97.4%). According to amino acid sequence identity, the Spike protein (56.9 to 86.2%) was the fourth most variable region (Table 2).

Spike



Partial S1

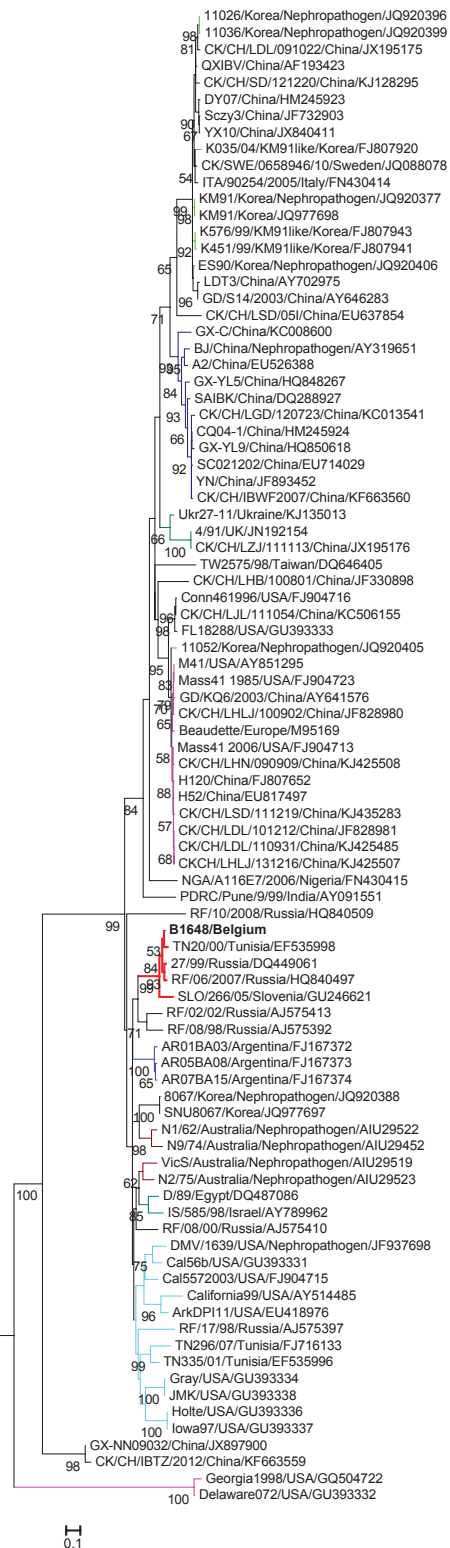


Figure 2. Maximum likelihood phylogenetic trees based on amino acid sequences of spike protein and nucleotide sequences of partial S1 gene. Bootstrap values ($n = 500$ replicates) of $<50\%$ are not shown. Strain B1648 cluster is shown in red.

4.1.4.4. Phylogenetic analysis and comparison alignments of the replicase transcriptase complex (polyprotein 1a (3949 aa) and 1b (2652 aa))

The replicase transcriptase complex (polyprotein 1a (3949 aa) and 1b (2652 aa)) maximum likelihood trees were constructed using the general time reversible model with gamma distribution and invariant sites (Figure 3). Based on the phylogenetic analysis of the replicase protein complex amino acid sequences, B1648 clustered with NGA/A116E7/2006 (1a, 1b), ITA/90254/2005 (1a) and UKr 27-11 (1b).

Polyprotein 1a (3949 aa) had the highest amino acid homology with strains Gray, NGA/A116E7/2006 and ITA/90254/2005 (93.3 to 94.2%), while polyprotein 1b (2652 aa) was closest to CK/CH/LDL/101212, CK/CH/LHLJ/131216 and H120 (97.3 to 97.4%). Overall, polyprotein 1b (95.3 to 97.4%) was more conserved than 1a (84.8 to 94.6%) (Table 2). Among the 15 NSPs of polyprotein 1ab, NSP3 (80.6 to 92.4%), NSP9 (69.1 to 99.1%) and NSP11 (69.8 to 86%) were most variable, whereas the other NSPs were generally more conserved (82.8 to 100%) (Supplementary Table S1).

4.1.4.5. Phylogenetic analysis and sequence comparison of amino acid sequences of E, M and N proteins

For construction of E or 3c (94 aa), M (225 aa) and N (409 aa) proteins maximum likelihood trees, the Jones Thornton Taylor model with gamma distribution sites was used (Figure 3). Based on the phylogenetic analysis of amino acid sequences of E protein, NGA/A116E7/2006, Ukr27-11, Cal5572003, Cal56b and many other Mass and non-Mass type strains were clustered together with B1648. Further, a sequence of 12 amino acids (36 nucleotides) was discontinuously deleted in the C-terminal of the B1648 E protein. The same 12 amino acids were deleted in strains NGA/A116E7/2006, Ukr27-11, Cal5572003 and Cal56b (Figure 4). According to amino acid sequences of the M protein, B1648 strain was clustered with NGA/A116E7/2006, UKr 27-11, QX-like ITA/90254/2005, QX-like CK/SWE/0658946/10 and many other non-Mass type strains. Based on the amino acid sequences of N protein, NGA/A116E7/2006, UKr 27-11, QX-like ITA/90254/2005, Beaudette, Mass type (1985) and many other Mass type and non-Mass type strains were clustered together with B1648.

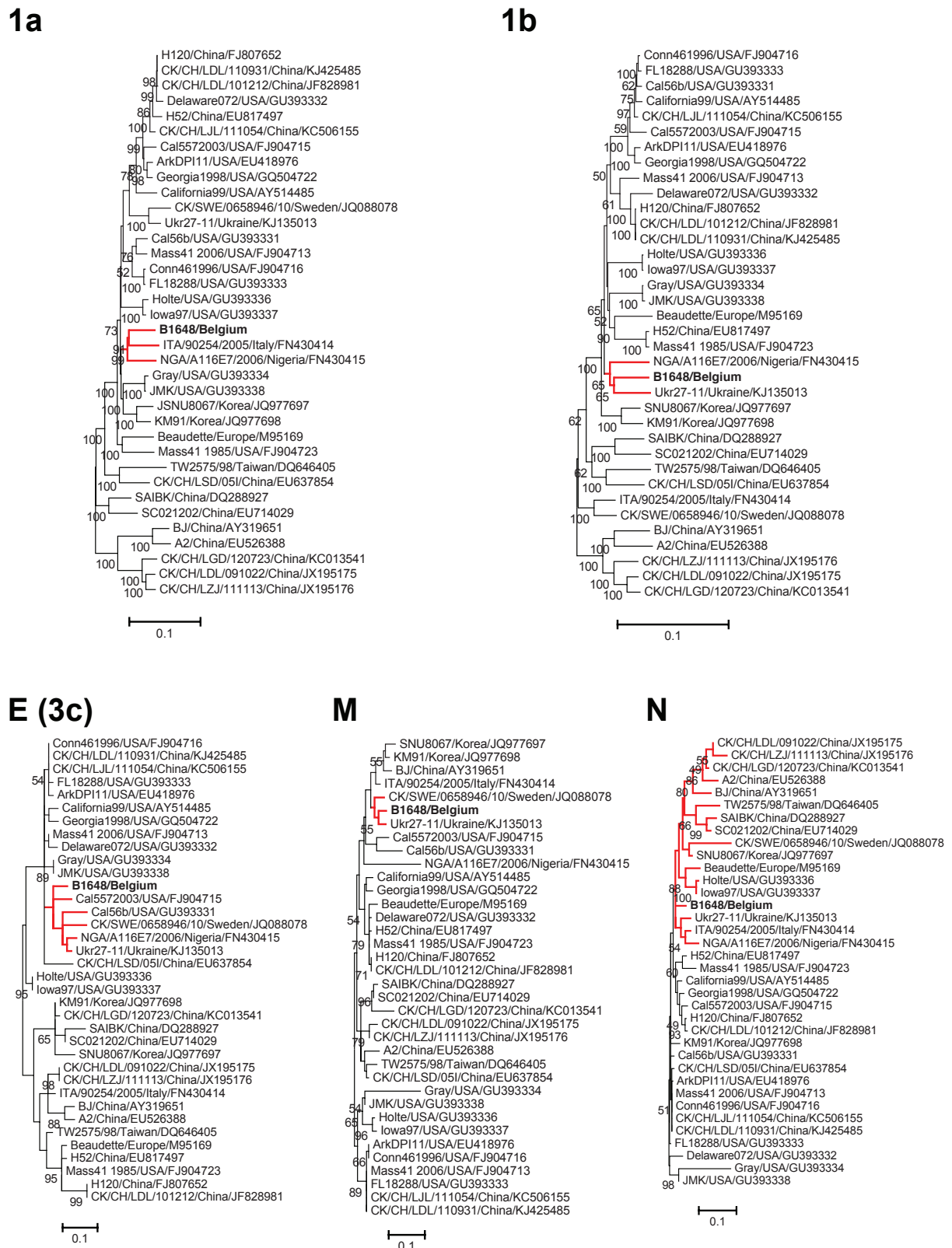


Figure 3. Maximum likelihood phylogenetic trees based on amino acid sequences of 1a, 1b, E (3c), M and N proteins. Bootstrap values (n = 500 replicates) of <50% are not shown. Strain B1648 cluster is shown in red.

The E or 3c (94 aa) protein had the highest amino acid identities to Mass 41(2006), Conn461996, CK/CH/LDL/110931 and CK/CH/LJL/111054 (93.1%). The M protein (225 aa) was closest to ITA/90254/2005, CK/SWE/0658946/10 and Ukr27-11 (94.6 to 96.6%). The N protein (409 aa) showed the highest amino acid identities to Mass 41(2006), and many other Mass and non-Mass type strains (96.7%).

ITA/90254/2005/Italy/FN430414	VNEFPKNGWNNKNPAIFQDVERHGKLS*
CK/SWE/0658946/10/Sweden/JQ088078	VNDFPKNGWNNKNPAIFQDVEPHHQLHS*
Beaudette/Europe/M95169	VNEFPKNGWNNKNPANFQDAQRD-KLYS*
H52/China/EU817497	VNEFPKNGWNNKNPANFQDVQRD-KLYS*
H120/China/FJ807652	VNEFPKNGWNNKNPANFQDVQRN-KLYS*
Mass41 1985/USA/FJ904723	VNEFPKNGWNNKNPANFQDVQRD-KLYS*
Mass41 2006/USA/FJ904713	VNEFPKNGWNNKSPANFQY---DGKLHT*
ArkDPI11/USA/EU418976	VNEFPKNGWNNKSPANFQY---DGKLHT*
Conn461996/USA/FJ904716	VNEFPKNGWNNKSPANFQY---DGKLHT*
Gray/USA/GU393334	VNEFPKNGWNNKIPENFQH---GGKLHT*
Holte/USA/GU393336	VNEFPKNGWNNKNPANFQY---GGKLHT*
B1648/Belgium	VNEFPKNGWK-----Y---G*----
NGA/A116E7/2006/Nigeria/FN430415	VNEFPKNGWK*-----
Ukr27-11/Ukraine/KJ135013	VNEFPKNGWKN-----G*----
Cal557 2003/USA/FJ904715	VNEFPKNGWKQ*-----
Cal56b/USA/GU393331	VNEFPKNGWKQ*-----
KM91/Korea/JQ977698	VNEFPKNGWNNKNPAIFQDVERHGKLS*

Figure 4. Amino acid sequence differences in C-terminal of E protein of B1648 strain with other Mass (red) and non-Mass type strains. In the B1648 strain 3' terminal E (3c) protein, a region of total 12 amino acids was discontinuously deleted (blue). The dashes (-) indicate the deleted sequences.

4.1.4.6. Accessory proteins alignments

There were 7 probable accessory proteins in the B1648 strain, such as 3a (57 aa), 3b (64 aa), 4b (94 aa), 4c (56 aa) 5a (65 aa), 5b (82 aa) and 6b (74 aa). The accessory proteins 3a (69.5% to 97.3%), 3b (51.2% to 96.4%), 4b (76.9% to 97%), 4c (46.4% to 100%) and 6b (15.9% to 96%) were variable whereas 5a (81.1% to 93.5%) and 5b (82.3% to 92.2%) were more conserved (Table 2). The highest amino acid identities of 3a, 3b, 4b, 4c, 5a, 5b and 6b were 97.3% (Ukr27-11 and TW2575/98), 96.4% (CK/CH/LDL/110931, California99 and many other non-Mass type strains), 97% (Ukr27-11), 100% (Ukr27-11), 98.4% (CK/SWE/0658946/10), 92.2% (Holte and Iowa97) and 96% (Ukr27-11, CK/SWE/0658946/10, Gray, ArkDPI11 and many other non-Mass type strains), respectively.

4.1.4.7. Recombination analysis

B1648 was used as a putative parental strain and 10 relevant pathogenic and vaccine strains were queried in the Simplot analysis (Figure 5). The B1648 strain was considered as parental strain, because the strains that clustered with B1648 (Figures 1–3), were reported after the B1648 outbreak. In gene 1a, a part of NSP2 and NSP4 showed a higher similarity to ITA/90254/2005; a part of NSP3 showed a higher similarity to ITA/90254/2005 and NGA/A116E7/2006, and part of NSP6 showed a higher similarity to CK/SWE/0658946/10. In the gene 1b, a part of NSP13 and NSP14 shared a higher similarity with NGA/A116E7/2006, and a part of NSP15 did that with UKr 27-11. In the S gene, a part of the S1 region showed similarities with Gray and UKr 27-11 and a part of S2 did that with NGA/A116E7/2006. The 4b, 4c and 5a genes were very similar to those of UKr 27-11.

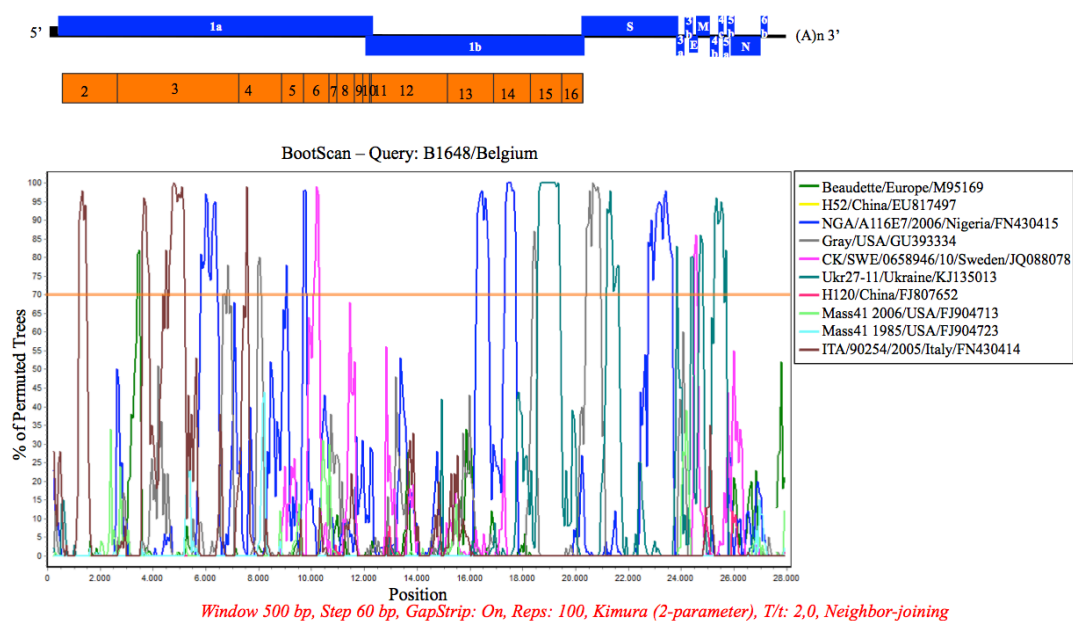


Figure 5. Simplot analysis (Simplot 3.5.1) of B1648 strain. The full genome sequence of B1648 strain was tested against 10 relevant IBV strains. The 70% bootstrap level is considered.

4.1.5. Discussion

The B1648 strain is a Belgian reference nephropathogenic IBV serotype. Earlier, in our laboratory it was demonstrated that B1648 was antigenically different from the Mass type and other variant strains. Furthermore, it was shown that Mass type vaccines (H120 and D274) did not provide protection (Lambrechts *et al.*, 1993; Pensaert and

Lambrechts, 1994). More recently, Cook *et al.* (2001) found that the 4/91 type (variant type) vaccine alone or the 4/91 and Ma5 (Mass type) combination vaccine protected against B1648 nephropathogenicity. In spite of the intensive vaccination program, the B1648 strain or its variants are still circulating or reemerging throughout Europe and North Africa (Bochkov *et al.*, 2006; Ducatez *et al.*, 2009; Krapež *et al.*, 2010; Toffan *et al.*, 2013b). Hence, in the present study the complete genome of the B1648 strain was characterized to speculate putative genetic factors that might be involved in the tissue tropism, and to understand their role in evolution (Lambrechts *et al.*, 1993; Meulemans *et al.*, 1987; Pensaert and Lambrechts, 1994).

The B1648 genome organization (5'-1a-1b-S-3a-3b-E-M-4b-4c-5a-5b-N-6b-3') was slightly different from most previously reported IBV genomes (5'-1a-1b-S-3a-3b-E-M-5a-5b-N-3'). 4b, 4c and 6b were additional ORFs present in the B1648 genome. Although 4b, 4c and 6b were present in the most of the IBV genomes, they have rarely been reported in literature (Abolnik, 2015; Hewson *et al.*, 2011; Xue *et al.*, 2012). ORFs 4b, 4c and 6b have also been reported in a turkey coronavirus (Cao *et al.*, 2008). The exact reason for the rare reports of these ORFs (4b, 4c and 6b) in most of the IBV genomes is not known. It could be that 4b, 4c and 6b ORFs are present in most of the IBV genomes, but that the success of their identification depends on the algorithms of ORF prediction software that was used. Recently, Bentley *et al.* (2013) has demonstrated and confirmed 4b as a 5th accessory protein in IBV, besides 3a, 3b, 5a and 5b. The 4b homologue of Middle East respiratory syndrome coronavirus (MERS-CoV) was found to be an interferon antagonist (Yang *et al.*, 2013). The 6b homologue of SARS coronavirus was found to induce apoptosis (Ye *et al.*, 2008). For IBV, further investigations are necessary to demonstrate the production of 4b, 4c and 6b proteins and to identify their functions in pathogenesis.

The phylogenetic analysis of the full-length genome, replicase transcriptase complex, spike protein, partial S1 gene and M protein has suggested that B1648 may have played an important role in evolution, because the strains which were clustered (NGA/A116E7/2006, UKr 27-11, QX-like ITA/90254/2005, QX-like CK/SWE/0658946/10, TN20/00, RF-27/99, RF/06/2007 and SLO/266/05) with B1648 were reported in Europe and North Africa, after the initial B1648 outbreak. The geographical proximity of all these countries and frequent movements of poultry and their products in between these countries might be an important reason for this

observed cluster. All the above clustered strains belong to a group referred to as non-Mass type strains. In the above-mentioned cluster, QX like ITA/90254/2005 and QX like CK/SWE/0658946/10 are presently predominant IBV strains in Europe (Germany, The Netherlands, Belgium, France, Sweden, Poland, Russia, Slovenia, Spain and the UK) (Abro *et al.*, 2012; Benyeda *et al.*, 2009; Cumming, 1969; Domanska-Blicharz *et al.*, 2006; Gough *et al.*, 2008; Krapez *et al.*, 2011; Valastro *et al.*, 2010; Worthington *et al.*, 2008). The QX IBV strains were first reported in China (Liu and Kong, 2004; YuDong *et al.*, 1998). The QX like IBV strains were later reported in Europe, which was mainly associated with the nephropathogenicity and cystic oviducts (Abro *et al.*, 2012; Benyeda *et al.*, 2009; Cook *et al.*, 2012; de Wit *et al.*, 2011). In Europe, the nephropathogenicity of QX like IBV strains may have derived from the initial European nephropathogenic strains like B1648. By natural recombination events segments of the B1648 genome may have been transferred into genomes of NGA/A116E7/2006, UKr 27-11, ITA/90254/2005 and CK/SWE/0658946/10. The emergence or evolution of different coronaviral genotypes or strains by recombination events has been well documented in IBV and other coronaviruses (Hughes, 2011; Thor *et al.*, 2011). Recombination analysis has suggested that the genetic recombination sites can be located in multiple genes (Lim *et al.*, 2011). Regions that have the highest occurrence of recombination were located on the parts of replicase transcriptase complex (NSP2, 3, 4, 6, 13 and 14) and spike protein. The rate of recombination may be one of the important mechanisms for generating genetic and antigenic diversity within IBV (Hughes, 2011; Thor *et al.*, 2011). Accumulation of mutations and recombination events between the live vaccines and field strains likely produce novel variant strains or recombinant strains like, NGA/A116E7/2006 or Ukr27-11 (Ducatez *et al.*, 2009). These novel strains are known to cause disease epidemics in chickens and vaccination failure (Lim *et al.*, 2011), and further studies are necessary to better understand the frequency of natural recombination events and which genes are preferentially involved in recombination.

Pairwise comparisons have shown that B1648 was closely related to pathogenic non-Mass type strains but not to Massachusetts type strains and vaccines. Based on the full-length genome, Nigerian reference IBADAN strain (NGA/A116E7/2006) was the closest relative with 91.6% nucleotide identity. Next closest were Ukrainian (UKr 27-11) and American (Gray and JMK) strains with 91.2% nucleotide identity. It is known

that Gray is a nephropathogen and JMK is a respiratory pathogen, but the information on NGA/A116E7/2006 and UKr 27-11 strains about their tissue tropism is not available. Pairwise comparisons of 1a, Spike, M and accessory proteins (3a, 3b, 4b, 4c, 5a, 5b and 6b) have suggested that B1648 was most closely related to non-Mass type strains. However, based on 1b, E and N proteins B1648 was closely related to both Mass and non-Mass types strains. All these comparisons have implicated that the determinants of nephropathogenicity (B1648 strain) might be located on the 1a, spike, M and accessory proteins. Many authors have shown that the pathogenicity determinants of IBV are multi-genic, and associated outside the spike protein (Ammayappan *et al.*, 2009; Armesto *et al.*, 2009; Britton *et al.*, 2005; Casais *et al.*, 2003; Hodgson *et al.*, 2006; Phillips *et al.*, 2012). With the well-studied coronavirus, murine hepatitis virus (MHV), NSP1, Nsp3 and Nsp14 have been linked with virulence (Eriksson *et al.*, 2008; Sperry *et al.*, 2005; Züst *et al.*, 2007). It is very well possible that the non-structural proteins (Nsp1 to Nsp11) encoded by ORF 1a may be strong candidates for being involved in the nephropathogenicity. However, this hypothesis has to be investigated and confirmed by RGS.

Classification of the IBV serotypes is mainly based on the variability of the spike protein or partial S1 fragment (Abro *et al.*, 2012; Cavanagh, 2007; Ducatez *et al.*, 2009; Rimondi *et al.*, 2009). According to partial S1 gene analysis, Tunisian (TN20/00), Russian (IBV-27/99 and RF/06/2007) and Slovenian (SLO/266/05) strains were clustered together with B1648. This cluster is referred to as B1648 genotype. Moreover, TN20/00 was the closest among all the reported IBV strains with 97.4% nucleotide homology. Next closest were RF-27/99 (96.4%), RF/06/2007 (96.1%) and SLO/266/05 (89.4%) (Bochkov *et al.*, 2006; Krapež *et al.*, 2010). The partial S1 fragment analysis has revealed that the B1648 genotype or its variants has been intermittently circulating in Europe and North Africa for over three decades (Bourogaa *et al.*, 2012; Capua *et al.*, 1999; Dolz *et al.*, 2006; Ducatez *et al.*, 2009; Meulemans *et al.*, 1987; Ovchinnikova *et al.*, 2011; Terregino *et al.*, 2006; Toffan *et al.*, 2013a; Tosi *et al.*, 2010). Although the B1648 strain outbreak has occurred in 1984, its origin remains still unidentified. This raises the question, whether B1648 type has emerged from another animal species, like MERS-CoV of humans emerged from bats/camels (Abdel-Moneim, 2014; Chastel, 2014). The comparison with MERS-CoV is interesting because it is also associated with kidney problems in

humans. However, the phylogenetic analysis, full-length nucleotide identities and recombination analysis has shown that B1648 is distinct from other known avian and mammalian coronaviruses, and provides no information on its origin (data not shown). Based on the danger of cross species jumps of coronaviruses, more epidemiologic and surveillance studies should be done on coronaviruses in species living in the wild. Gammacoronaviruses could be circulating asymptotically in wild birds as reservoirs, before emerging as a novel pathogenic IBV strains in chickens (Kim and Oem, 2014; Muradrasoli *et al.*, 2010). In this context, efforts should be done to generate a database of full-length sequences of coronaviruses in wild animals e.g., wild migratory birds.

In summary, the present study has demonstrated that B1648 is a distinct strain setting it apart from all strains reported so far in Europe and other parts of the world. Partial S1 gene analysis has suggested that B1648 genotype or its variants has been circulating in Europe and North Africa for over three decades. The pathogenicity determinants of B1648 strain might be located on the 1a, spike, M and accessory proteins (3a, 3b, 4b, 4c, 5a, 5b and 6b). However, the conclusions of this chapter should be confirmed by RGS and *in vivo* chicken experiments. Thus, one should be careful with over interpreting the results of this study.

4.1.6. Acknowledgments

This research was supported by the Indian Council of Agricultural Research (ICAR, Pusa, New Delhi-110012 (29-1/2009-EQR/Edn)). Vishwanatha RAP Reddy and Hans J Nauwynck are members of the BELVIR consortium (IAP, phase VII) sponsored by Belgian Science Policy Office (BELSPO). The authors acknowledge Magda De Keyzer and Lieve Sys for their excellent technical assistance.

4.1.7. References

- Abdel-Moneim, A.S., 2014. Middle East respiratory syndrome coronavirus (MERS-CoV): evidence and speculations. *Arch Virol* 159, 1575-1584.
- Abdel-Moneim, A.S., El-Kady, M.F., Ladman, B.S., Gelb, J., 2006. S1 gene sequence analysis of a nephropathogenic strain of avian infectious bronchitis virus in Egypt. *Virol J* 3, 78.
- Abolnik, C., 2015. Genomic and single nucleotide polymorphism analysis of infectious bronchitis coronavirus. *Infect Genet Evol* 32, 416-424.

- Abro, S.H., Renström, L.H., Ullman, K., Isaksson, M., Zohari, S., Jansson, D.S., Belák, S., Baule, C., 2012. Emergence of novel strains of avian infectious bronchitis virus in Sweden. *Vet Microbiol* 155, 237-246.
- Altschul, S.F., Gish, W., Miller, W., Myers, E.W., Lipman, D.J., 1990. Basic local alignment search tool. *J Mol Biol* 215, 403-410.
- Ammayappan, A., Upadhyay, C., Gelb, J., Vakharia, V.N., 2009. Identification of sequence changes responsible for the attenuation of avian infectious bronchitis virus strain Arkansas DPI. *Arch Virol* 154, 495-499.
- Ammayappan, A., Vakharia, V.N., 2009. Complete nucleotide analysis of the structural genome of the infectious bronchitis virus strain md27 reveals its mosaic nature. *Viruses* 1, 1166-1177.
- Armesto, M., Cavanagh, D., Britton, P., 2009. The replicase gene of avian coronavirus infectious bronchitis virus is a determinant of pathogenicity. *PLoS One* 4, e7384.
- Bankevich, A., Nurk, S., Antipov, D., Gurevich, A.A., Dvorkin, M., Kulikov, A.S., Lesin, V.M., Nikolenko, S.I., Pham, S., Prjibelski, A.D., Pyshkin, A.V., Sirotkin, A.V., Vyahhi, N., Tesler, G., Alekseyev, M.A., Pevzner, P.A., 2012. SPAdes: a new genome assembly algorithm and its applications to single-cell sequencing. *J Comput Biol* 19, 455-477.
- Bayry, J., Goudar, M.S., Nighot, P.K., Kshirsagar, S.G., Ladman, B.S., Gelb, J., Ghalsasi, G.R., Kolte, G.N., 2005. Emergence of a nephropathogenic avian infectious bronchitis virus with a novel genotype in India. *J Clin Microbiol* 43, 916-918.
- Benyeda, Z., Mató, T., Süveges, T., Szabó, E., Kardi, V., Abonyi-Tóth, Z., Rusvai, M., Palya, V., 2009. Comparison of the pathogenicity of QX-like, M41 and 793/B infectious bronchitis strains from different pathological conditions. *Avian Pathol* 38, 449-456.
- Bochkov, Y.A., Batchenko, G.V., Shcherbakova, L.O., Borisov, A.V., Drygin, V.V., 2006. Molecular epizootiology of avian infectious bronchitis in Russia. *Avian Pathol* 35, 379-393.
- Bourogaa, H., Hellal, I., Hassen, J., Fathallah, I., Ghram, A., 2012. S1 gene sequence analysis of new variant isolates of avian infectious bronchitis virus in Tunisia. *Veterinary medicine* 3, 41-48.
- Britton, P., Evans, S., Dove, B., Davies, M., Casais, R., Cavanagh, D., 2005. Generation of a recombinant avian coronavirus infectious bronchitis virus using transient dominant selection. *J Virol Methods* 123, 203-211.
- Cao, J., Wu, C.C., Lin, T.L., 2008. Complete nucleotide sequence of polyprotein gene 1 and genome organization of turkey coronavirus. *Virus Res* 136, 43-49.

- Capua, I., Minta, Z., Karpinska, E., Mawditt, K., Britton, D., Cavanagh, D., Gough, R.E., 1999. Co-circulation of four types of infectious bronchitis virus (793/B, 624/I, B1648 and Massachusetts). *Avian Pathol* 28, 587-592.
- Casais, R., Dove, B., Cavanagh, D., Britton, P., 2003. Recombinant avian infectious bronchitis virus expressing a heterologous spike gene demonstrates that the spike protein is a determinant of cell tropism. *J Virol* 77, 9084-9089.
- Cavanagh, D., 2005. Coronaviruses in poultry and other birds. *Avian Pathol* 34, 439-448.
- Cavanagh, D., 2007. Coronavirus avian infectious bronchitis virus. *Vet Res* 38, 281-297.
- Cavanagh, D., Davis, P.J., Cook, J.K., 1992. Infectious bronchitis virus: evidence for recombination within the Massachusetts serotype. *Avian Pathol* 21, 401-408.
- Chastel, C., 2014. [Middle East respiratory syndrome (MERS): bats or dromedary, which of them is responsible?]. *Bull Soc Pathol Exot* 107, 69-73.
- Cook, J.K., Chesher, J., Baxendale, W., Greenwood, N., Huggins, M.B., Orbell, S.J., 2001. Protection of chickens against renal damage caused by a nephropathogenic infectious bronchitis virus. *Avian Pathol* 30, 423-426.
- Cook, J.K., Jackwood, M., Jones, R.C., 2012. The long view: 40 years of infectious bronchitis research. *Avian Pathol* 41, 239-250.
- Cumming, R.B., 1969. The control of avian infectious bronchitis/nephrosis in Australia. *Aust Vet J* 45, 200-203.
- de Wit, J.J., Nieuwenhuisen-van Wilgen, J., Hoogkamer, A., van de Sande, H., Zuidam, G.J., Fabri, T.H., 2011. Induction of cystic oviducts and protection against early challenge with infectious bronchitis virus serotype D388 (genotype QX) by maternally derived antibodies and by early vaccination. *Avian Pathol* 40, 463-471.
- Dolz, R., Pujols, J., Ordonez, G., Porta, R., Majo, N., 2006. Antigenic and molecular characterization of isolates of the Italy 02 infectious bronchitis virus genotype. *Avian Pathol* 35, 77-85.
- Domanska-Blicharz, K., Minta, Z., Smietanka, K., Porwan, T., 2006. New variant of IBV in Poland. *Vet Rec* 158, 808.
- Ducatez, M.F., Martin, A.M., Owoade, A.A., Olatoye, I.O., Alkali, B.R., Maikano, I., Snoeck, C.J., Sausy, A., Cordioli, P., Muller, C.P., 2009. Characterization of a new genotype and serotype of infectious bronchitis virus in Western Africa. *J Gen Virol* 90, 2679-2685.
- Eriksson, K.K., Cervantes-Barragán, L., Ludewig, B., Thiel, V., 2008. Mouse hepatitis virus liver pathology is dependent on ADP-ribose-1"-phosphatase, a viral function conserved in the alpha-like supergroup. *J Virol* 82, 12325-12334.

- Gough, R.E., Cox, W.J., de B Welchman, D., Worthington, K.J., Jones, R.C., 2008. Chinese QX strain of infectious bronchitis virus isolated in the UK. *Vet Rec* 162, 99-100.
- Hewson, K.A., Ignjatovic, J., Browning, G.F., Devlin, J.M., Noormohammadi, A.H., 2011. Infectious bronchitis viruses with naturally occurring genomic rearrangement and gene deletion. *Arch Virol* 156, 245-252.
- Hodgson, T., Britton, P., Cavanagh, D., 2006. Neither the RNA nor the proteins of open reading frames 3a and 3b of the coronavirus infectious bronchitis virus are essential for replication. *J Virol* 80, 296-305.
- Hopkins, S.R., 1974. Serological comparisons of strains of infectious bronchitis virus using plaque-purified isolants. *Avian Dis* 18, 231-239.
- Huang, Y., Lau, S.K., Woo, P.C., Yuen, K.Y., 2008. CoVDB: a comprehensive database for comparative analysis of coronavirus genes and genomes. *Nucleic Acids Res* 36, D504-511.
- Hughes, A.L., 2011. Recombinational histories of avian infectious bronchitis virus and turkey coronavirus. *Arch Virol* 156, 1823-1829.
- Johnson, R.B., Marquardt, W.W., 1975. The neutralizing characteristics of strains of infectious bronchitis virus as measured by the constant-virus variable-serum method in chicken tracheal cultures. *Avian Dis* 19, 82-90.
- Kim, H.R., Oem, J.K., 2014. Surveillance of avian coronaviruses in wild bird populations of Korea. *J Wildl Dis* 50, 964-968.
- Kottier, S.A., Cavanagh, D., Britton, P., 1995. Experimental evidence of recombination in coronavirus infectious bronchitis virus. *Virology* 213, 569-580.
- Krapež, U., Slavec, B., Barlič-Maganja, D., Rojs, O.Z., 2010. Molecular analysis of infectious bronchitis viruses isolated in Slovenia between 1990 and 2005: a retrospective study. *Virus Genes* 41, 414-416.
- Krapez, U., Slavec, B., Rojs, O.Z., 2011. Circulation of infectious bronchitis virus strains from Italy 02 and QX genotypes in Slovenia between 2007 and 2009. *Avian Dis* 55, 155-161.
- Lambrechts, C., Pensaert, M., Ducatelle, R., 1993. Challenge experiments to evaluate cross-protection induced at the trachea and kidney level by vaccine strains and Belgian nephropathogenic isolates of avian infectious bronchitis virus. *Avian Pathol* 22, 577-590.
- Lim, T.H., Lee, H.J., Lee, D.H., Lee, Y.N., Park, J.K., Youn, H.N., Kim, M.S., Lee, J.B., Park, S.Y., Choi, I.S., Song, C.S., 2011. An emerging recombinant cluster of nephropathogenic strains of avian infectious bronchitis virus in Korea. *Infect Genet Evol* 11, 678-685.

- Liu, S., Kong, X., 2004. A new genotype of nephropathogenic infectious bronchitis virus circulating in vaccinated and non-vaccinated flocks in China. *Avian Pathol* 33, 321-327.
- Mahmood, Z.H., Sleman, R.R., Uthman, A.U., 2011. Isolation and molecular characterization of Sul/01/09 avian infectious bronchitis virus, indicates the emergence of a new genotype in the Middle East. *Vet Microbiol* 150, 21-27.
- Meir, R., Rosenblut, E., Perl, S., Kass, N., Ayali, G., Perk, S., Hemsani, E., 2004. Identification of a novel nephropathogenic infectious bronchitis virus in Israel. *Avian Dis* 48, 635-641.
- Meulemans, G., Carlier, M.C., Gonze, M., Petit, P., Vandebroek, M., 1987. Incidence, characterisation and prophylaxis of nephropathogenic avian infectious bronchitis viruses. *Vet Rec* 120, 205-206.
- Muradrasoli, S., Bálint, A., Wahlgren, J., Waldenström, J., Belák, S., Blomberg, J., Olsen, B., 2010. Prevalence and phylogeny of coronaviruses in wild birds from the Bering Strait area (Beringia). *PLoS One* 5, e13640.
- Ovchinnikova, E.V., Bochkov, Y.A., Shcherbakova, L.O., Nikonova, Z.B., Zinyakov, N.G., Elatkin, N.P., Mudrak, N.S., Borisov, A.V., Drygin, V.V., 2011. Molecular characterization of infectious bronchitis virus isolates from Russia and neighbouring countries: identification of intertypic recombination in the S1 gene. *Avian Pathol* 40, 507-514.
- Pensaert, M., Lambrechts, C., 1994. Vaccination of chickens against a Belgian nephropathogenic strain of infectious bronchitis virus B1648 using attenuated homologous and heterologous strains. *Avian Pathol* 23, 631-641.
- Phillips, J.E., Jackwood, M.W., McKinley, E.T., Thor, S.W., Hilt, D.A., Acevedo, N.D., Williams, S.M., Kissinger, J.C., Paterson, A.H., Robertson, J.S., Lemke, C., 2012. Changes in nonstructural protein 3 are associated with attenuation in avian coronavirus infectious bronchitis virus. *Virus Genes* 44, 63-74.
- Rimondi, A., Craig, M.I., Vagnozzi, A., König, G., Delamer, M., Pereda, A., 2009. Molecular characterization of avian infectious bronchitis virus strains from outbreaks in Argentina (2001-2008). *Avian Pathol* 38, 149-153.
- Shaw, K., Britton, P., Cavanagh, D., 1996. Sequence of the spike protein of the Belgian B164S isolate of nephropathogenic infectious bronchitis virus. *Avian Pathol* 25, 607-611.
- Song, C.S., Lee, Y.J., Kim, J.H., Sung, H.W., Lee, C.W., Izumiya, Y., Miyazawa, T., Jang, H.K., Mikami, T., 1998. Epidemiological classification of infectious bronchitis virus isolated in Korea between 1986 and 1997. *Avian Pathol* 27, 409-416.
- Sperry, S.M., Kazi, L., Graham, R.L., Baric, R.S., Weiss, S.R., Denison, M.R., 2005. Single-amino-acid substitutions in open reading frame (ORF) 1b-nsp14 and

- ORF 2a proteins of the coronavirus mouse hepatitis virus are attenuating in mice. *J Virol* 79, 3391-3400.
- Terregino, C., Maria, S.B., Giovanni, O., Cristian, D.B., Alessandra, D., 2006. Survey on circulation of infectious bronchitis virus strains in Northern Italy. *Italiana Journal of Animal Science* 5, 309-311.
- Thor, S.W., Hilt, D.A., Kissinger, J.C., Paterson, A.H., Jackwood, M.W., 2011. Recombination in avian gamma-coronavirus infectious bronchitis virus. *Viruses* 3, 1777-1799.
- Toffan, A., Bonci, M., Bano, L., Bano, L., Valastro, V., Vascellari, M., Capua, I., Terregino, C., 2013a. Diagnostic and clinical observation on the infectious bronchitis virus strain Q1 in Italy. *Vet Ital* 49, 347-355.
- Toffan, A., Bonci, M., Bano, L., Valastro, V., Vascellari, M., Capua, I., Terregino, C., 2013b. Diagnostic and clinical observation on the infectious bronchitis virus strain Q1 in Italy. *Vet Ital* 49, 347-355.
- Tosi, G., Taddei, R., Barbieri, I., Fiorentini, L., Massi, P. 2010. Caratterizzazione molecolare dei ceppi di virus della bronchite infettiva aviaria isolati in Italia nel periodo 2007–2009 e nel primo bimestre del 2010. In: In proceedings of the 49th Annual Conference of Acts Italian society of Avian Pathology (SIPA), Forli, Italy, 217-224.
- Valastro, V., Monne, I., Fasolato, M., Cecchettin, K., Parker, D., Terregino, C., Cattoli, G., 2010. QX-type infectious bronchitis virus in commercial flocks in the UK. *Vet Rec* 167, 865-866.
- Wang, C.H., Hsieh, M.C., Chang, P.C., 1996. Isolation, pathogenicity, and H120 protection efficacy of infectious bronchitis viruses isolated in Taiwan. *Avian Dis* 40, 620-625.
- Wang, S., Sundaram, J.P., Spiro, D., 2010. VIGOR, an annotation program for small viral genomes. *BMC Bioinformatics* 11, 451.
- Winterfield, R.W., Hitchner, S.B., 1962. Etiology of an infectious nephritis-nephrosis syndrome of chickens. *Am J Vet Res* 23, 1273-1279.
- Woo, P.C., Lau, S.K., Lam, C.S., Tsang, A.K., Hui, S.W., Fan, R.Y., Martelli, P., Yuen, K.Y., 2014. Discovery of a novel bottlenose dolphin coronavirus reveals a distinct species of marine mammal coronavirus in *Gammacoronavirus*. *J Virol* 88, 1318-1331.
- Worthington, K.J., Currie, R.J., Jones, R.C., 2008. A reverse transcriptase-polymerase chain reaction survey of infectious bronchitis virus genotypes in Western Europe from 2002 to 2006. *Avian Pathol* 37, 247-257.

- Xue, Y., Xie, Q., Yan, Z., Ji, J., Chen, F., Qin, J., Sun, B., Ma, J., Bi, Y., 2012. Complete genome sequence of a recombinant nephropathogenic infectious bronchitis virus strain in China. *J Virol* 86, 13812-13813.
- Yang, Y., Zhang, L., Geng, H., Deng, Y., Huang, B., Guo, Y., Zhao, Z., Tan, W., 2013. The structural and accessory proteins M, ORF 4a, ORF 4b, and ORF 5 of Middle East respiratory syndrome coronavirus (MERS-CoV) are potent interferon antagonists. *Protein Cell* 4, 951-961.
- Ye, Z., Wong, C.K., Li, P., Xie, Y., 2008. A SARS-CoV protein, ORF-6, induces caspase-3 mediated, ER stress and JNK-dependent apoptosis. *Biochim Biophys Acta* 1780, 1383-1387.
- YuDong, W., YongLin, W., ZiChun, Z., GenChe, F., YiHai, J., XiangE, L., Jiang, D., ShuShuang, W., 1998. Isolation and identification of glandular stomach type IBV (QXIBV) in chickens. *Chinese Journal of Animal Quarantine* 15, 1-3.
- Zhao, F., Zou, N., Wang, F., Guo, M., Liu, P., Wen, X., Cao, S., Huang, Y., 2013. Analysis of a QX-like avian infectious bronchitis virus genome identified recombination in the region containing the ORF 5a, ORF 5b, and nucleocapsid protein gene sequences. *Virus Genes* 46, 454-464.
- Zhou, S., Tang, M., Jiang, Y., Chen, X., Shen, X., Li, J., Dai, Y., Zou, J., 2014. Complete genome sequence of a novel infectious bronchitis virus strain circulating in China with a distinct S gene. *Virus Genes* 49, 152-156.
- Züst, R., Cervantes-Barragán, L., Kuri, T., Blakqori, G., Weber, F., Ludewig, B., Thiel, V., 2007. Coronavirus non-structural protein 1 is a major pathogenicity factor: implications for the rational design of coronavirus vaccines. *PLoS Pathog* 3, e109.

CHAPTER 4.2.

Productive replication of nephropathogenic infectious bronchitis virus in peripheral blood monocytic cells, a strategy for viral dissemination and kidney infection in chickens

Vishwanatha R.A.P. Reddy, Ivan Trus, Lowiese M. B. Desmarets, Yewei Li,
Sebastian Theuns, and Hans J. Nauwynck

Veterinary Research (2016), 47:70

4.2.1. Abstract

In the present study, the replication kinetics of nephropathogenic (B1648) and respiratory (Massachusetts-M41) IBV strains were compared *in vitro* in respiratory mucosa explants and blood monocytes (KUL01⁺ cells), and *in vivo* in chickens to understand why some IBV strains have a kidney tropism. B1648 was replicating somewhat better than M41 in the epithelium of the respiratory mucosa explants and used more KUL01⁺ cells to penetrate the deeper layers of the respiratory tract. B1648 was productively replicating in KUL01⁺ monocytic cells in contrast with M41. In B1648 inoculated animals, $10^{2.7-6.8}$ viral RNA copies/100 mg were detected in tracheal secretions at 2, 4, 6, 8, 10 and 12 days post inoculation (dpi), $10^{2.4-4.5}$ viral RNA copies/ml in plasma at 2, 4, 6, 8, 10 and 12 dpi and $10^{1.8-4.4}$ viral RNA copies/ 10^6 mononuclear cells in blood at 2, 4, 6 and 8 dpi. In M41 inoculated animals, $10^{2.6-7.0}$ viral RNA copies/100 mg were detected in tracheal secretions at 2, 4, 6, 8 and 10 dpi, but viral RNA was not demonstrated in plasma and mononuclear cells (except in one chicken at 6 dpi). Infectious virus was detected only in plasma and mononuclear cells of the B1648 group. At euthanasia (12 dpi), viral RNA and antigen positive cells were detected in lungs, liver, spleen and kidneys of only the B1648 group and in tracheas of both the B1648 and M41 group. In conclusion, only B1648 can easily disseminate to internal organs via a cell-free and -associated viremia with KUL01⁺ cells as important carrier cells.

4.2.2. Introduction

Avian infectious bronchitis virus (IBV) causes mild to acute respiratory disease in chickens, characterized by coughing, sneezing, tracheal rales and dyspnea (Cavanagh and Naqi, 2003a). IBV belongs to the order of the *Nidovirales*, family *Coronaviridae*, subfamily *Coronavirinae* and genus *Gammacoronavirus* (Woo *et al.*, 2014). Worldwide, IBV causes huge economic losses in both broilers and layers. IBV has a tropism not only for the epithelium of the respiratory tract but also for the epithelium of kidneys, oviduct, gastrointestinal tract (oesophagus, proventriculus, duodenum, jejunum, bursa of Fabricius, caecal tonsils, rectum and cloaca) and testes (Cavanagh, 2007; Jackwood, 2012). IBV is clinically associated with poor performance of birds, reduced egg production and quality, as well as increased predisposition to other secondary bacterial infection (Cavanagh, 2005). IBV is highly contagious. Currently,

multiple serotypes of IBV exist, and new variants emerge due to frequent point mutations and recombination events in the viral genome (Jackwood, 2012). Vaccination failure is very common against IBV due to poor or no cross-protection between different IBV serotypes (Cook *et al.*, 2001; Lambrechts *et al.*, 1993; Pensaert and Lambrechts, 1994).

The first IBV was isolated from birds showing respiratory problems in the United States in 1931 (Fabricant, 1998). In the early 1950s, the well-known respiratory Massachusetts type of IBV (Mass) was isolated in the United States. In subsequent years, Mass-type (prototype: M41) strains have been identified worldwide, and many variants emerged. Some IBV strains were called nephropathogenic because the initial respiratory infection was followed by severe kidney infection. Important clinical signs of nephropathogenic IBV strains include increased water consumption, low body weight gain, watery droppings and significant mortality. Necropsy of birds that died during a nephropathogenic infection reveals enlarged and pale kidneys with urates in the collecting tubules (Cook *et al.*, 2012). In the 1960s, the first nephropathogenic IBV strains were reported in the US and Australia, and later worldwide. In the last 15 years, nephropathogenic IBV strains have been emerging as most prevalent IBV strains in commercial poultry (Abdel-Moneim *et al.*, 2006; Bayry *et al.*, 2005; Lim *et al.*, 2011; Mahmood *et al.*, 2011; Meir *et al.*, 2004). The B1648 strain is a Belgian reference nephropathogenic IBV serotype, that was responsible for large outbreaks of kidney disease in broiler farms in Belgium, The Netherlands and Northern France, and was first isolated in 1984 (Cook *et al.*, 2012; Meulemans *et al.*, 1987; Pensaert and Lambrechts, 1994; Reddy *et al.*, 2015).

In September 2012, a novel coronavirus emerged in humans, designated Middle East respiratory syndrome coronavirus (MERS-CoV). MERS-CoV has a higher mortality rate (>35%) than another well-known coronavirus, the severe acute respiratory syndrome coronavirus (SARS-CoV) (9.6%). The MERS-CoV infected patients usually end up with a severe pneumonia complicated with kidney failure. The severity of MERS CoV infections in humans, caused by its extra-pulmonary infection of kidneys have prompted us to question why this virus has a strong tropism for the kidneys. The same question has been raised for the kidney tropism of certain IBV strains, for the past 25 years. (Cook *et al.*, 2012; Meulemans *et al.*, 1987; Pensaert and Lambrechts, 1994; Reddy *et al.*, 2015).

In mammals, many highly pathogenic viruses or virus strains exploit and replicate productively in macrophages to cause severe systemic disease (Cline *et al.*, 2013; Dewerchin *et al.*, 2005; Hoeve *et al.*, 2012; Zhou *et al.*, 2014). Because monocytes/macrophages are usually the first line of defense against virus entry, the successful replication of virus in these cells may hamper their immunological functions and by the migratory characteristics of these cells, virus is disseminated throughout the body. In this context, peripheral blood mononuclear cells (PBMC) were used to elucidate replication kinetics of IBV nephropathogenic (B1648) and respiratory (M41) strains.

Hence, in the present study, we aimed to explore the tissue tropism characteristics of IBV nephropathogenic (B1648) and respiratory (M41) strains in chickens. To this end, replication kinetics of IBV B1648 and M41 were evaluated *in vitro* in tracheal mucosa explants and blood monocytes by a reproducible quantitative analysis system using confocal microscopy (Frydas *et al.*, 2013; Vairo *et al.*, 2013; Vandekerckhove *et al.*, 2010). A new 5' RT-qPCR was validated and used for comparing *in vivo* the viral replication kinetics in the respiratory tract and dissemination in blood of IBV B1648 and M41 (Desmarets *et al.*, 2016). Elucidating the tissue tropism mechanisms of B1648 and M41 is important to plan better prevention strategies for emerging highly nephropathogenic IBV infections.

4.2.3. Materials and Methods

4.2.3.1. IBV B1648 and M41 replication characteristics in tracheal mucosa explants and peripheral blood monocytes

4.2.3.1.1. Viruses

The virulent nephropathogenic IBV B1648 and the respiratory prototype M41 were used in this study. B1648 is a Belgian field isolate obtained in 1984 and described previously (Lambrechts *et al.*, 1993; Meulemans *et al.*, 1987; Reddy *et al.*, 2015). M41 with unknown passage history was obtained from the avian pathology laboratory, Ghent University (Pensaert *et al.*, 1981). Virus was propagated in specific pathogen free (SPF) 10 days old embryonated chicken eggs. From both B1648 and M41, a second passage was produced and utilized in the present experiment. The allantoic fluids were harvested 48 hours after infection, cleared by low-speed centrifugation

and stored at -70°C. Virus titration was performed in 10 days old chicken embryos by inoculation of 10-fold dilutions via allantoic route and expressed as 50% egg infectious dose per ml (EID₅₀/ml).

4.2.3.1.2. Virus titration

Intracellular and extracellular virus titers were determined by an EID₅₀ assay using embryonated chicken eggs. Embryonated chicken eggs were obtained from an SPF flock and used when the embryos were 10 days old. Ten-fold dilutions of virus were prepared in PBS (1x Dulbecco's phosphate buffered saline (DPBS) with 0.9 mM CaCl₂, 0.5 mM MgCl₂ × 6H₂O and 20 mg/L phenol red) (Jackwood, 2012) and 100 µl of the dilutions were inoculated into the allantoic cavity of eggs. Eggs were incubated at 37°C for 7 days. The embryos were collected and examined for the presence of embryo dwarfing and curling, which is characteristic for an IBV infection. Based on the observations, end points were calculated (Cook *et al.*, 1976; Cook *et al.*, 2012). Virus titers were assessed by a fifty percent end-point, according to the method of Reed and Muench, and expressed as EID₅₀/ml.

4.2.3.1.3. Isolation and cultivation of chicken tracheal mucosa explants

This study was performed in agreement with the guidelines of the local Ethical and Animal Welfare Committee of the Faculty of Veterinary Medicine and Bio-Science Engineering of Ghent University. The chicken tracheal mucosa explants were prepared as described previously (Reddy *et al.*, 2014). Briefly, three eight-week-old specific-pathogen free (SPF) chickens were euthanized by intravenous injection of sodium pentobarbital (100 mg/kg) in the brachial wing vein. Tracheas were collected and carefully split into two equal halves with surgical blades (Swann-Morton). Tracheal mucosal explants covering a total area of 10 mm² were made and placed on top of fine-meshed gauzes in six-well culture plates (Nunc), epithelium upwards. The explants were maintained in serum-free medium (50% Ham's F12 (Gibco)/50% DMEM (Gibco)) supplemented with 100 U/mL penicillin (Continental Pharma), 0.1 mg/mL streptomycin (Certa), 1 µg/mL gentamycin (Gibco) and 25 mM HEPES (Gibco). The epithelium of the explants was slightly immersed in the fluid to achieve an air liquid interface. Explants were maintained up to 96 hours at 37°C and 5% CO₂.

4.2.3.1.4. Isolation of blood monocytes

Five ml blood was collected on heparin (15 U/ml) (Leo) from the brachial wing vein of three chickens. Monocytes were isolated from chicken PBMC by Ficoll-paque gradient centrifugation as described by the manufacturer (Pharmacia Biotech AB). Mononuclear cells were resuspended in RPMI-1640 (Gibco) medium containing 10% fetal calf serum (FCS, Gibco), 100 U/ml penicillin (Continental Pharma), 0.1 mg/ml streptomycin (Certa), 1 µg/ml gentamycin (Gibco), and 1% non-essential amino acids (Gibco). Afterwards, 2×10^6 cells/ml were seeded in a 24-well plate (Nunc) and cultivated at 37°C with 5% CO₂. Non-adherent cells were removed by washing two times with RPMI-1640 medium at 2 and 24 h after seeding. The adherent cell population consisted of $80.2 \pm 7.3\%$ of monocytes, based on the fluorescent staining with the monocyte/macrophage marker KUL01 (Mast *et al.*, 1998). KUL01⁺ cells were cultured up to 96 hours at 37°C and 5% CO₂. All experiments were performed in triplicate.

4.2.3.1.5. IBV inoculation and sample collection of tracheal mucosa explants and monocytes

Tracheas of three chickens were used. Explants were inoculated with IBV B1648 and M41 at 24 h of cultivation. For the inoculation, explants were taken from their gauze and placed at the bottom of a 24-well plate with the epithelial surface upwards. Explants were washed twice with warm serum-free medium and inoculated with 1 ml of a virus stock containing $10^{7.0}$ EID₅₀ (1 h, 37°C, 5% CO₂). In *in vitro* tracheal mucosa experiments, the local mucus layer and other innate defense barriers reduce infectivity of the mucosa. Therefore, the mucosal explants were washed before inoculation to remove mucus and other innate defense barriers and high virus titers were used (10^7 EID₅₀/ml) in order to have sufficient virus to reach the epithelial cells. In addition, the main aim of this study was to evaluate replication kinetics at early time points, before the viability of the mucosal explants goes down, i.e. 96 h of cultivation and 72 h after virus inoculation. To meet the above expectations, the use of a high virus titer for the inoculation of *in vitro* mucosal explants is a general standardized protocol in our laboratory (Glorieux *et al.*, 2011; Steukers *et al.*, 2011, 2012; Vairo *et al.*, 2013). After one hour of virus incubation, the inoculated explants were washed three times with warm medium and placed back on the gauze. Explants were collected at 0, 6, 12, 24, 48 and 72 hours post-inoculation (hpi), embedded in Methocel[®] (Fluka) and frozen at -70°C.

Monocytes were inoculated with IBV B1648 and M41 at a multiplicity of infection (m.o.i.) of 5. To maintain uniformity and consistency, the virus titer of inoculum, incubation time, washing steps and sample collection time points should be similar in TOC and monocyte cultures under *in vitro* conditions. Therefore, the same virus titer was used to inoculate *in vitro* cultured monocytes. After 1 h of virus incubation (37°C, 5% CO₂), cells were washed three times with warm RPMI-1640 medium and further incubated in medium. Cells and supernatant were collected at 0, 6, 12, 24, 48 and 72 hpi for viral antigen quantification and virus titration. The cells were removed from the well by scraping and added to the pellet for determination of intracellular virus titers. Virus was released from the cells by 2 freeze-thaw cycles. The supernatants were used for determination of extracellular virus titers. The samples were stored at -70°C until virus titration on embryonated eggs.

4.2.3.1.6. Identification and quantification of IBV infected cells in the tracheal mucosa explants and monocytes

A double immunofluorescence staining was performed to identify and quantify individual IBV-positive cells. At 0, 6, 12, 24, 48 and 72 hpi, 15 consecutive cryosections of 10 µm were made from the frozen tracheal explants and fixed (4% paraformaldehyde for 10 minutes and 0.1% Triton[®] X-100 for 2 minutes). The cryosections were first stained for monocytes/macrophages (KUL01 marker), and next for IBV antigens. The cryosections were incubated (1 h, 37°C) with mouse monoclonal anti-chicken monocyte/macrophage (KUL01) antibodies (Southern Biotech) (1:250 in PBS containing 10% negative goat serum) and washed three times after incubation. Cryosections were then incubated (1 h, 37°C) with Texas Red-labelled goat anti-mouse IgG₁ antibodies (Molecular Probes) (1:250 in PBS containing 10% negative goat serum and 10% negative chicken serum). Subsequently, after washing, the sections were incubated (1 h, 37°C) with a polyvalent IBV hyperimmune serum conjugated with FITC (Lambrechts *et al.*, 1993; Pensaert and Lambrechts, 1994) (1:20 in PBS for B1648; 1:7 in PBS for M41). Finally, after washing, the sections were incubated (10 min, room temperature [RT]) with Hoechst 33342 (1:100 in PBS), washed and mounted with glycerin-DABCO (Janssen Chimica).

Based on cross serum neutralization tests, B1648 is distantly related to respiratory IBV strains. FITC-conjugated antibodies were prepared from a polyclonal hyperimmune serum against B1648 strain, and their reactivity against B1648 infected cells was quite different from the reactivity against M41 infected cells (Lambrechts *et al.*, 1993; Pensaert and Lambrechts, 1994). As a result, the concentration of FITC-conjugated polyclonal anti-B1648 antibodies that is needed to detect IBV-positive cells was higher for M41 than for B1648 (Pensaert *et al.*, 1981). The IBV-positive cell quantification done with FITC-conjugated polyclonal anti-B1648 antibodies was confirmed by monoclonal antibodies directed against the nucleocapsid protein (Ignjatovic and McWaters, 1991). The number of virus-infected cells was determined in 15 consecutive cryosections in both the epithelium and lamina propria of the tracheal mucosa explants. Further, at each time point, the number of infected KUL01⁺ cells was calculated both in the epithelium and lamina propria.

Monocytes were fixed in 4% paraformaldehyde for 10 minutes and 0.1% Triton[®] X-100 for 2 minutes at 0, 6, 12, 24, 48 and 72 hpi. IBV-positive cells in monocytes were visualized using the same technique as for the cryosections. The percentage of B1648 and M41-positive cells was determined for the KUL01⁺ cells (colocalization). A reproducible quantitative analysis system was followed for the elucidation of IBV replication in the tracheal mucosal explants and blood monocytes/macrophages (KUL01⁺ cells) by using a confocal microscopy (Leica TCS SPE confocal microscope) (Frydas *et al.*, 2013; Vairo *et al.*, 2013; Vandekerckhove *et al.*, 2010).

4.2.3.2. Replication kinetics of IBV B1648 and M41 in chickens

4.2.3.2.1. Experimental design

Table 1. Experimental design of *in vivo* IBV (B1648/M41) infection study.

Group		Time of inoculation (days post inoculation)			
Virus strain	Number of animals	Observation of clinical signs	Tracheal swab collection	Blood collection (plasma and PBMC*)	Euthanasia
B1648	3	-3 to 12	0, 2, 4, 6, 8, 10, 12	0, 2, 4, 6, 8, 10, 12	12
M41	3	-3 to 12	0, 2, 4, 6, 8, 10, 12	0, 2, 4, 6, 8, 10, 12	12
PBS control	3	-3 to 12	0, 2, 4, 6, 8, 10, 12	0, 2, 4, 6, 8, 10, 12	12

* Peripheral blood mononuclear cells.

The experimental setup is presented in Table 1. Nine 3-week-old SPF White Leghorn chickens were individually tagged and 3 chickens per group were housed in separate negative pressure (150 pa) isolation units (IM 1500, Montair). Before the start of the experiment, an acclimatization period of two-weeks was respected. Drinking water and food were provided *ad libitum*. The experimental design was evaluated and approved by the Ethical and Animal Welfare Committee of the Faculty of Veterinary Medicine of Ghent University (EC 2014/160).

4.2.3.2.2. Virus inoculation

Three 5-week-old chickens were inoculated with the virulent nephropathogenic B1648 strain or respiratory M41 via intratracheal (200 µl), nasal (50 µl each nostril) and ocular routes (50 µl each eye) with 10^3 EID₅₀/400 µl. The main aim of our *in vivo* study was to study the replication kinetics of IBV in the respiratory mucosa and its spread via blood to internal organs (0 to 12 dpi). To conduct this *in vivo* study successfully, mortality should not be induced. Based on our experience of past experiments and available literature, we have selected 10^3 EID₅₀/400 µl to keep the chance of mortality at a minimal level (Ariaans *et al.*, 2008; Lambrechts *et al.*, 1993; Tang *et al.*, 2008). The control chickens were mock inoculated with PBS and served as a negative control group.

4.2.3.2.3. Clinical signs and water consumption

Clinical signs, such as depression, huddling together, ruffled feathers, sneezing, coughing, tracheal rales and dyspnoea were recorded daily from -3 until 12 days post inoculation (dpi). Drinkers were regularly weighed in each group to calculate water consumption per bird.

4.2.3.2.4. Post mortem findings

At 12 dpi, the chickens from the three groups were humanely euthanized. During necropsy, all tissues were examined macroscopically. After macroscopical examination, two samples were collected from the following tissues: trachea, lungs, liver, spleen and kidneys. The first tissue sample was stored at -70°C for viral RNA quantification by RT-qPCR. The second tissue sample was embedded in Methocel® (Fluka) and was snap frozen for immunofluorescence staining.

4.2.3.2.5. Standardization of SYBR green-based RT-qPCR assay for ORF 1a gene

To avoid the detection of subgenomic mRNAs, the real-time 5' RT-qPCR primers were designed by targeting the highly conserved region of open reading frame (ORF) 1a of B1648 strain (Table 2). Then, a single step SYBR green-based 5' RT-qPCR assay was developed for ORF1a gene.

Table 2. Primers used for real-time RT-PCR of ORF 1a.

Primer name	Gene	Primer sequence	Amplico Size
cDNA_fw	ORF 1a	5'-GGT GTT AGG CTT ATA GTT CCT CAG-3'	254 nt
cDNA_rv	ORF 1a	5'-TAA ACA TTA GGG TTG ACA CCA GT-3'	
T7_fw	ORF 1a	5'-TAA TAC GAC TCA CTA TAG GGG GTG TTA GGC TTA TAG TTC CTC AG-3'	
qPCR_fw	ORF 1a	5'-GCT ATT GTA GAG GTA GTG TAT GTG AG-3'	176 nt
qPCR_rv	ORF 1a	5'-AGG GTT GAC ACC AGT AAA GAA T-3'	

4.2.3.2.6. Primer design and *in silico* validation

Multiple sequence alignments were performed with the relevant IBV sequences of GenBank in the MEGA software version 5.2.2. The real-time RT-qPCR primers were designed using the online web tool Primer 3 plus <http://www.bioinformatics.nl/cgi-bin/primer3plus/primer3plus.cgi/>. The sequences of the primers for real-time RT-qPCR targeting ORF 1a and amplicon size are listed in Table 2. Primer-specificity was assessed *in silico* by use of the Basic Local Alignment Search Tool (BLAST) in public databases and by aligning these primers to ORF 1a genes of pan IBV strains of the worldwide. The risk of primer-dimer formation, and the presence of hairpins at the annealing site were analyzed using OligoAnalyzer 3.1 (Integrated DNA Technologies) with a correction for ion concentrations set at 50 mM for Na⁺ and 3 mM for Mg²⁺. All primers used in this study were synthesized by Integrated DNA Technologies and purified by standard desalting.

4.2.3.2.7. Preparation of RNA standards for absolute quantification

Standard RNA for absolute quantification was prepared from B1648. Viral RNA of the B1648 was extracted using the QIAamp Viral RNA Mini Kit (Qiagen). A synthetic fragment containing the amplicon size of 254 nt of ORF 1a gene was generated *in vitro* to prepare the standard RNA for absolute quantification. The RNA

was reverse-transcribed into cDNA with the QIAGEN OneStep RT-PCR Kit (Qiagen), using primer set ORF 1a cDNA_fw/cDNA_rv (Table 2). ORF 1a cDNA_fw primer was modified to T7_fw with a T7 promoter sequence at its 5' end by Herculanase II fusion DNA polymerase (Agilent Technologies Inc., Santa Clara, CA, USA). The T7 promoter sequence incorporation was necessary for subsequent *in vitro* transcription (Table 2). A 50 µl OneStep RT-PCR (Qiagen) reaction mixture consisting 10 µl OneStep RT-PCR buffer (Qiagen), 2 µl dNTP (10 mM) mix, 3 µl forward primer (10 µM), 3 µl reverse primer (10 µM), 2 µl OneStep RT-PCR enzyme mix, 20 µl nuclease free water and 10 µl RNA. To generate the cDNA fragment, a reverse transcription step of 30 min at 50°C and an enzyme activation step of 15 min at 95°C were followed by 35 cycles each denaturation 30 s at 94°C, annealing 30 s at 48°C and extension 1 min at 72°C. A final extension step was performed for 10 min at 72°C and stored at 4°C until further processing. Then, the cDNA fragment was analyzed by 2% agarose gel electrophoresis, and fragments with the correct length were excised and purified from gel using the Nucleospin Gel and PCR-Clean up kit (Macherey-Nagel). The cDNA was either used directly for *in vitro* transcription or stored at -70°C. *In vitro* transcription of RNA was performed by incubation for 1h at 37°C with 10x transcription buffer, 500 µM rNTPs and 20 U T7 RNA Polymerase-Plus Enzyme Mix (Applied Biosystems). Template DNA was removed by treatment with enzyme 2U DNase I (Sigma Aldrich) for 15 min at 37°C. Then, enzyme DNase I inactivation was done for 10 min at 75°C. Finally, the *in vitro* generated RNA was purified using the RNeasy Mini Kit (Qiagen) and the amount of RNA was determined using the Nanodrop 2000 Spectrophotometer (Thermo Scientific). RNA standards were stored in single-use aliquots of 20 µl (8 ng/µl, 5.27×10^{10} copies/µl) volume at -70°C. Ten microliters of RNA was used for preparation of a standard curve, and the remainder (6 µl) was used to determine the RNA concentration with the Nanodrop 2000 Spectrophotometer. The ENDMEMO online web tool was used to calculate the number of RNA copies per microliter (<http://endmemo.com/bio/dnacopynum.php>).

4.2.3.2.8. SYBR Green based one step RT-qPCR protocol

In order to generate a standard curve, the concentration of RNA was measured as described above, and further serially ten-fold diluted in nuclease free water (Gibco). RT-qPCR reaction mixtures (20 µl) consisted of 10 µl Precision OneStep qRT-PCR Mastermix with SYBR Green and ROX (Primer Design), 200 nM (0.4 µl/reaction) of

each primer (qPCR_fw and qPCR_rv), 6.2 μ l nuclease free water and 3 μ l of standard RNA template or H₂O. Reaction mixtures were loaded in MicroAmp Optical 96-Well Reaction plates (Applied Biosystems), sealed with MicroAmp Optical Adhesive Films (Applied Biosystems), and experiments were performed in a StepOnePlus apparatus (Applied Biosystems). A reverse transcription step of 10 min at 55°C and an enzyme activation step at 95°C for 8 min were followed by 40 cycles, each 10 s at 95°C and 60 s at 58°C. Afterwards, a first-derivative melting curve analysis was performed by heating the mixture to 95°C for 15 s, then cooling to 60°C for 1 min, and heating back to 95°C at 0.3°C increments. Results were analyzed using the StepOnePlus Software version 2.2. The baseline was set automatically, and the threshold was placed manually in the exponential phase of the amplification reaction. Melt curve analysis and agarose gel electrophoresis were performed to assess specificity of the reactions. Amplification efficiency was determined by running a standard curve over a linear dynamic range (LDR) from 7 log₁₀ copies/reaction to 1 log₁₀ copies/reaction in 1:10 dilution steps. Each dilution point of the standard curve was analyzed in triplicate and also three non-template control reactions (nuclease free water) were included in each experiment.

4.2.3.2.9. Collection of tracheal secretions, plasma and PBMCs

Tracheal secretions and 2 ml of blood [with EDTA (VWR)] were collected from each chicken at 0, 2, 4, 6, 8, 10 and 12 dpi. Immediately after collection, tracheal secretions were immersed in transport medium containing PBS [1x Dulbecco's PBS (DPBS) with 0.9 mM CaCl₂, 0.5 mM MgCl₂ × 6H₂O and 20 mg/L phenol red] supplemented with 10% FCS, 1000 U/ml penicillin, 1 mg/ml streptomycin and 0.5 mg/ml kanamycin. Plain swabs were weighed before and after swabbing, and viral RNA copies were calculated per 100 mg of secretions. Plasma was harvested from blood after centrifugation (300g, 10 min) and the remaining pellet was used for isolation of PBMCs (mononuclear cells). Mononuclear cells were isolated by Ficoll-paque gradient centrifugation as described above (section A). Infection in mononuclear cells was evaluated by three methods. With the first method, 200,000 mononuclear cells were used to make cytopins and to perform immunostainings (protocol was described in section A), to quantitate the number of viral antigen positive cells. With the second method and third method, 10⁶ mononuclear cells were lysed by one freeze-thaw cycle to determine the number of viral RNA copies by RT-qPCR, and to confirm

the presence of infectious virus by virus isolation, respectively. Plasma and 10^6 mononuclear cells were stored at -70°C until use.

4.2.3.2.10. RT-qPCR in tracheal secretions, plasma and mononuclear cells

Viral RNA was extracted from tracheal secretions, plasma and mononuclear cells using the QIAamp Viral RNA Mini Kit (Qiagen). Three μl of RNA was used per RT-qPCR reaction. Viral RNA extracts from tracheal secretions, plasma and mononuclear cells were analyzed in duplicate RT-qPCR reactions as described above.

4.2.3.2.11. Virus isolation in plasma and mononuclear cells

Virus isolation from the plasma and 10^6 mononuclear cells samples were performed on 10 days old embryonated SPF eggs, to confirm the presence of infectious virus (protocol described in section A). If embryo dwarfing and curling lesions were not observed after the first inoculation, up to five blind passages of the samples were performed.

4.2.3.2.12. RT-qPCR and immunofluorescence staining of tissues

RNA was extracted from tissues using the QIAamp cadior Pathogen Mini Kit (Qiagen). Quantification of the number of viral RNA copies in tissues (RNA copies/g) was similar like in other samples. IBV-positive cells in tissues were visualized and quantified using the same technique as for the cryosections of tracheal mucosa explants. Twenty consecutive cryosections of $10\ \mu\text{m}$ were analyzed per tissue. The average number of infected cells was expressed per $10\ \text{mm}^2$ of tissue.

4.2.3.2.13. Statistical analysis

SigmaPlot (Systat Software, Inc.) software was used to analyse the data statistically with one-way analysis of variance (ANOVA). Viral loads in tracheal secretions, plasma and mononuclear cells were log-transformed prior to analysis. The quantification limit of RT-qPCR was $3.4\ \log_{10}$ copies/ml (quantification limit is the concentration/amount of viral RNA copies, which can be quantified reliably). The detection limit of RT-qPCR was $2.4\ \log_{10}$ copies/ml (detection limit is the minimal concentration of viral that can be detected). The results of three independent experiments were shown as mean \pm standard deviation (SD). P values of < 0.05 were considered to be significant.

4.2.4. Results

4.2.4.1. IBV B1648 and M41 replication characteristics in respiratory mucosa and KUL01⁺ cells

4.2.4.1.1. B1648 and M41 replication in tracheal mucosa explants

Inoculation of chicken tracheal mucosa explants with IBV B1648 and M41 led to the appearance of viral antigen positive (infected) cells in the epithelium and lamina propria of the tracheal mucosa starting from 6 hpi (Figure 1). In the epithelial layer of the tracheal mucosa, the number of B1648 and M41 infected cells gradually increased until 12 hpi, and later gradually decreased up to 72 hpi (Figure 1A). The number of B1648 infected cells in the epithelium was significantly higher than M41 infected cells at 6 (B1648: 2856.3 ± 217.2 [which equals $37.2 \pm 2.8\%$ of the epithelial cells], M41: 877.0 ± 142.7 [$11.2 \pm 2.9\%$], $P = 0.0002$), 12 (B1648: 6490.3 ± 298.9 [$82.5 \pm 4.1\%$], M41: 4380.0 ± 203.1 [$57.6 \pm 3.4\%$], $P = 0.0005$) and 24 hpi (B1648: 4077.3 ± 225.4 [$51.8 \pm 4.8\%$], M41: 3064.3 ± 144.9 [$38.9 \pm 3.0\%$], $P = 0.0028$). The number of M41 infected cells was significantly higher than B1648 infected cells at 48 hpi (B1648: 664.7 ± 164.7 , M41: 1446.7 ± 354.3 , $P = 0.0257$) and were slightly higher at 72 hpi (B1648: 130.0 ± 62.4 , M41: 179.3 ± 67.6 , $P = 0.4057$). From 48 hpi, the epithelial layer was almost totally gone, which explained the drop of positive cells.

In the lamina propria of the tracheal mucosa, B1648 and M41 infected cells were visible from 6 hpi and increased in number over time (Figure 1A). In the lamina propria, the average number of B1648 infected cells was only slightly higher than M41 infected cells at 6, 12, 24 and 48 hpi ($P = 0.6433$ to 0.1578) but significantly higher at 72 hpi ($P = 0.0249$).

Double immunofluorescence staining was performed for the identification of IBV susceptible cells. IBV infected KUL01⁺ cells were detected in the epithelium and lamina propria of the respiratory mucosa inoculated with both B1648 and M41 (Figure 1A). In the epithelium, the average number of B1648 infected KUL01⁺ cells was slightly higher than M41 infected KUL01⁺ cells at 24 and 48 hpi ($P = 0.2302$ to 0.0705) but significantly higher at 72 hpi ($P = 0.0270$). In the lamina propria, the average number of B1648 infected KUL01⁺ cells was higher than M41 infected KUL01⁺ cells at 12, 24, 48 and 72 hpi ($P = 0.0686$ to 0.0550). Interestingly, the

number of infected KUL01⁺ cells (monocytic cells) started to increase from 12 hpi, when the total number of IBV infected cells started to decrease. Representative images of IBV infected cells and IBV infected KUL01⁺ cells are given in Figure 1B.

The above results indicate that in the epithelium B1648 replicated better than M41 until 24 hpi. Then, the replication pattern changed. B1648 exploited more infected KUL01⁺ cells but without significant differences with M41 in most of the times post inoculation evaluated.

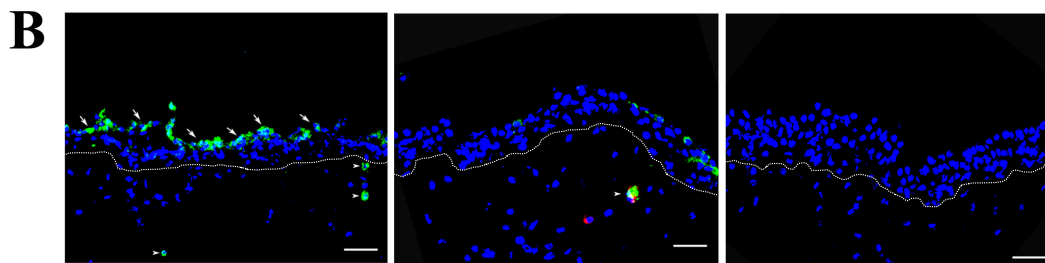
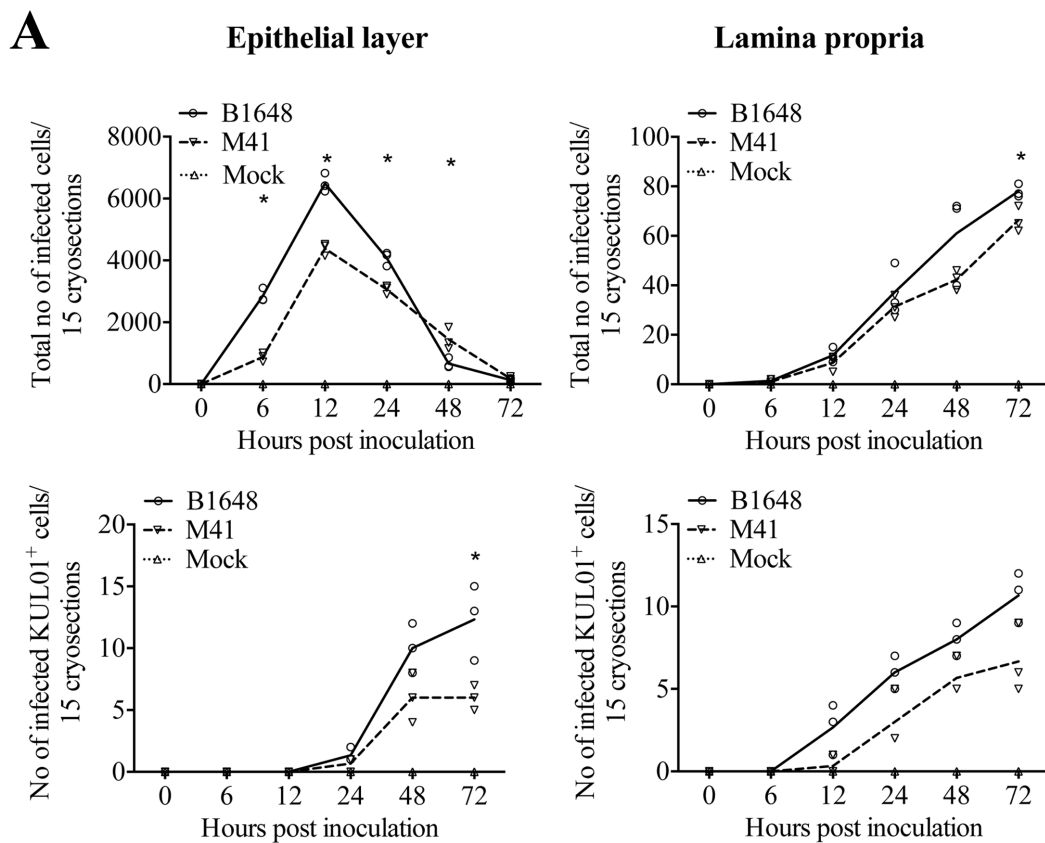


Figure 1. IBV infected cell quantification (A) and antigen expression (B) in tracheal mucosa explants. (A) Number of IBV B1648 and M41 infected cells and infected KUL01⁺ cells were quantified in the epithelial layer and lamina propria of tracheal mucosa explants. Fifteen consecutive cryosections were analysed at 0, 6, 12, 24, 48 and 72 hpi to quantify infected cells. The number of infected KUL01⁺ cells starts to

increase from 12 hpi, when the total number of IBV infected cells starts to decrease. Lines represent the evolution of arithmetic means without any transformation of original data. Solid line represents mean values of B1648, dashed line represents mean values of M41 and dotted line represents mean values of mock. An asterisk (*) indicates a significant difference ($P < 0.05$) between B1648 and M41. (B) Representative confocal photomicrograph illustrating IBV infected cells (left panel) in the epithelium (arrows) and lamina propria (arrowheads), and IBV infected KUL01⁺ cell (middle panel) in lamina propria (arrowhead) of the tracheal mucosa. Mock-inoculated tracheal mucosa (right panel). Green fluorescence visualises IBV antigens. KUL01⁺ cells are visualised by red fluorescence. Cell nuclei were stained with Hoechst (blue). White dotted line indicates the BM. Scale bar represents 50 μ m.

4.2.4.1.2. IBV B1648 and M41 replication in blood monocytic cells (KUL01⁺ cells)

The replication kinetics of IBV B1648 and M41 were compared in the peripheral blood monocytic cells (KUL01⁺ cells) (Figure 2). In blood monocytes (KUL01⁺ cells), the percentage of B1648 infected cells was significantly higher than M41 infected cells at 12 (B1648: $9.7 \pm 1.3\%$, M41: $2.2 \pm 1.9\%$, $P = 0.0051$), 24 (B1648: $16.0 \pm 2.6\%$, M41: $2.3 \pm 1.5\%$, $P = 0.0013$), 48 (B1648: $21.1 \pm 6.0\%$, M41: $1.4 \pm 1.7\%$, $P = 0.0053$) and 72 hpi (B1648: $46.0 \pm 8.6\%$, M41: $2.2 \pm 1.7\%$, $P = 0.0010$). Virus titers were analyzed in the cell lysate (intracellular virus) and supernatant (extracellular virus) of the infected blood monocytes. The intracellular and extracellular B1648 virus titers increased over time until 24 hpi, and later reached a plateau or slightly decreased up to 72 hpi. The intracellular virus titers with strain B1648 were significantly higher than M41 strain at 12 ($P = 0.0115$), 24 ($P = 0.0152$), 48 ($P = 0.0014$) and 72 hpi ($P = 0.0063$). The extracellular titers with B1648 were higher than with M41 at 12 hpi ($P = 0.0501$), and were significantly higher at 24 ($P = 0.0077$), 48 ($P = 0.0118$) and 72 hpi ($P = 0.0270$). On the contrary, no increase in viral titers was seen in cell lysate and supernatant of blood monocytic cells infected with M41, with a slope comparable to the inactivation curve. Over all, the above results demonstrated that only B1648 could establish a productive infection in the peripheral blood monocytic cells (KUL01⁺ cells).

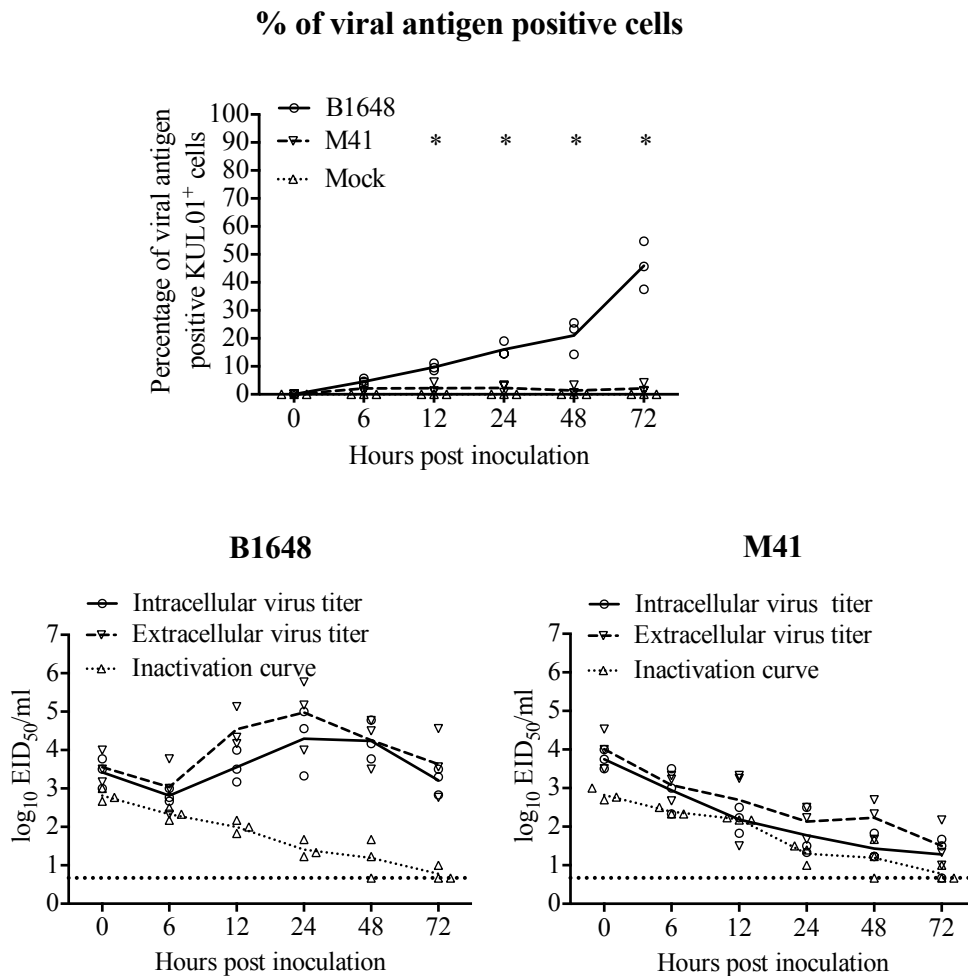


Figure 2. IBV replication kinetics in blood monocytes (KUL01⁺ cells). The monocytes were inoculated with IBV B1648 or M41 at a m.o.i. = 5. Percentage of viral antigen positive KUL01⁺ cells was determined in B1648 and M41 infected blood mononuclear cells at 0, 6, 12, 24, 48 and 72 hpi by double immunofluorescence. For viral antigen positive cells, the solid line represents the mean values of the B1648 group, the dashed line represents the mean values of the M41 group and the dotted line represents the mean values of the mock group. Intracellular and extracellular virus titers of cell lysate and supernatant were determined at designated time points. For viral titers, the solid line represents the mean values of the intracellular virus titers, the dashed line represents the mean values of the extracellular virus titers and the dotted line represents the mean values of the inactivation curve. An asterisk (*) indicates a significant difference of viral antigen positive KUL01⁺ cells between B1648 and M41 ($P < 0.05$). The inactivation curve shows the drop of virus titers at 37°C in culture medium due to inactivation events.

4.2.4.2. Replication kinetics between B1648 and M41 strains in chickens

4.2.4.2.1. Clinical signs and water consumption

After inoculation with B1648 and M41, all chickens showed signs of illness characterized by depression, ruffled feathers, huddling together, tracheal rales, sneezing, coughing and dyspnoea from 2 dpi to 10 dpi. None of the control chickens showed any clinical signs during the whole experiment. Water consumption was increased in the B1648 group (1370.7 g/bird) compared to the control group (853.7 g/bird) and the M41 group (792.2 g/bird). Reduced body weight gain was observed in the B1648 group compared to the control group and the M41 group (data not shown).

4.2.4.2.2. Post mortem findings

Chickens were euthanized at 12 dpi. Tissue samples of trachea, lungs, liver, spleen and kidneys were collected from all three groups. At necropsy, enlarged kidneys were observed in animals of the B1648 group. No lesions were observed in kidneys of the M41 group (Figure 3). Gross lesions were not observed in trachea, lungs, liver and spleen of animals of the B1648, M41 and control groups.

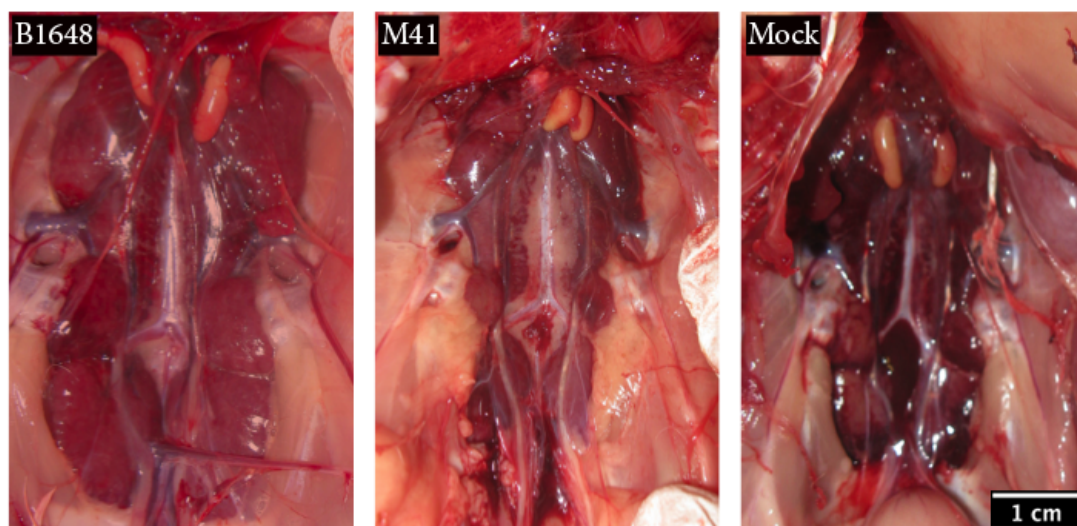


Figure 3. Representative photographs of kidneys after euthanasia (12 dpi). Kidneys were collected from chickens inoculated with IBV B1648 and M41, and PBS (mock). The kidneys of the chicken infected with B1648 were clearly enlarged.

4.2.4.2.3. Standardization of SYBR green-based RT-qPCR assay for ORF 1a gene and interpretation of results

SYBR green-based one step RT-qPCR was performed to generate a standard curve, using 1:10 serially diluted standard RNA templates. The results indicated that the standard curve had a wide dynamic range (10^1 - 10^7 copies/reaction) with the high linear correlation ($R^2 = 0.9999$) between the cycle threshold (Ct) value and template concentration (Figure 4A). The slope of the standard curve was -3.297. The amplification efficiency of the RT-qPCR assay was 102.3%, according to the slope of the exponential phase in the amplification chart (Figure 4B). Melt curve analysis showed amplification of a specific product with a melting peak at 78.31°C (Figure 4C), which was confirmed by the agarose gel electrophoresis analysis. Amplification was not observed in the non-template control. RNA extracts from samples were analyzed in duplicate reactions. Quantification of the viral RNA copies was possible if the Cq values of both reactions fell within the LDR of the RT-qPCR assay. Samples with a specific melt curve were considered positive but not quantifiable when the Cq value of the reactions fell at Cq values higher than the lowest peak of the LDR.

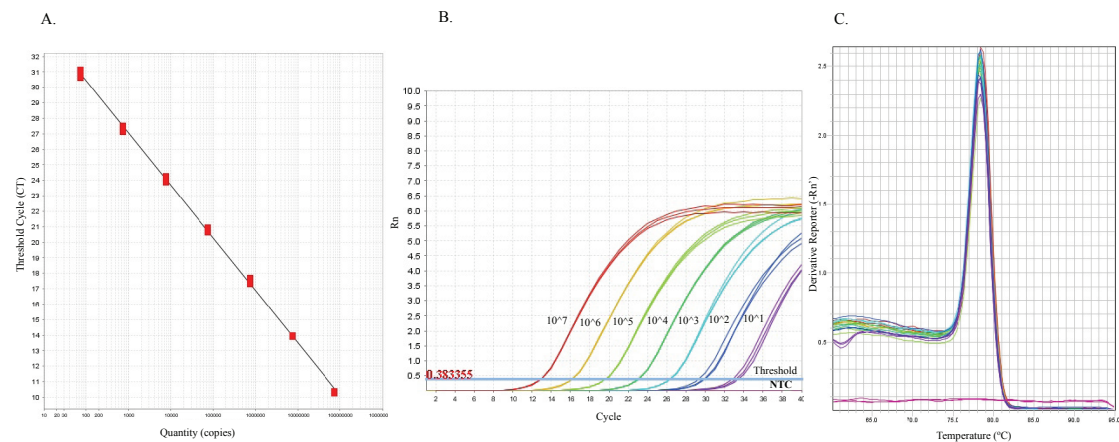


Figure 4. Standardization of SYBR green-based RT-qPCR for ORF 1a gene. (A) Standard curve, (B) amplification plot and (C) melt curve analysis over a linear dynamic range from 1 log₁₀ to 7 log₁₀ copies/reaction.

4.2.4.2.4. RT-qPCR for tracheal secretions, plasma and mononuclear cells

Viral RNA in tracheal secretions, plasma and mononuclear cells was quantified by RT-qPCR (Figure 5). The virus-shedding pattern in tracheal mucosa was the same until 10 dpi for both B1648 and M41. Viral shedding in tracheal mucosa was

identified from 2 to 12 dpi in the B1648 group with a maximum number of $10^{6.8}$ viral RNA copies/100 mg, and from 2 to 10 dpi in the M41 group with a maximum number of $10^{7.0}$ viral RNA copies/100 mg. In the B1648 group, two chickens were positive at 10 and 12 dpi. Two chickens were positive at 10 dpi, in the M41 group. In tracheal secretions, viral RNA copies were not significantly different between the B1648 and M41 groups.

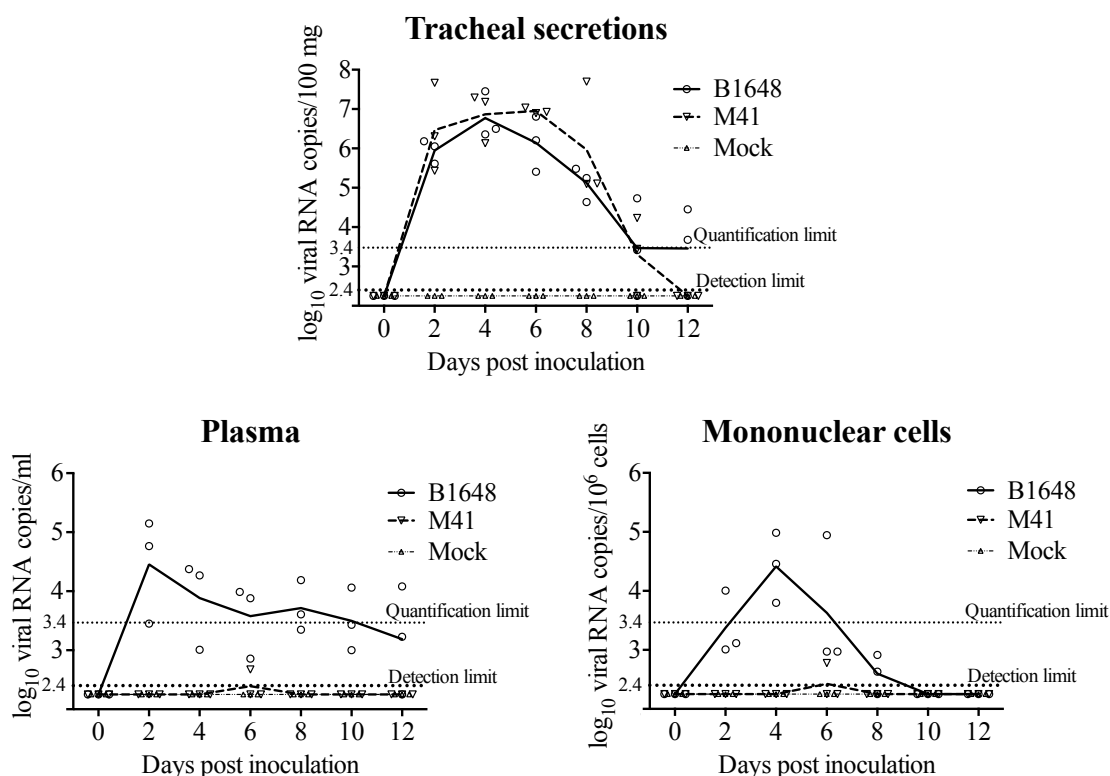


Figure 5. IBV RNA in tracheal secretions, plasma and mononuclear cells. Samples were collected from IBV B1648 and M41, and PBS (mock) inoculated chickens at 0, 2, 4, 6, 8, 10 and 12 dpi. Viral RNA was measured by RT-qPCR. Solid and dashed lines represent mean viral RNA copies per strain and per day. Mock is represented by the dash-dotted line. The quantification limit of RT-qPCR was $3.4 \log_{10}$ copies/ml (dotted line). The detection limit of RT-qPCR was $2.4 \log_{10}$ copies/ml (bold dotted line).

In plasma, viral RNA was first detected in the B1648 group at 2 dpi and was observed until the end of the study (12 dpi, $n = 2$), with a peak number of $10^{4.5}$ viral RNA copies/ml. In the M41 group, viral RNA was not detected in plasma, except of one animal at 6 dpi ($n = 1$, $10^{2.6}$ viral RNA copies/ml).

In mononuclear cells, viral RNA was first detected in the B1648 group at 2 dpi and lasted until 8 dpi (n = 2) with a peak number of $10^{4.4}$ viral RNA copies/ 10^6 cells. In contrast, viral RNA was not detected in mononuclear cells of the M41 inoculated animals, except of one chicken at 6 dpi (n = 1, $10^{2.8}$ viral RNA copies/ 10^6 cells).

The statistical analysis was not performed on viral RNA copies in plasma and mononuclear cells because the M41 group was negative except of one chicken at 6 dpi.

4.2.4.2.5. Immunostainings of cytopinned mononuclear cells

Immunofluorescence stainings of 200,000 cytopinned mononuclear cells revealed B1648 infected cells at 2 (2/3 animals), 4 (3/3) and 6 (2/3) dpi, and B1648 infected KUL01⁺ cells at 4 (1/3) and 6 (1/3) dpi. Infected cells were not observed in cytopinned mononuclear cells of M41 and control groups (Figure 6).

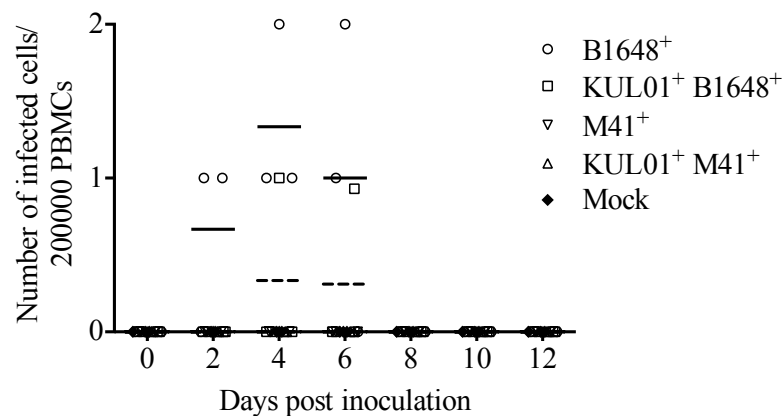


Figure 6. Quantification and identification of IBV B1648 and M41 infected total and KUL01⁺ PBMC. IBV B1648 and M41, and PBS (mock) inoculated blood samples were collected at 0, 2, 4, 6, 8, 10 and 12 dpi; 200,000 mononuclear cells were cytopinned and immunostainings were performed. B1648⁺ infected PBMC were observed at 2, 4 and 6 dpi and KUL01⁺B1648⁺ infected cells were observed at 4 and 6 dpi.

4.2.4.2.6. Virus isolation in plasma and mononuclear cells

To demonstrate the presence of infectious virus from plasma and mononuclear cells of infected animals, virus isolation was performed by several passages on 10 days old embryonated B1648 inoculated eggs (Cook *et al.*, 1976). After two blind passages, plasma of all B1648 inoculated animals at 2, 4, 6, 8, 10 and 12 dpi and mononuclear cells of all B1648 inoculated animals at 2, 4, 6 and 8 dpi caused clear dwarfing and

curling of inoculated embryos (Table 3). With mononuclear cells of the B1648 group, lesions were observed in one out of three chickens at 10 and 12 dpi, after two blind passages. Even after five blind passages, plasma and mononuclear cells from the M41 group showed no embryonic lesions, demonstrating the absence of infectious virus.

Table 3. Infectious virus in tracheal swabs, plasma and mononuclear cells. Tracheal swabs, plasma and mononuclear samples were collected in chickens at different time points post inoculation of IBV B1648 and M41. Infectious virus was measured by inoculating embryonated eggs.

Samples	IBV strain	Number of positive animals per three inoculated animals at ... days post inoculation (n =3)						
		0	2	4	6	8	10	12
Plasma	B1648	0/3	3/3	3/3	3/3	3/3	3/3	3/3
	M41	0/3	0/3	0/3	0/3	0/3	0/3	0/3
	Control	0/3	0/3	0/3	0/3	0/3	0/3	0/3
Mononuclear cells	B1648	0/3	3/3	3/3	3/3	3/3	1/3	1/3
	M41	0/3	0/3	0/3	0/3	0/3	0/3	0/3
	Control	0/3	0/3	0/3	0/3	0/3	0/3	0/3

4.2.4.2.7. RT-qPCR and immunofluorescence staining of tissues

Viral RNA was measured in samples of trachea, lungs, liver, spleen, and kidneys by RT-qPCR (Figure 7). Viral RNA was present in all collected tissues of the B1648 group and, only in tracheal samples of the M41 group (B1648: $10^{4.9 \pm 0.5}$ copies/g, M41: $10^{3.4 \pm 0.5}$ copies/g). The average B1648 viral RNA content in the lungs, liver, spleen and kidneys were $10^{5.8 \pm 1.0}$ copies/g, $10^{3.0 \pm 2.6}$ copies/g, $10^{5.5 \pm 0.5}$ copies/g and $10^{8.1 \pm 0.3}$ copies/g, respectively. Immunofluorescence staining was performed on tissues to quantify viral antigen positive cells (Figure 8). IBV infected cells were detected in the tracheal mucosa of animals inoculated with both strains (B1648: $0.33 \pm 0.06/10 \text{ mm}^2$, M41: $0.40 \pm 0.33/10 \text{ mm}^2$) and in the lungs ($0.96 \pm 0.13/10 \text{ mm}^2$), liver ($1.86 \pm 0.80/10 \text{ mm}^2$), spleen ($1.81 \pm 1.16/10 \text{ mm}^2$) and kidneys ($85.71 \pm 12.06/10 \text{ mm}^2$) of only animals inoculated with B1648.

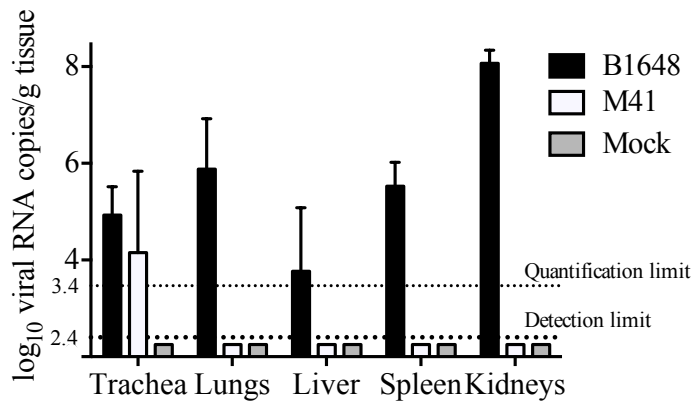


Figure 7. Viral RNA copies in the trachea, lungs, liver, spleen and kidneys at 12 dpi. Tissues were collected at euthanasia (12 dpi) from chickens inoculated with IBV B1648 and M41, and PBS (mock). Viral RNA copies (\log_{10} viral RNA copies/g of tissue) were measured by RT-qPCR. The quantification limit of RT-qPCR was 3.4 \log_{10} copies/ml (dotted line). The detection limit of RT-qPCR was 2.4 \log_{10} copies/ml (bold dotted line).

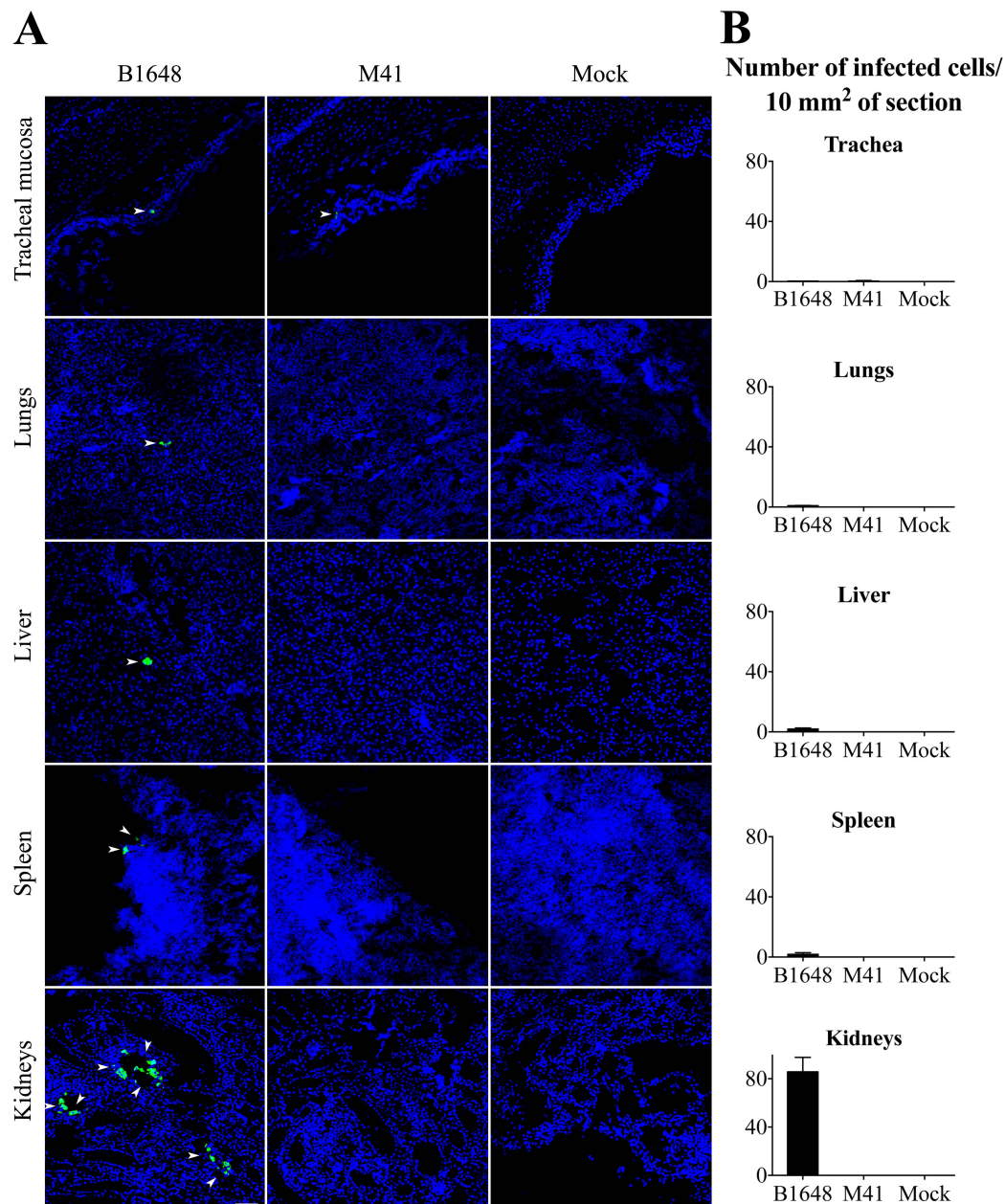


Figure 8. IBV infected cell localization (A) and quantification (B) in various tissues at 12 dpi. Trachea, lungs, liver, spleen and kidneys were collected from IBV B1648 and M41, and PBS (mock) inoculated chickens at 12 dpi. (A) Representative confocal photomicrographs illustrating viral antigen positive cells (arrowheads). Green fluorescence visualises IBV antigens. Cell nuclei were stained with Hoechst (blue). Scale bar represents 50 μm . (B) Quantification of viral antigen positive cells was performed per 20 consecutive cryosections of 10 μm tissue. Viral antigen positive cells were quantified in the tracheal mucosa of B1648 and M41 infected animals and in the lungs, liver, spleen and kidneys of only B1648 infected animals. The average number of viral antigen positive cells present in different tissues is presented per 10 μm^2 . For each tissue, mean and standard deviation (SD) are shown.

4.2.5. Discussion

Despite the circulation of nephropathogenic and respiratory IBV strains for over five to six decades, it is not well understood why some IBV strains have a kidney tropism (Cavanagh, 2007; Cook *et al.*, 2012; Reddy *et al.*, 2015). Hence, we have investigated the replication patterns of IBV nephropathogenic (B1648) and respiratory (M41) strains *in vitro*, in respiratory mucosa explants and peripheral blood monocytes, and in chickens.

The replication kinetics and invasion strategies of IBV B1648 and M41 were better understood by the work done with respiratory mucosa explants. Similar to many other IBV viruses, B1648 and M41 are epitheliotropic in the respiratory mucosa (Cavanagh, 2005, 2007; Cook *et al.*, 2012). Replication kinetics of B1648 and M41 in the respiratory mucosa explants have revealed some important differences between these strains. B1648 replicated somewhat better than M41 in the epithelium of the respiratory mucosa at 6, 12 and 24 hpi ($P < 0.05$). Consequently, B1648 destroyed the epithelial layer more severely than M41. The desquamation of the cells present in the epithelial layer is the main reason for the decreased number of IBV infected cells after 24 hpi (Raj and Jones, 1997). Above results indicated that B1648 was highly virulent compared to M41 in the epithelial layer of respiratory mucosa.

There have been several reports on the virulence of IBV strains in *in vitro* tracheal organ cultures. Chhabra *et al.* (Chhabra *et al.*, 2016) and Raj and Jones (1996b) have reported that in tracheal organ cultures, the M41 strain was highly pathogenic compared to the variant nephropathogenic IS/885/00-like and QX-like IBV strains and other variant strains (Strain G and strain 6/1432/81). In addition, Abd El Rahman *et al.* (Abd El Rahman *et al.*, 2009) have shown that Beaudette (highly passaged Massachusetts-derived strain) and QX were highly pathogenic compared to Italy 02 and 4/91 variant strains (Bourisnell *et al.*, 1985). M41 strain used in the present study seems to be somewhat less virulent than other M41 strains reported in literature (Chhabra *et al.*, 2016; Raj and Jones, 1996b).

Although speculative, a hypothesis can be formed to explain the lower virulence of M41 strain *in vitro*, which was used in the present study. The passage history of the strain and genome sequence should be considered. The passage history of the present

study M41 strain is unknown (Cook *et al.*, 1976; Pensaert *et al.*, 1981). For IBV isolation from infected chickens, sometimes several passages of the strain in embryonated eggs are necessary to observe characteristic clinical signs of infection on embryos (Cook *et al.*, 1976). The repeated passages may alter the virulence and antigenicity of the virus (Cook *et al.*, 1976). If the present study M41 strain has been serially passaged in the past, then it may have lost part of its replication ability, and it may not be able to replicate or show virulence to the extent that is associated with other reported M41 strains (Chhabra *et al.*, 2016; Raj and Jones, 1996b). Therefore, it is important to give more emphasis on the passage history of the strains to have a better understanding about their virulence and its associated biological properties (Zhang *et al.*, 2015). The genome sequence of the present study M41 strain may be different from those of the M41 strains reported by Chhabra *et al.* (Chhabra *et al.*, 2016), Raj and Jones (Raj and Jones, 1996b) and Abd El Rahman *et al.* (Abd El Rahman *et al.*, 2009). At present, there is no information available on the full genome sequence of M41 strain used in the present study. In the future, our M41 strain will be sequenced and analyzed. However, in contrast with the *in vitro* findings, our M41 was replicating better than the B1648 IBV strain *in vivo* demonstrating the fitness of our M41 in birds. Therefore, one should be careful with over interpreting the *in vitro* results.

Similar replication differences were observed in tracheal organ cultures with many other IBV strains and serotypes (Cubillos *et al.*, 1991; Raj and Jones, 1996a, b). Recently, Wickramasinghe *et al.* (2011) have reported that the attachment patterns of spike proteins were correlated with the tissue tropism and pathogenicity differences between IBV Beaudette, vaccine H120, M41 and B1648 strains. In general, the differences in virulence of strains at the respiratory mucosa might be related to the presence/absence, and/or differential expression of receptors on susceptible epithelial cells, antiviral responses of the host cells and immune-evasion mechanisms developed by the IBV strain (Widagdo *et al.*, 2016). It would be interesting to compare the replication kinetics in *in vitro* tracheal mucosa explants, between B1648 and other worldwide important IBV strains such as variant nephropathogenic IS/885/00-like and QX-like strains, recent variant M41 strains and variant Italy 02 and 4/91 strains (Cook *et al.*, 2012).

During the epithelial cell layer infection, both B1648 and M41 infected cells penetrated through the basement membrane (BM) into the lamina propria. The number of B1648 viral antigen positive cells in the lamina propria was quite higher than the number of M41 viral antigen positive cells at 6, 12, 24 and 48 hpi, and was significantly higher at 72 hpi ($P < 0.05$). Certain infected cells were identified as KUL01⁺ cells (monocytic cells) and, whose number started to increase from 12 hpi, where the total number of IBV infected cells started to decrease. It could be that the infected monocytic cells (KUL01⁺ cells) that increased after 12 hpi, started to cross the BM to enter the lamina propria and underlying layers. These infected monocytic cells (KUL01⁺ cells) may play a crucial role in dissemination of virus to the blood circulation and internal organs. Therefore, monocytic cells may be identified as carrier cells that breach through the BM to reach underlying layers of the respiratory mucosa. The use of monocytic cells by nephropathogenic IBV as a Trojan horse to penetrate through connective tissues is in line with what has been observed with equine herpes virus 1 (EHV1) and European equine arteritis virus in the respiratory mucosa of horses (Gryspeerd *et al.*, 2010; Vairo *et al.*, 2013; Vairo *et al.*, 2012; Vandekerckhove *et al.*, 2010). In our study, many infected cells in the epithelium and lamina propria were observed. Because only a certain percentage was identified as KUL01⁺, efforts will be made to identify the KUL01 negative IBV infected cells in the lamina propria of tracheal mucosa explants.

The percentage of infected peripheral blood monocytes (KUL01⁺ cells) and virus production was higher ($P < 0.05$) with B1648 than with M41 at 12, 24, 48 and 72 hpi. The intracellular and extracellular titers showed that B1648 has a strong productive replication in the peripheral blood monocytes. The decrease or no change in the intracellular and extracellular virus titers of B1648 strain at 48 and 72 hpi may be due to the absence of available susceptible cells or due to an antiviral response (e.g. interferon). This is in line with the Middle East respiratory syndrome coronavirus (MERS-CoV) and dengue virus interactions with human macrophages, and classical swine fever virus interactions with monocyte derived dendritic cells (Carrasco *et al.*, 2004; Chen and Wang, 2002; Zhou *et al.*, 2014). Absence of increase of percentage of infected cells and virus titers in the cell lysate and supernatant with M41 demonstrated that the M41 infection of monocytes was abortive. The productive replication of B1648 and abortive replication of M41 is most probably the result of differences at

certain steps of the replication cycle (entry, disassembly, genome release, transcription, translation and assembly). This issue will be further explored in the future.

In general, coughing, dyspnea, tracheal rales, depression, ruffled feathers and huddling together are characteristic clinical signs of IB in chickens (Cavanagh and Naqi, 2003a). Increased water consumption is a typical clinical sign of nephropathogenic IB and was recorded in the B1648 group (Cavanagh and Naqi, 2003b; Meir *et al.*, 2004; Raj and Jones, 1997). Reduced body weight gain was another important clinical sign noticed in the B1648 group (data not shown). At postmortem, swollen kidneys were principal macroscopic lesions recorded in the B1648 group, which is consistent with other nephropathogenic strains (Cavanagh and Naqi, 2003a).

RT-qPCR is a reproducible and reliable method for rapid quantification of IBV RNA in clinical samples (Callison *et al.*, 2006; Meir *et al.*, 2010; Roh *et al.*, 2014). At present, most of the available RT-qPCR assays, which target the nucleocapsid gene, 5' untranslated region, or the S1 gene of the IBV genome are not efficient to quantify B1648 and M41 strains in a consistent way, by the highly flexible and cost effective SYBR green method (Callison *et al.*, 2006; Meir *et al.*, 2010; Roh *et al.*, 2014). Other RT-qPCR assays that target the 3' end of the viral genome (Acevedo *et al.*, 2013; Chousalkar *et al.*, 2009; Hewson *et al.*, 2009), usually give a 3-4 log₁₀ overestimation of viral genomic RNA, as this 3' RT-qPCR detects not only genomic RNA, but also all subgenomic mRNAs (Desmarets *et al.*, 2016). Indeed, during coronavirus replication, RNA dependent RNA polymerase synthesizes genomic RNA, as well as minus strand and subgenomic mRNAs. Based on our past experience with feline coronavirus quantification, 5' RT-qPCR is the most consistent and reliable quantification method, because it evades overestimation of genomic RNAs than 3' RT-qPCR (Desmarets *et al.*, 2013; Desmarets *et al.*, 2016). Thus, 5' RT-qPCR was developed to avoid quantification of the subgenomic mRNAs.

After inoculation of virus, both B1648 and M41 initiate extensive virus replication in the epithelium of the upper respiratory tract (URT) and shed virus in the respiratory secretions between 2 to 12 dpi. In contrast to the *in vitro* results in tracheal mucosa explants, the replication of B1648 and M41 were very similar except that B1648 replication was persisting longer (12 dpi). It would have been interesting, if tracheal

swabs and mucosal tissues were collected at 6, 12, 24, 48 and 72 hpi (similar to *in vitro* experiments) to better understand the infection kinetics at the epithelial layer and lamina propria layer of *in vivo* tracheal mucosa and to compare it with *in vitro* results. The primary local replication of both B1648 and M41 at the URT allows horizontal transmission virus to susceptible birds and ensures virus circulation in birds (Ignjatovic and Sapats, 2000).

Viral RNA was detected in plasma of B1648 inoculated animals at 2 (n = 3), 4 (n = 3), 6 (n = 3), 8 (n = 3), 10 (n = 3) and 12 dpi (n = 2) at a concentration of $10^{2.4-4.5}$ and in mononuclear cells of B1648 inoculated animals at 2 (n = 3), 4 (n = 3), 6 (n = 3) and 8 (n = 2) dpi at a concentration of $10^{1.8-4.4}$ viral RNA copies/ 10^6 mononuclear cells. These B1648 viral RNA copies of plasma and mononuclear cells were originated from infectious virus as confirmed by virus isolation. In M41 inoculated animals, viral RNA was present in only one animal at 6 dpi in plasma and mononuclear cells but no infectious virus could be demonstrated by virus isolation. Infected cells were demonstrated by immunofluorescence in cytopinned mononuclear cells at 2 (n = 2), 4 (n = 3) and 6 dpi (n = 2) with B1648. M41 infected cells were never demonstrated. These results demonstrated the onset of a cell free and cell-associated viremia at 2 dpi with B1648. This indicates that cell free B1648 virus and/or B1648 infected cells are able to enter in to the blood circulation very quickly. The potential spread of B1648 from blood into the internal organs was demonstrated. In contrast with B1648, infectious virus was not demonstrated for M41 to reach the blood circulation and internal organs. Pseudorabies virus and classical swine fever virus are other examples of viruses that result in a combination of cell free and cell-associated viremia leading to the viral spread in mammals (Nawynck and Pensaert, 1995; Pensaert *et al.*, 2004). For many avian viral infections, there is no information on the viremic phase and its pathogenic consequences.

The infected mononuclear cells were mainly KUL01⁺ cells but also some KUL01 negative cells were present. The latter were not identified. They could be unidentified blood monocytic cells (KUL01 negative), B and T lymphocytes. The KUL01 marker is not reported to identify all the monocytic cells of the blood circulation (Mast *et al.*, 1998). Hence, the role of blood dendritic cells, KUL01 negative monocytic cells, B and T lymphocytes in B1648 infection kinetics and dissemination needs to be elucidated in future work.

In the B1648 group, cell-free virus in plasma persisted until the end of the study (12 dpi). Different sources may have continuously contributed to the cell-free virus in plasma during the course of B1648 infection. At early time points (2 and 4 dpi), cell free virions produced by tracheal epithelial cells may have infiltrated into the underlying submucosal layers. Then, through capillaries cell-free virions may have reached blood circulation. At 6 and 8 dpi, infected blood mononuclear cells may have released virus in plasma. The presence of infectious virus in plasma at later time points (10 and 12 dpi) but not in mononuclear cells indicated that cell free virions from infected internal organs may have leaked into the blood circulation. In the M41 group, the absence of viral RNA and infectious virus, especially at later time points (8, 10 and 12 dpi), is also an indication that infectious virus could not have reached internal organs.

Viral RNA and antigen positive cells were only detected in lungs, liver, spleen and kidneys of B1648 infected animals at 12 dpi, demonstrating that only B1648 was disseminated through the mononuclear cells and plasma but not M41 at that stage of infection. In the M41 group, the possibility of presence of viral RNA and antigen positive cells in tissues at earlier time points (6, 8 and 10 dpi) cannot be completely excluded. B1648 replicated more productively in the kidneys compared to lungs, liver and spleen, illustrating the high nephropathogenicity of B1648 (Cook *et al.*, 2012; Meulemans *et al.*, 1987; Pensaert and Lambrechts, 1994). Infected KUL01⁺ cells (colocalization) were not observed in the tissues. This demonstrates that once the virus reached internal organs, it is replicating in non-KUL01⁺ cells (Cook *et al.*, 2012). In kidneys it is known that it replicates in tubular cells.

In this study, we observed several differences between B1648 and M41 strains at the level of mononuclear cells (KUL01⁺ cells). Firstly, the number of B1648 infected KUL01⁺ cells in the lamina propria of *in vitro* tracheal mucosa explants was quite higher than M41. Secondly, the percentage of infected cells and virus production in the *in vitro* inoculated blood mononuclear cells (KUL01⁺ cells) was higher for B1648 than for M41. Thirdly, viral RNA copies were detected in mononuclear cells of all B1648 infected chickens and exceptionally with M41. The results above implicate that monocytic cells may be important carrier cells, which are required for the progress of B1648 disease. The productive and sustainable replication of B1648 virus in blood

monocytic cells (KUL01⁺ cells) may represent an important strategy used by B1648 to disseminate virus to the kidneys and other internal organs.

Even though M41 infected KUL01⁺ cells were observed in the lamina propria of the tracheal mucosa explants, the abortive replication of M41 in monocytic cells (KUL01⁺ cells) most probably hampered the dissemination of M41 via blood to reach the kidneys and other internal organs. Furthermore, the replication ability of M41 may be lowest in the lamina propria and underlying layers to release cell free virus. Therefore, it can be stated that the M41 strain that was used in the present study can replicate only in the respiratory mucosa, and cannot spread to the internal organs for further disease progression. The results presented here are somewhat different with those from other reports, where Massachusetts type strains (M41) were detected in kidneys (Butcher *et al.*, 1990; Ganapathy *et al.*, 2005; Li and Yang, 2001; Owen *et al.*, 1991). Some other studies with the M41 reference strain have shown only mild histopathological lesions with the absence of viral antigen positive cells (Benyeda *et al.*, 2010). The basis for the differences between the different studies is not clear but might be due to different M41 strains, passage levels, experimental design and conditions, nutrition, environment, intercurrent infections, age/breed of the birds, and detection techniques (Benyeda *et al.*, 2009; Raj and Jones, 1997).

Otherwise, M41 strains used in recent reports might be mutants/variants of the prototype M41. Mutation and recombination events are common in coronaviruses, which are likely to contribute to the emergence of new variants/mutants and outbreaks of new diseases (Jia *et al.*, 1995; Woo *et al.*, 2009). Currently, at least 8 full genome sequences of M41 are available in Genbank. The full genome sequence of the latest M41_2006 was closest (90.8%) to the B1648 full genome sequence compared to earlier Mass 41_1965-85 (89.7%) full genome sequences (Reddy *et al.*, 2015). It could be that the recent M41 strains may be recombinant viruses like M41_2006 with only the spike gene from the prototype M41 and the remaining genome regions from Connecticut and California serotypes (McKinley *et al.*, 2011). The Mass type (M41) is identified/classified based on the sequence of its spike gene (3500 bp) only, but one should consider that remaining genomic regions (24000 bp) may also play an important role in the pathogenicity of the virus (Armesto *et al.*, 2009; Reddy *et al.*, 2015). Thus, in the near future, full sequences should be considered and not only parts of it. Therefore, the full genome sequence of the M41 strain used in the present study

will be elucidated to understand its evolutionary relationship with other Massachusetts type strains.

The cell-associated viremia in mononuclear leukocytes and cell free virus in plasma and the replication in kidneys of B1648 virus infected chickens is very similar to another coronavirus, MERS-CoV in humans. MERS-CoV was also reported in whole blood and plasma of humans (Chan *et al.*, 2013; Drosten *et al.*, 2013; Guery *et al.*, 2013). In addition, MERS-CoV is replicating in monocytic cells and kidneys, resulting in high mortality in humans (Chan *et al.*, 2013; Drosten *et al.*, 2013; Eckerle *et al.*, 2013; Guery *et al.*, 2013; Zhou *et al.*, 2014).

In summary, B1648 and M41 strains followed different tissue tropism mechanisms. Both B1648 and M41 strains successfully invade and replicate in the epithelium of the respiratory mucosa. B1648 uses more mononuclear cells as carrier cells to breach through the underlying layers of the respiratory mucosa. The penetration through the deeper layers of the respiratory mucosa was more intensive with B1648 compared to M41. B1648 spreads via a cell free and cell-associated viremia to target organs such as kidneys, liver, spleen and lungs whereas M41 does not do this. B1648 showed a fully productive replication in the KUL01⁺ blood monocytic cells. B1648 replication was more productive in kidneys and less in liver, spleen and lungs. During M41 infection, the infected KUL01⁺ cells could not be able to infiltrate into the circulation or were abortive in the submucosal layers of the upper respiratory tract (trachea and bronchi). Our study unveils hitherto unknown, but crucial aspects of the tissue tropism of B1648 and M41 strains. B1648 has achieved highly nephropathogenic hallmarks by exploiting the carrier mononuclear cells in an active manner, whereas M41 is not nephropathogenic due to the abortive nature of M41 infection of mononuclear cells.

4.2.6. Acknowledgments

This research was supported by the Indian Council of Agricultural Research - International Fellowship (ICAR, Pusa, New Delhi-110012 (29-1/2009-EQR/Edn)) and Ghent University - Special Research Fund. Vishwanatha RAP Reddy and Hans J Nauwynck are members of the BELVIR consortium (IAP, phase VII) sponsored by Belgian Science Policy Office (BELSPO). The authors acknowledge Magda De Keyzer, Lieve Sys, Melanie Bauwens, Ytse Noppe and Zeger Van den Abeele for their

excellent technical assistance. The local Ethical and Animal Welfare Committee of the Faculty of Veterinary Medicine of Ghent University approved the animal experiment (EC 2014/160).

4.2.7. References

- Abd El Rahman, S., El-Kenawy, A.A., Neumann, U., Herrler, G., Winter, C., 2009. Comparative analysis of the sialic acid binding activity and the tropism for the respiratory epithelium of four different strains of avian infectious bronchitis virus. *Avian Pathol* 38, 41-45.
- Abdel-Moneim, A.S., El-Kady, M.F., Ladman, B.S., Gelb, J., 2006. S1 gene sequence analysis of a nephropathogenic strain of avian infectious bronchitis virus in Egypt. *Virology* 3, 78.
- Acevedo, A.M., Perera, C.L., Vega, A., Rios, L., Coronado, L., Relova, D., Frias, M.T., Ganges, L., Nunez, J.I., Perez, L.J., 2013. A duplex SYBR Green I-based real-time RT-PCR assay for the simultaneous detection and differentiation of Massachusetts and non-Massachusetts serotypes of infectious bronchitis virus. *Mol Cell Probes* 27, 184-192.
- Ariaans, M.P., Matthijs, M.G., van Haarlem, D., van de Haar, P., van Eck, J.H., Hensen, E.J., Vervelde, L., 2008. The role of phagocytic cells in enhanced susceptibility of broilers to colibacillosis after Infectious Bronchitis Virus infection. *Vet Immunol Immunopathol* 123, 240-250.
- Armesto, M., Cavanagh, D., Britton, P., 2009. The replicase gene of avian coronavirus infectious bronchitis virus is a determinant of pathogenicity. *PLoS One* 4, e7384.
- Bayry, J., Goudar, M.S., Nighot, P.K., Kshirsagar, S.G., Ladman, B.S., Gelb, J., Ghalsasi, G.R., Kolte, G.N., 2005. Emergence of a nephropathogenic avian infectious bronchitis virus with a novel genotype in India. *J Clin Microbiol* 43, 916-918.
- Benyeda, Z., Mató, T., Süveges, T., Szabó, E., Kardi, V., Abonyi-Tóth, Z., Rusvai, M., Palya, V., 2009. Comparison of the pathogenicity of QX-like, M41 and 793/B infectious bronchitis strains from different pathological conditions. *Avian Pathol* 38, 449-456.
- Benyeda, Z., Szeredi, L., Mató, T., Süveges, T., Balka, G., Abonyi-Tóth, Z., Rusvai, M., Palya, V., 2010. Comparative histopathology and immunohistochemistry of QX-like, Massachusetts and 793/B serotypes of infectious bronchitis virus infection in chickens. *J Comp Pathol* 143, 276-283.
- Bournsnel, M.E., Binns, M.M., Foulds, I.J., Brown, T.D., 1985. Sequences of the nucleocapsid genes from two strains of avian infectious bronchitis virus. *J Gen Virol* 66 (Pt 3), 573-580.

- Butcher, G.D., Winterfield, R.W., Shapiro, D.P., 1990. Pathogenesis of H13 nephropathogenic infectious bronchitis virus. *Avian Dis* 34, 916-921.
- Callison, S.A., Hilt, D.A., Boynton, T.O., Sample, B.F., Robison, R., Swayne, D.E., Jackwood, M.W., 2006. Development and evaluation of a real-time Taqman RT-PCR assay for the detection of infectious bronchitis virus from infected chickens. *J Virol Methods* 138, 60-65.
- Carrasco, C.P., Rigden, R.C., Vincent, I.E., Balmelli, C., Ceppi, M., Bauhofer, O., Tache, V., Hjertner, B., McNeilly, F., van Gennip, H.G., McCullough, K.C., Summerfield, A., 2004. Interaction of classical swine fever virus with dendritic cells. *J Gen Virol* 85, 1633-1641.
- Cavanagh, D., 2005. Coronaviruses in poultry and other birds. *Avian Pathol* 34, 439-448.
- Cavanagh, D., 2007. Coronavirus avian infectious bronchitis virus. *Vet Res* 38, 281-297.
- Cavanagh, D., Naqi, S.A., 2003a. *Infectious Bronchitis*, Vol 11, 11 Edition. Iowa state press, Ames, Iowa.
- Cavanagh, D., Naqi, S.A., 2003b. *Infectious bronchitis*, 11 Edition. Iowa state press, Ames, Iowa, 20 p.
- Chan, R.W., Chan, M.C., Agnihothram, S., Chan, L.L., Kuok, D.I., Fong, J.H., Guan, Y., Poon, L.L., Baric, R.S., Nicholls, J.M., Peiris, J.S., 2013. Tropism of and innate immune responses to the novel human betacoronavirus lineage C virus in human ex vivo respiratory organ cultures. *J Virol* 87, 6604-6614.
- Chen, Y.C., Wang, S.Y., 2002. Activation of terminally differentiated human monocytes/macrophages by dengue virus: productive infection, hierarchical production of innate cytokines and chemokines, and the synergistic effect of lipopolysaccharide. *J Virol* 76, 9877-9887.
- Chhabra, R., Kuchipudi, S.V., Chantrey, J., Ganapathy, K., 2016. Pathogenicity and tissue tropism of infectious bronchitis virus is associated with elevated apoptosis and innate immune responses. *Virology* 488, 232-241.
- Chousalkar, K.K., Cheetham, B.F., Roberts, J.R., 2009. LNA probe-based real-time RT-PCR for the detection of infectious bronchitis virus from the oviduct of unvaccinated and vaccinated laying hens. *J Virol Methods* 155, 67-71.
- Cline, T.D., Karlsson, E.A., Seufzer, B.J., Schultz-Cherry, S., 2013. The hemagglutinin protein of highly pathogenic H5N1 influenza viruses overcomes an early block in the replication cycle to promote productive replication in macrophages. *J Virol* 87, 1411-1419.
- Cook, J.K., Chesher, J., Baxendale, W., Greenwood, N., Huggins, M.B., Orbell, S.J., 2001. Protection of chickens against renal damage caused by a nephropathogenic infectious bronchitis virus. *Avian Pathol* 30, 423-426.

- Cook, J.K., Darbyshire, J.H., Peters, R.W., 1976. The use of chicken tracheal organ cultures for the isolation and assay of avian infectious bronchitis virus. *Arch Virol* 50, 109-118.
- Cook, J.K., Jackwood, M., Jones, R.C., 2012. The long view: 40 years of infectious bronchitis research. *Avian Pathol* 41, 239-250.
- Cubillos, A., Ulloa, J., Cubillos, V., Cook, J.K., 1991. Characterisation of strains of infectious bronchitis virus isolated in Chile. *Avian Pathol* 20, 85-99.
- Desmarests, L.M., Theuns, S., Olyslaegers, D.A., Dedeurwaerder, A., Vermeulen, B.L., Roukaerts, I.D., Nauwynck, H.J., 2013. Establishment of feline intestinal epithelial cell cultures for the propagation and study of feline enteric coronaviruses. *Vet Res* 44, 71.
- Desmarests, L.M., Vermeulen, B.L., Theuns, S., Conceicao-Neto, N., Zeller, M., Roukaerts, I.D., Acar, D.D., Olyslaegers, D.A., Van Ranst, M., Matthijnssens, J., Nauwynck, H.J., 2016. Experimental feline enteric coronavirus infection reveals an aberrant infection pattern and shedding of mutants with impaired infectivity in enterocyte cultures. *Sci Rep* 6, 20022.
- Dewerchin, H.L., Cornelissen, E., Nauwynck, H.J., 2005. Replication of feline coronaviruses in peripheral blood monocytes. *Arch Virol* 150, 2483-2500.
- Drosten, C., Seilmaier, M., Corman, V.M., Hartmann, W., Scheible, G., Sack, S., Guggemos, W., Kallies, R., Muth, D., Junglen, S., Muller, M.A., Haas, W., Guberina, H., Rohnisch, T., Schmid-Wendtner, M., Aldabbagh, S., Dittmer, U., Gold, H., Graf, P., Bonin, F., Rambaut, A., Wendtner, C.M., 2013. Clinical features and virological analysis of a case of Middle East respiratory syndrome coronavirus infection. *Lancet Infect Dis* 13, 745-751.
- Eckerle, I., Muller, M.A., Kallies, S., Gotthardt, D.N., Drosten, C., 2013. In-vitro renal epithelial cell infection reveals a viral kidney tropism as a potential mechanism for acute renal failure during Middle East Respiratory Syndrome (MERS) Coronavirus infection. *Virology* 453, 359.
- Fabricant, J., 1998. The early history of infectious bronchitis. *Avian Dis* 42, 648-650.
- Frydas, I.S., Verbeeck, M., Cao, J., Nauwynck, H.J., 2013. Replication characteristics of porcine reproductive and respiratory syndrome virus (PRRSV) European subtype 1 (Lelystad) and subtype 3 (Lena) strains in nasal mucosa and cells of the monocytic lineage: indications for the use of new receptors of PRRSV (Lena). *Vet Res* 44, 73.
- Ganapathy, K., Cargill, P.W., Jones, R.C., 2005. Effects of cold storage on detection of avian infectious bronchitis virus in chicken carcasses and local antibodies in tracheal washes. *J Virol Methods* 126, 87-90.
- Glorieux, S., Bachert, C., Favoreel, H.W., Vandekerckhove, A.P., Steukers, L., Reckecki, A., Van den Broeck, W., Goossens, J., Croubels, S., Clayton, R.F., Nauwynck, H.J., 2011. Herpes simplex virus type 1 penetrates the basement membrane in human nasal respiratory mucosa. *PLoS One* 6, e22160.

- Gryspeerdt, A.C., Vandekerckhove, A.P., Garre, B., Barbe, F., Van de Walle, G.R., Nauwynck, H.J., 2010. Differences in replication kinetics and cell tropism between neurovirulent and non-neurovirulent EHV1 strains during the acute phase of infection in horses. *Vet Microbiol* 142, 242-253.
- Guery, B., Poissy, J., el Mansouf, L., Sejourne, C., Ettahar, N., Lemaire, X., Vuotto, F., Goffard, A., Behillil, S., Enouf, V., Caro, V., Mailles, A., Che, D., Manuguerra, J.C., Mathieu, D., Fontanet, A., van der Werf, S., group, M.E.-C.s., 2013. Clinical features and viral diagnosis of two cases of infection with Middle East Respiratory Syndrome coronavirus: a report of nosocomial transmission. *Lancet* 381, 2265-2272.
- Hewson, K., Noormohammadi, A.H., Devlin, J.M., Mardani, K., Ignjatovic, J., 2009. Rapid detection and non-subjective characterisation of infectious bronchitis virus isolates using high-resolution melt curve analysis and a mathematical model. *Arch Virol* 154, 649-660.
- Hoeve, M.A., Nash, A.A., Jackson, D., Randall, R.E., Dransfield, I., 2012. Influenza virus A infection of human monocyte and macrophage subpopulations reveals increased susceptibility associated with cell differentiation. *PLoS One* 7, e29443.
- Ignjatovic, J., McWaters, P.G., 1991. Monoclonal antibodies to three structural proteins of avian infectious bronchitis virus: characterization of epitopes and antigenic differentiation of Australian strains. *J Gen Virol* 72 (Pt 12), 2915-2922.
- Ignjatovic, J., Sapats, S., 2000. Avian infectious bronchitis virus. *Rev Sci Tech* 19, 493-508.
- Jackwood, M.W., 2012. Review of infectious bronchitis virus around the world. *Avian Dis* 56, 634-641.
- Jia, W., Karaca, K., Parrish, C.R., Naqi, S.A., 1995. A novel variant of avian infectious bronchitis virus resulting from recombination among three different strains. *Arch Virol* 140, 259-271.
- Lambrechts, C., Pensaert, M., Ducatelle, R., 1993. Challenge experiments to evaluate cross-protection induced at the trachea and kidney level by vaccine strains and Belgian nephropathogenic isolates of avian infectious bronchitis virus. *Avian Pathol* 22, 577-590.
- Li, H., Yang, H., 2001. Sequence analysis of nephropathogenic infectious bronchitis virus strains of the Massachusetts genotype in Beijing. *Avian Pathol* 30, 535-541.
- Lim, T.H., Lee, H.J., Lee, D.H., Lee, Y.N., Park, J.K., Youn, H.N., Kim, M.S., Lee, J.B., Park, S.Y., Choi, I.S., Song, C.S., 2011. An emerging recombinant cluster of nephropathogenic strains of avian infectious bronchitis virus in Korea. *Infect Genet Evol* 11, 678-685.

- Mahmood, Z.H., Sleman, R.R., Uthman, A.U., 2011. Isolation and molecular characterization of Sul/01/09 avian infectious bronchitis virus, indicates the emergence of a new genotype in the Middle East. *Vet Microbiol* 150, 21-27.
- Mast, J., Goddeeris, B.M., Peeters, K., Vandesande, F., Berghman, L.R., 1998. Characterisation of chicken monocytes, macrophages and interdigitating cells by the monoclonal antibody KUL01. *Vet Immunol Immunopathol* 61, 343-357.
- McKinley, E.T., Jackwood, M.W., Hilt, D.A., Kissinger, J.C., Robertson, J.S., Lemke, C., Paterson, A.H., 2011. Attenuated live vaccine usage affects accurate measures of virus diversity and mutation rates in avian coronavirus infectious bronchitis virus. *Virus Res* 158, 225-234.
- Meir, R., Maharat, O., Farnushi, Y., Simanov, L., 2010. Development of a real-time TaqMan RT-PCR assay for the detection of infectious bronchitis virus in chickens, and comparison of RT-PCR and virus isolation. *J Virol Methods* 163, 190-194.
- Meir, R., Rosenblut, E., Perl, S., Kass, N., Ayali, G., Perk, S., Hemsani, E., 2004. Identification of a novel nephropathogenic infectious bronchitis virus in Israel. *Avian Dis* 48, 635-641.
- Meulemans, G., Carlier, M.C., Gonze, M., Petit, P., Vandebroek, M., 1987. Incidence, characterisation and prophylaxis of nephropathogenic avian infectious bronchitis viruses. *Vet Rec* 120, 205-206.
- Nawynck, H.J., Pensaert, M.B., 1995. Cell-free and cell-associated viremia in pigs after oronasal infection with Aujeszky's disease virus. *Vet Microbiol* 43, 307-314.
- Owen, R.L., Cowen, B.S., Hattel, A.L., Naqi, S.A., Wilson, R.A., 1991. Detection of viral antigen following exposure of one-day-old chickens to the Holland 52 strain of infectious bronchitis virus. *Avian Pathol* 20, 663-673.
- Pensaert, M., Lambrechts, C., 1994. Vaccination of chickens against a Belgian nephropathogenic strain of infectious bronchitis virus B1648 using attenuated homologous and heterologous strains. *Avian Pathol* 23, 631-641.
- Pensaert, M.B., Debouck, P., Reynolds, D.J., 1981. An immunoelectron microscopic and immunofluorescent study on the antigenic relationship between the coronavirus-like agent, CV 777, and several coronaviruses. *Arch Virol* 68, 45-52.
- Pensaert, M.B., Sanchez, R.E., Jr., Ladekjaer-Mikkelsen, A.S., Allan, G.M., Nauwynck, H.J., 2004. Viremia and effect of fetal infection with porcine viruses with special reference to porcine circovirus 2 infection. *Vet Microbiol* 98, 175-183.
- Raj, G.D., Jones, R.C., 1996a. Immunopathogenesis of infection in SPF chicks and commercial broiler chickens of a variant infectious bronchitis virus of economic importance. *Avian Pathol* 25, 481-501.

- Raj, G.D., Jones, R.C., 1996b. An in vitro comparison of the virulence of seven strains of infectious bronchitis virus using tracheal and oviduct organ cultures. *Avian Pathol* 25, 649-662.
- Raj, G.D., Jones, R.C., 1997. Infectious bronchitis virus: Immunopathogenesis of infection in the chicken. *Avian Pathol* 26, 677-706.
- Reddy, V.R., Steukers, L., Li, Y., Fuchs, W., Vanderplasschen, A., Nauwynck, H.J., 2014. Replication characteristics of infectious laryngotracheitis virus in the respiratory and conjunctival mucosa. *Avian Pathol* 43, 450-457.
- Reddy, V.R., Theuns, S., Roukaerts, I.D., Zeller, M., Matthijnsens, J., Nauwynck, H.J., 2015. Genetic Characterization of the Belgian Nephropathogenic Infectious Bronchitis Virus (NIBV) Reference Strain B1648. *Viruses* 7, 4488-4506.
- Roh, H.J., Hilt, D.A., Jackwood, M.W., 2014. Detection of infectious bronchitis virus with the use of real-time quantitative reverse transcriptase-PCR and correlation with virus detection in embryonated eggs. *Avian Dis* 58, 398-403.
- Steukers, L., Vandekerckhove, A.P., Van den Broeck, W., Glorieux, S., Nauwynck, H.J., 2011. Comparative analysis of replication characteristics of BoHV-1 subtypes in bovine respiratory and genital mucosa explants: a phylogenetic enlightenment. *Vet Res* 42, 33.
- Steukers, L., Vandekerckhove, A.P., Van den Broeck, W., Glorieux, S., Nauwynck, H.J., 2012. Kinetics of BoHV-1 dissemination in an in vitro culture of bovine upper respiratory tract mucosa explants. *ILAR J* 53, E43-54.
- Tang, M., Wang, H., Zhou, S., Tian, G., 2008. Enhancement of the immunogenicity of an infectious bronchitis virus DNA vaccine by a bicistronic plasmid encoding nucleocapsid protein and interleukin-2. *J Virol Methods* 149, 42-48.
- Vairo, S., Van den Broeck, W., Favoreel, H., Scagliarini, A., Nauwynck, H., 2013. Development and use of a polarized equine upper respiratory tract mucosal explant system to study the early phase of pathogenesis of a European strain of equine arteritis virus. *Vet Res* 44, 22.
- Vairo, S., Vandekerckhove, A., Steukers, L., Glorieux, S., Van den Broeck, W., Nauwynck, H., 2012. Clinical and virological outcome of an infection with the Belgian equine arteritis virus strain 08P178. *Vet Microbiol* 157, 333-344.
- Vandekerckhove, A.P., Glorieux, S., Gryspeerdt, A.C., Steukers, L., Duchateau, L., Osterrieder, N., Van de Walle, G.R., Nauwynck, H.J., 2010. Replication kinetics of neurovirulent versus non-neurovirulent equine herpesvirus type 1 strains in equine nasal mucosal explants. *J Gen Virol* 91, 2019-2028.
- Wickramasinghe, I.N., de Vries, R.P., Grone, A., de Haan, C.A., Verheije, M.H., 2011. Binding of avian coronavirus spike proteins to host factors reflects virus tropism and pathogenicity. *J Virol* 85, 8903-8912.

- Widagdo, W., Raj, V.S., Schipper, D., Kolijn, K., van Leenders, G.J., Bosch, B.J., Bensaid, A., Segales, J., Baumgartner, W., Osterhaus, A.D., Koopmans, M.P., van den Brand, J.M., Haagmans, B.L., 2016. Differential expression of the MERS-coronavirus receptor in the upper respiratory tract of humans and dromedary camels. *J Virol*.
- Woo, P.C., Lau, S.K., Huang, Y., Yuen, K.Y., 2009. Coronavirus diversity, phylogeny and interspecies jumping. *Exp Biol Med (Maywood)* 234, 1117-1127.
- Woo, P.C., Lau, S.K., Lam, C.S., Tsang, A.K., Hui, S.W., Fan, R.Y., Martelli, P., Yuen, K.Y., 2014. Discovery of a novel bottlenose dolphin coronavirus reveals a distinct species of marine mammal coronavirus in *Gammacoronavirus*. *J Virol* 88, 1318-1331.
- Zhang, S., Xiang, J., Van Doorselaere, J., Nauwynck, H.J., 2015. Comparison of the pathogenesis of the highly passaged MCMV Smith strain with that of the low passaged MCMV HaNa1 isolate in BALB/c mice upon oronasal inoculation. *Vet Res* 46, 94.
- Zhou, J., Chu, H., Li, C., Wong, B.H., Cheng, Z.S., Poon, V.K., Sun, T., Lau, C.C., Wong, K.K., Chan, J.Y., Chan, J.F., To, K.K., Chan, K.H., Zheng, B.J., Yuen, K.Y., 2014. Active replication of Middle East respiratory syndrome coronavirus and aberrant induction of inflammatory cytokines and chemokines in human macrophages: implications for pathogenesis. *J Infect Dis* 209, 1331-1342.

CHAPTER 5.

GENERAL DISCUSSION

Respiratory tract infections are very common in worldwide poultry industry. A wide variety of respiratory viruses have been associated with the respiratory tract of poultry, and may cause high morbidity and mortality in chickens (Jones, 2010). Infectious laryngotracheitis virus (ILTV) and infectious bronchitis virus (IBV) are two of the most devastating respiratory viruses in commercial poultry worldwide (Cavanagh, 2007; Cook *et al.*, 2012; Fuchs *et al.*, 2007; Jones, 2010; Menendez *et al.*, 2014). The alphaherpesvirus ILTV and the coronavirus IBV are highly contagious avian viruses. Nostrils and eyes are the main portals of entry of ILTV and IBV. Although, ILTV and IBV are circulating already for several decades, their replication kinetics at the primary replication site and invasion mechanism are largely unknown (Cavanagh, 2007; May and Tittsler, 1925; Menendez *et al.*, 2014; Schalk and Hawn, 1931). In this study, several aspects of the pathogenesis of ILTV and IBV infections were examined under *in vitro* and *in vivo* conditions.

Establishment of *in vitro* tracheal and conjunctival mucosal explant models of chickens

ILTV replicates initially in the epithelial cells of the upper respiratory and conjunctival mucosae (Garcia *et al.*, 2013; Guy and Bagust, 2003). After initial replication, ILTV may penetrate through the basement membrane (BM) to spread through underlying layers (Glorieux *et al.*, 2009; Steukers *et al.*, 2011). During severe infection, chickens end up with marked gasping, open mouth breathing, expectoration of bloody mucus and asphyxiation (Fuchs *et al.*, 2007). The replication kinetics and invasion mechanisms at the initial replication site are largely not understood. These mechanisms are important to understand the pathogenesis and dissemination of virus to internal organs. The *in vivo* experiments are involved with high costs, and challenged with ethical questions (Bang and Bang, 1967; Kirkpatrick *et al.*, 2006). Thus, the establishment of *in vitro* organ cultures is necessary to investigate specific questions about replication kinetics and invasion mechanisms. Chicken tracheal and conjunctival mucosal explants were collected from 4 to 8 weeks old chickens and cultured at an air liquid interface (chapter 3.1.). One side of the mucosal tissue was exposed to air, the other side was exposed to serum free medium. This positioning mimics physiological conditions of respiratory mucosa (Glorieux *et al.*, 2009). In contrast to cell cultures, the *in vitro* explant models maintain morphology, cell-cell and cell-extracellular matrix interactions, and ultimately the 3D architecture of tissues

(Glorieux *et al.*, 2009; Lin *et al.*, 2001; Schmidt *et al.*, 1996; Steukers *et al.*, 2012; Yoon *et al.*, 2002). The *in vitro* explant models are in line with the “three Rs” ethical dogma: Reduction, Refinement and Replacement. Refinement is minimizing the pain, Reduction is lowering the number of animals and Replacement is using *in vitro* alternatives instead of living animals (Russell and Burch, 1959). The use of *in vitro* models reduces inter-animal variation and experiment-to-experiment variations. Furthermore, the natural route of infection is well mimicked with these models.

By light microscopy and fluorescent terminal deoxynucleotidyl transferase dUTP nick end-labelling (TUNEL) staining it was demonstrated that the organ culture could successfully be maintained up to 96 h of cultivation. The tracheal ring culture with alternating air and medium exposure is another commonly used method to study host pathogen interactions in chickens (Reemers *et al.*, 2009). However, the explant culture on metal gauze with air liquid interface resembles better than the *in vivo* conditions. All together, this study established an *in vitro* model that very closely mimics the *in vivo* physiological situation.

The established *in vitro* tracheal and conjunctival explant models are useful to study infection kinetics of avian viruses and/or pathogens

The *in vitro* tracheal and conjunctival mucosal explant models were used to test whether ILTV (U76/1035) successfully infects and replicates in the mucosae (chapter 3.1.). The *in vitro* mucosal explant models were susceptible to ILTV infection. By confocal microscopy, a complete 3D picture of horizontal and vertical spread of ILTV was elucidated. From 24 hpi, ILTV spreads in a plaquewise manner through both tracheal and conjunctival mucosal explants. ILTV spreads laterally in both mucosae (latitude) and vertically through the BM of the mucosae (invasion depth). The plaque latitude increased with time and breached through the BM from 48 hpi. At later time points (72 hpi), ILTV was replicating more extensively in the conjunctival mucosa compared with the tracheal mucosa. This is due to variation in its tropism for the tracheal and conjunctival mucosa (Kirkpatrick *et al.*, 2006). ILTV invasion through the BM is very limited, when compared to mammal alphaherpesviruses SHV1, BHV1 and HSV1, which are all highly invasive (Glorieux *et al.*, 2011a; Glorieux *et al.*, 2009; Steukers *et al.*, 2011). The limited invasion of ILTV through the BM agrees with the *in vivo* pathogenesis of ILTV, where no clear evidence exists for viraemia

(Garcia *et al.*, 2013; Guy and Bagust, 2003). In addition, this study clearly confirmed that ILTV penetrates through the BM of the tracheal and conjunctival mucosae. Indeed, Zhao *et al.* (2013) and Roy *et al.* (2015) have reported ILTV in the internal organs of infected chickens.

The above results have proved that ILTV (U76/1035) is well adapted to replicate and spread in the *in vitro* tracheal and conjunctival mucosae. Thus, these established *in vitro* explant models are valuable tools to elucidate replication kinetics of other avian respiratory viruses, bacteria, fungi and other pathogens.

ILTV effects on apoptosis were evaluated for both tracheal and conjunctival mucosae by TUNEL assay. Among large number of ILTV-positive cells, only few ILTV infected cells were observed to be TUNEL-positive in both mucosae, and this observation corroborated that ILTV blocks apoptosis. Many other alphaherpesviruses such as HSV1, HSV2 and SHV1 were reported to show low levels of apoptosis in infected cells (Aleman *et al.*, 2001; Asano *et al.*, 1999; Glorieux *et al.*, 2011). Further, apoptotic cells were observed in the vicinity of ILTV infected cells and these could be local immune cells (leukocytes) or uninfected bystander cells (Aleman *et al.*, 2001; Asano *et al.*, 1999). Usually, alphaherpesviruses evade the immune response by inhibiting apoptosis of infected cells (Aleman *et al.*, 2001; Asano *et al.*, 1999; Galvan and Roizman, 1998; Glorieux *et al.*, 2011a; Winkler *et al.*, 1999). This could be a strategy of ILTV to survive in infected cells long enough to support virus replication. After spreading through the BM, ILTV reaches the lamina propria and underlying mucosal layers. Then, ILTV may reach sensory nerves and the trigeminal ganglion. Finally, in the trigeminal ganglion ILTV establishes latency and makes from an animal a lifelong virus carrier.

ILTV infected muroid plugs/casts are associated with extracellular DNA fibrous structures but not with mucins (MUC5AC and MUC5B)

An acute ILTV infection is associated with marked dyspnea, gasping, suffocation and increased mortality in chickens due to presence of the muroid plugs/casts in the trachea (Linares *et al.*, 1994). It has been speculated that the muroid plugs/casts are formed due to mucus hypersecretion, however there are no published reports supporting this hypothesis (Garcia *et al.*, 2013; Linares *et al.*, 1994). In chapter 3.2, we first evaluated if main respiratory mucins MUC5AC and MUC5B were produced

in the mucosa of normal and ILTV infected chickens. Second, the tracheal mucosal thickness and the tracheal lumen diameter were compared between normal and ILTV infected chickens to understand their role in obstruction of the trachea. Third, the mucoid plugs/casts present inside the trachea were stained for mucins and nuclear DNA fibrous structures (extracellular traps). Fourth and last, the effect of ILTV on the formation of DNA fibrous structures from nuclei of blood heterophils was evaluated.

MUC5AC and MUC5B were found to be the common mucins produced by the epithelium of the larynx, trachea and bronchi of normal chickens. This finding is in line with the respiratory mucosa of humans and pigs (Kirkham *et al.*, 2002). The mucin (MUC5AC and MUC5B) production was higher in larynx and trachea compared to bronchi, which is from an anatomical point of view more relevant in the defense against pathogens/foreign substances. An important observation of this study was that mucins (MUC5AC and MUC5B) were exclusively present in the dorsal tracheal region (thinner) of the cranial and middle part of tracheal mucosa of normal chickens. In evolution, this property may have been developed to block the initial entry of pathogens at the dorsal surface. ILTV infects mainly the lateral and ventral areas. In ILTV infected chickens, the tracheal lumen diameter was reduced with almost 40% than tracheal lumen diameter of control chickens, and was caused by a strongly increased tracheal mucosal thickness. The reduced tracheal lumen and its associated increased mucosal thickness are most probably due to severe congestion, edema and heavy infiltration of heterophils, macrophages, lymphocytes and plasma cells in the mucosa and underlying layers (Devlin *et al.*, 2006; Garcia *et al.*, 2013; Hayashi *et al.*, 1985). This observation strongly demonstrated that the reduced tracheal lumen due to the increased mucosal thickness is one of the important reasons for the obstruction of the trachea during an acute ILTV infection.

Mucins (MUC5AC and MUC5B) were scarcely observed in the mucosa of the respiratory tract and almost absent in the mucoid plugs/casts in the trachea of ILTV infected chickens. This observation does not fit with the speculation that the mucoid plugs/casts are associated with mucus hypersecretion (Garcia *et al.*, 2013; Linares *et al.*, 1994). Surprisingly, DNA fibrous structures (ETs) were observed in $10.0 \pm 7.3\%$ nuclei of the cells from ILTV infected mucoid plugs/casts. The absence of mucins in the mucoid plugs/casts and presence of DNA fibrous structures (ETs) in the nuclei of the mucoid plugs/casts of ILTV is in line with what has been reported in the sputum and

mucus of cystic fibrosis patients (Henke *et al.*, 2004; Lethem *et al.*, 1990; Rubin, 2007). Further, these DNA fibrous structures (ETs) were demonstrated in $2.0 \pm 0.1\%$ nuclei from ILTV inoculated blood heterophils at 24 hpi.

In general, extracellular DNA network (ETs) formation is a defense mechanism of host cells towards pathogenic microorganisms (Goldmann and Medina, 2012). During acute ILTV infection, the formation of extracellular DNA networks may also be a strategy to restrict virus replication and remove the virus in the respiratory mucosa. Further, these DNA fibrous structures may trap lipids, proteins, cations, cellular debris and other non-mucin components to form a jelly plug in the trachea, and obstruct normal air passage and may cause suffocation and mortality in chickens (Garcia *et al.*, 2013; Lethem *et al.*, 1990). Acute ILTV associated gasping, marked dyspnea, open mouth breathing and asphyxiation could be reduced by aerosol administration of DNase I (Rogers, 2007; Shak, 1995).

IBV B1648 is a distinct strain from all the available worldwide IBV strains

IBV has a tropism for the epithelial cells of the respiratory tract, kidneys, oviduct and alimentary tract of chickens. Massachusetts type strains (prototype: M41) cause mainly respiratory problems. Some IBV strains were described as nephropathogenic since the respiratory infection is followed by a severe kidney infection and increased mortality. Strain B1648 is a well-studied Belgian reference nephropathogenic IBV that became an important strain across the European continent. Despite the intensive vaccination program, IBV B1648 or its variants are still circulating through Europe and North Africa (Bochkov *et al.*, 2006; Ducatez *et al.*, 2009; Krapež *et al.*, 2010; Toffan *et al.*, 2013b). In the present PhD thesis, the full genome sequence of IBV B1648 was characterized to speculate possible genetic factors, which might be associated with the nephropathogenicity, and to understand its position in evolution (chapter 4.1.).

Thirteen open reading frames (ORFs) were predicted in B1648 genome. 4b, 4c and 6b were additional ORFs present in the B1648 genome when compared with most available IBV genomes, and were rarely reported in the literature (Abolnik, 2015; Hewson *et al.*, 2011). The success of ORFs identification depends on the algorithm of ORF prediction software that was used. NGA/A116E7/2006, UKr 27-11, QX-like ITA/90254/2005, QX-like CK/SWE/0658946/10, TN20/00, RF-27/99, RF/06/2007

and SLO/266/05 were grouped with B1648, according to the phylogenetic analysis of the full-length genome, replicase transcriptase complex, Spike protein, S1 gene and M protein, and this group was referred as non-Mass type strains. All the above grouped strains were reported after the first B1648 outbreak in Belgium, hence in the evolution, segments of the B1648 genome may have transferred into these strains. In IBV and other coronaviruses, the emergence of new coronaviral genotypes/strains by recombination events has been well reported (Hughes, 2011; Thor *et al.*, 2011). Further, based on the recombination analysis, the recombination sites were distributed in several genes of the B1648 genome.

According to pairwise comparison of the full genome, B1648 was closely related to NGA/A116E7/2006 (91.6%), UKr 27-11 (91.2%), Gray (91.2%) and JMK strains (91.2%), and these strains were earlier described as non-Mass type strains. B1648 was also closely related to non-Mass type strains, based on pairwise comparison of 1a, Spike, M and accessory proteins (3a, 3b, 4b, 4c, 5a, 5b and 6b). According to the 1b, E and N proteins, B1648 was closely related to most of the IBV strains. Pairwise comparison has implicated that the pathogenicity determinants of B1648 strain might be located on 1a, Spike, M and accessory proteins. Recently, many researchers have reported that the pathogenicity determinants of IBV are polygenic, and located outside the Spike protein (Ammayappan *et al.*, 2009; Armesto *et al.*, 2009; Britton *et al.*, 2005; Casais *et al.*, 2003; Hodgson *et al.*, 2006; Phillips *et al.*, 2012). In murine hepatitis virus (MHV), another well-studied coronavirus, some authors have shown that the Nsp1, Nsp3 and Nsp14 are pathogenicity factors. In nephropathogenic IBV, the non-structural proteins of ORF 1a might be associated with nephropathogenicity. However, this hypothesis should be further investigated by reverse genetics system (RGS).

The development of IBV Beaudette strain infectious clones or RGS has opened up the possibility to modify IBV spike, 3a, 3b, 5, E, M, N and other accessory proteins, to understand their role in the pathogenicity (Britton *et al.*, 2005; Casais *et al.*, 2005; Casais *et al.*, 2003; Hodgson *et al.*, 2006). Based on these IBV RGS studies, Armesto *et al.* (2009) have shown that the replicase gene (polyprotein 1ab) might be a determinant of the pathogenicity. However, further studies are necessary to understand the role of individual Nsps of the replicase gene in the pathogenicity (Armesto *et al.*, 2009). Currently, RGS (Beau-R) is available only for a Beaudette

strain (Britton *et al.*, 2005; Casais *et al.*, 2001). Beaudette strain is a laboratory adapted non-virulent attenuated strain (Beaudette and Hudson, 1937; Casais *et al.*, 2001). Hence, Beaudette strain infectious clone is not an ideal model to study the pathogenicity determinants of the virulent IBV strains. In the future, more studies should be performed with RGS of virulent IBV strains to understand the role of individual Nsps of the replicase gene or other structural proteins.

Based on the sequence of the partial S1 fragment, TN20/00, RF-27/99, RF/06/2007 and SLO/266/05 strains were closest related and grouped with B1648, and named as B1648 genotype. Phylogenetic analysis and pairwise comparisons have suggested that B1648 is a distinct genotype, which has been intermittently circulating in Europe and North Africa for over three decades (Bourogaa *et al.*, 2012; Capua *et al.*, 1999; Dolz *et al.*, 2006; Ducatez *et al.*, 2009; Meulemans *et al.*, 1987; Ovchinnikova *et al.*, 2011; Terregino *et al.*, 2006; Toffan *et al.*, 2013a; Tosi *et al.*, 2010). Further, the knowledge on the pathogenicity and tissue tropism of the strains NGA/A116E7/2006, Ukr27-11, TN20/00, RF-27/99, RF/06/2007 and SLO/266/05 are necessary to understand whether these strains are really nephropathogenic.

Cell-free and cell-associated viremia in NIBV strain B1648 infection: a strategy for viral dissemination to kidneys

In spite of the circulation of nephropathogenic (B1648) and respiratory strains (M41) for many decades, it is not well understood why some IBV strains have a kidney tropism. Therefore, replication kinetics of IBV B1648 (nephropathogenic) and M41 (respiratory) were studied *in vitro* in tracheal mucosa explants and blood monocytes and *in vivo* in chickens (chapter 4.2.).

Two important questions were answered in the work done with respiratory mucosa explants, namely i) what is the strategy that B1648 uses to invade at the level of the respiratory tract and ii) how does B1648 reach the blood circulation to disseminate virus to the kidneys. B1648 and M41 replicate in the epithelium of the respiratory mucosa similar to other IBV viruses. B1648 was highly virulent than M41 in the epithelium of the respiratory mucosa. With many other IBV strains and serotypes, similar replication differences were reported in tracheal organ cultures (Chhabra *et al.*, 2016; Cubillos *et al.*, 1991; Raj and Jones, 1996a, b). The antiviral responses of the host cells, presence/absence, and/or differential expression of receptors on

susceptible epithelial cells and immune-evasion mechanisms developed by the IBV strain might be important factors determining the differences in virulence of strains at the tracheal mucosa (Widagdo *et al.*, 2016).

After epithelium infection, B1648 and M41 viral antigen positive cells breached through the basement membrane (BM) into the lamina propria. In the lamina propria, the number of B1648 infected cells was slightly higher at 6, 12, 24 and 48 hpi, and was significantly higher at 72 hpi. Infected KUL01⁺ cells (monocytic cells) were observed in the both epithelium and lamina propria, for both B1648 and M41. The number of B1648 infected KUL01⁺ cells in the epithelium were somewhat higher than M41 infected cells at 24 and 48 hpi, and significantly higher at 72 hpi. The number of B1648 infected KUL01⁺ cells in the lamina propria was higher than M41 infected cells. The infected KUL01⁺ cells may have acted as carrier cells to disseminate virus through BM to reach underlying layers of the respiratory mucosa. This invasion mechanism is in line with equine herpes virus 1 (EHV1) and equine arteritis virus in the respiratory mucosa of horses (Gryspeerd *et al.*, 2010; Vairo *et al.*, 2013; Vairo *et al.*, 2012; Vandekerckhove *et al.*, 2010). In summary, B1648 was replicating quite better than M41 in the respiratory mucosa explants and B1648 exploited more infected KUL01⁺ cells to breach through the underlying layers of the respiratory mucosa compared to M41.

The percentage of infected peripheral blood monocytes (KUL01⁺ cells) was higher with B1648 than M41. B1648 showed 20-700 times higher viral titers than M41 in both cell lysate and supernatant of the inoculated blood monocytes. With M41, no or little increase in viral titers was seen in cell lysate and supernatant of blood monocytic cells. All together, B1648 productively replicates in the peripheral blood monocytes whereas M41 aborts. Similar to this study, productive replication of viruses in monocytic cells have been reported with many of the mammalian viruses such as, dengue virus with human macrophages, classical swine fever virus with monocyte derived dendritic cells, Middle East respiratory syndrome coronavirus (MERS-CoV) with human macrophages and monocyte derived dendritic cells, and feline infectious peritonitis virus with peripheral blood monocytes. On the other hand, an abortive replication has been observed with EHV1 and feline enteric coronavirus in blood monocytes, with severe acute respiratory syndrome coronavirus (SARS-CoV) in blood macrophages and monocyte derived dendritic cells, and with influenza virus in

mouse dendritic cells (Carrasco *et al.*, 2004; Chen and Wang, 2002; Chu *et al.*, 2014; Dewerchin *et al.*, 2005; Ioannidis *et al.*, 2012; Zhou *et al.*, 2014).

In the *in vivo* study, all chickens inoculated with IBV B1648 and M41 were infected and developed clinical signs, such as ruffled feathers, huddling together, tracheal rales, coughing and dyspnea. Increased water consumption and reduced body weight gains were typical with B1648 inoculated chickens. Enlarged kidneys was the most important gross lesion observed in the B1648 group, which is similar to other nephropathogenic strains (Cavanagh and Naqi, 2003).

The highest viral shedding in the upper respiratory tract (URT) secretions occurred between 2 and 8 dpi. Such a respiratory shedding allows horizontal transmission of IBV to susceptible birds and ensures virus circulation in birds (Ignjatovic and Sapats, 2000). In contrast to the *in vitro* results in tracheal mucosa explants, the replication of B1648 and M41 were very similar except that B1648 replication was persisting longer (12 dpi). Further, it would have been interesting, if tracheal swabs and mucosal tissues were collected at 6, 12, 24, 48 and 72 hpi to better understand the replication characteristics at the epithelium and lamina propria of *in vivo* tracheal mucosa and to compare it with *in vitro* results.

In B1648 inoculated animals, $10^{2.4-4.5}$ viral RNA copies/ml were detected in plasma at 2, 4, 6, 8, 10 and 12 dpi and $10^{1.8-4.4}$ viral RNA copies/ 10^6 mononuclear cells at 2, 4, 6 and 8 dpi. Virus isolation has confirmed that these B1648 viral RNA copies of plasma and mononuclear cells were infectious virus. In M41 inoculated animals, viral RNA was detected in only one animal at 6 dpi in plasma and mononuclear cells but the infectivity could not be demonstrated by virus isolation. The infected cells were observed in cytopinned mononuclear cells at 2, 4 and 6 dpi with B1648 but not with M41. These results demonstrated the onset of cell free and cell-associated viremia at 2 dpi with B1648 strain. This indicates that cell free B1648 virus and B1648 infected cells are able to spread through the epithelium and underlying submucosal layers of the respiratory tract to enter in to the blood circulation very quickly (before 48 hpi). Thus the potential spread of B1648 strain from blood into the internal organs was demonstrated. The combination of a cell free and cell-associated viremia of B1648 strain is in line with pseudorabies virus and classical swine fever virus dissemination in pigs (Nawynck and Pensaert, 1995; Pensaert *et al.*, 2004).

Viral RNA and antigen positive cells were only detected in kidneys, liver, lungs and spleen of B1648 infected animals at 12 dpi, providing evidence that only B1648 productively infects internal organs, whereas M41 does not. B1648 replicated more actively in the kidneys compared to lungs, liver and spleen, explaining the nephropathogenicity of B1648 (Cook *et al.*, 2012; Meulemans *et al.*, 1987; Pensaert and Lambrechts, 1994).

The cell-associated viremia in mononuclear leukocytes and cell free virus in plasma of B1648 virus infected chickens might be extrapolated to MERS-CoV tissue tropism mechanisms in humans. The comparison with MERS-CoV is compelling because it is also associated with severe kidney problems and high mortality in humans (Chan *et al.*, 2013; Drosten *et al.*, 2013; Eckerle *et al.*, 2013; Guery *et al.*, 2013). Moreover, MERS-CoV replicates in a productive way in human macrophages and its presence was also reported in whole blood and plasma of humans (Chan *et al.*, 2013; Drosten *et al.*, 2013; Guery *et al.*, 2013; Zhou *et al.*, 2014). At present, there is no detailed information on MERS-CoV disease, and no good animal models to study the pathogenesis of MERS-CoV (Momattin *et al.*, 2013; Vijay and Perlman, 2016). Thus, although speculative, a correlation can be made between coronaviruses of chickens and humans to understand their evolution and replication mechanism and to plan control and prevention strategies in a better way.

In conclusion, B1648 and M41 infection kinetics and pathogenesis mechanisms were different (Figure 1). Both B1648 and M41 strains successfully replicate and invade in the epithelium of the respiratory mucosa. B1648 uses more KUL01⁺ cells (monocytes/macrophages) as carrier cells to transport via the underlying layers of the respiratory mucosa. B1648 penetrates more vigorously than M41 in the deeper underlying layers of the respiratory mucosa. B1648 disseminates via a cell free and cell-associated viremia to target organs such as kidneys, liver, spleen and lungs whereas M41 does not do this. Only B1648 showed a fully productive replication in the KUL01⁺ peripheral blood monocytic cells. B1648 replicates more productively in kidneys when compared to liver, spleen and lungs. The M41 infected KUL01⁺ cells could not be able to disseminate into the circulation or were abortive in the lamina propria and underlying layers of the upper respiratory tract. Our study unravels very important invasion and tissue tropism mechanisms of B1648 and M41 strains. B1648 has become nephropathogenic mainly by productively replicating in carrier

mononuclear cells, and M41 is not nephropathogenic due to abortive replication in mononuclear cells.

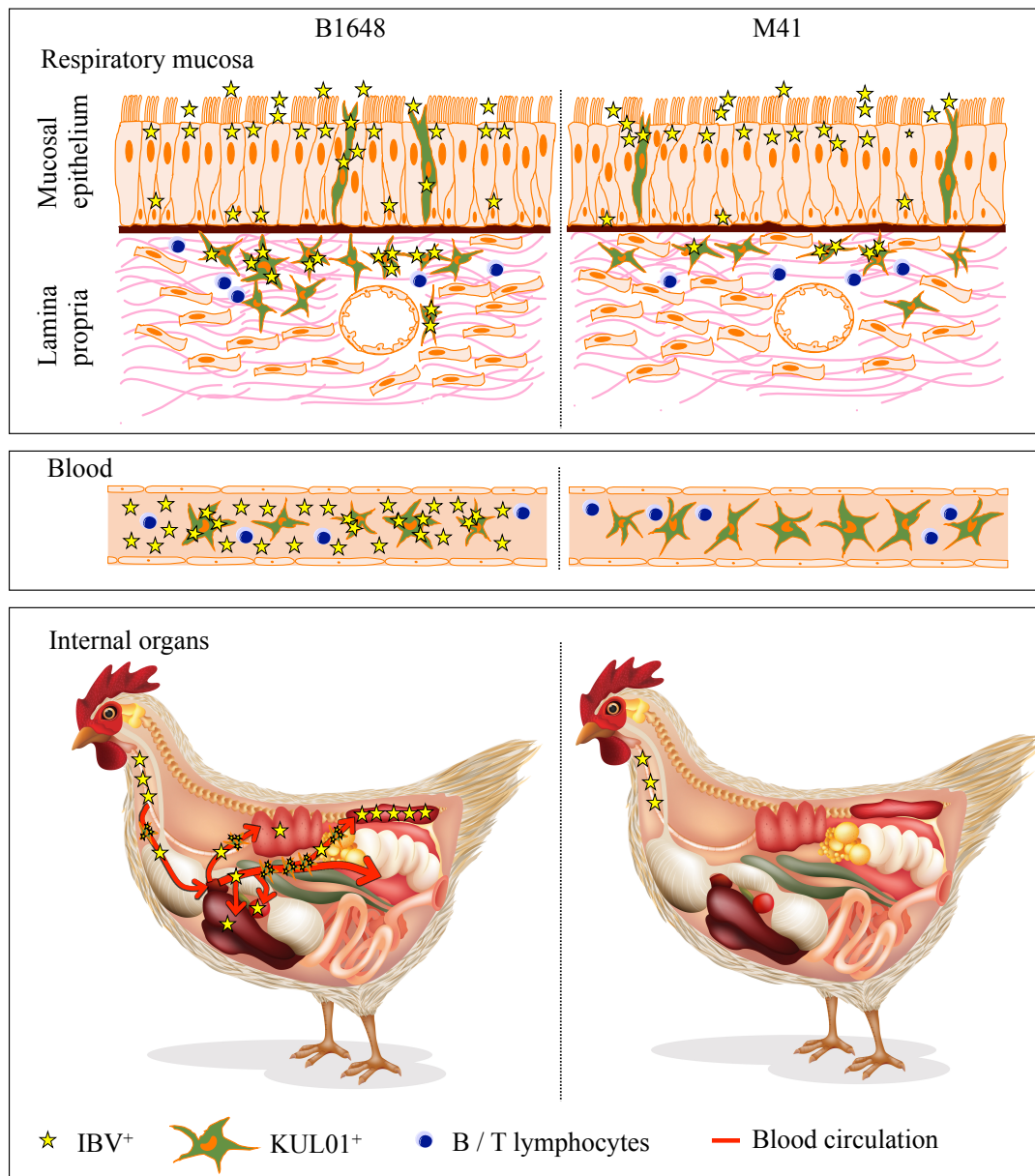


Figure 1. Hypothetical model of IBV B1648 and M41 replication kinetics in respiratory mucosa, blood and internal organs of chickens. Stars represent infectious virus. Star number and infectivity are directly proportional to each other. After natural entry of virus through nostrils, both nephropathogenic IBV B1648 and M41 replicate in the respiratory mucosa. B1648 uses a higher number of infected KUL01⁺ cells as carriers to penetrate deeper in the layers of the respiratory mucosa in contrast to M41. B1648 productively infects KUL01⁺ blood monocyctic cells while M41 infection is abortive. Only B1648 disseminates via a cell-associated viremia in mononuclear leukocytes and cell free virus in plasma to reach lungs, liver, spleen and kidneys.

Only B1648 shows a productive infection in kidneys and to a less degree in lungs, liver and spleen.

Future perspectives

The current thesis was dealt with the many important aspects of the pathogenesis of ILTV and IBV under *in vitro* and *in vivo* conditions. The knowledge gained in this pathogenesis study can be used in the development of new antiviral compounds and vaccines, especially against acute ILT and nephropathogenic IB diseases.

- We found ILTV spreads by a plaquewise manner in the tracheal and conjunctival mucosae and subsequently penetrates the BM. The trypsin-like serine protease in SHV1 and the heterodimeric complex of gE/gI in BHV1, were reported to be involved in penetration of the BM (Glorieux *et al.*, 2011b; Steukers, 2013). Similarly, ILTV might follow one of these mechanisms to penetrate the BM. The use of antiviral compounds against trypsin-like serine protease and heterodimeric complex of gE/gI will be an interesting strategy to stop ILTV invasion. The established *in vitro* mucosal explant models will be ideal tools to check new antiviral compounds.
- Aerosol administration of DNase I could be used to prevent acute ILT associated mucoid plugs/casts formation, and further helpful to reduce gasping, open mouth breathing and suffocation problems in chickens.
- Blocking IBV entry pathways to epithelial cells and NIBV to monocytes can prevent the IBV infection. However, many questions on virus entry steps are necessary to be addressed in the future. First, binding and internalization into epithelial cells and monocytic cells should be studied. Second, the internalization pathways and regulators can be evaluated to find the targets. Third, the receptors associated with the binding and internalization should be elucidated. Finally, differences between respiratory IBV and NIBV strains at binding and internalization would be interesting to study.
- Further pathogenesis studies should be performed on currently available variant respiratory and nephropathogenic IBV strains to understand their tissue tropism mechanisms and differences.

- Construction and manipulation of infectious clones of the virulent ILTV genome, respiratory IBV and NIBV genome is needed for the development of novel vaccines.
- The egg inoculation and primary cells studies with ILTV and IBV are tedious, cumbersome and hamper long-term studies. To obtain reproducible and relevant results, there is an increased demand for the well-characterized continued cell lines, which retain the phenotypic and functional characteristics of their non-transformed primary cells.

These studies would be helpful to plan effective preventive and control strategies against ILT and IB diseases.

References

- Abolnik, C., 2015. Genomic and single nucleotide polymorphism analysis of infectious bronchitis coronavirus. *Infect Genet Evol* 32, 416-424.
- Aleman, N., Quiroga, M.I., Lopez-Pena, M., Vazquez, S., Guerrero, F.H., Nieto, J.M., 2001. Induction and inhibition of apoptosis by pseudorabies virus in the trigeminal ganglion during acute infection of swine. *J Virol* 75, 469-479.
- Ammayappan, A., Upadhyay, C., Gelb, J., Vakharia, V.N., 2009. Identification of sequence changes responsible for the attenuation of avian infectious bronchitis virus strain Arkansas DPI. *Arch Virol* 154, 495-499.
- Armesto, M., Cavanagh, D., Britton, P., 2009. The replicase gene of avian coronavirus infectious bronchitis virus is a determinant of pathogenicity. *PLoS One* 4, e7384.
- Asano, S., Honda, T., Goshima, F., Watanabe, D., Miyake, Y., Sugiura, Y., Nishiyama, Y., 1999. US3 protein kinase of herpes simplex virus type 2 plays a role in protecting corneal epithelial cells from apoptosis in infected mice. *J Gen Virol* 80 (Pt 1), 51-56.
- Bang, B.G., Bang, F.B., 1967. Laryngotracheitis virus in chickens. A model for study of acute nonfatal desquamating rhinitis. *J Exp Med* 125, 409-428.
- Beaudette, F., Hudson, C.B., 1937. Cultivation of the virus of infectious bronchitis. *J Am Vet Med Assoc* 90, 51-58.
- Bochkov, Y.A., Batchenko, G.V., Shcherbakova, L.O., Borisov, A.V., Drygin, V.V., 2006. Molecular epizootiology of avian infectious bronchitis in Russia. *Avian Pathol* 35, 379-393.

- Bourogaa, H., Hellal, I., Hassen, J., Fathallah, I., Ghram, A., 2012. S1 gene sequence analysis of new variant isolates of avian infectious bronchitis virus in Tunisia. *Veterinary medicine* 3, 41-48.
- Britton, P., Evans, S., Dove, B., Davies, M., Casais, R., Cavanagh, D., 2005. Generation of a recombinant avian coronavirus infectious bronchitis virus using transient dominant selection. *J Virol Methods* 123, 203-211.
- Capua, I., Minta, Z., Karpinska, E., Mawditt, K., Britton, D., Cavanagh, D., Gough, R.E., 1999. Co-circulation of four types of infectious bronchitis virus (793/B, 624/I, B1648 and Massachusetts). *Avian Pathol* 28, 587-592.
- Carrasco, C.P., Rigden, R.C., Vincent, I.E., Balmelli, C., Ceppi, M., Bauhofer, O., Tache, V., Hjertner, B., McNeilly, F., van Gennip, H.G., McCullough, K.C., Summerfield, A., 2004. Interaction of classical swine fever virus with dendritic cells. *J Gen Virol* 85, 1633-1641.
- Casais, R., Davies, M., Cavanagh, D., Britton, P., 2005. Gene 5 of the avian coronavirus infectious bronchitis virus is not essential for replication. *J Virol* 79, 8065-8078.
- Casais, R., Dove, B., Cavanagh, D., Britton, P., 2003. Recombinant avian infectious bronchitis virus expressing a heterologous spike gene demonstrates that the spike protein is a determinant of cell tropism. *J Virol* 77, 9084-9089.
- Casais, R., Thiel, V., Siddell, S.G., Cavanagh, D., Britton, P., 2001. Reverse genetics system for the avian coronavirus infectious bronchitis virus. *J Virol* 75, 12359-12369.
- Cavanagh, D., 2007. Coronavirus avian infectious bronchitis virus. *Vet Res* 38, 281-297.
- Cavanagh, D., Naqi, S.A., 2003. *Infectious Bronchitis*, Vol 11, 11 Edition. Iowa state press, Ames, Iowa.
- Chan, R.W., Chan, M.C., Agnihothram, S., Chan, L.L., Kuok, D.I., Fong, J.H., Guan, Y., Poon, L.L., Baric, R.S., Nicholls, J.M., Peiris, J.S., 2013. Tropism of and innate immune responses to the novel human betacoronavirus lineage C virus in human ex vivo respiratory organ cultures. *J Virol* 87, 6604-6614.
- Chen, Y.C., Wang, S.Y., 2002. Activation of terminally differentiated human monocytes/macrophages by dengue virus: productive infection, hierarchical production of innate cytokines and chemokines, and the synergistic effect of lipopolysaccharide. *J Virol* 76, 9877-9887.
- Chhabra, R., Kuchipudi, S.V., Chantrey, J., Ganapathy, K., 2016. Pathogenicity and tissue tropism of infectious bronchitis virus is associated with elevated apoptosis and innate immune responses. *Virology* 488, 232-241.
- Chu, H., Zhou, J., Wong, B.H., Li, C., Cheng, Z.S., Lin, X., Poon, V.K., Sun, T., Lau, C.C., Chan, J.F., To, K.K., Chan, K.H., Lu, L., Zheng, B.J., Yuen, K.Y., 2014. Productive replication of Middle East respiratory syndrome coronavirus in

- monocyte-derived dendritic cells modulates innate immune response. *Virology* 454-455, 197-205.
- Cook, J.K., Jackwood, M., Jones, R.C., 2012. The long view: 40 years of infectious bronchitis research. *Avian Pathol* 41, 239-250.
- Cubillos, A., Ulloa, J., Cubillos, V., Cook, J.K., 1991. Characterisation of strains of infectious bronchitis virus isolated in Chile. *Avian Pathol* 20, 85-99.
- Devlin, J.M., Browning, G.F., Hartley, C.A., Kirkpatrick, N.C., Mahmoudian, A., Noormohammadi, A.H., Gilkerson, J.R., 2006. Glycoprotein G is a virulence factor in infectious laryngotracheitis virus. *J Gen Virol* 87, 2839-2847.
- Dewerchin, H.L., Cornelissen, E., Nauwynck, H.J., 2005. Replication of feline coronaviruses in peripheral blood monocytes. *Arch Virol* 150, 2483-2500.
- Dolz, R., Pujols, J., Ordonez, G., Porta, R., Majo, N., 2006. Antigenic and molecular characterization of isolates of the Italy 02 infectious bronchitis virus genotype. *Avian Pathol* 35, 77-85.
- Drosten, C., Seilmaier, M., Corman, V.M., Hartmann, W., Scheible, G., Sack, S., Guggemos, W., Kallies, R., Muth, D., Junglen, S., Muller, M.A., Haas, W., Guberina, H., Rohnisch, T., Schmid-Wendtner, M., Aldabbagh, S., Dittmer, U., Gold, H., Graf, P., Bonin, F., Rambaut, A., Wendtner, C.M., 2013. Clinical features and virological analysis of a case of Middle East respiratory syndrome coronavirus infection. *Lancet Infect Dis* 13, 745-751.
- Ducatez, M.F., Martin, A.M., Owoade, A.A., Olatoye, I.O., Alkali, B.R., Maikano, I., Snoeck, C.J., Sausy, A., Cordioli, P., Muller, C.P., 2009. Characterization of a new genotype and serotype of infectious bronchitis virus in Western Africa. *J Gen Virol* 90, 2679-2685.
- Eckerle, I., Muller, M.A., Kallies, S., Gotthardt, D.N., Drosten, C., 2013. In-vitro renal epithelial cell infection reveals a viral kidney tropism as a potential mechanism for acute renal failure during Middle East Respiratory Syndrome (MERS) Coronavirus infection. *Virol J* 10, 359.
- Fuchs, W., Veits, J., Helferich, D., Granzow, H., Teifke, J.P., Mettenleiter, T.C., 2007. Molecular biology of avian infectious laryngotracheitis virus. *Vet Res* 38, 261-279.
- Galvan, V., Roizman, B., 1998. Herpes simplex virus 1 induces and blocks apoptosis at multiple steps during infection and protects cells from exogenous inducers in a cell-type-dependent manner. *Proc Natl Acad Sci U S A* 95, 3931-3936.
- Garcia, M., Spatz, S., Guy, J.S., 2013. *Laryngotracheitis*, Vol 13. Ames: Blackwell, 161-179 pp.
- Glorieux, S., Bachert, C., Favoreel, H.W., Vandekerckhove, A.P., Steukers, L., Rekecki, A., Van den Broeck, W., Goossens, J., Croubels, S., Clayton, R.F., Nauwynck, H.J., 2011a. Herpes simplex virus type 1 penetrates the basement membrane in human nasal respiratory mucosa. *PLoS One* 6, e22160.

- Glorieux, S., Favoreel, H.W., Meesen, G., de Vos, W., Van den Broeck, W., Nauwynck, H.J., 2009. Different replication characteristics of historical pseudorabies virus strains in porcine respiratory nasal mucosa explants. *Vet Microbiol* 136, 341-346.
- Glorieux, S., Favoreel, H.W., Steukers, L., Vandekerckhove, A.P., Nauwynck, H.J., 2011b. A trypsin-like serine protease is involved in pseudorabies virus invasion through the basement membrane barrier of porcine nasal respiratory mucosa. *Vet Res* 42, 58.
- Goldmann, O., Medina, E., 2012. The expanding world of extracellular traps: not only neutrophils but much more. *Front Immunol* 3, 420.
- Gryspeerd, A.C., Vandekerckhove, A.P., Garré, B., Barbé, F., Van de Walle, G.R., Nauwynck, H.J., 2010. Differences in replication kinetics and cell tropism between neurovirulent and non-neurovirulent EHV1 strains during the acute phase of infection in horses. *Vet Microbiol* 142, 242-253.
- Guery, B., Poissy, J., el Mansouf, L., Sejourne, C., Ettahar, N., Lemaire, X., Vuotto, F., Goffard, A., Behillil, S., Enouf, V., Caro, V., Mailles, A., Che, D., Manuguerra, J.C., Mathieu, D., Fontanet, A., van der Werf, S., group, M.E.-C.s., 2013. Clinical features and viral diagnosis of two cases of infection with Middle East Respiratory Syndrome coronavirus: a report of nosocomial transmission. *Lancet* 381, 2265-2272.
- Guy, J.S., Bagust, T.J., 2003. *Diseases of Poultry*, Vol 11 Ames: Blackwell.
- Hayashi, S., Odagiri, Y., Kotani, T., Horiuchi, T., 1985. Pathological changes of tracheal mucosa in chickens infected with infectious laryngotracheitis virus. *Avian Dis* 29, 943-950.
- Henke, M.O., Renner, A., Huber, R.M., Seeds, M.C., Rubin, B.K., 2004. MUC5AC and MUC5B Mucins Are Decreased in Cystic Fibrosis Airway Secretions. *Am J Respir Cell Mol Biol* 31, 86-91.
- Hewson, K.A., Ignjatovic, J., Browning, G.F., Devlin, J.M., Noormohammadi, A.H., 2011. Infectious bronchitis viruses with naturally occurring genomic rearrangement and gene deletion. *Arch Virol* 156, 245-252.
- Hodgson, T., Britton, P., Cavanagh, D., 2006. Neither the RNA nor the proteins of open reading frames 3a and 3b of the coronavirus infectious bronchitis virus are essential for replication. *J Virol* 80, 296-305.
- Hughes, A.L., 2011. Recombinational histories of avian infectious bronchitis virus and turkey coronavirus. *Arch Virol* 156, 1823-1829.
- Ignjatovic, J., Sapats, S., 2000. Avian infectious bronchitis virus. *Rev Sci Tech* 19, 493-508.
- Ioannidis, L.J., Verity, E.E., Crawford, S., Rockman, S.P., Brown, L.E., 2012. Abortive replication of influenza virus in mouse dendritic cells. *J Virol* 86, 5922-5925.

- Jones, R.C., 2010. Viral respiratory diseases (ILT, aMPV infections, IB): are they ever under control? *Br Poult Sci* 51, 1-11.
- Kirkham, S., Sheehan, J.K., Knight, D., Richardson, P.S., Thornton, D.J., 2002. Heterogeneity of airways mucus: variations in the amounts and glycoforms of the major oligomeric mucins MUC5AC and MUC5B. *Biochem J* 361, 537-546.
- Kirkpatrick, N.C., Mahmoudian, A., Colson, C.A., Devlin, J.M., Noormohammadi, A.H., 2006. Relationship between mortality, clinical signs and tracheal pathology in infectious laryngotracheitis. *Avian Pathol* 35, 449-453.
- Krapež, U., Slavec, B., Barlič-Maganja, D., Rojs, O.Z., 2010. Molecular analysis of infectious bronchitis viruses isolated in Slovenia between 1990 and 2005: a retrospective study. *Virus Genes* 41, 414-416.
- Lethem, M.I., James, S.L., Marriott, C., Burke, J.F., 1990. The origin of DNA associated with mucus glycoproteins in cystic fibrosis sputum. *Eur Respir J* 3, 19-23.
- Lin, C., Holland, R.E., Jr., Williams, N.M., Chambers, T.M., 2001. Cultures of equine respiratory epithelial cells and organ explants as tools for the study of equine influenza virus infection. *Arch Virol* 146, 2239-2247.
- Linares, J.A., Bickford, A.A., Cooper, G.L., Charlton, B.R., Woolcock, P.R., 1994. An outbreak of infectious laryngotracheitis in California broilers. *Avian Dis* 38, 188-192.
- May, H.G., Tittsler, R.P., 1925. Tracheolaryngitis in poultry. *J Am Vet Med Assoc* 67, 229-231.
- Menendez, K.R., Garcia, M., Spatz, S., Tablante, N.L., 2014. Molecular epidemiology of infectious laryngotracheitis: a review. *Avian Pathol* 43, 108-117.
- Meulemans, G., Carlier, M.C., Gonze, M., Petit, P., Vandebroek, M., 1987. Incidence, characterisation and prophylaxis of nephropathogenic avian infectious bronchitis viruses. *Vet Rec* 120, 205-206.
- Momattin, H., Mohammed, K., Zumla, A., Memish, Z.A., Al-Tawfiq, J.A., 2013. Therapeutic options for Middle East respiratory syndrome coronavirus (MERS-CoV)--possible lessons from a systematic review of SARS-CoV therapy. *Int J Infect Dis* 17, e792-798.
- Nawynck, H.J., Pensaert, M.B., 1995. Cell-free and cell-associated viremia in pigs after oronasal infection with Aujeszky's disease virus. *Vet Microbiol* 43, 307-314.
- Ovchinnikova, E.V., Bochkov, Y.A., Shcherbakova, L.O., Nikonova, Z.B., Zinyakov, N.G., Elatkin, N.P., Mudrak, N.S., Borisov, A.V., Drygin, V.V., 2011. Molecular characterization of infectious bronchitis virus isolates from Russia and neighbouring countries: identification of intertypic recombination in the S1 gene. *Avian Pathol* 40, 507-514.

- Pensaert, M., Lambrechts, C., 1994. Vaccination of chickens against a Belgian nephropathogenic strain of infectious bronchitis virus B1648 using attenuated homologous and heterologous strains. *Avian Pathol* 23, 631-641.
- Pensaert, M.B., Sanchez, R.E., Jr., Ladekjaer-Mikkelsen, A.S., Allan, G.M., Nauwynck, H.J., 2004. Viremia and effect of fetal infection with porcine viruses with special reference to porcine circovirus 2 infection. *Vet Microbiol* 98, 175-183.
- Phillips, J.E., Jackwood, M.W., McKinley, E.T., Thor, S.W., Hilt, D.A., Acevedol, N.D., Williams, S.M., Kissinger, J.C., Paterson, A.H., Robertson, J.S., Lemke, C., 2012. Changes in nonstructural protein 3 are associated with attenuation in avian coronavirus infectious bronchitis virus. *Virus Genes* 44, 63-74.
- Raj, G.D., Jones, R.C., 1996a. Immunopathogenesis of infection in SPF chicks and commercial broiler chickens of a variant infectious bronchitis virus of economic importance. *Avian Pathol* 25, 481-501.
- Raj, G.D., Jones, R.C., 1996b. An in vitro comparison of the virulence of seven strains of infectious bronchitis virus using tracheal and oviduct organ cultures. *Avian Pathol* 25, 649-662.
- Reemers, S.S., Groot Koerkamp, M.J., Holstege, F.C., van Eden, W., Vervelde, L., 2009. Cellular host transcriptional responses to influenza A virus in chicken tracheal organ cultures differ from responses in in vivo infected trachea. *Vet Immunol Immunopathol* 132, 91-100.
- Rogers, D.F., 2007. Mucoactive agents for airway mucus hypersecretory diseases. *Respir Care* 52, 1176-1193; discussion 1193-1177.
- Roy, P., Fakhrul Islam, A.F., Burgess, S.K., Hunt, P.W., McNally, J., Walkden-Brown, S.W., 2015. Real-time PCR quantification of infectious laryngotracheitis virus in chicken tissues, faeces, isolator-dust and bedding material over 28 days following infection reveals high levels in faeces and dust. *J Gen Virol* 96, 3338-3347.
- Rubin, B.K., 2007. Mucus structure and properties in cystic fibrosis. *Paediatr Respir Rev* 8, 4-7.
- Russell, W.M.S., Burch, R.L., 1959. *The principles of humane experimental technique*. Methuen, London, UK.
- Schalk, A.F., Hawn, M.C., 1931. An apparent new respiratory disease of chicks. *J Am Vet Med Assoc* 78, 413-422.
- Schmidt, D., Hubsch, U., Wurzer, H., Heppt, W., Aufderheide, M., 1996. Development of an in vitro human nasal epithelial (HNE) cell model. *Toxicol Lett* 88, 75-79.
- Shak, S., 1995. Aerosolized recombinant human DNase I for the treatment of cystic fibrosis. *Chest* 107, 65S-70S.

- Steukers, L., 2013. Unraveling Herpesvirus Mucosal Invasion in an Exvivo Organ Culture. Ghent University, Merelbeke, Belgium.
- Steukers, L., Vandekerckhove, A.P., Van den Broeck, W., Glorieux, S., Nauwynck, H.J., 2011. Comparative analysis of replication characteristics of BoHV-1 subtypes in bovine respiratory and genital mucosa explants: a phylogenetic enlightenment. *Vet Res* 42, 33.
- Steukers, L., Vandekerckhove, A.P., Van den Broeck, W., Glorieux, S., Nauwynck, H.J., 2012. Kinetics of BoHV-1 dissemination in an in vitro culture of bovine upper respiratory tract mucosa explants. *ILAR J* 53, E43-54.
- Terregino, C., Maria, S.B., Giovanni, O., Cristian, D.B., Alessandra, D., 2006. Survey on circulation of infectious bronchitis virus strains in Northern Italy. *Italina Journal of Animal Science* 5, 309-311.
- Thor, S.W., Hilt, D.A., Kissinger, J.C., Paterson, A.H., Jackwood, M.W., 2011. Recombination in avian gamma-coronavirus infectious bronchitis virus. *Viruses* 3, 1777-1799.
- Toffan, A., Bonci, M., Bano, L., Bano, L., Valastro, V., Vascellari, M., Capua, I., Terregino, C., 2013a. Diagnostic and clinical observation on the infectious bronchitis virus strain Q1 in Italy. *Vet Ital* 49, 347-355.
- Toffan, A., Bonci, M., Bano, L., Valastro, V., Vascellari, M., Capua, I., Terregino, C., 2013b. Diagnostic and clinical observation on the infectious bronchitis virus strain Q1 in Italy. *Vet Ital* 49, 347-355.
- Tosi, G., Taddei, R., Barbieri, I., Fiorentini, L., Massi, P. 2010. Caratterizzazione molecolare dei ceppi di virus della bronchite infettiva aviaria isolati in Italia nel periodo 2007–2009 e nel primo bimestre del 2010. In: In proceedings of the 49th Annual Conference of Acts Italian society of Avian Pathology (SIPA), Forli, Italy, 217-224.
- Vairo, S., Van den Broeck, W., Favoreel, H., Scagliarini, A., Nauwynck, H., 2013. Development and use of a polarized equine upper respiratory tract mucosal explant system to study the early phase of pathogenesis of a European strain of equine arteritis virus. *Vet Res* 44, 22.
- Vairo, S., Vandekerckhove, A., Steukers, L., Glorieux, S., Van den Broeck, W., Nauwynck, H., 2012. Clinical and virological outcome of an infection with the Belgian equine arteritis virus strain 08P178. *Vet Microbiol* 157, 333-344.
- Vandekerckhove, A.P., Glorieux, S., Gryspeerdt, A.C., Steukers, L., Duchateau, L., Osterrieder, N., Van de Walle, G.R., Nauwynck, H.J., 2010. Replication kinetics of neurovirulent versus non-neurovirulent equine herpesvirus type 1 strains in equine nasal mucosal explants. *J Gen Virol* 91, 2019-2028.
- Vijay, R., Perlman, S., 2016. Middle East respiratory syndrome and severe acute respiratory syndrome. *Curr Opin Virol* 16, 70-76.

- Widagdo, W., Raj, V.S., Schipper, D., Kolijn, K., van Leenders, G.J., Bosch, B.J., Bensaid, A., Segales, J., Baumgartner, W., Osterhaus, A.D., Koopmans, M.P., van den Brand, J.M., Haagmans, B.L., 2016. Differential expression of the MERS-coronavirus receptor in the upper respiratory tract of humans and dromedary camels. *J Virol*.
- Winkler, M.T., Doster, A., Jones, C., 1999. Bovine herpesvirus 1 can infect CD4(+) T lymphocytes and induce programmed cell death during acute infection of cattle. *J Virol* 73, 8657-8668.
- Yoon, J.H., Moon, H.J., Seong, J.K., Kim, C.H., Lee, J.J., Choi, J.Y., Song, M.S., Kim, S.H., 2002. Mucociliary differentiation according to time in human nasal epithelial cell culture. *Differentiation* 70, 77-83.
- Zhao, Y., Kong, C., Cui, X., Cui, H., Shi, X., Zhang, X., Hu, S., Hao, L., Wang, Y., 2013. Detection of infectious laryngotracheitis virus by real-time PCR in naturally and experimentally infected chickens. *PLoS One* 8, e67598.
- Zhou, J., Chu, H., Li, C., Wong, B.H., Cheng, Z.S., Poon, V.K., Sun, T., Lau, C.C., Wong, K.K., Chan, J.Y., Chan, J.F., To, K.K., Chan, K.H., Zheng, B.J., Yuen, K.Y., 2014. Active replication of Middle East respiratory syndrome coronavirus and aberrant induction of inflammatory cytokines and chemokines in human macrophages: implications for pathogenesis. *J Infect Dis* 209, 1331-1342.

CHAPTER 6.

SUMMARY - SAMENVATTING

Summary

Infectious laryngotracheitis virus (ILTV) and infectious bronchitis virus (IBV) are two important avian respiratory viruses, which cause major economic losses in the worldwide commercial poultry. ILTV and IBV enter through respiratory and ocular routes. The ILTV and IBV invasion strategies at entry sites and subsequent pathogenesis mechanisms are poorly understood. Therefore, we aimed to evaluate replication characteristics of ILTV and IBV under *in vitro* and *in vivo* conditions.

In **Chapter 1**, an overview of the current knowledge of ILTV and IBV were given. In this chapter, historical background, classification, virus structure, replication, pathogenesis, clinical signs and pathology of ILTV and IBV were discussed.

In **Chapter 2**, the aims of this study were presented. The first aim was to study the replication kinetics of ILTV under *in vitro* respiratory and conjunctival mucosa explant models. The second aim was to understand if there is any change of mucin secretion in ILTV infected animals leading to the mucoid plugs/casts in the lumen of the respiratory tract. The third aim was to characterize the complete genome of the nephropathogenic B1648 strain to understand its epidemiological relationship with other IBV strains and genetic factors that may be associated with nephropathogenicity. The fourth and last aim was to elucidate how NIBV (B1648) has a strong tropism for the kidneys.

In **Chapter 3.1**, the first aim was addressed. *In vitro* tracheal and conjunctival mucosa explant models were developed of three chickens. Light microscopy and a fluorescent terminal deoxynucleotidyl transferase mediated dUTP nick end labeling (TUNEL) staining were used to evaluate the viability of the mucosal explants. *In vitro* chicken tracheal and conjunctival mucosa explant models were maintained up to 96h without significant changes in cell viability. These mucosal models were inoculated with ILTV and collected at 0, 24, 48 and 72h post inoculation (pi). ILTV was found to spread in a plaquewise manner in the mucosa. The three-dimensional changes of an ILTV plaque were quantitatively analysed. Plaque latitude increased over time up to 72h pi. ILTV showed a restricted penetration through the basement membrane (BM) (31% of the plaques in the trachea and 43% of the plaques in the conjunctiva at 48h pi). Further, the effect of ILTV on the cell viability of tracheal and conjunctival mucosae indicated that ILTV blocks apoptosis in infected cells but induces apoptosis

in neighboring uninfected cells. Overall, tracheal and conjunctival mucosal explant models were valuable and reproducible tools to study the early events of ILTV infection under *in vitro* conditions.

In **Chapter 3.2**, the second aim was addressed. First, we examined the expression of MUC5AC and MUC5B in the mucosa of larynx, trachea and bronchi of normal and ILTV infected chickens. Second, the mucoid plugs/casts present inside the trachea were stained for mucins (MUC5AC and MUC5B) and nuclear DNA fibrous structures (extracellular traps). The results showed that MUC5AC and MUC5B were extensively produced in the epithelium of the respiratory mucosa of normal chickens. Interestingly, the MUC5AC and MUC5B mucins were only present at the dorsal tracheal region (thinner) of the cranial and middle part of tracheal mucosa of normal chickens. The tracheal mucosal thickness was nearly 6.5 times higher in ILTV infected chickens compared to control chickens, and which is the main reason for almost 40% reduced diameter of the lumen in infected trachea. MUC5AC and MUC5B mucins were hardly observed in the mucosa of the respiratory tract and in the mucoid plugs/casts of the ILTV infected chickens. Surprisingly, DNA fibrous structures were present in $10.0 \pm 7.3\%$ nuclei of the cells from ILTV infected mucoid plugs/casts. Upon inoculation of isolated blood heterophils with ILTV, DNA fibrous structures were observed in $2.0 \pm 0.1\%$ nuclei of heterophils at 24 hours post inoculation (hpi). In summary, ILTV infected mucoid plugs/casts are not associated with MUC5AC and MUC5B mucins but with DNA fibrous structures, and are contributing to tracheal obstruction, and finally asphyxiation in chickens.

In **Chapter 4.1**, the third aim was addressed. The complete genome of Belgian NIBV reference B1648 strain was characterized to understand its evolutionary relationship with other IBV strains, and to identify the genetic factors, which may be associated with the nephropathogenic nature of this strain. Thirteen open reading frames (ORFs) were predicted in the B1648 strain (5'UTR-1a-1ab-S-3a-3b-E-M-4b-4c-5a-5b-N-6b-3'UTR). ORFs 4b, 4c and 6b were present in B1648 and most of the other IBV complete genomes. Based on the phylogenetic analysis of the full-length genome, replicase transcriptase complex, spike protein, partial S1 gene and M protein, B1648 strain was grouped with non-Massachusetts type strains (NGA/A116E7/2006, UKr 27-11, QX-like ITA/90254/2005, QX-like CK/SWE/0658946/10, TN20/00, IBV-27/99, RF/06/2007 and SLO/266/05). According to the partial S1 fragment, strains

TN20/00, IBV-27/99, RF/06/2007 and SLO/266/05 were grouped with B1648 and further, designated as B1648 genotype. The full-length genome of the B1648 strain shares the highest sequence homology with UKr 27-11, Gray, JMK, and NGA/A116E7/2006 (91.2 to 91.6%), but was less related with reference Beaudette and Massachusetts type strains (89.7%). Nucleotide and amino acid sequence analyses have revealed that the B1648 strain may have played an important role in the recent evolution of IBV in Europe and North Africa. The possible pathogenicity determinants of B1648 strain might be located on the 1a, spike, M and accessory proteins (3a, 3b, 4b, 4c, 5a and 5b). Overall, B1648 is a distinct strain setting it apart from all strains reported so far in Europe and other parts of the world.

In **Chapter 4.2**, the fourth aim was addressed. Nephropathogenic (B1648) and respiratory (M41) IBV infection kinetics were elucidated *in vitro* in respiratory mucosa explants and blood monocytes (KUL01⁺ cells) by a reproducible quantitative analysis system using confocal microscopy. A new real time quantitative polymerase chain reaction (5' RT-qPCR) was validated and used to evaluate B1648 and M41 infection kinetics *in vivo* in chickens. B1648 strain was replicating slightly better in the epithelium of the respiratory mucosa explants than M41 strain and used more KUL01⁺ cells (monocytes/macrophages) as carriers to transport the deeper layers of the respiratory tract in contrast to M41. Nephropathogenic B1648 virus productively infected KUL01⁺ blood monocytic cells whereas the infection with respiratory M41 virus was abortive. *In vivo*, IBV respiratory shedding was similar for both strains. Viral RNA copies were detected in plasma and mononuclear cells of B1648 inoculated chickens. In M41 inoculated chickens, viral RNA copies were not observed in plasma and mononuclear cells (except at one time point for plasma and mononuclear cells of one chicken at 6 dpi). Based on virus isolation, plasma and mononuclear cell samples of B1648 inoculated chickens were positive for infectious virus in contrast with M41 inoculated chickens. In addition, viral antigen KUL01⁺ cells were identified in mononuclear cells of only B1648 inoculated chickens. Viral RNA copies and antigen positive cells were observed in kidneys, spleen, lungs and liver of chickens infected with B1648 but not with M41, at 12 dpi (euthanasia). In summary, both B1648 and M41 replicate extensively in the epithelium of the tracheal mucosa, after which only B1648 can disseminate to internal organs through cell associated viremia in mononuclear leukocytes and cell free virus in plasma. This

study clearly demonstrated that the tissue tropism differences between IBV B1648 and M41 can be explained by the susceptibility of KUL01⁺ monocytic cells.

In **Chapter 5**, all data obtained in this study were reviewed and discussed. *In vitro* tracheal and conjunctival mucosal explant models were successfully established for chickens. These *in vitro* explants were susceptible to ILTV. ILTV spreads in a plaque-wise manner in the mucosa and penetrates underlying layers in a restricted manner. The ILTV infected mucoid plugs/casts are associated with DNA fibrous structures but not with mucins (MUC5AC and MUC5B). IBV B1648 is distinct from all other IBV strains reported so far in Europe and other parts of the world and may have played an important role in evolution. IBV B1648 can easily disseminate to internal organs via cell-free viremia in plasma and cell-associated viremia in mononuclear cells with KUL01⁺ cells as important carrier cells.

Samenvatting

Infectieuze laryngotracheïtis virus (ILTV) en infectieuze bronchitis virus (IBV) zijn twee belangrijke aviaire respiratoire virussen die wereldwijd enorme economische verliezen veroorzaken bij nutspluimvee. ILTV en IBV dringen binnen via respiratoire en oculaire route. De ILTV en IBV invasie strategieën op deze plaatsen en de ermee gepaarde pathogenesemechanismen zijn onvoldoende gekend. Daarom hebben we tot doel de vermeerderingskarakteristieken van ILTV en IBV onder *in vitro* en *in vivo* omstandigheden te bestuderen.

Een overzicht van de beschikbare kennis van ILTV en IBV werd gegeven in **Hoofdstuk 1**. De historische achtergrond, indeling, virusstructuur, vermeerdering, pathogenese, ziektebeelden en pathologie van ILTV en IBV werden hier besproken.

In **Hoofdstuk 2** werden de beoogde doelstellingen beschreven. De eerste doelstelling was de vermeerderingskinetiek van ILTV met behulp van *in vitro* respiratoire en conjunctivale mucosa explantmodellen te bestuderen. De tweede doelstelling bestond uit het onderzoeken van een mogelijke verandering in mucine secretie in ILTV-geïnfecteerde dieren dat aanleiding geeft tot mucoïede plugs/casts in het lumen van het ademhalingsstelsel. De derde doelstelling was de karakterisatie van het volledig genoom van de nefropathogene stam B1648 zodat de epidemiologische relatie met andere IBV stammen en genetische factoren die mogelijks geassocieerd zijn met nefropathogeniciteit beter begrepen kunnen worden. De vierde en laatste doelstelling was het ophelderen van hoe NIBV (B1648) een sterk tropisme voor de nieren heeft verworven.

Hoofdstuk 3.1 geeft een antwoord op de eerste doelstelling. Er werden *in vitro* tracheale en conjunctivale mucosa explanten gemaakt van drie verschillende kippen. De viabiliteit van de mucosale explanten werd beoordeeld door middel van lichtmicroscopie en een fluorescente terminal deoxynucleotidyl transferase mediated dUTP nick end labeling (TUNEL) kleuring. De *in vitro* kippen tracheale en conjunctivale mucosa explantmodellen werden tot 96 uur lang gehouden zonder dat er significante verschillen gezien werden in de levensvatbaarheid van de cellen. De explanten werden geïnfecteerd met ILTV en verzameld op 0, 24, 48 en 72 uur na inoculatie (post inoculatie, pi). ILTV bleek van cel-tot-cel te spreiden in de mucosa met de vorming van een plaque als gevolg. De drie-dimensionele veranderingen van

een plaque werden kwantitatief geanalyseerd. De breedte (latitude) van de plaques nam toe tot 72 uren pi. ILTV vertoonde een beperkte penetratie door de basaal membraan (BM) (31% van de plaques in de trachea en 43% van de plaques in de conjunctiva op 48 uur pi). Het effect van ILTV op de levensvatbaarheid van de cellen werd nagegaan in tracheale en conjunctivale mucosa. ILTV blokkeerde apoptose in geïnfecteerde cellen maar induceerde apoptose in naburige niet-geïnfecteerde cellen. Algemeen genomen kunnen tracheale en conjunctivale mucosale explantmodellen beschouwd worden als waardevolle en reproduceerbare tools om de eerste gebeurtenissen in een ILTV-infectie onder *in vitro* omstandigheden te kunnen bestuderen.

De tweede doelstelling werd behandeld in **Hoofdstuk 3.2**. Ten eerste werd de expressie van MUC5AC en MUC5B ter hoogte van de mucosa van de larynx, trachea en bronchen bij gezonde en ILTV-geïnfecteerde kippen nagegaan. Ten tweede werden de mucoïde plugs/casts die aanwezig waren in de trachea gekleurd voor mucines (MUC5AC en MUC5B) en DNA fibreuze structuren (extracellulaire traps). MUC5AC en MUC5B werd sterk geproduceerd door het epitheel in de respiratoire mucosa bij gezonde kippen. MUC5AC en MUC5B waren enkel aanwezig in het dorsale tracheale gebied (dunner) van het proximale en middelste deel van de tracheale mucosa bij gezonde kippen. De dikte van de tracheale mucosa was bijna 6,5 keer toegenomen in ILTV-geïnfecteerde kippen vergeleken met gezonde kippen, wat dus de hoofdreden is voor de vernauwing van de diameter van het lumen van om en bij de 40% bij geïnfecteerde dieren. De MUC5AC en MUC5B mucines werden nauwelijks waargenomen in de mucosa van het ademhalingsstelsel noch in de mucoïde plugs/casts bij ILTV-geïnfecteerde dieren. Verrassend genoeg waren DNA fibreuze structuren aanwezig bij $10.0 \pm 7.3\%$ van de kernen van cellen in ILTV-geïnfecteerde mucoïde plugs/casts. Na inoculatie van geïsoleerde bloedheterofielen met ILTV werden deze structuren 24 uur pi waargenomen in $2.0 \pm 0.1\%$ van de kernen. Samengevat, ILTV-geïnfecteerde mucoïde plugs/casts worden niet geassocieerd met MUC5AC en MUC5B mucines maar met DNA fibreuze structuren en dragen bij tot de obstructie van de luchtpijp met verstikking tot gevolg.

In **Hoofdstuk 4.1** werd de derde doelstelling besproken. Het volledige genoom van de Belgische NIBV referentiestam B1648 werd gekarakteriseerd om zijn evolutionaire relatie met andere IBV stammen te kunnen begrijpen, en om genetische factoren te

identificeren die mogelijks geassocieerd zijn met de nefropathogene natuur van deze stam. Dertien “open reading frames” (ORFs) werden voorspeld in de B1648 stam (5'UTR-1a-1ab-S-3a-3b-E-M-4b-4c-5a-5b-N-6b-3'UTR). ORFs 4b, 4c en 6c waren aanwezig in B1648, alsook in de meeste andere IBV volledige genomen. Gebaseerd op de fylogenetische analyse van het full-length genoom werden het replicase transcriptase complex, het spike eiwit, een gedeeltelijk S1 gen en het M-eiwit van B1648 gegroepeerd met die van niet-Massachusetts type stammen (NGA/A116E7/2006, UKr 27-11, QX-like ITA/90254/2005, QX-like CK/SWE/0658946/10, TN20/00, IBV-27/99, RF/06/2007 and SLO/266/05). Als gevolg van het gedeeltelijk S1 fragment werden de TN20/00, IBV-27/99, RF/06/2007 en SLO/266/05 stammen gegroepeerd met B1648 en werden ze verder vernoemd als B1648 genotype. Het full-length genoom van de B1648 stam vertoonde een erg hoge sequentie homologie met UKr 27-11, Gray, JMK en NGA/A116E7/2006 (91.2 tot 91.6%), maar was minder gerelateerd met de Beaudette en Massachusetts type referentie stammen (89.7%). Nucleotide en aminozuursequentie analyses brachten aan het licht dat de B1648 stam mogelijks een belangrijke rol gespeeld heeft in de recente evolutie van IBV in Europa en Noord-Afrika. De mogelijke pathogeniciteitsbepalende factoren van B1648 kunnen zich bevinden in de 1a, spike, M en accessoire eiwitten (3a, 3b, 4b, 4c, 5a en 5b). Algemeen genomen is de B1648 stam een stam die zich onderscheidt van alle stammen die tot nu toe in Europa en andere werelddelen werden gerapporteerd.

In **Hoofdstuk 4.2** werd de vierde doelstelling behandeld. Nefropathogene (B1648) en respiratoire (M41) IBV-infectiekinetieken werden opgesteld in *in vitro* respiratoire mucosa explanten en bloedmonocyten (KUL01⁺ cellen) door middel van een reproduceerbaar kwantitatief analysesysteem en confocale microscopie. Een nieuwe real time quantitative polymerase chain reaction (5' RT-qPCR) werd gevalideerd en gebruikt om de infectiekinetiek van B1648 en M41 bij levende kippen te bestuderen. De B1648 stam vermeerderde iets meer, vergeleken met de M41 stam, in het epitheel van respiratoire mucosa explanten en gebruikte meer KUL01⁺ cellen (monocyten/macrofagen) als carrier om zo dieper in de lagen van het respiratoire stelsel te geraken. De nefropathogene stam B1648 infecteerde succesvol KUL01⁺ cellen, terwijl een infectie met de respiratoire M41 stam mislukte. *In vivo* bleek de IBV uitscheiding vergelijkbaar met beide stammen. Bij B1648-geïnfecteerde kippen

werden er virale RNA kopijen teruggevonden in plasma en mononucleaire cellen. Bij M41-geïnfecteerde kippen werden er geen RNA kopijen gevonden in deze cellen of plasma (behalve in plasma en in mononucleaire cellen van één kip op 6 dagen na inoculatie). Volgens de virusisolatie waren stalen met plasma en mononucleaire cellen afkomstig van B1648-geïnfecteerde dieren positief voor infectieus virus in tegenstelling tot M41-geïnfecteerde dieren. Bovendien werden viraal antigeen-positieve KUL01⁺ cellen enkel geïdentificeerd in mononucleaire cellen van B1648-geïnfecteerde kippen. Op 12 dagen na inoculatie (euthanasie) werden virale RNA kopijen en antigen positieve cellen gevonden in de nieren, de milt, de longen en de lever van kippen geïnfecteerd met B1648, maar niet bij dieren geïnfecteerd met M41. Samengevat, zowel B1648 als M41 vermeederen in het epitheel van de tracheale mucosa, waarna enkel B1648 verder kan spreiden naar interne organen via een celgeassocieerde viremie in mononucleaire leukocyten en celvrij in plasma. Deze studie demonstreerde duidelijk dat de weefselvoorkeuren tussen IBV B1648 en M41 kunnen verklaard worden door de gevoeligheid van de KUL01⁺ monocytische cellen voor een IBV infectie.

Alle gegevens worden kort aangekaart en grondig bediscussieerd in **Hoofdstuk 5**. *In vitro* tracheale en conjunctivale mucosale explantmodellen voor kippen werden succesvol ontwikkeld. Deze *in vitro* explanten waren gevoelig voor ILTV-infectie. ILTV spreidt van cel tot cel in de mucosa met de vorming van een plaque als gevolg en penetreert de onderliggende lagen op een beperkte manier. De ILTV-geïnfecteerde mucoïede plugs/casts werden in verband gebracht met DNA fibreuze structuren maar niet met mucines (MUC5AC en MUC5B). IBV B1648 kan gemakkelijk spreiden naar interne organen via een celvrije viremie in plasma en via een celgeassocieerde viremie in mononucleaire cellen met KUL01⁺ cellen als belangrijke carriercellen.

CURRICULUM VITAE

Personal contact

Vishwanatha R.A.P. Reddy
Laboratory of Virology
Faculty of Veterinary Medicine, Ghent University
Salisburylaan 133, 9820 Merelbeke, Belgium
Phone: +32 9 264 73 87/Mobile: +32 466 04 31 03
E-mail: Reddy.Vishwanatha@UGent.be
apvishireddy@gmail.com/vishwanathareddyap@gmail.com

Vishwanatha Reddy Avalakuppa Papi Reddy was born in Kolar, Karnataka, India. He obtained his Bachelor degree in Veterinary Science and Animal Husbandry (B.V.Sc and A.H.) from Bangalore Veterinary College, Karnataka Veterinary, Animal, and Fisheries Sciences University (KVAFSU - Bidar), in August 2007. In September 2008, he was awarded with a scholarship from the Indian Veterinary Research Institute (IVRI) to pursue his Master of Veterinary Science (M.V.Sc.) in Veterinary Biochemistry. Purification and identification of Matrix metalloproteinase 7 (MMP7, matrilysin) protein of canine mammary tumor tissue was performed during his Masters studies. He obtained his M.V.Sc. in 2010. In December 2011, he started his Ph.D. under supervision of Professor Hans Nauwynck in the Laboratory of Virology, Department of Virology, Parasitology and Immunology, Faculty of Veterinary Medicine, Ghent University. Indian Council of Agricultural Research - International Fellowship (ICAR IF - 2011/12) and Ghent University special research fund (BOF - 2015) sponsored his Ph.D. project. In Nauwynck's laboratory, he has elucidated the replication kinetics of infectious laryngotracheitis virus (ILTV) and infectious bronchitis virus (IBV) under *in vitro* and *in vivo* conditions. He also worked on fowl poxvirus (FPV) and Marek's disease virus (MDV). He has published several first-author and co-author papers in international peer-reviewed journals, and has made oral and poster presentations in various international scientific conferences and symposiums.

Scientific awards and distinctions

1. Awarded BOF-Special research fund for finalizing PhD at Ghent University (2015-16).
2. Awarded Indian council of agricultural research international fellowship for three years to pursue PhD at Ghent University (ICAR-IF - 2011-12).
3. Selected for Assistant professor job in the department of physiology and animal biochemistry, recruited by Karnataka animal and fishery Sciences University, Karnataka state, India (KVAFSU - 2011-12).
4. Qualified national eligibility test (NET) for Assistant Professor job, conducted by the agricultural scientists recruitment board (ASRB) in September 2010.
5. 20th rank in the all India entrance examination for admission to post graduate programme in animal biotechnology (IVRI), conducted by the ICAR (2008-09).
6. 4th rank in the all India entrance examination for admission to PhD programme in animal biochemistry, conducted by the Indian veterinary research institute (IVRI) (2010-11).

7. 6th rank in the all India entrance examination for admission to PhD programme in animal biochemistry, conducted by the National dairy research institute (NDRI) (2010-11).
8. Indian veterinary research institute (IVRI) research fellowship for M.V.Sc programme (Animal Biochemistry) (2008-10).
9. Awarded Jindal merit scholarship for undergraduate programme (2003-2006).

Publications in international scientific journals

1. **Reddy, V. R.**, Trus I., Desmarests, L. M. B., Li Y., Theuns, S., & Nauwynck, H. J. Productive replication of nephropathogenic infectious bronchitis virus strain B1648 in the peripheral blood monocyctic cells, a strategy for viral dissemination and kidney infection in chickens. *Veterinary Research*. 2016 Jul 13;47(1):70.
2. **Reddy, V. R.**, Theuns, S., Roukaerts, I. D., Zeller, M., Matthijssens, J., & Nauwynck, H. J. Genetic Characterization of the Belgian Nephropathogenic Infectious Bronchitis Virus (NIBV) Reference Strain B1648. *Viruses*. 2015 Aug 7;7(8):4488-506.
3. **Reddy, V. R.**, Steukers, L., Li, Y., Fuchs, W., Vanderplasschen, A., & Nauwynck, H. J. Replication characteristics of infectious laryngotracheitis virus in the respiratory and conjunctival mucosa. *Avian Pathology*. 2014; 43 (5): 450-7.
4. **Reddy, V. R.**, Trus I., Vercammen, F., & Nauwynck, H. J. Contemporary outbreaks of different avipoxviruses in Humboldt Penguins of Wild Animal Park Planckendael and in chickens of commercial poultry farms in Belgium. *Flemish veterinary journal* (*in press*).
5. **Reddy, V. R.**, Trus I., & Nauwynck, H. J. Drop of MUC5AC and MUC5B mucin production in infectious laryngotracheitis virus (ILTV) infected respiratory mucosa and absence in mucoid plugs/casts. *Virus Research*. 2017); 227: 135-142
6. Watteyn, A., Devreese, M., Plessers, E., Wyns, H., Garmyn, A., **Reddy, V. R.**, ... Croubels, S. Efficacy of gamithromycin against *Ornithobacterium 2* rhinotracheale in turkey poultts pre-infected with avian Metapneumovirus. *Avian Pathology* (*in press*).
7. Li, Y., Negussie, H., Qiu, Y., **Reddy, V. R.**, & Nauwynck, H. J. Early events of canine herpesvirus 1 infections in canine respiratory and genital mucosae by the use of ex vivo models. *Research in Veterinary Science*, 2016, 105, 205–208.
8. Trus, I., Frydas, I. S., **Reddy, V. R.**, Bonckaert, C., Li, Y., Kvisgaard, L. K., . . . Nauwynck, H. J. Immunity raised by recent European subtype 1 PRRSV strains allows better replication of East European subtype 3 PRRSV strain Lena than that raised by an older strain. *Veterinary Research*, 2016, 47(1), 15.
9. Li, Y., Van Cleemput, J., Qiu, Y., **Reddy, V. R.**, Mateusen, B., & Nauwynck, H. J. Ex vivo modeling of feline herpesvirus replication in ocular and respiratory mucosae, the primary targets of infection. *Virus Research*. 2015 Dec 2;210:227-31.
10. Frydas, I. S., Trus, I., Kvisgaard, L. K., Bonckaert, C., **Reddy, V. R.**, Li, Y., . . . Nauwynck, H. J. Different clinical, virological, serological and tissue tropism outcomes of two new and one old Belgian type 1 subtype 1 porcine reproductive and respiratory virus (PRRSV) isolates. *Veterinary Research*. 2015 Mar 21;46:37.
11. Gowda, T. K., **Reddy, V. R.**, Devleeschauwer, B., Zade, N. N., Chaudhari, S. P., Khan, W. A., . . . Patil, A. R. Isolation and Seroprevalence of *Aeromonas* spp. Among Common Food Animals Slaughtered in Nagpur, Central India. *Foodborne Pathogens and Disease*. 2015;12(7):626-30.

12. BV Sunil Kumar, Meena Kataria, GVPPS Ravi Kumar, K Aswani Kumar and **AP Vishwanatha Reddy**. Partial sequence clone of canine mammary tumor metalloproteases MMP-11 catalytic domain. Online journal of veterinary research. 12(1): 66-73, 2011.

Manuscripts under preparation

1. **Reddy, V. R.**, Trus I., & Nauwynck, H. J. Infection kinetics of fowl poxvirus in respiratory mucosa explants of chickens.
2. **Reddy, V. R.**, Vercammen, F., & Nauwynck, H. J. First outbreak of avian poxvirus in Griffon vulture (*Gyps fulvus*) of Wild Animal Park Planckendael in Belgium.

Publications in national scientific journals

1. **Vishwanatha Reddy AP**, Sunil Kumar BV, Ranganath GJ, Aswani Kumar K, Maiti SK and Meena Kataria. Isolation, Purification and Identification of Matrilysin protein from canine mammary tumor tissue and its relative quantification in normal and tumor cases by Indirect ELISA. Indian journal of veterinary pathology. 35(1): 8-12, 2011.
2. Ranganath GJ, Ram Kumar, **Vishwanatha Reddy AP**, Mayilkumar K, Pawaiya, RVS and Biplab Debroy. Comparative study on the expression pattern of the proliferating cell markers PCNA and Ki67 in canine mammary tumors. Indian journal of veterinary pathology. 35 (1): 13-17, 2011.
3. Ranganath GJ, Ram Kumar, **Vishwanatha Reddy AP**, Mayilkumar K, Pawaiya, RVS and Biplab Debroy. Expression pattern of c-erb2 and Estrogen receptor- α in spontaneous canine mammary tumors. Indian journal of veterinary pathology. 35 (2), 2011.

Conference abstracts

1. **Reddy, V. R.**, & Nauwynck, H. J. The replication characteristics of infectious laryngotracheitis virus (ILTV) in the respiratory and conjunctival mucosa. 11th International Symposium on Marek's Disease and Avian Herpesviruses, Tours, France (2016).
2. **Reddy, V. R.**, Trus, I., & Nauwynck, H. J. Study of mucus plugs/casts in the early acute infectious laryngotracheitis infection. 11th International Symposium on Marek's Disease and Avian Herpesviruses, Tours, France (2016).
3. **Reddy, V. R.**, Trus I., Desmarests, L. M. B., Li Y., Theuns, S., & Nauwynck, H. J. Comparison of respiratory (M41) and nephropathogenic (B1648) infectious bronchitis viruses in in vitro and in vivo conditions. 9th international symposium on avian corona- and pneumoviruses. COST European Cooperation in Science and Technology, Utrecht, Netherlands (2016).
4. **Reddy, V. R.**, Theuns, S., Matthijssens, J., & Nauwynck, H. J. Genetic characterization of the Belgian nephropathogenic infectious bronchitis virus (NIBV) reference strain B1648. COST European Cooperation in Science and Technology, Utrecht, Netherlands (2016).
5. **Reddy, V. R.**, Trus, I., Li, Y., & Nauwynck, H. J. Replication characteristics of respiratory and nephropathogenic infectious bronchitis virus (IBV) strains M41 and B1648 in respiratory mucosa and monocytes. Veterinary Virology, 10th

- International congress. European Society of Veterinary Virology (ESVV), Montpellier, France (2015).
6. **Reddy VR**, Trus I, Li Y, & Nauwynck, H. J. The invasion mechanisms of infectious laryngotracheitis virus (ILTV) in the respiratory and conjunctival mucosa. Veterinary Virology, 10th International congress. European Society of Veterinary Virology (ESVV), Montpellier, France (2015).
 7. **Reddy VR**, Steukers L, Li Y, Fuchs W, Vanderplasschen A, Nauwynck H. J. “The replication characteristics of infectious laryngotracheitis virus (ILTV) in the respiratory and conjunctival mucosa” Second annual meeting, Belgian Society for Virology, The Royal Academies for Science and the Arts Hertogsstraat/Rue Ducale 1, Brussels, Belgium (2014).
 8. Trus, I., Frydas, I. S., **Reddy, V. R.**, Bonckaert, C., Li, Y., Kvisgaard, L. K., . . . Nauwynck, H. J. “The immunity raised by recent European subtype1 porcine reproductive and respiratory syndrome virus (PRRSV) strains allows spatial expansion of highly virulent East European subtype 3 PRRSV strains” Second annual meeting, Belgian Society for Virology, The Royal Academies for Science and the Arts Hertogsstraat/Rue Ducale 1, Brussels, Belgium (2014).
 9. Watteyn, A., Devreese, M., Plessers, E., Wynsa, H., Garmynb, A., **Reddy, V. R.**, . . . Croubels, S. “Efficacy of a single bolus administration of gamithromicin against *Ornithobacterium rhinotracheale* infection in turkeys” 14th European poultry conference: Conference information and proceedings, Stavanger, Norway (2014).

Oral presentations

1. **Reddy VR**, Nauwynck H. The replication characteristics of infectious laryngotracheitis virus (ILTV) in the respiratory and conjunctival mucosa. 11th International Symposium on Marek’s Disease and Avian Herpesviruses, Tours, France (2016).
2. **Reddy VR**, Trus I, Desmarests L, Li Y, Theuns S, Nauwynck H. Comparison of respiratory (M41) and nephropathogenic (B1648) infectious bronchitis viruses in in vitro and in vivo conditions. 9th international symposium on avian corona- and pneumoviruses. COST European Cooperation in Science and Technology, Utrecht, Netherlands (2016).
3. **Reddy VR**, J. Matthijnsens, Theuns S, Nauwynck H. Genetic characterization of the Belgian nephropathogenic infectious bronchitis virus (NIBV) reference strain B1648. COST European Cooperation in Science and Technology, Utrecht, Netherlands (2016).
4. **Reddy VR**, Trus I, Li Y, Nauwynck H. Replication characteristics of respiratory and nephropathogenic infectious bronchitis virus (IBV) strains M41 and B1648 in respiratory mucosa and monocytes. Veterinary Virology, 10th International congress. European Society of Veterinary Virology (ESVV), Montpellier, France (2015).

Acknowledgments

On every accomplishment of a person there are many known and unknown helping hands and it is always pleasure to remember and thank them at the end.

First of all, I would like to thank my Supervisor Prof. Hans J. Nauwynck for accepting me as a doctoral student in the Laboratory of Virology, Faculty of Veterinary Medicine, and Ghent University. In the past 4 years and 10 months, his critical comments and guidance have changed my amateur research approach. I have enjoyed your perfect choice of my Ph.D. project on avian viruses, as I had no idea on virology and veterinary research. I will always be proud that you are my mentor. Your perseverance to get through the funding of this project is highly appreciated. I would like to thank Indian Council of Agricultural Research (ICAR) for International fellowship and Ghent University for finalizing special research fund (BOF).

I would like to express my sincere gratitude to the guidance committee members, Prof. Dr. Richard Ducatelle and Prof. Dr. Katleen Hermans, for reading of this thesis and comments. I highly appreciate the members of the examination board: Dr. Sjaak de Wit, Prof. Dr. Kannan Ganapathy and Prof. Dr. An Garmy, for the careful reading of this thesis and providing me useful comments and suggestions, which improved the thesis quality.

Magda, your help is highly appreciated, especially for the maintenance of stables and isolators during chicken experiments. I would like to thank Lieve for her help during initial days of my research and her assistance on basic virology techniques. Melanie thank you for the help to process samples during animal experiments. You made my sample-processing job easy. Ytse, your help for qPCR is highly appreciated and also for diagnosis of Pox. Your help has improved the quality of my IBV research. I would also like to thank Carine, Nele and Chanthal for their excellent technical assistance. Zeger, thank you for your help during animal experiments and excellent technical assistance. Best wishes for your work and endeavors. Dirk, thank you for solving all type of computer problems. Mieke, administrative help before and after my arrival to Belgium is highly appreciated. Loes, thank you very much for your help during animal experiments and best wishes for your future endeavors.

Ivan, you have assisted me in most parts of my research work and helped for statistical analysis. I learnt many things from you, especially animal experiments design, maintenance and successful execution. There are no words to appreciate your help and suggestions. Of course, I cannot forget our endless discussions on almost all contemporary topics of the world. I wish you a lot of successes with your future work and life. Bas, thank you for helping me to initiate collaboration with Prof. Dr. Jelle for genome sequencing and interpretation of results. Your help also appreciated for qPCR optimization. I have learnt a lot of things from you and enjoyed the discussions with you. I would like to wish you a lot of successes in your academic and life. And good luck with your animal experiments. Lowiese, your strategies and suggestions have helped a lot to improve my research quality. You have solved many of my technical research problems. You are one of the best researchers and asset of this lab. I hope you will stay only in academic research and wish you a lot of successes with your future endeavors. Caroline, thank you very much for your help and suggestions during animal experiments and for diagnosis. I appreciate your help for translation of my thesis summary and abstract of one paper. Good luck with your PhD defence and Best wishes for your future endeavors. Lennert, thank you very much for your help and critical suggestions during my initial days of PhD. Inge, I wish a lot of success with your defence starting of next year. We also collaborated for a paper. Thank you for your suggestions and comments. Isaura, good luck for finishing your PhD and thank you for suggestions on PCR. Haile, I would like to wish you a lot of success with your PhD defence in the starting of next year and best wishes for job searching. We had lively discussions on many topics and thank you for your comments and suggestions. Yewei, we have collaborated for many explant experiments and

animal experiments with successful outcome. I appreciate your help during this period and wish you a lot of success for your defence in the starting of next year. Pepe, good luck for finishing your PhD and thank you for lively discussions on many topics. Ilias, we did an animal experiment together and thank you for your suggestions during my PhD period. Depu, I appreciate your motivation during my initial days of PhD and I was happy to discuss with you. Amy, I appreciate your help during my initial days of PhD. And thank you for mucin antibodies that helped for one publication. Hossein, we had some active discussions on varied topics and thank you for your comments and suggestions during this period. Thoung, we have almost started and finishing same time. I wish you a lot of success with your defence next month and your future endeavors. Wenfeng, thank you for the lively discussions and suggestions for the past four years. Best wishes for your future career. Charlie and Kevin, we have started almost at the same time. I really enjoyed both of your company in the Belgium and I wish you both a lot of success. Eleni, it was interesting discussions with you for the last one year in our chamber. Best wishes for your future career and life. Ting ting, it was good discussion with you and good luck with your PhD research and life. Garba, it was good discussion with you, and good luck with your doctoral research and life in the Belgium. Wendy, good luck with your project. If you want to know something about IBV, feel free to contact me. Delphine, best wishes for your doctoral research and thank you.

I would like to thank all my colleagues of the lab: Jing, Fang, Jiexiong, Bo, Kathlyn, Sebastiaan, Gaetan, Tuan, Katrien, Jolien and Quintin. I appreciate all your company in the lab.

I highly appreciate the members of the India platform for their passion, selflessness and commitment to promote European research culture in the Indian universities/culture. After my association with the India platform, both my professional and personal lifestyle was improved tremendously in the Ghent. I would be sincerely great full to Prof. Balu, Nele, Marianne, Jakob, Sarika and Saraha for their support and suggestions.

Deruddera jozef (my house owner) is the best person I have ever seen in the Belgium and always be grateful to him. I will be indebted to him in my whole life for his service.

I will be always great full to Dr. Meena Kataria for her guidance, patience and support during masters. I am thankful to Dr. Joshi, Dr Bhaskar Sharma, Dr. Mohini Sainin and Dr. Sanjeev bhure.

I will be always great full to my career guide Kanta for his constant motivation and suggestions. His association has changed my career path. I also like to thank my best friends since my failure days, Govardhan, Mohan, Manjunatha Reddy, Venki anna, Sudharshan, Badri, Sivabala, Shankarmurthy, Anand, Bradman and Advocate. I am thankful to my IVRI friends, Prbhya, Murugavel and Amith. Aswani and Ravi sir help was highly appreciated during my IVRI days and for the success of ICAR project. I am thankful to Koli ramesha, Sajjan, Arun GB, Pathu sir and Kotresh sir for their help during IVRI days. I am great full to my UG friends: Bradman, Sridhar, Bhaskar, Kantha, Guru, Yathisha, Kaddi sathisha, Pithamagan and Mahan. I would like to thank Bablu, Shankara, Munirathnam, athma and Sheena.

I would like to thank Hemant and Prabhu for warm Indian dishes and good company in the Belgium. Sathya and Shivu for help and suggestions during initial days of the Belgium.

I am always great full and indebted to Eranagari and kollepa family members for their hope, support and sacrifice. I would be great full to Rangappa (Virginia, USA), for his constant encouragement and suggestion for my career. I am fortunate to have person like him. Finally, I would like to thank Amma, Jalajakshi, Suresh, Rajanna, Kittanna, Shreramma and Tanuja.